QUANTIFYING BED STABILITY: THE MISSING TOOL FOR ESTABLISHING MECHANISTIC HYDROLOGICAL LIMITS

A thesis presented in partial fulfilment of the requirements for the degree of
Doctor of Philosophy
in
Geography
at Massey University, Palmerston North,
New Zealand.

Andrew J. Neverman

2018

Typeset with LaTeX

Primary Supervisor:
Professor Ian C. Fuller

Co-Supervisors:
Professor Russell G. Death
Associate Professor Jon N. Procter
Dr. Ranvir Singh

Examiners:
Professor David J. Gilvear
Dr. Jon F. Tunnicliffe
Dr. Sam T. McColl

Abstract

Sediment transport processes are a key mechanism of ecological change in riverine systems, and certain levels of sediment flux are necessary for healthy ecosystem functioning. Altered flow regimes and sediment mobility are contributing to a global problem of higher substrate embeddedness reducing the frequency of substrate scour events and leading to increases in periphyton accrual. Excess periphyton accrual leads to fish and invertebrate kills from oxygen depletion, degraded ecological health, altered sediment dynamics, deterioration in water taste, and odour nuisance. In recent decades, reports of toxic periphyton proliferations have increased and are linked with health problems in humans including asthma, skin rashes, liver damage, and the death of domestic dogs. Excess periphyton accrual is prominent in impounded catchments where dams have a considerable impact on flow and sediment regimes. With at least 3,700 large dams currently under construction or in the planning phase the problem is set to increase in the foreseeable future.

Hydrological limits are widely implemented by authorities in an attempt to manage periphyton accrual. Hydrological limits are frequently based on flow-ecology relationships but are often ineffective. Sediment transport thresholds have been found to have a better relationship with periphyton accrual than hydrological metrics. Flow-ecology relationships do not account for the mechanisms of periphyton removal (scour, abrasion, and molar action) which are likely to vary between sites at equivalent flows, and the species-specific resistance to each mechanism also likely varies. Abrasion and molar action result from transport of sediment. Improving the effectiveness of hydrological limits as a tool for river management therefore relies on setting flows with the aim of inducing sediment transport to initiate mechanisms of periphyton scour. This will require models which can accurately predict the flow required to induce different phases of sediment transport. The research presented in this thesis focuses on improving the estimation of gravel entrainment to advance entrainment models as a means of setting hydrological limits to induce molar action and improve the effectiveness of periphyton removal.

A literature review of methods for estimating gravel particle entrainment thresholds in natural channels revealed a considerable gap in methods being available to quantify substrate characteristics to calculate resistance thresholds. The review also found significant challenges in identifying the onset of gravel transport in natural channels, and difficulty obtaining corresponding hydrodynamic data to identify entrainment thresholds. Further, the review found seepage was an important component of hydrodynamic forces for inducing particle entrainment in flumes, but seepage is not considered in conventional entrainment formulae, and is not measured alongside bedload transport data in the field.

A suite of tools is identified and developed to improve the quantification of substrate structure and resistance, identification of incipient motion, and quantification of entrainment thresholds in natural gravel beds to advance the assessment of bed mobility. Optical and ranging techniques are compared to identify an optimal approach to remotely quantify substrate structure. Both approaches were found to produce a comparable quantification of surface roughness using point cloud elevations, but identified different trends in surface layer development. Quantification of surface layer development was found to be sensitive to the cell size used to grid the data, and this sensitivity increased with higher-order statistical moments which were used to describe armouring. Airborne optical sensors were found to be the most versatile method for remote characterisation of gravel-bed surface structure, with a larger range of metrics being derivable from the same dataset to quantify a wider range of substrate structural and textural characteristics.

Whilst quantifying bed structure is critical for developing bed mobility models, measuring the resistive force of the bed created by the structural arrangement of particles is required for model calibration and empirical data collection. A protocol was developed to use a modified penetrometer to quantify the resistive force of the armour (active) layer in gravel-bed channels. The modifications made to the penetrometer made it sensitive to variations in armour layer compactness, and allowed for adaptive penetration depths enabling variations in armour layer thickness to be accounted for. The protocol and modified penetrometer provide a significant advancement in the ability to empirically quantify bed resistance and relate bed structure to potential bed mobility, and build on the remote sensing methods to provide a suite of bed resistance parameters for entrainment models.

Measurement of bed mobility is also critical for calibrating entrainment models and relating ecological metrics to bed mobility thresholds. Both direct and indirect measurement of bed mobility have benefits for research and river management. Tick-box indices are frequently used in ecological studies to provide an indirect assessment of substrate (in)stability (i.e. bed mobility). These indices often provide a poor approximation of bed mobility, and do not relate well with biotic communities, but their low-cost and rapidity make them a valuable tool for research and management. An improved index is developed to provide rapid, low-cost assessment of bed mobility. This index improves on previous methods by focusing on objective measurements of parameters where low-cost approaches are available, or providing a framework for scoring parameters where visual assessment is required. The index scores correlated well with tracer particle data, and were found to relate to accrual of *Phormidium* biomass. This index therefore provides a means to rapidly and cost-effectively estimate bed mobility and predict periphyton accrual.

Direct measurement of bed mobility is also required to provide an empirical dataset for the calibration of particle entrainment and transport models, and for the empirical derivation of hydrological limits. A multi-sensor system was developed to measure the onset of particle movement, and record corresponding hydrodynamic data, including bed seepage, to identify hydraulic entrainment thresholds in natural channels, and therefore address the challenges of identifying bedload entrainment thresholds identified in the literature review. A pilot study testing the system identified bed seepage and turbulence intensity as key predictors of particle entrainment, and discharge and mean velocity as the worst predictors. These findings challenge the use of discharge and mean velocity as the metrics used to set hydrological limits if mechanistic limits based on bed mobility-ecology relationships are to be established effectively.

These tools provide a means for scientists to study bedload entrainment and transport, identify their thresholds, and relate the frequency and magnitude of these processes to benthic community dynamics. This research will form the basis for establishing the mechanisms required to achieve removal of excess periphyton and establish hydrological limits to ensure these mechanisms function and effective removal of periphyton is achieved to maintain ecosystem health.

Acknowledgements

Whilst each chapter contains specific acknowledgements, there are many people I would like to emphasise my thanks to who have been key to my journey during the construction of this thesis.

First of all I would like to thank Professor Ian Fuller and Professor Russell Death for conceiving the idea of this thesis and considering me to be up to the task, and Associate Professor Jon Procter and Dr. Ranvir Singh for joining the project and providing valuable expertise.

The expertise and ideas which were produced in supervisory meetings would never have lead to any data or new knowledge being produced without the technical expertise provided by David Feek (Massey University) and Dave Reid (Essential Electronics and Security Limited, Levin) throughout this research. Sincere thanks are given to David Feek for his many hours of technical assistance with the development, construction, and installation of the sensors and field apparatus used in this thesis, and his repeat sacrifice of dry days in the office to get the job done. Dave Reid was instrumental in developing the brains behind the impact plate geophone and was more than generous with donating his time in-kind to meet our limited budget. Without skilled technicians the state of science would be very poor indeed.

I am thankful to Horizons Regional Council (HRC), in particular Brent Watson and Jeff Watson who were always accommodating, and supported the project through funding and provision of data. Paul Peters is also thanked for supporting the installation of sensors at Mais Reach.

I also thank Dr. Lorenzo Picco and Dr. Riccardo Rainato for hosting me on my trips to Vienna and Padova, and allowing me to join in with the research in the Rio Cordon basin. These were great experiences and provided me with a deeper understanding of geomorphic processes and research beyond the New Zealand context. I am also thankful to them for the introduction to proper coffee and pasta.

Without financial support it would have been impossible to do any of this research. Funding for the project was provided by many parties, including: Massey University (Doctoral Scholarship), TrustPower (Windfarm Bursary), Tilt Renewables (WindFarm Bursary), MacMillan Brown Agricultural Research Scholarship, Royal Society of New Zealand (New Zealand Ecohydraulics Trust Travel Award), IPENZ Rivers Group (Student Research Grant), NZ Hydrological Society (Grant in Aid of Research, Grant in Aid of Travel), Perpetual Guardian (Kathleen Spragg Travel Grant), NZ Geographical Society Manawatu Branch (Postgraduate Research Fund).

I have also been fortunate to receive excellent support outside of my project. On this note I would like to thank Professor Danny Donaghy for providing independent mentoring throughout the PhD process, and for the many Saturday open mats.

To my parents, I thank my mother, Sharyon Neverman, for instilling in me from an early age the inclination to do research if I ever had a question which others could not provide an answer to. And to my father, Geoffrey Neverman, for teaching me that if you can't buy it off the shelf you can make it. And if you can buy it off the shelf, you can probably make it better and cheaper anyway. These foundations are the reason I have made it to this point.

Most importantly, I am grateful to Charlotte Holdsworth for putting up with me throughout this ordeal, and supporting my need to get butter chicken or dumplings on a regular basis. She has also been my primary field assistant, UAV spotter, spell-checker, and sounding board. Without her, this would have been a very different experience.

Contents

List of Figures

List of Tables

List of Equations

General Introduction

Water abstraction and storage modifies the physical and chemical habitat of rivers leading to dramatically altered river ecology, such as the increased accrual of periphyton (Graf, 2006; Poff *et al.* 2007). Periphyton accrual is increasingly reaching prolific levels as a result of lower flows, increased nutrient availability, and increased substrate stability. Excess periphyton accrual has a number of negative impacts on aquatic ecosystems including oxygen depletion, fluctuations in dissolved oxygen, and alteration of sediment dynamics (Biggs, 1990; Fovet *et al.* 2012). These impacts may lead to fish and invertebrate kills. Some periphyton, such as cyanobacteria, can have major implications for human health, and the genus *Phormidium* has been attributed to the death of domestic dogs via neurotoxicosis (Baker *et al.* 2001; Hamill, 2001; McAllister *et al.* 2016; McAllister *et al.* 2018). Non-toxic periphyton may also cause problems by creating a deterioration in water taste, creating an odour nuisance, and blocking pipes and filters (Adin & Alon, 1986; Litrico *et al.* 2011).

Authorities have responded to these issues by placing limits on water quantity and quality and are beginning to recognise the need to set regulations for other physical habitat characteristics. But increasing demand is being placed on authorities to allow water storage and abstraction to supply water to growing communities and economies. During the 20^{th} Century the human population increased fourfold, freshwater abstraction increased eightfold, and one large dam was constructed per day on average (World Commission on Dams, 2000; Richter *et al.* 2003). Planning or construction of at least a further 3,700 large dams is currently underway globally (Zarfl *et al.* 2015). Tensions between the societal need for water and the associated impact on freshwater ecosystems is therefore set to increase throughout the 21^{st} Century.

A large body of literature is available upon which to draw limits for measures such as nutrients, but limited research is available on hydrological limits. Hydrological limits involve the regulation of flows to produce a flow regime which sustains a healthy ecosystem. Where hydrological limits are implemented to achieve specific outcomes, such as periphyton reduction, the approach is known as objective-based flow setting (Acreman & Dunbar, 2004), which is the focus of this thesis.

Hydrological limits include minimum flows, flushing flows, and hydropeaking, which are collectively referred to as environmental flows. Hydrological limits are commonly set using rules-of-thumb, such as FRE_3 or the Montana Method (see Tennant, 1976; Clausen & Biggs, 1997), based on flow-ecology relationships identified from other sites. The issue with this conventional approach to identifying limits is it assumes stationarity in the system (Poff, 2017), and uniformity between sites. After reviewing 165 papers, covering four decades, Poff & Zimmerman (2010) concluded that the global literature is not suitable for identifying flow-ecology relationships, largely due to the variation in metrics used to describe both flow and ecology. This thesis adds to this argument by suggesting the effect of flow on ecology is over simplified and misses the effect of geomorphic processes, such as sediment transport, which alter benthic communities. Whilst these geomorphic processes are driven by flow, and therefore their effect on benthic communities can be related back to threshold flows for the geomorphic processes, the lack of attribution of geomorphic processes to ecological outcomes inhibits the transfer of thresholds to other sites, and is likely the reason rule-of-thumb approaches perform so poorly on a site-by-site basis. The use of FRE_3, the frequency of events exceeding three times the median flow, as an indicator of periphyton removal in New Zealand is a prime example of this. At a regional level FRE_3 is a predictor of periphyton removal on average across sites, but Hoyle *et al.* (2017) found periphyton removing flows ranged from 1.7 - 14.5 times the median flow at individual sites. Hoyle *et al.* (2017) found sediment entrainment models to be better predictors of periphyton accrual than hydrological metrics, and attributed the variation in flow thresholds for periphyton removal to the differences in sediment processes occurring at equivalent flows, and the different mechanism of periphyton removal at each site (hydraulic scour, abrasion by fines, or molar action by coarse particles). Acknowledging the need to set flows which target mechanisms to achieve objectives has recently been highlighted by Poff (2017) as a key step towards improving environmental flow science. It is therefore critical that management of benthic communities takes an holistic approach and considers the systems as a whole, combining ecologic, hydrologic, and geomorphic knowledge (Acreman & Dunbar, 2004; Poole, 2010).

In order for hydrological limits to be based on sediment transport thresholds accurate measurement or prediction of sediment entrainment and transport rates are required. Both measuring and predicting these thresholds has remained elusive, particularly for coarse particle transport; despite being an area of active research for over a century (Herschel, 1878; Shields, 1936; Einstein, 1937; White, 1940; Soar & Downs, 2017; Javernick *et al.* 2018; Rickenmann, 2018). This has also made it challenging to study the relationships between benthic communities and sediment processes, making it difficult to identify the sediment process thresholds required to achieve desired ecological outcomes. Improving the effectiveness of setting hydrological limits therefore requires new methods and models to measure and predict sediment process thresholds, both to study the relationship with ecology and to develop appropriate hydrological limits.

Aims and Objectives

This thesis focuses on developing tools to measure substrate structure and resistance, hydraulic entrainment thresholds for bedload entrainment, and to quantify bed mobility as these tasks remain challenging. The intention is to provide tools which can be used both to study the relationship between bedload transport and periphyton removal to identify bedload transport thresholds for the removal of periphyton by site and species, as well as to identify flow thresholds required to induce the magnitude and frequency of bedload transport needed to achieve periphyton removal at a specific site so effective hydrological limits can be set.

The objectives of the thesis are to:

i.) synthesise the vast geomorphic and hydraulic literature on measuring bedload transport and initiation thresholds to identify methodologies which may improve the measurement and modelling of bedload transport processes to relate to ecological outcomes, and to identify where new tools are required to address known knowledge gaps

ii.) improve quantification of the resistance of gravel beds for entrainment and transport model parameterisation by:

   a.) evaluating the suitability of emerging remote/proximal sensing approaches for quantifying the structural development of the surface layer to provide an assessment of bed stability, and provide parameters to improve the development of gravel entrainment and transport models

   b.) developing a method to quantify armour layer compactness

iii.) develop an objective approach for the rapid assessment of reach-scale bed stability

iv.) develop a methodology to improve the identification of site-specific bedload transport thresholds by recording bedload transport events and obtaining corresponding data suitable for identifying entrainment thresholds, to lead to improved entrainment models which could be used for objective-based hydrological limits setting to manage nuisance periphyton.

Thesis Organization

This thesis comprises a series of chapters, each written for publication as separate manuscripts in relevant journals, followed by a final synthesis and conclusions chapter. The structure of these manuscripts has been retained as they were submitted to the journals (i.e. journal specific constrictions such as word count and section structure), thus, there is some degree of repetition of material such as site descriptions, and some difference in notation between chapters. Where possible, formatting is made consistent between chapters to attain coherency of the thesis, such as the use of continual figure and table numbering, and a single combined bibliography. Each chapter also has an introduction and summary separate from the manuscript introduction and summary/conclusion which describe how the chapter fits the thesis, and summarises the chapter in the context of the thesis, respectively.

Chapter 1 introduces the limitations of the present method of hydrological limit setting in the context of flushing flows for periphyton management, identifies the relationship between periphyton removal and sediment transport processes, and makes a case for using bedload entrainment thresholds as a target for initiating phase 3 removal of periphyton (molar action). Chapter 1 then provides a synthesis of literature on bedload entrainment mechanisms and methods for measuring bedload entrainment and its thresholds, and identifies knowledge and methodology gaps which form the foundation of subsequent chapters. Chapter 1 is published as a paper in Environmental Management (Springer) as: Neverman, A. J., Fuller, I. C., Death, R. G., Singh, R., & Procter, J. N. (2018). Towards mechanistic hydrological limits: a literature synthesis to improve the study of direct linkages between sediment transport and periphyton accrual in gravel-bed rivers. Environmental Management. 62, 740-755. doi:10.1007/s00267-018-1070-1.

Chapter 2 provides a comparison of Structure-from-Motion photogrammetry (SfMp) and Terrestrial Laser Scanning (TLS) for quantifying surface layer structural development. Metrics derived from the elevation data of point clouds captured using TLS have been shown to relate to the development of the surface layer in some flume and field studies, but the cost of terrestrial laser scanners and the labour-intensive acquisition of grain-scale topographic data in the field using TLS have limited the uptake of this approach for river management. The relatively low cost of small Unmanned Aerial Systems (sUAS, also known as UAVs, RPAS, or drones) has led to wide use of SfMp in the geosciences in the past five years to generate topographic point clouds. The use of SfMp affords an opportunity to capture grain-scale topographic point clouds over large spatial extents relatively cheaply and rapidly. However, applying the same processing to SfMp point clouds as TLS point clouds to quantify surface structural development may be inappropriate as differences in the errors and biases of TLS and SfMp led to the creation of point clouds with differing characteristics and representation of the real surface. This means the metrics developed from TLS point clouds to quantify surface structure may produce different results when derived from SfMp point clouds. Chapter 2 addresses this issue by providing a comparison of metrics from both survey methods, and provides a discussion around which methods are better suited to quantifying surface structure in gravel beds. Chapter 2 has been accepted for publication and is in press in a special issue on Structure-from-Motion photogrammetry for river management in Progress in Physical Geography as: Neverman, A. J., Fuller, I. C., Procter, J. N., & Death, R. G. (In Press). Terrestrial Laser Scanning and Structure-from-Motion Photogrammetry concordance analysis for describing the surface layer of gravel beds. Progress in Physical Geography.

Chapter 3 develops a method for quantifying the compactness of the active layer in gravel beds. This was done as compactness is often cited as a critical component of bed resistance, but no methods are available for objectively quantifying compactness in the field beyond providing a means to compare the relative compactness of sites. Chapter 3 provides a method for measuring the resistive force of the active layer using a penetrometer, providing a quantification of compactness measured in Newtons. This provides a unit which is easily related to measures of entrainment forces such as shear stress. Chapter 3 therefore provides a tool for improving the quantification of bed resistance to entrainment, and provides a parameter for improved entrainment models. Chapter 3 is in preparation as a manuscript to Earth Surface Processes and Landforms as: Neverman, A. J., Fuller, I. C., & Death, R. G. (In Prep). A technique to rapidly quantify active layer compactness in gravel-bed streams.

Chapter 4 develops a method for the rapid assessment of substrate stability at the reach scale. Such methods have been popular in ecological research as they provide a rapid, low cost approach to measuring bed stability which does not require extensive expertise, allowing a large number of sites to be assessed and repeatedly monitored by a wide range of stakeholders. However, currently available methods are either subjective and their results are not transferrable between sites or observers, or they relate poorly to ecological communities. Chapter 4 develops a method which improves on previous approaches by using cheap, easy to use methods to quantify a range of geomorphic and hydraulic parameters which relate to intrinsic bed stability thresholds, and using a categorised visual assessment approach to reduce the user bias associated with visual assessment scoring for parameters where (cheap or rapid) objective measurement techniques were not available. Chapter 4 is in preparation as a manuscript to Freshwater Biology as: Neverman, A. J., Death, R. G., Fuller, I. C., & McAllister, T. G. (In Prep). A new rapid assessment technique for measuring bed stability in gravel substrates.

Chapter 5 addresses the challenge of recording incipient motion and associated thresholds in natural channels by developing an approach to install impact plate geophones coupled with a high-frequency velocity sensor in dynamic gravel beds. Chapter 5 makes a first attempt to relate changes in the bed seepage regime to the entrainment of coarse particles in a natural channel using differential piezometers to record continuous bed seepage data. This chapter is in review as a manuscript to Journal of Geophysical Research: Earth Surface as: Neverman, A.J., Fuller, I.C., Procter, J.N., Singh, R., & Death, R.G. (In Review). Implementation of a multi-sensor system to identify streamwise hydrodynamic and vertical bed seepage thresholds for particle entrainment in gravel-bed rivers.

Chapter 6 provides a synthesis of Chapters 1-5 in the context of using bed mobility thresholds to set hydrological limits, and identifies future research trajectories. Chapter 6 highlights the advancement to measuring bed mobility afforded by the methods developed in Chapters 2-5, particularly in regard to empirical quantification of entrainment thresholds in natural channels. Chapter 6 identifies a need to use the tools developed in Chapters 2-5 to study the relationship between periphyton accrual and bed mobility to identify critical bed mobility thresholds for limiting periphyton accrual before effective hydrological limits can be set.

Chapter 1

Towards Mechanistic Hydrological Limits: A Literature Synthesis to Improve the Study of Direct Linkages Between Sediment Transport and Periphyton Accrual in Gravel-Bed Rivers

Introduction of Chapter 1 to Thesis

Chapter 1 highlights the current limitations of setting flushing flow targets using flow-ecology relationships, and presents a case for moving towards mechanistic flow targets based on identifying thresholds to initiate the physical processes which scour periphyton. Whilst this chapter focuses specifically on flushing flows, the concept is applicable to the wider family of hydrological limits. Chapter 1 focuses on using gravel entrainment thresholds to identify the flows required to induce molar action as a mechanism to remove periphyton. Our limited ability to accurately model entrainment thresholds is highlighted and a need to improve our ability to measure the various parameters which condition entrainment thresholds is identified. Chapter 1 provides a literature synthesis of methods to measure bedload transport and incipient motion, hydrodynamic entrainment forces, and substrate characteristics with a focus on measurement in natural channels. Limitations of various methods are outlined and gaps in our ability to measure some parameters due to a lack of appropriate methods being available are identified. The identified gaps provide the basis for developing the methods in subsequent chapters.

This chapter has been published in Environmental Management (Springer) as:

Neverman, A. J., Fuller, I. C., Death, R. G., Singh, R., & Procter, J. N. (2018). Towards mechanistic hydrological limits: a literature synthesis to improve the study of direct linkages between sediment transport and periphyton accrual in gravel-bed rivers. Environmental Management. 62, 740-755. doi : 10.1007/s00267-018-1070-1

1.1 Abstract

Altered hydrological, sediment, and nutrient regimes can lead to dramatic increases in periphyton abundance in rivers below impoundments. Flushing flows are a commonly adopted strategy to manage the excess periphyton that can accumulate, but in practice they often prove ineffective. Designing hydrological regimes that include flushing flows may be overlooking key processes in periphyton removal, particularly the role of abrasion and molar action induced by substrate movement. Setting flow targets which aim to initiate substrate movement are likely to improve periphyton removal, but an understanding of the site-specific thresholds for substrate entrainment and periphyton removal is required. Despite decades of entrainment studies accurate and consistent measurement and prediction of substrate entrainment remains elusive, making it challenging to study the relationship between substrate movement and periphyton removal, and to set flow targets. This paper makes a case for using substrate entrainment and transport thresholds as the target metric for flushing flows to manage excess periphyton accrual. This paper critically reviews the determinants of periphyton accrual and associated management methods. This paper also aims to provide a reference for interdisciplinary research on periphyton removal by summarising the geomorphic and hydraulic literature on methods for estimating and measuring substrate entrainment and transport. This will provide a basis for ecologists to identify tools for quantifying entrainment and transport thresholds so they are better placed to explore the direct linkages between phases of sediment transport and periphyton accrual. These linkages need to be identified in order for river managers to set effective flushing flow targets.

1.2 Introduction

During the 20th Century an average of one large dam was constructed per day to provide water for irrigation, power generation, domestic and industrial use, or flood control (World Commission on Dams, 2000). Construction of dams to store and extract surface waters has become one of the major issues of water management in the 21st century (Poff *et al.* 2007, 2015). At least 3,700 large dams are currently under construction or being planned around the world (Zarfl *et al.* 2015). Dams can dramatically alter river ecology by interrupting species migration pathways, altering the physical and chemical habitat of a river and/or changing the hydrological and geomorphological regime (Graf, 2006; Poff *et al.* 2007). These changes often result in dramatic increases in periphyton biomass that in-turn alter the species composition and food web downstream of many dams (Davie & Mitrovic, 2014). Periphyton is the term for a range of benthic organisms, including filamentous algae, bacteria, fungi, cyanobacteria, and diatoms. Altered flow conditions, increased nutrient levels and temperatures, and decreased substrate movement are often postulated to drive excess periphyton accrual (Biggs, 1985, 1990; McAllister *et al.* 2016). Excess periphyton accrual leads to fish and invertebrate kills from oxygen depletion, degraded ecological health, altered sediment dynamics, deterioration in water taste, odour nuisance, fluctuations in dissolved oxygen, and blockages of irrigation takes and water filtration systems (Adin & Alon, 1986; Biggs, 1990; Lozano *et al.* 2010; Litrico *et al.* 2011; Fovet *et al.* 2012). In recent decades, reports of toxic periphyton proliferations have increased and are linked with health problems in humans including asthma, skin rashes, liver damage, and the death of domestic dogs (Baker *et al.* 2001; Wood *et al.* 2007; McAllister *et al.* 2016). The causes, impacts, and mitigation methods for excess periphyton accrual are summarised in Figure 1.1. Hydrological limits (which includes environmental flows, flushing flows, pulsed flows, and minimum flows) are commonly used

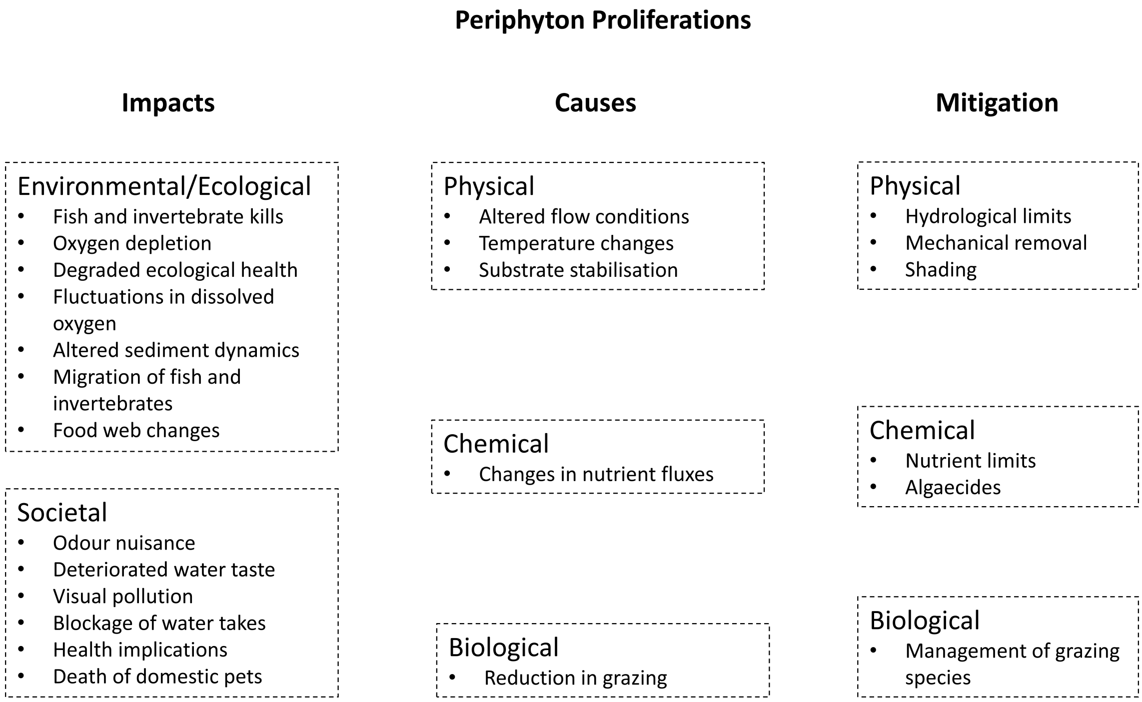

Figure 1.1: Impacts, causes, and mitigation methods for periphyton proliferations.

to manage periphyton accrual, but the physical processes which remove periphyton are often overlooked in the design phase (Figure 1.2). Instead, hydrological indices are linked directly to ecological outcomes (de Jalón *et al.* 2017; James *et al.* 2017), often leading to large discrepancies in the effectiveness of hydrological limits.

This paper discusses the need for hydrological regimes to be designed with the aim of controlling site-specific physical processes that link directly with periphyton accrual. The paper focuses on the role of sediment transport as a key physical process for limiting periphyton accrual and builds a case for the need to set hydrological limits based on coarse sediment entrainment thresholds. Managing sediment supply is beyond the scope of this paper, which instead focuses on local sediment mobilisation. A brief review of the knowledge gaps in predicting entrainment thresholds is presented, followed by a discussion of what techniques have recently become available to fill these gaps. This paper aims to summarise the vast literature on predicting and measuring entrainment thresholds and bedload transport in the fluvial geomorphology and hydraulics literature to form a basis for ecologists and interdisciplinary researchers to develop programmes to better understand the relationship between sediment movement and periphyton removal so effective flushing flows can be developed.

1.3 Managing Periphyton Removal with Physical Process Targets

Managing the hydrological regime to initiate substrate entrainment offers managers a tool for regulating periphyton accrual, and may be used to supplement other management strategies in Figure 1.1. However, the approach to identifying effective flows for periphyton removal needs revising. A review of 165 papers by Poff & Zimmerman (2010) suggested global literature is not suitable for drawing clear statistical relationships between ecological responses and flow alteration as the metrics used to describe flow alteration and ecological responses vary significantly, inhibiting quantitative comparison. Poff & Zimmerman (2010) also conclude that the current body of literature lacks enough information to examine species-specific responses to flow alteration, or to categorise flow regimes by geographic setting. Being able to calculate site specific thresholds for periphyton removal is critical as suboptimal flows may lead to increased periphyton accrual despite lower flows leading to removal at other sites (Table 1.1).

In New Zealand the frequency of high flow events exceeding 3 times the median flow, known as FRE_3, has been identified as a predictor of periphyton abundance in streams (Clausen & Biggs, 1997), and has consequently been used as a rule-of-thumb for defining periphyton-removing flows (e.g. Booker, 2013; Lessard *et al.* 2013; McAllister *et al.* 2016). However, subsequent work by some of these authors have found a weaker linkage between FRE_3 and measures of periphyton biomass (e.g. Snelder *et al.* 2014). Whilst rules-of-thumb may predict regional average flows required to achieve a particular periphyton biomass, they fail to account for the site-specific processes of periphyton removal, which will vary between sites (Biggs *et al.* 1999; Hoyle *et al.* 2017). A recent study by Hoyle *et al.* (2017) found flows ranging from 1.7 - 14.5 times the median flow were required to remove periphyton, and linked the variation in thresholds to different mechanisms of removal operating at each site. Periphyton removal may result from one or multiple mechanisms: scour, abrasion, and molar action (Tsujimoto & Tashiro, 2004; Francoeur & Biggs, 2006). Scour relates to the removal of periphyton by hydraulic forces such as excess shear stress or drag, and can occur at shear stresses lower than those required to mobilise sand (Hoyle *et al.* 2017). Abrasion refers to the detachment of periphyton by sediment in transport. Some authors have referred to abrasion as resulting from suspended sediment (e.g. Francoeur & Biggs, 2006), but strictly speaking by definition suspended load does not come in to contact with the bed during transport, and therefore periphyton attached to the bed. In this sense we refer to abrasion as occurring from overpassing bedload contacting periphyton attached to a static bed, resulting in detachment. It is likely previous works have referred to abrasion as resulting from suspended sediments as they were really referring to the transport of fine

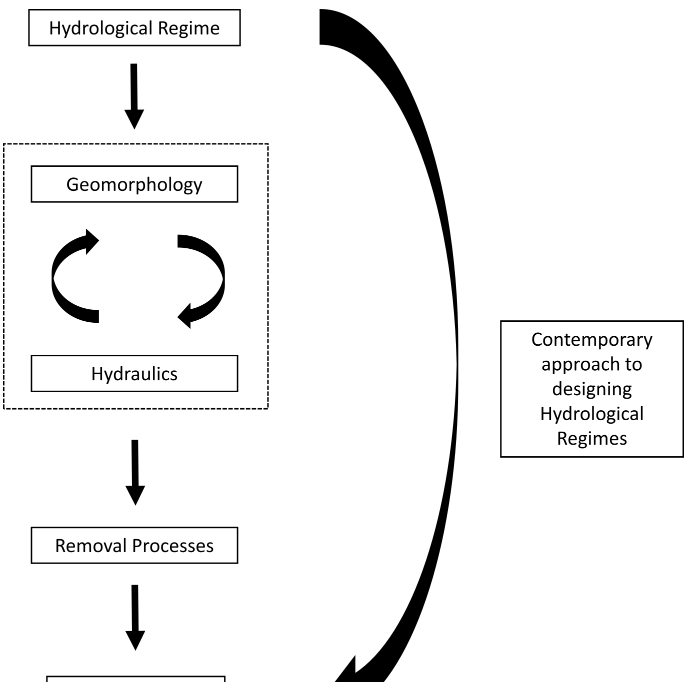

Figure 1.2: Conceptual model of the approach needed to design effective hydrological regimes vs. the approach used in many contemporary methods. Adapted from de Jalón *et al.* (2017).

material. Abrasion requires shear stresses high enough to transport sediment, either from upstream or to entrain fine sediment from the bed, but not high enough to mobilise the bed sediments upon which the periphyton is attached. Molar action requires mobilisation of the bed sediments upon which periphyton is attached, which requires higher shear stresses than abrasion (assuming non-equal mobility).

Given these processes of removal occur on a continuum of shear stresses, we propose periphyton removal occurs in phases; phase 1: only hydraulic force mechanisms active, phase 2: abrasion becomes active, and phase 3: molar action becomes active. At each phase, mechanisms active during the previous phase may also be active. The boundaries between these phases relate to phases of bedload transport. Phase 1 periphyton removal occurs prior to bedload transport. Phase 2 periphyton removal relates to the first phase of bedload transport, overpassing, where fine sediment is transported over a static, stable armoured bed (Jackson & Beschta, 1982), and includes size-selective entrainment of finer particles (i.e. no disruption of armour layer particles), but uncertainty exists regarding the key grain size for abrasion (Hoyle *et al.* 2017). Phase 3 periphyton removal relates to the second phase of bedload transport where shear stresses are capable of disrupting the armour layer and the substrate becomes mobile (Jackson & Beschta, 1982). This relates to processes of size-selective transport (of larger particles with periphyton attached), general mobility, and fully mobile conditions depending on the structure of the bed and the effect of protrusion and hiding on the condition of equal mobility (see Ashworth & Ferguson, 1989).

Differences in the sediment transport processes occurring at equivalent flows is therefore likely to be one of the major factors leading to the mixed success of hydrological indices as determinants of periphyton accrual (Biggs *et al.* 1999). Variation in how these processes affect different species of periphyton is also critical, and differing community compositions between sites will further exacerbate inter-site variability. Hoyle *et al.* (2017) found 1D hydraulic models which estimated sediment mobility thresholds had a higher predictive power of periphyton removal than FRE_3. In a study of hydrological limit effectiveness on the Opihi-Opuha River system Lessard *et al.* (2013) found flushing flows were not effective at controlling nuisance periphyton which dominated post construction of the Opuha Dam. Lessard *et al.* (2013) attribute the lower periphyton biomass at a study control site to the active abrasion and scour processes which were no longer operating in the reaches below the dam, despite the implemented flushing flows.

The key to improving the effectiveness of flushing flows may therefore lie in managing for the site-specific physical processes which scour periphyton. It is therefore critical that hydrological limits be translated into specific physical objectives for which flow targets can be set (Kondolf & Wilcock, 1996). The three phases of removal outlined above are directly linked to different physical processes and therefore provide a basis for establishing a physical objectives approach. As these phases are directly linked to different phases of sediment transport, sediment entrainment and transport models may provide a better tool for river managers to calculate the flows required for periphyton removal. However, the models used currently provide limited reliability for predicting entrainment and transport. Further research is also required to understand species-specific resilience to each of the phases of removal, but this requires accurate data on entrainment and transport upon which relationships can be drawn.

Early sediment entrainment literature used deterministic models which focused on identifying a critical velocity or discharge for entrainment (e.g. Carling, 1983; Komar, 1987). This was followed by a body of research which emphasised the limitations of this approach and stressed the stochastic nature of bedload transport and spatial variability of entrainment forces (Wilcock *et al.* 1996; Milan *et al.* 2001). This stochastic nature is attributed to spatial and temporal variability in the range of complex geomorphic and hydrodynamic controls on entrainment thresholds such as grain size distribution, surface armouring, and velocity fluxes. This leads to variability in erosion and deposition processes at different scales, so it is important to consider scale when assessing substrate stability thresholds.

At a given moment, discrete zones of differing mobility may occur within a reach due to localised variations in shear stress, absolute grain size, and grain size distribution (Lisle *et al.* 2000), with some sections of the bed mobile whilst the majority of the bed may be immobile. Threshold adjustment may lead to stabilisation of these patches, leading to temporal variations in stability (Lisle *et al.* 2000). This also leads to spatial and temporal variations in the phase of periphyton removal.

Bedload transport is also dependant on the degree of sediment supply, depending on the spatial and temporal scale of observations (Wilcock & Southard, 1989), which, along with variations in entrainment forces, conditions whether a channel is supply- or transport-limited. Sediment supply influences the mobility of patches, with sediment-rich channels being shown to have greater frequency of fully mobile areas, whilst sediment-limited channels have more zones of partial transport (Lisle *et al.* 2000; Venditti *et al.* 2010). Variations in sediment supply alter the coarseness of the bed surface, with reduction in sediment supply leading to coarsening of the bed surface (Dietrich *et al.* 1989; Lisle *et al.* 1993). Sediment supply also varies spatially, with the upper reaches of channels often being supply-limited (Kammerlander *et al.* 2017). Sediment supply conditions may therefore be a determining factor in which phase of periphyton removal is most dominant at a site, and how this varies longitudinally.

Stream morphology also influences the distribution of distinct zones of differing mobility by conditioning hydrodynamics, and creating a feedback loop with erosion and deposition processes leading to alterations in channel morphology. In alternate bar channels, Lisle *et al.* (1993) and Lisle *et al.* (2000) noted zones of bedload transport were controlled by bar morphology which produced a lane of continuous transport, but the lane coarsened and bed mobility reduced under decreasing sediment supply with near constant boundary shear stress. At channel meanders, cross-sectional velocity distributions alter zones of mobility. Braided channels exhibit distinct zones of highly variable mobility, such as in chutes and pools, and less propensity to reach threshold adjustment, leading to rapid evolution of the bed at the reach scale (Ashmore & Parker, 1983; Ashworth & Ferguson, 1986; Ashworth *et al.* 1992). Alternatively, step-pool channels have relatively stable planform, but may have high mobility in the pools.

It is therefore critical that the scale-dependence of bedload transport be considered when assessing bed stability, and bedload models are applied at appropriate scales to manage hydrological limits and periphyton biomass.

Despite the development in our understanding of the complexity of inputs required for accurate entrainment models, researchers and managers rely on the outputs of simplified entrainment models well beyond the known limits of their assumptions (Lorang & Hauer, 2003). The use of hydrologic metrics such as FRE_3 for flushing flows is a clear example of this. Lorang & Hauer (2003) attribute the reliance on these flawed simple models to difficulty in finding alternatives because of differences in terminology and notation, and difficulty finding them in the literature. Hoyle *et al.* (2017) also note the need for models to deal with all aspects of site-specific hydraulic and geomorphic characteristics.

Whilst the above text has highlighted the potential benefit substrate entrainment equations may have for determining flow requirements to manage periphyton accrual, these need to be assessed specifically for each site's geomorphic and hydrodynamic conditions. This requires more advanced models capable of including 4-Dimensional hydrodynamics, which are missed in conventional, often flume-derived, equations. Parameters which adequately describe substrate structure are also critical. The use of such models requires managers to be able to obtain adequate input data. Managers therefore need a range of methodologies, outlined below, which can supply the required data. Development of such models also needs to consider what data can be obtained, and how. Subsequent sections in this paper identify the geomorphic and hydrodynamic processes which control substrate entrainment, and available or emerging methods to quantify these controls at appropriate spatial and temporal scales.

Velocity ($\mathbf{m\,s^{-1}}$)	**Change in Periphyton**	**Paper**
< 0.5	Increase	Horner & Welch (1981)
> 0.5	Decrease	”
> 0.6	Decrease	Horner *et al.* (1990)
0.2 - 0.58	Decrease	Biggs & Gerbeaux (1993)
0.6 - 0.9	Decrease	Jowett & Biggs (1997)
< 0.6	Increase	”
< 0.3	Increase	”
0.18 - 0.2	Increase	Biggs *et al.* (1998)
> 0.2	Decrease	”
0.05 - 0.95	Decrease	Bourassa & Cattaneo (1998)
0.025 - 0.055	Increase	Townsend & Padovan (2005)
0.3 - 1.0	Decrease	Ryder *et al.* (2006)
1	Decrease/ Increase	Watts *et al.* (2006)
> 0.2	Decrease/Increase	Flinders & Hart (2009)
> 1.5	Decrease/Increase	”
0.9	Increase	Davie & Mitrovic (2014)

Table 1.1: Changes in periphyton biomass under different velocities. Adapted from Davie & Mitrovic (2014).

1.4 Entrainment Mechanisms and Thresholds

Identifying the boundary between abrasion and molar action will be a critical step for understanding periphyton removal dynamics and determining flow targets. The boundary between these phases is marked by the onset of incipient motion for gravel particles, which is determined by their entrainment thresholds. Substrate entrainment thresholds are notoriously difficult to determine, and the numerous formulae proposed in the literature are a testament to this difficulty. Fluvial geomorphologists have primarily been interested in determining the dimensionless critical shear stress for the median grain size to identify incipient motion thresholds. Flume-derived formulae for shear stress dominate the literature (Ergenzinger & De Jong, 2003) as the spatial variability of natural fluvial systems makes model development using field data challenging due to a lack of control (Miller *et al.* 1977). Many of these formulae are derivatives of Shields (1936) parameter (Buffington & Montgomery, 1997), and are capable of predicting incipient motion of substrate in flumes (within an envelope, see Miller *et al.* 1977), but do not work well in natural channels with observed entrainment often varying significantly from predicted.

Systematic methodological biases contribute to the variation in determining the critical shear stress for a given particle size. Buffington & Montgomery (1997) demonstrate that variations in the definition of shear stress and particle motion are major contributing factors to this systematic bias, along with variation in the methods used to measure various model parameters. Definitions of motion are often qualitative such as individual initial motion, several grains moving, weak, medium, or general (Kramer, 1935; Alfadhli

& Yang, 2014). A two-fold difference in critical shear stress values is observed between the three definitions of motion used by Kramer (1935) (Buffington & Montgomery, 1997). Magnitude differences are also seen between theoretically-based estimates which often estimate incipient motion of a single grain, versus reference-based estimates which relate to movement of mixed gravels (Buffington & Montgomery, 1997). It is therefore critical to differentiate between these definitions when developing and reporting on field studies. Critical shear stress for identifying incipient motion will be needed to understand the boundary between phase 2 and phase 3 removal to identify which phase is required to remove periphyton. Where phase 3 is required, flushing flows will need to produce bedload transport, although the magnitude of transport required is unclear at present, but likely varies between sites and periphyton species. Given a need for bedload transport to be occurring, flushing flows need to exceed the threshold for individual grain incipient motion, and will need to be based on reference thresholds which describe mobility of the entire bedload distribution and correlate to a dimensionless transport rate (Parker *et al.* 1982; Buffington & Montgomery, 1997; Mueller *et al.* 2005). Competency-based methods only describe mobility of the coarsest bedload material which may have lower thresholds due to protrusion and lower intergranular friction angles (Buffington *et al.* 1992; Buffington & Montgomery, 1997), and therefore do not give a true indication of transport rate which is likely more relevant to benthic communities.

To improve the effectiveness of flushing flows by inducing molar action improved bedload transport models are required to accurately define target flows. These models should be developed using empirical data derived from natural channels, which needs to include data on hydrological connectivity and substrate characteristics, and should aim to relate to bedload transport rates. This requires multivariate data for a range of hydrodynamic and sedimentological parameters. This section outlines the variables which have been identified in the literature as mechanisms of substrate entrainment and should be included as variables in future field-based experiments to model substrate entrainment and transport thresholds.

1.4.1 Mechanisms of Entrainment

Particle entrainment is the result of the forces applied to the substrate by hydrodynamic processes exceeding the resistance of the substrate to movement. Entrainment models therefore require components that equate hydrodynamic forces with resistance forces (Andrews, 1983), and these models need to handle spatio-temporal variation. This section outlines various entrainment processes and substrate characteristics identified in the literature as affecting entrainment.

1.4.1.1 Hydraulic entrainment forces

There are a range of hydrodynamic processes which effect substrate entrainment (Shields, 1936; Einstein & El-Samni, 1949; Reid & Frostick, 1986; Smart & Habersack, 2007; Smart *et al.* 2010), and detailed measurement of hydrodynamics can elucidate entrainment mechanisms (Yager *et al.* 2015). However, investigating the relationship between time-averaged streamwise velocity or critical discharge and entrainment has dominated the research in field-based studies (Carling, 1983; Ferguson, 1994; Wilcock *et al.* 1996) to overcome the challenges of quantifying flow heterogeneity. Flows in the near-bed region, where substrate is entrained, are complex, with flow moving in the downstream, cross stream, and vertical directions, and instantaneous velocities fluctuating in all directions at high temporal rates, resulting in what is collectively known as turbulence, which has been challenging to quantify in the field, yet may be critical to understanding entrainment mechanisms.

Turbulence is an important mechanism of particle entrainment (Zanke, 2003; Vollmer & Kleinhans, 2007; Paiement-Paradis *et al.* 2011; Smith & Yager, 2012; Radice *et al.* 2013; Yager *et al.* 2015). Smart *et al.* (2010) and Jaeger & Smart (2012) have shown turbulence alone can induce substrate movement when the instantaneous fluctuations increase. As velocity fluctuations increase, time-averaged velocities are also likely to increase. Time-averaged measurements may therefore have been acting as a proxy for turbulence. As the relationship between turbulence magnitude and time-averaged velocity is not linear, this may explain, partly, why there are so many variations in critical velocities for entrainment.

Pressure fluctuations resulting from turbulence may also create entrainment forces (Papanicolaou *et al.* 2002; Wu & Chou, 2003; Zanke, 2003; Smith & Yager, 2012). Such pressure fluctuations also occur in natural channels in the near-bed region due to the difference between pressure in the bed and at the water-sediment interface, and as advecting pressure fluctuations in the form of eddies and vortices. The combination of pressure variations around the surface grains and passing eddy cells and vortex streets is capable of entraining clasts (Smart & Habersack, 2007; Smart *et al.* 2010; Jaeger & Smart, 2012).

Turbulence and near-bed velocities are also affected by seepage (Chen & Chiew, 2004; Dey & Nath, 2009; Patel *et al.* 2017). Seepage also alters the relative submerged weight of individual particles (Lu *et al.* 2008), altering their critical entrainment thresholds. Lu *et al.* (2008) suggest that seepage has the greatest impact on particle stability as it alters the equilibrium of resistance and entrainment forces by affecting both hydrodynamics and bed structure (Patel *et al.* 2017). Francalanci *et al.* (2008) suggest it is the lack of consideration of the 3-Dimensionality of flows, such as seepage direction, which leads to the poor predictive power of Shields equation in natural channels. Shields equation assumes hydrostatic pressure, which does not occur in natural alluvial beds.

Whilst it is important to identify entrainment thresholds for individual grains to recognise entrainment mechanisms and thresholds for modelling and identify the boundary between abrasion and molar action phases, it is important to note that time-averaged velocities are strongly influenced by local bed conditions (Nikora *et al.* 2001). Accordingly, time-averaged velocity measures are more suited to identifying thresholds for highly localised grain movement (i.e. individual grains) than for transport rates. There is a growing body of literature supporting the use of double-averaging of hydrodynamics for the study of spatially and temporally heterogenous flows in mobile beds (Pokrajac *et al.* 2008). Double-averaging involves a two-step process of averaging the Navier-Stokes equation in time (i.e. Reynold-averaging) and space (volume- or area-averaging) (Pokrajac *et al.* 2008; Nikora *et al.* 2013). Double-averaging has mainly been applied in fixed bed flumes to date (Nikora *et al.* 2013). Obtaining spatio-temporal velocity data in the field remains challenging, particularly in the near bed region, making double-averaging of natural open channel flows even more challenging. However, double-averaging offers significant potential for modelling entrainment spatially in the field, as it provides flow parameters that can be related to roughness parameters obtained from the same spatial domain, potentially offering a powerful tool when combined with spatially varied roughness maps of the bed surface (e.g. Entwistle & Fuller, 2009; Milan, 2009). As such double-averaging may be suited to studies of bedload rates and reference shear stress, or for differentiating habitat patches hydraulically. However, double-averaging may mask the actual mechanism of entrainment at a site, as double-averaging aims to simplify flow fluctuations, yet it is these fluctuations which entrain the particles. Understanding the mechanisms of entrainment is critical to understanding how management practises will affect substrate movement dynamics and predicting the associated impact on periphyton accrual. The use of flow metrics therefore needs to be carefully selected to match the aims of the research or management objectives.

1.4.1.2 Substrate resistance

The ability of hydrodynamic processes to entrain substrate is determined by the resistance of the bed to the hydrodynamic forces. Entrainment thresholds are conditioned by several characteristics of substrate surfaces, including: grain protrusion (Fenton & Abbott, 1977); bed packing (Papanicolaou *et al.* 2002); grain size and placement (Downes *et al.* 1998); and bedform clusters (Church *et al.* 1998; Wittenberg & Newson, 2005; Papanicolaou *et al.* 2012). Whilst many entrainment equations rely on quantifying clast size to determine resistance thresholds, very few consider how the arrangement of surrounding grains affects these thresholds. This is largely due to a lack of methodologies being available to quantify the arrangement of substrate at suitable spatial scales. Establishing such methods is critical if resistance thresholds are to be accurately quantified.

Quantifying substrate arrangement is also critical to understanding local hydrodynamics, and therefore predicting entrainment forces. A complex feedback loop exists between hydrodynamics and substrate fabric. For example, turbulent kinetic energy can be increased twofold by the introduction of flow perturbations from bedform clusters (Lacey & Roy, 2007). Clusters and other bedforms may be created by local hydrodynamic conditions such as the presence of seepage (Patel *et al.* 2017). Clusters contribute to the high spatial variability in boundary shear stress and the associated size selective transport observed in natural channels (Lisle & Madej, 1992). The resulting non-uniformity in sediment transport causes local variations in armouring of the surface substrate (Lisle & Madej, 1992; Church *et al.* 1998; Powell, 1998), exacerbating the stochastic nature of entrainment. Micro-topography of the substrate surface should therefore be accounted for in bedload transport equations (Billi, 1988).

1.5 Measurement of Entrainment and Resistance Forces

To date research on the incipient motion of substrate has largely been inhibited by an inability to accurately quantify relevant hydrodynamic processes and substrate characteristics at the appropriate scale. New field-based techniques are essential to quantify these variables in natural channels to accurately identify incipient motion thresholds, and to provide data to develop and validate models of incipient motion thresholds and bedload transport rates (Ergenzinger & De Jong, 2003). The past decade has seen a range of technologies with high spatial and temporal resolution become more widely available which may overcome many previous difficulties. This section discusses methodologies which may be used to quantify the geomorphic and hydrodynamic variables which have been identified as key controls and drivers of entrainment and transport rates in the previous section.

1.5.1 Assessment of Resistance

1.5.1.1 Grain size distribution

Individual grain density is a major component of entrainment thresholds. One of the major limitations in quantifying grain size is the logistical constraints on measuring grains over large spatial extents at suitably high resolutions to understand spatial variations in substrate characteristics. Common methods for quantifying grain density typically measure grain axis lengths from a sample of surface grains over a geomorphic unit or reach scale using manual sampling procedures which have significant limitations (Wolman, 1954; Bunte & Abt, 2003; Green, 2003). A representative grain metric is then derived from the samples, commonly the D_{50} or D_{84}, to represent grain size over the survey area. Known densities for the dominant clast lithology are then used to calculate resistance thresholds for the representative clast fraction. Such approaches do not capture the spatial variability in grain size over the geomorphic unit or reach scale.

Recent developments in remote sensing approaches may offer an improvement over manual sampling, allowing *in situ* measurement of individual grains over large extents. 3D point clouds derived using techniques such as Terrestrial Laser Scanning (TLS) or Structure-from-Motion photogrammetry (SfM) surveys are capable of grain scale topographic measurements, and can cover large spatial extents, with registration errors as low as 6 mm (Lague *et al.* 2013). Point clouds have been used to estimate grain-size, either by using relationships between the surface roughness and empirically derived grain size data (Pearson *et al.* 2017; Vázquez-Tarrío *et al.* 2017), or through the use of edge detection algorithms for point clouds (Measures & Tait, 2008). The former is well established in the geomorphic literature (Heritage & Milan, 2009; Westoby *et al.* 2015; Bertin & Friedrich, 2016; Pearson *et al.* 2017; Woodget & Austrums, 2017).Vázquez-Tarrío *et al.* (2017) found almost a 1:1 ratio of fit between point cloud roughness and Wolman derived grain size distributions (GSDs). However, this method may better determine the c-axis length of grains rather than their b-axis and is only suited to well-sorted substrates (Heritage & Milan, 2009; Pearson *et al.* 2017). It may therefore be challenging to adapt this technique to use with entrainment models which often rely on b-axis measurements.

Use of 3D point clouds has largely been limited to subaerial gravel surfaces due to challenges in obtaining subaqueous surface measurements. Studies have been carried out using SfM to conduct subaqueous surveys (Woodget *et al.* 2015; Dietrich, 2016), but this largely requires shallow flows with low turbidity and flat surfaces. Bathymetric LiDAR and bathymetric aDcp are also capable of subaqueous topographic surveying, but require advancements to increase spatial resolution to provide grain-scale analysis (Milan & Heritage, 2012).

Optical granulometry techniques offer another approach to determining the length of clast axes. These approaches complement the point cloud approach as optical granulometry is suited to the measurement of clast a- and b-axes.

Optical granulometry techniques can be broadly classified as statistical correlation or object-based image analysis (OBIA) approaches (Carbonnneau *et al.* 2018; Woodget *et al.* 2018). Statistical correlation approaches aim to correlate properties of image patches with grain size statistics using methods such as image texture mapping (Verdú *et al.* 2005; Dugdale *et al.* 2010). OBIA approaches include visual clast identification in terrestrial photographs, termed photo-sieving (Adams, 1979; Ibbeken & Schleyer, 1986), and automated clast boundary identification from terrestrial or aerial images (Graham *et al.* 2005a; Graham *et al.* 2005b). OBIA techniques have the advantage of being able to sample the entire substrate surface without the need for empirical datasets for calibration (for a review see Dugdale *et al.* 2010). Westoby *et al.* (2015) found digital grain analysis to be accurate to within <2 mm of dry-sieving control samples.

Increasing availability of small Unmanned Aerial Systems (sUAS) to rapidly obtain high resolution image sets over large spatial extents is increasing interest in optical granulometry techniques, but have fundamental issues regarding constraint of image scale and blurring in images (Carbonnneau *et al.* 2018). Carbonneau & Dietrich (2017) found the image scaling issue could be overcome using direct georeferencing, with errors ranging from 0.2-4%. Carbonnneau *et al.* (2018) have recently presented a proof-of-concept for robotic photo-sieving which further overcomes these limitations by using an SfM photogrammetry workflow to directly georeference aerial images obtained with an sUAS, removing the need for ground validation.

Tamminga *et al.* (2015) found strong empirical relationships (r^2= 0.82) between sUAS orthomosaic image texture and manual photo-sieving of close range images, although

Woodget & Austrums (2017) failed to recreate these relationships. Woodget & Austrums (2017) suggest their poor results, along with those of de Haas *et al.* (2014), relate to image blur created by sUAS platform vibrations not being adequately removed by the camera gimbal. Woodget *et al.* (2018) demonstrate the improvement of particle measurement provided by using 3-axis camera gimbal stabilisation, reducing the second limitation of sUAS imagery highlighted by Carbonnneau *et al.* (2018).

Advances in optical granulometry therefore offer an advantage over traditional manual sampling for grain size determination as they allow large spatial areas to be covered relatively quickly using sUAS surveys, effectively bridging the gap between high resolution and large spatial extent which has often been a trade-off. The high accuracy these techniques are capable of (Westoby *et al.* 2015) along with increasing ability to capture higher resolution data offers researchers the potential to differentiate sand from gravel in an automated way (Carbonnneau *et al.* 2018). Optical granulometry using sUAS offers potential for ecologists to describe gravel substrate and relate substrate characteristics to processes of periphyton removal to better understand scouring mechanisms specific to various species: a critical step towards better management of periphyton accrual.

1.5.1.2 Substrate structure

As outlined, a complex feedback loop exists between local bed structure and near-bed hydrodynamics. Surface roughness plays a major role in altering near-bed hydrodynamics. Surface roughness also alters the exposure of clasts to entrainment forces. Surface roughness is the product of the individual grains protruding from the mean bed surface, and from bed formations such as clusters. This often leads to larger grains being more exposed to entrainment forces and smaller clasts being shielded from entrainment forces (Fenton & Abbott, 1977). This can mean the relationship between predicted and actual onset of motion breaks down. Protruding grains and bedforms also alter near-bed hydrodynamics, effecting velocity, turbulent kinetic energy, and shear stress (Lisle & Madej, 1992; Lacey & Roy, 2007).

The effect of bed roughness on entrainment thresholds and hydrodynamics is well established with several conventional approaches to quantify it, ranging from subjective indices, to empirical quantification using characteristic grain sizes (Fuller *et al.* 2003b; Neverman *et al.* 2016). The main limitation with these approaches is they are often applied at the reach scale. Direct sampling approaches also usually require removal of clasts for measurement. To improve estimates of entrainment thresholds and transport rates there is a need to quantify surface roughness at the grain to patch scale *in situ* (e.g. Entwistle & Fuller, 2009; Milan, 2009). Surface roughness can be quantified from point clouds using the statistical properties of the point elevations, such as the standard deviation (e.g. Brasington *et al.* 2012; Brodu & Lague, 2012; Lague *et al.* 2013; Bertin *et al.* 2017; Pearson *et al.* 2017). This approach is well established in the geosciences, but is often limited to subaerial gravel surfaces due to the limitations of many sensors. Subaqueous topographic surveying using acoustic Doppler current profilers (aDcp) (Milan & Heritage, 2012; Williams *et al.* 2013) or optical bathymetric mapping (Williams *et al.* 2014; Woodget *et al.* 2015) techniques are beginning to emerge for grain-scale mapping, but are not widely used to date beyond proof-of-concept.

Point clouds and digital terrain models (DTMs) have also been used to quantify surface armouring (Aberle & Nikora, 2006; Bertin & Friedrich, 2018), imbrication (Millane *et al.* 2006; Bertin & Friedrich, 2016; Bertin *et al.* 2017), and grain exposure (Hodge *et al.* 2013), but these metrics have received significantly less attention and present a fruitful avenue for future research. Papanicolaou *et al.* (2012) have demonstrated the use of manual image analysis techniques to quantify bedform clusters. Clustering metrics, such as surface percentage composed of clusters (Piedra *et al.* 2012), or types of cluster present, could be developed using such techniques for use in the field.

It is clear that remote sensing approaches offer a step-change in the way substrate characteristics are quantified for substrate and entrainment modelling, and offer powerful tools for studying the relationship between periphyton dynamics and geomorphic processes.

1.5.1.3 Bed compaction

Bed compaction has a significant effect on entrainment thresholds (Carling, 1983), but has been poorly studied. Aberle & Nikora (2006) demonstrated a technique to assess gravel-bed armouring using the skewness of point-cloud elevations. Bed armouring has also been measured using a penetrometer in a few studies (Sear, 1992; Sear, 1995; Milan *et al.* 2001). However, there is no consistent approach to how a penetrometer can be used to quantify armour layer development, and often this method is used in a more qualitative fashion. Both approaches show promise for quantifying armouring, but more rigorous testing and standardising is required if they are to be widely adopted to further geomorphic and ecological understanding.

1.5.2 Measurement of Entrainment Forces

1.5.2.1 Near-bed hydraulics

Surrogate methods for measuring bedload transport, such as impact plates, hydrophones, and magnetometers, have been found to be suitable for detecting the onset of motion. Datasets on hydrodynamic metrics with corresponding resolution to such bedload transport datasets are required to identify mechanisms of incipient motion to allow quantification of entrainment thresholds. Near-bed velocity and turbulence are key catalysts for substrate entrainment, but it is unclear which characteristic of velocity induces entrainment, and which mechanism of entrainment dominates. It is likely that these vary between sites. The main limitation with recording velocity in natural channels is the lack of suitable sensors. High resolution near-bed velocity profiles can provide information on which processes are active at a site and how they link with incipient motion. Several useful metrics including average velocities, instantaneous velocities, instantaneous velocity fluctuations (turbulence), and turbulence intensity can be derived from high frequency near-bed velocity data (Tennekes & Lumley, 1972). This kind of data has been captured in flume experiments using, among other things, acoustic Doppler and laser Doppler instruments (Chen & Chiew, 2004; Jaeger & Smart, 2012), but field equivalents are rare. The measurement of near-bed velocity in natural channels is challenged by the difficulty of maintaining sensors in mobile beds. Furthermore, this mobility means the near-bed zone is also vertically mobile making it difficult to record near-bed velocity throughout bed adjustments.

Fluctuations in pressure can also entrain substrate, without changes in velocity. Smart & Habersack (2007), Smart *et al.* (2010), and Jaeger & Smart (2012) have demonstrated the use of differential pressure transducers to measure pressure fluctuations at the bed surface that were correlated with entrainment events. Differential pressure sensors, however, require frequent calibration which makes their long-term deployment at remote locations difficult.

1.5.2.2 Seepage

Conventional quantification of the flow field for entrainment studies has focused on streamwise flow, but in alluvial channels flow also moves vertically. The vertical flow of water between the surface water column and the bed, known as seepage, injection, or suction, has largely been ignored in entrainment formulae, but can have large impacts on near-bed entrainment forces (Francalanci *et al.* 2008). Deshpande & Kumar (2016) found time-averaged near-bed velocities, Reynolds stresses, roughness sublayer thickness, and shear velocities increase under downward seepage conditions resulting in rapid bedload movement. Lu *et al.* (2008) provide a comprehensive review of seepage studies in flumes, and conclude that seepage conditions have a significant impact on near-bed flow structure and velocity. Furthermore, they conclude that extensive areas of seepage will alter shear stress by changing the total mass of the surface flow. In fact, seepage may be why flume derived equations do not work well in natural alluvial channels. Alfadhli & Yang (2014) re-examined 329 datasets and concluded that deviations from Shields curve were best explained by variation in upward velocity induced by seepage.

Future research on incipient motion and bedload transport must consider the influence of seepage and will require development of techniques to measure seepage in natural channels, particularly during high flows. This may involve differential piezometers, or seepage meters (e.g. Zhu *et al.* 2015) adapted for use in non-wadeable conditions and permanent installations. This will allow rates or changes in rates of seepage along hydraulic gradients to be evaluated for their role in substrate entrainment.

1.6 Identifying the Onset of Motion and Transport Rates

In order to identify hydrological thresholds for managing ecological health the exact moment that biomass removal processes begin needs to be recorded. Hoyle *et al.* (2017) demonstrate that molar action requires the highest grain stresses to occur. Drag and abrasion processes begin to operate below these stresses. Thresholds for bedload transport, which initiates molar action, therefore offer the most useful target for hydrological limits to manage periphyton abundance as they guarantee the activation of all three removal processes. Measuring site-specific entrainment and transport thresholds is therefore critical for periphyton management. A wide range of approaches have been used to measure bedload transport either by direct measurement or through surrogate measurement techniques (Leopold & Emmett, 1976; Reid *et al.* 1984; Wilcock *et al.* 1996; Tunnicliffe *et al.* 2000; Mizuyama *et al.* 2010; Rickenmann *et al.* 2014; Mao *et al.* 2016). A range of these approaches are discussed below.

1.6.1 Direct Measurement of Bedload

Traditionally, substrate movement was measured by tracking the movement of clasts or trapping of bedload material. Tracer particles are the most widely used method for estimating bedload transport in gravel-bed rivers (e.g. Ashworth & Ferguson, 1989; Death & Winterbourn, 1995). Pit trap and basket type samplers are also common and overcome the recovery limitations of tracer clasts (Reid *et al.* 1980; Leopold & Emmett, 1997; Bunte & Abt, 2003; Rickenmann *et al.* 2012). The major limitation of these methods for initiation of motion research is the inability to record the exact timing of clast movement, unless specialist systems such as pressure cells are used in traps, or smart tracers are used for particle tracking (e.g. Rickenmann *et al.* 2012; Cassel *et al.* 2017). These are difficult to establish in larger, mobile beds. Quantifying transport rates is also challenging due to a lack of ability to sample the entire bedload.

1.6.2 Surrogate Measurement of Bedload Transport

Surrogate methods, which use sensors to record the signal created by either the passage of clasts in transport, or the movement of the bedload layer, offer an alternative to the infamously difficult task of directly measuring substrate movement. A large range of these sensors are available and mostly use electromagnetic (Brayshaw, 1985; Tunnicliffe *et al.* 2000), or acoustic sensors (Lorang & Tonolla, 2014; Tsakiris *et al.* 2014). They in turn can be active or passive. Active sensors are those which emit their own signal and record properties of the reflected signal, whereas passive sensors record signals generated naturally (Gray *et al.* 2010). Direct application is where sensors generate a signal when the sediment in transport contacts the sensor. Indirect methods record the bedload without direct contact.

1.6.2.1 Passive bedload sensors

Passive sensors have been used in bedload research for over 30 years, and are more commonly used than active sensors. Passive electromagnetic sensors generally comprise of a magnetometer which records changes in the magnetic field produced by either tagged clasts (Reid *et al.* 1984; Brayshaw, 1985) or clasts with sufficient ferric content (e.g. Tunnicliffe *et al.* 2000). Passive acoustic sensors typically consist of either a hydrophone or geophone which record the vibrations caused by clasts contacting other clasts, or contacting a resonator (steel plate or pipe) (Lorang & Tonolla, 2014; Mao *et al.* 2016). Indirect sensors are highly sensitive to contamination from surrounding noise (Lorang & Tonolla, 2014; Barrière *et al.* 2015), severely limiting where they can be used. Attaching the hydrophone to a resonator eliminates considerable noise contamination, but requires the sensor to be installed in the bed where it may be buried or scoured out (Lorang & Tonolla, 2014).

Both electromagnetic and acoustic sensors suffer from limited spatial coverage, limits on clast size detection, and sensitivity to noise. Installing an array of sensors across the channel may overcome the spatial limitations, but will be difficult in larger and/or mobile channels. Clasts as small as 4 mm have been measured using electromagnetic sensors (Tunnicliffe *et al.* 2000), and filtering techniques have allowed fine and coarse bedload fractions to be separated in acoustic signals (Mao *et al.* 2016). It is also impossible to discern if recorded clasts originate locally or have been transported from upstream. Passive acoustic sensors have an advantage over electromagnetic sensors as they do not require ferric content in the bedload.

1.6.2.2 Active bedload sensors

There is a growing body of literature demonstrating the potential of active sensors for bedload monitoring, but the application of active sensors has largely been limited to feasibility studies (e.g. Yu *et al.* 2012; Chen *et al.* 2014) as opposed to long-term monitoring. Active electromagnetic sensors use radar transceivers to emit a pulse which is reflected from sediment (Shrestha *et al.* 2005), and the reflected signal (echo) recorded (Gray *et al.* 2010). Ferric clasts are not required. Active acoustic sensors come in a range of forms, including side-scan sonar (Kenyon & Belderson, 1973; Hamill *et al.* 2018) and acoustic Doppler current profilers (Milan & Heritage, 2012). Active acoustics emit sound pulses and record the returned signal. These methods can be used to measure bedload transport directly by measuring bed movement and velocity, or calculate transport flux by cross-section differencing or dune tracking (Spicer *et al.* 1997; Traykovski *et al.* 1998; Shrestha *et al.* 2005). The major advantage of active sensors is the ability to mount them out of the water column on bridges or cableways (Spicer *et al.* 1997).

One of the main limitations with active acoustic sensors is the variability of measurements (Rennie & Villard, 2004), and noise from suspended sediment (Stark *et al.* 2014). It is also important to note that bedload velocities recorded by active acoustics may be biased by stationary bed particles and may not represent heterogeneous bedload processes (Stark *et al.* 2014). Wang *et al.* (2016) demonstrate the need to incorporate other data including sediment chemical properties, water temperature, and suspended sediment concentration in radar processing as these parameters can affect the radar signal. This may increase cost, but, the results of Shrestha *et al.* (2005) suggest radar-based methodologies are worth the extra cost for active monitoring of bedload.

1.7 Synthesis

Declining ecological health from the reduction of substrate movement events is an increasing problem globally and maintaining the natural flow regime to ensure these occur is now commonly advocated for management of ecological health (Poff *et al.* 1997). Where hydrological regimes are altered by dams or water abstraction hydrological limits are used to replicate the natural flow regime with respect to magnitude, frequency, duration, and timing of natural flow events (Poff *et al.* 1997). Often these hydrological regimes are designed to reduce periphyton accrual, however, the critical threshold for flows to effectively remove periphyton is poorly understood, and the flows that transpire are often ineffective. This ineffectiveness is a result of the physical processes which scour periphyton being poorly understood. It is critical for future river management that we understand exactly what environmental flows are most effective for limiting periphyton accrual. Hoyle *et al.* (2017) demonstrated that periphyton removal is more strongly correlated with substrate movement than hydrological indices because movement thresholds relate directly to removal processes. Designing hydrological regimes to induce substrate entrainment and transport may hold the key to more effective environmental flows. Despite decades of research on incipient motion and bedload transport, we are unfortunately still some way from the answer.

Nevertheless, this paper discusses many of the recent technological advances which have the potential to rapidly improve our understanding of the site specific spatio-temporal variation in sediment dynamics and the associated effect on periphyton accrual (Table 1.2). Arising from this discussion, to better manage environmental flows we must:

- Increase the high spatial and temporal resolution of datasets
- Quantify:
    - bed compaction
    - substrate structure
    - near-bed velocity and pressure fluctuations
    - the exact moment substrate entrainment begins
- Record appropriate geomorphic and hydrodynamic variables simultaneously
- Focus more research in natural channels

- Develop models for identifying site- and species-specific entrainment and removal thresholds

One of the significant limitations highlighted in this paper has been the difficulty in applying appropriate techniques to natural channels. However, natural channels are where the management needs are, and there are now a range of options for future research to adapt flume techniques to the field. Furthermore, it is critical that a framework is established for choosing the appropriate site-specific methods to ensure that future research identifies applicable thresholds at appropriate resolution. If geomorphologists can identify the suite of critical parameters that initiate substrate movement, and how best to measure these *in situ*, ecologists will be better placed to explore the direct linkages between scour, abrasion, and molar action processes and periphyton accrual. This in turn will hopefully yield more informed environmental flow regimes that may allow better mitigation of the detrimental effects of flow modification.

1.8 Acknowledgements

The authors thank anonymous referees for their constructive comments on previous versions of this manuscript, which have been helpful in focusing this paper. Andrew Neverman is in receipt of a Massey University Doctoral Scholarship, and thanks Manaaki Whenua for supporting this work from Strategic Science Investment Funding.

Summary of Chapter 1 for Thesis

This chapter has highlighted the need for hydrological limits to be set using mechanistic targets based on physical processes as opposed to the present reliance on flow-ecology relationships. Sediment entrainment and transport thresholds were identified as potential mechanistic targets for establishing more effective flushing flows to manage excess periphyton accrual. The chapter has identified the present challenge of modelling and predicting entrainment and transport thresholds which inhibits their use in management. A number of recent methodological advancements which may address some of these limitations have been identified, and knowledge and methodological gaps which need addressing have been outlined. In particular, there is a need to increase the spatial and temporal resolution of datasets, quantify bed compactness, substrate structure, near-bed velocity and pressure fluctuations, be able to record the exact moment substrate entrainment begins, record appropriate geomorphic and hydrodynamic variables simultaneously, and focus more research in natural channels. Chapters 2-5 present the development of a number of methods to fill these methodological gaps.

Table 1.2: Data capture and analysis methods to improve incipient motion research.

Process	Data/Methodology	Analysis	Applicable Scale	Limitations
Substrate				
Roughness	3D Point-clouds	Standard deviation of elevation or similar	Grain Scale/Habitat Patch/Geomorphic Unit/Reach	Require expertise to conduct surveys, requires user to be at the site, temporally discrete
Compaction	Penetrometer	Penetration Index	Geomorphic Unit/Reach	Limited/no consistent methodology or proof of concept
Clustering	UAV aerial images	Manual Image Analysis	Habitat Patch/Geomorphic Unit/Reach	Time consuming, subjective. Limited testing of the technique
Imbrication	3D Point-clouds	Imbrication Index	Patch/ Geomorphic Unit/Reach	Application to date has been limited to patch scale, requiring hyper-resolution data. Limited testing of the technique
Water working	3D Point-clouds	Detrended Elevation, Skewness	Habitat Patch/Geomorphic Unit/Reach	Limited testing of the technique. Research to date limited to flume experiments
Entrainment and Transport Processes	Tracer Clasts/Clast Trackers	Recording movement of tagged clasts	Geomorphic Unit/Reach	Low recovery rate of tagged clasts, difficulties tagging clasts *in situ*, assumptions of when clasts moved and under which conditions
	Traps	Recording density of trapped sediment	Reach	Traps are limited by trapping capacity and efficiency
	Passive acoustics: Impact Plate geophone/ Japanese Acoustic Pipe/ Hydrophones	Signal Processing	Transect/Reach	Issues distinguishing signal from noise, need to have a permanent structure to secure device to.
	Passive electromagnetics	Signal Processing	Transect/Habitat Patch/Geomorphic Unit/Reach depending on use/distribution of seeded clasts	Limited to sites where substrate has sufficient ferric content or else seeded clasts are required.
	Active acoustics: Sonar/aDcp	Signal Processing	At-a-point/Transect/Habitat Patch/Geomorphic Unit/Reach	High setup costs, difficult to use in continuous monitoring applications, limitations in signal processing
	Active electromagnetics: GPR	Signal Processing	At-a-point/Transect	Still a relatively untested method
Hydraulic				
Critical Velocity	Velocity Sensor	Velocity at onset of motion	At-a-point	Difficulty finding readily available sensors capable of recording accurate data at suitably high temporal resolutions

Continued on next page

Process	Data/Methodology	Analysis	Applicable Scale	Limitations
Continued from previous page				
	aDcp	Velocity at onset of motion	Transect/Reach	Difficulty measuring velocities accurately in the turbulent near-bed region
Seepage	Differential Piezometers	Hydraulic Gradient Changes	Reach	Limited spatial resolution
	Seepage Meters	Rate of seepage	At-a-point	Limited to application during wadeable flows
Pressure Fluctuations	Differential Pressure Transducer	Variation in pressure between the substrate surface and subsurface	At-a-point	Need for frequent calibration, not readily available off the shelf for this application

Concluded

Chapter 2

Terrestrial Laser Scanning and Structure-from-Motion Photogrammetry concordance analysis for describing the surface layer of gravel beds

Introduction of Chapter 2 to Thesis

Chapter 1 highlighted the need to improve the quantification of substrate structure which is fundamental before considering how the structured substrate may move and for modelling the influence of the bed surface on near-bed hydrodynamics and associated forces, and therefore formed the basis of objective ii-a. Chapter 2 addresses objective ii-a by comparing the quantification of surface layer structural development using Terrestrial Laser Scanning (TLS) and Structure-from-Motion photogrammetry (SfMp) derived point clouds. Characteristics of TLS points have been related to armouring development, but the logistical challenges of obtaining suitable TLS datasets in the field have limited their wider application for quantifying gravel substrates at the grain scale beyond the extent of a patch. SfMp using Unmanned Aerial Systems allows rapid data capture of grain-scale point clouds at reach-scale extents, but SfMp produces point clouds with different characteristics to TLS point clouds. Applying the same analysis to SfMp point clouds as TLS point clouds to describe surface structure may therefore not be appropriate. This chapter highlights the differences in the metrics derived from each type of cloud and develops our understanding of how bed structure should best be quantified.

This chapter has been accepted for publication and is in press in Progress in Physical Geography as:

Neverman, A. J., Fuller, I. C., Procter, J. N., & Death, R. G. (In Press). Terrestrial Laser Scanning and Structure-from-Motion Photogrammetry concordance analysis for describing the surface layer of gravel beds. Progress in Physical Geography.

2.1 Abstract

Terrestrial Laser Scanning (TLS) and Structure-from-Motion photogrammetry (SfMp) offer rapid, non-invasive surveying of *in situ* gravels. Numerous studies have used the point clouds derived from TLS or SfMp to quantify surface layer characteristics, but direct comparison of the methods for grain-scale analysis has received relatively little attention to date. Comparing equivalent products of different data capture methods is critical as differences in errors and sampling biases between the two methods may produce different outputs, effecting further analysis. The sampling biases and errors related to SfMp and TLS lead to differences in the point clouds produced by each method. The metrics derived from the point clouds are therefore likely to differ, potentially leading to different inputs for entrainment threshold models, different trends in surface layer development being identified, and different trajectories for physical processes and habitat quality being predicted.

This paper provides a direct comparison between TLS and SfMp surveys of an exposed gravel bar for three different survey periods following inundation and reworking of the bar surface during high flow events. The point clouds derived from the two methods are used to describe changes in the character of the surface layer between bar inundation events, and comparisons are made with descriptions derived from conventional pebble counts. The results found differences in the metrics derived using each method do exist, but the grid resolution used to detrend the surfaces and identify spatial variations in surface layer characteristics had a greater impact than survey method. Further research is required to understand the significance of these variations for quantifying surface texture and structure, and predicting entrainment thresholds and transport rates.

2.2 Introduction

The structural organisation of heterogeneous sediment is a key component of gravel-bed rivers (Hodge *et al.* 2009b; Yu *et al.* 2012). The organisation of particles in the bed conditions entrainment of individual grains, increasing or decreasing the stability of the bed and the frequency of substrate scour and bedload transport events. Substrate scouring events are a key driver of disturbance for aquatic communities (Resh *et al.* 1988; Lake, 2000; Death, 2008, 2010). Decreasing frequency of substrate scour events from increased substrate stability is a growing problem in streams globally, leading to a reduction in habitat, alterations to riverine food webs, and increases in periphyton and macrophyte accrual (Neverman *et al.* 2018). Managing flow regimes and bed conditions to ensure disturbance events occur requires accurate measurement of substrate resistance, and identification of entrainment thresholds (see Neverman *et al.* 2018, for further discussion). Quantifying the texture (particle size distribution) and structure (arrangement of particles) (Buffington & Montgomery, 1999; Bertin & Friedrich, 2018) of gravel bed surfaces is an important component of quantifying substrate resistance and identifying entrainment thresholds. Heritage & Milan (2009) cite a range of difficulties in characterising surface grain size, attributed to sediment patchiness (e.g. Buffington & Montgomery, 1999); inconsistent sampling approaches (e.g. Fraccarollo & Marion, 1995); operator bias (e.g. Wohl *et al.* 1996); and insufficient sample size (e.g. Church *et al.* 1987). Many conventional descriptors of substrate characteristics are derived from pebble counts using the Wolman (1954) surface sampling protocol (Heritage & Milan, 2009), and typically use a representative grain size percentile (usually D_{50} or D_{84}) to quantify characteristics such as surface roughness (e.g. Clifford *et al.* 1992; Gomez, 1993; Fuller *et al.* 2003a; Neverman *et al.* 2016). Moments (statistics which describe the distribution of data about a point, such as variation and skewness) of the grain-size distribution can also describe gravel substrates (Van der Lingen, 1968; Folk, 1980). To date these metrics have received considerably less attention in the literature than surface roughness, but may prove valuable in improving the accuracy of entrainment and transport models.

The conventional application of these metrics has largely been limited to small areas of the surface layer, such as single facies or different geomorphic units, which leads to discrepancies between methods and deviations from true values (Bunte *et al.* 2009; Heritage & Milan, 2009). This limited spatial coverage is a product of differences in sampling protocols and the laborious nature of many of the methods used to derive grain size which often require manual sampling in the field or time-consuming manual post-processing (Bunte *et al.* 2009; Heritage & Milan, 2009). The time-consuming nature of field-based grain size analysis also reduces the frequency of repeat surveys, limiting the ability of managers to detect changes in system trajectories and adjust management schemes accordingly (see Larsen *et al.* 2004).

The ability to rapidly measure variations in grain-scale morphology *in situ*, at extents beyond the patch scale, may provide new opportunities to quantify substrate characteristics and develop accurate entrainment and transport models, leading to improved management of riverine systems. Advancements in optical gravelometry automation have begun to make analysis of substrates beyond the patch scale feasible (e.g. Carbonneau *et al.* 2004, 2005; Dugdale *et al.* 2010; Carbonnneau *et al.* 2018; Woodget *et al.* 2018). Terrestrial Laser Scanning (TLS) and Structure-from-Motion photogrammetry (SfMp) also offer surveying of substrates at the grain-scale, over large spatial extents (Hodge *et al.* 2009a,b; Brasington *et al.* 2012; Westoby *et al.* 2012; Hodge *et al.* 2013; Williams *et al.* 2014; Woodget *et al.* 2015; Woodget & Austrums, 2017). Numerous studies have used the point clouds derived from TLS and SfMp to quantify surface roughness (Heritage & Milan, 2009; Brasington *et al.* 2012; Bertin & Friedrich, 2013; Baewert *et al.* 2014; Bertin & Friedrich, 2016; Trevisani & Cavalli, 2016; Vázquez-Tarrío *et al.* 2017; Woodget & Austrums, 2017). Where previous studies have quantified roughness using a characteristic grain size (e.g. Carling, 1983; Clifford *et al.* 1992), an emerging trend in fluvial geomorphology has been estimating characteristic grain sizes using surface roughness measured from point clouds (Pearson *et al.* 2017; Vázquez-Tarrío *et al.* 2017). The relationship between surface roughness and the D_{50} or D_{84} is well documented using both TLS and SfMp. There is a growing body of work comparing SfMp and photo-sieving (Woodget & Austrums, 2017; Woodget *et al.* 2018), but SfMp and TLS estimates are rarely compared.

The focus on quantifying grain size and surface roughness reflects the dominance of these characteristics in entrainment models, but grain resistance is also altered by other characteristics of the substrate such as mortaring (Hodge *et al.* 2013), grain protrusion (Fenton & Abbott, 1977), bed packing (Sear, 1992, 1996; Papanicolaou *et al.* 2002), grain size and arrangement (Downes *et al.* 1998), and clustering (Wittenberg & Newson, 2005). These characteristics have been difficult to quantify in the field to date and are rarely included as parameters in entrainment threshold models. Several studies have used statistical moment coefficients derived from TLS point clouds to describe the surface texture and structure of gravel beds (Smart *et al.* 2004; Aberle & Nikora, 2006; Aberle *et al.* 2006; Aberle, 2007; Hodge *et al.* 2009a; Ockelford & Haynes, 2013). Whilst this work has shown promise, the method has not been widely applied in natural channels. But with the increasing adoption of SfMp, and the emergence of sUAS-borne LiDAR, for grain-scale modelling at the reach scale and beyond, point cloud analysis offers considerable potential for improving the quantification of substrate texture and structure for entrainment threshold modelling.

It is important to compare emerging techniques, and better understand what the data reveals (Viles, 2016). To the knowledge of the authors statistical moments of SfMp point clouds have not been used to quantify gravel bed surface texture and structure and compared to TLS point cloud moments. This paper compares the statistical moment coefficients derived from TLS and SfMp surveys of a 2,700 m^2 subaerial bar from multi-temporal surveys following successive inundation of the bar by high flow events over a 1-year period, building on the work of Aberle & Nikora (2006). Such a comparison is important as the point clouds produced by TLS and SfMp produce different models of the real surface due to differences in sampling biases and errors (Figure 2.1). Scientists and river managers need to understand whether the use of TLS or SfMp may create different outcomes for quantifying substrate characteristics as these variations may alter management decisions.

The paper aims to make a comparison between the values derived from independent TLS and SfMp point clouds for a range of metrics used to describe surface layer texture and structure, and provide some direction for which method is most beneficial for river managers and scientists to characterise surface layer texture and structure to improve estimation of entrainment thresholds.

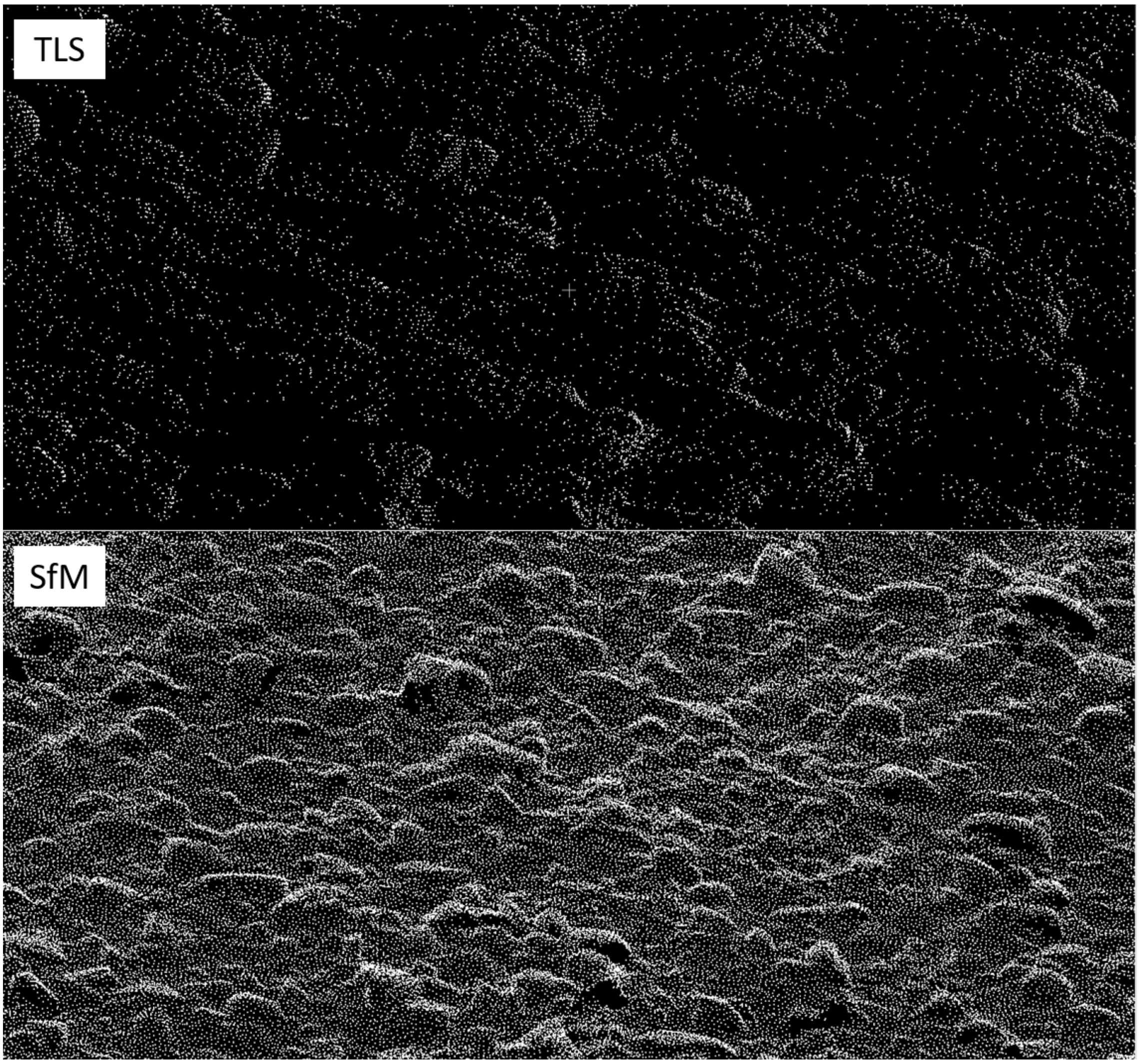

Figure 2.1: Example of a patch of gravel from the same extent in the TLS and SfMp clouds. Note the SfMp cloud has considerably more data points, and less occluded spots.

2.3 Study Site

The 2,700 m^2 bar which is the focus of this study is located in the Pohangina River: a wandering gravel-bed river (*sensu* Ferguson & Werritty, 1983) draining a 547 km^2 catchment in the eastern Wanganui Basin at the margin of the North Island axial ranges in New Zealand (Figure 2.2). The Pohangina runs parallel to the western front of the Ruahine Ranges, until its confluence with the Manawatu River at the western end of the Manawatu Gorge. The catchment has a steep 0.004 gradient, and the channel has a sinuosity of 1.3 (Fuller, 2007). A temperate maritime climate exists in the Manawatu region with rainfall ranging from 800 mm at the coast to >5000 mm in the ranges (Heerdegen & Shepherd, 1992; Clement *et al.* 2010). In 2004 a 150-year storm event caused significant flooding in the Manawatu region (Fuller, 2007). During the flood event the Pohangina expended 14,400 x 103 J, eroding 0.36 km^2 of floodplain (Fuller, 2007).

The study site is located at a site known as Mais Reach, which is used for flow monitoring by Horizons Regional Council. The mean flow at Mais Reach is 17 $m^3 s^{-1}$, mean annual low flow (MALF) is 2.3 $m^3 s^{-1}$, and the mean annual flood (MAF) is 489 $m^3 s^{-1}$ (Henderson & Diettrich, 2007). Repeat surveys were conducted on a single subaerial gravel bar, chosen for its ease of access and opportunity to scan from the true left and true right banks (i.e. left and right bank in the direction of flow, respectively) with a Terrestrial Laser Scanner. The areal extent of the survey area was slightly different each time due to minor changes in channel morphology, stage, and scanner occlusion by vegetation growth between surveys, but covered approximately 2,700 m^2. Only the downstream end of the bar was surveyed because of challenges in accessing the banks in the upper section due to dense vegetation limiting the ability to establish suitable scanning positions.

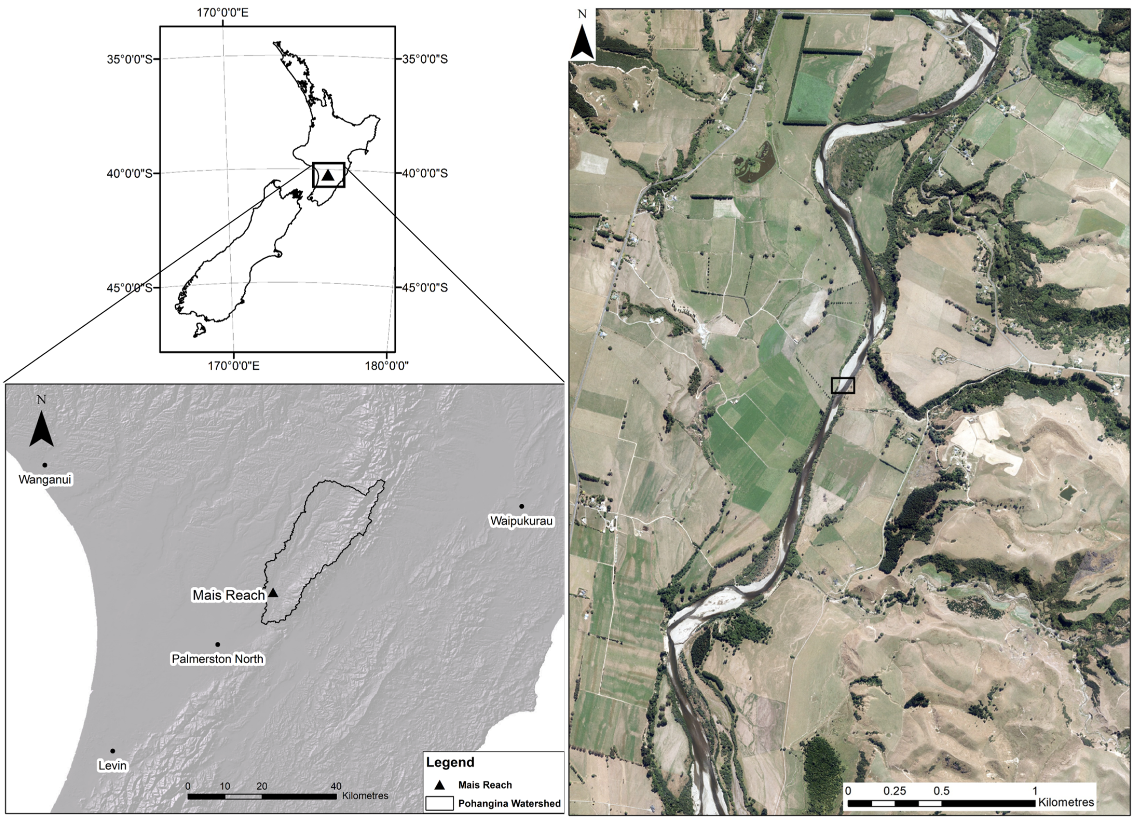

Figure 2.2: Location of the Pohangina River catchment, North Island, New Zealand (left), and the study site at Mais Reach indicated by the black box (right) which shows the extent of Figure 2.3.

2.4 Methodology

2.4.1 Data Acquisition

2.4.1.1 Survey control

To improve consistency of point cloud registrations a network of survey control pegs was established prior to the first survey, providing repeat stations for the TLS setup, and registration of the TLS and SfMp point clouds. A network of seven survey pegs (Figure 2.3) was established on the elevated floodplain. The control peg coordinates were established in the New Zealand Transverse Mercator 2000 (NZTM2000) projection using a Trimble® R8 RTK-dGPS base station and rover with accuracy and precision measured as 2 cm. The two pegs established on the true left were lost due to bank erosion between the October 2015 and August 2016 surveys, so new pegs were established using the five pegs on the true right as control (Figure 2.3).

2.4.1.2 Terrestrial Laser Scanner surveys

TLS surveys were conducted using a Leica® MS50 MultiStation. Several considerations are needed when establishing TLS surveys. Occlusion of the laser beam is common on rough topographic surfaces, producing point clouds which only sample the face of objects visible to the scanner, resulting in gaps in the point cloud where the scanner could not see the reverse side of objects, known as occlusion (Hodge *et al.* 2009b; Nouwakpo *et al.* 2016). TLS also positively biases sampling with increased distance from the scanner as the angle of incidence becomes lower (Brasington *et al.* 2012). Point spacing increases with distance from the scanner and vice versa, creating spatial variations in point density (Girardeau-Montaut *et al.* 2005; Sotoodeh, 2006). To limit these issues the gravel bar was surveyed from multiple scanning positions around its perimeter to reduce occlusion in the final point cloud. Scanning positions were located on the elevated banks when possible to create higher angles of incidence and therefore reduce the positive bias in sampling. When the left bank was not accessible due to high flows for the October 2015 survey the TLS scans were conducted from pegs 1 and 3 on the true right, and from a temporary position along the true left of the bar surface (Figure 2.3). The December 2015 survey used scanning positions at pegs 1, 3, and 8. The August 2016 survey used pegs 1 and 9. The use of different scanning positions is due to variations in visibility of the bar produced by changing riparian vegetation structure and bar configuration between surveys.

The bar was separated into an upstream and downstream section for ease of surveying, and each section was scanned separately from the left and right banks, with point spacing set for the centre of the section. This approach created a more uniform point spacing. Point spacing was set at 10 mm as this provided the best trade-off between time efficiency, representation of the substrate surface, and reduction of scatter/noise in the point clouds. TLS scanning distances ranged from 11-100 m so are not considered close-range (*sensu* Hodge *et al.* 2009b). The MS50 laser beam has a footprint of 8 x 20 mm at 50 m, and 16 by 25 mm at 100 m, and a range noise (distance measurement accuracy) of 2 mm at 100 m for 1000 Hz scans as used for this study (Leica Geosystems AG, 2014). The footprint size is important to consider as it adds further uncertainties, particularly for grains smaller than the footprint. The MS50 has a filter designed to remove mixed-pixel errors (Leica Geosystems AG, 2014), which occur when light is reflected from two surfaces at different distances from the scanner (Hodge *et al.* 2009b). Leica Cyclone 8.1 was used to merge the scans and manually remove woody debris and water strikes from the clouds.

Figure 2.3: Distribution of the survey peg network at Mais Reach (top) displayed on an aerial image from 2016 showing the bar configuration for the August 2016 survey. Pegs from the benchmark survey are displayed in green, the temporary peg used for the October 2015 survey is shown in red (indicating the extent of the bar in October 2015), and pegs 8 and 9 which replaced 6 and 7 are shown in blue. Arrow indicates flow direction. The bottom image shows an example of the GCPs used in the August 2016 survey, allowing rapid deployment, and automatic recognition of targets during processing. DJI® Phantom 3 battery shown for scale.

2.4.1.3 Structure-from-Motion photogrammetry

Image datasets for the Structure-from-Motion (SfMp) surveys were collected using a DJI® Phantom 3 Professional small Unmanned Aerial System (sUAS) with the factory standard 12 MP camera with a 94° field of view (FOV) and 20 mm focal length (35 mm equivalent). The sUAS was flown at 3 m above ground level (AGL) to achieve a ground sampling distance (GSD) of 1.5 mm. Surveys were conducted using a grid pattern to collect nadir images, with flight parameters set to achieve 80% front and side overlap of image pairs. The grid was flown a second time to collect low oblique images. This approach reduces systematic errors (see Westoby *et al.* 2012; James & Robson, 2014; Clapuyt *et al.* 2016). 12 Ground Control Points (GCPs) were used as control for each survey. The GCP positions were surveyed using the MS50 in Total Station mode from peg 1 to maintain the same registration errors as the TLS surveys. The GCPs were surveyed in the same NZTM2000 projection used for the control peg network. 80 mm steel discs on a 150 mm long spike (driven into the bed) painted fluorescent orange were used as GCPs in the 2015 surveys. For the 2016 survey, 12-bit targets from Agisoft® PhotoScan were used, allowing automatic identification of the targets during processing. These targets were printed on orange A4 paper, laminated, and glued to 450 mm x 450 mm industrial carpet squares, which allowed rapid deployment of the GCPs, whilst remaining heavy enough to stay in place (Figure 2.3).

Agisoft® PhotoScan Professional (version 1.2.5 build 2706) was used to process the images using the standard SfMp workflow which is well described in the literature (e.g. Westoby *et al.* 2012). Image alignment was optimised using the 12 GCPs. Tie points with high uncertainty were removed using the *Gradual Selection* tool with intuitive threshold selection, reducing the number of tie points by an order of magnitude. The model was optimised following each stage of the gradual selection process, removing images that no longer had tie points in the sparse cloud. A 2.5-Dimensional height field (with the bounding box aligned to the geographic coordinate system) dense cloud was generated using ultra high quality and aggressive depth filtering to reduce the chance of artefacts being introduced. This had a significant beneficial impact on the quality of the dense clouds produced with reduction in noise visually apparent.

2.4.2 Point Cloud Processing

The large datasets created by the TLS and SfMp surveys are difficult to visualise with standard GIS packages (Brasington *et al.* 2012). CloudCompare (`http://www.danielgm.net/cc`) is an open-source freeware GIS package optimised for displaying and analysing point clouds. The point clouds were imported into CloudCompare, where the CANUPO plugin (see Brodu & Lague, 2012) was used to segregate vegetation from gravel and remove the vegetation. Vegetation was virtually absent from all 2015 surveys, but small bushes of Lupin were present in the August 2016 surveys. Visual analysis of the clouds following vegetation cleaning suggested most vegetation was successfully removed, except for some data points which were indistinguishable in elevation from larger gravel clasts, but these were relatively sparse. We therefore consider vegetation will have no significant impact on our analysis.

The benchmark survey of the control pegs was imported into CloudCompare and used to register the TLS and SfMp clouds using the *Align* tool by manually picking points. Registration errors are presented in Table 2.1. The TLS and SfMp clouds for each survey were subtracted from one another to assess the correspondence between the surface registrations and to assess the SfMp clouds for distortion (see Carbonneau & Dietrich, 2017). The clouds were differenced in CloudCompare using cloud-to-cloud (C2C) differencing with the results split for the x, y, and z directions. Distortion was assessed using the difference in the z direction (Δz). The difference was found to be challenging to interpret due to occlusion in the TLS cloud leading to large differences being measured where there was SfMp data. To overcome this issue, the point clouds were gridded to a 0.5 m grid, and the average elevation of the points within each grid cell was assigned to the cell value. These grids were then differenced. This reduced some of the complexity in analysing the differences. Figure 2.4 shows a box plot of the cloud-to-cloud results for Δz for the gridded data. No dishing or doming distortion (see Carbonneau & Dietrich, 2017) was noticed in the clouds, but some tilt differences were observed, particularly in the October 2015 SfMp cloud (Figure 2.5). Whilst iterative closest point (ICP) matching could be used to finely register the clouds and correct the SfMp distortions, this was not performed as the aim of this paper is to compare the differences in the TLS and SfMp clouds as independent products. ICP algorithms are also designed to work on datasets which represent the same shape. As demonstrated in Figure 2.1, TLS and SfM produce clouds with quite different shapes, so fine registration of these clouds may not be appropriate and could give misleading results.

Local detrending is a standard method in the literature to remove the effect of bed form on local surface roughness (Brasington *et al.* 2012; Pearson *et al.* 2017; Vázquez-Tarrío *et al.* 2017). Following Vázquez-Tarrío *et al.* (2017), a mesh was created to produce a surface representative of the mean elevation for each point cloud. This was done twice using different grid sizes to analyse the effect of grid resolution on the final outputs. The cell sizes chosen were 1 x 1 m (grid 1) and 0.25 x 0.25 m (grid 2). The mesh was subtracted from the point cloud using the cloud-to-mesh (C2M) tool in CloudCompare to produce elevations relative to the local trend ($z_{detrended}$). The cloud extents were clipped so TLS and SfMp cloud pairs had the same extent, and the artefacts produced at the edge of the clouds during detrending were removed (see Pearson *et al.* 2017). The total number of points in the final clouds ranged from 887,201 to 8,959,257 (Table 2.1), with higher point densities in the SfMp clouds.

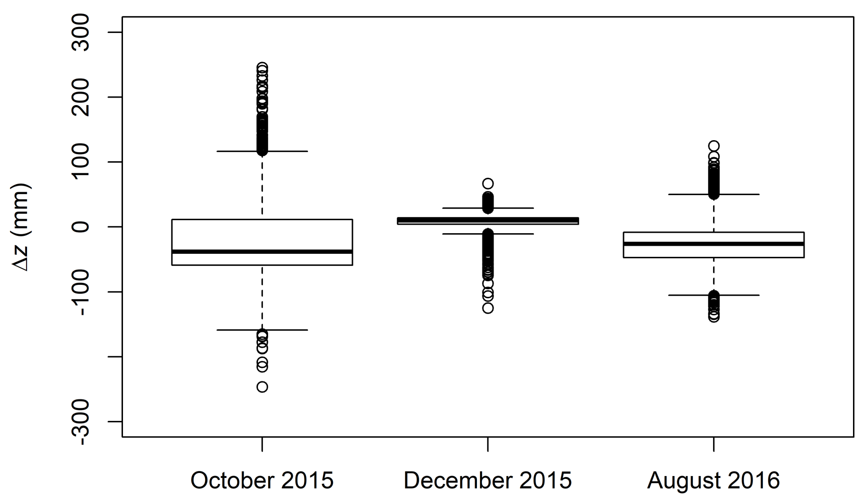

Figure 2.4: Difference in the z direction between points in the SfMp and TLS clouds.

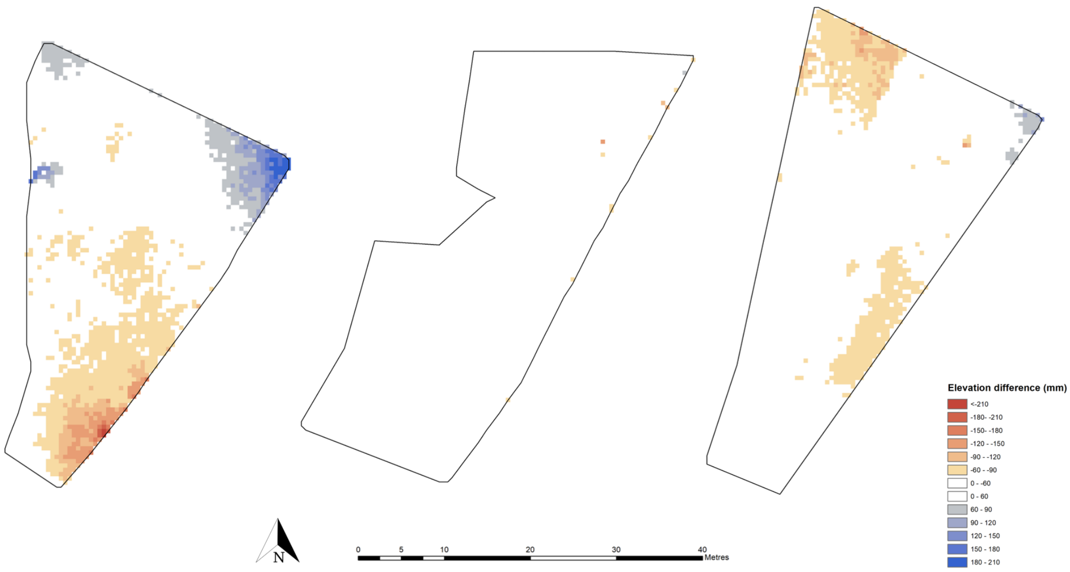

Figure 2.5: Rasters showing the difference in elevation between the SfMp and TLS clouds. The clouds were gridded to 0.5 m resolution, with cell values representing the mean elevation. Areas in red represent cells where the TLS was lower than the SfMp. Areas below 60 mm difference (approximately the D_{84}) are thresholded out as these areas tended to show pixels where the SfMp cloud had data points in occluded areas of the TLS, or at the base of grains where TLS had only sampled the top of the grain. It is worth noting the largest b-axis measured in a pebble sample exceeded 256 mm, and therefore differences in the clouds are within the range of b-axis measurements at the site. The black outline represents the survey boundary.

Table 2.1: RMS registration errors for each survey and total number of points in each point cloud.

Survey Date	**Survey Method**	**RMS error (mm)**	**Total Points**
October 2015	TLS	14	4,481,828
	SfM	14	7,555,690
December 2015	TLS	4	1,924,318
	SfM	15	7,296,085
August 2016	TLS	7	887,201
	SfM	8	8,959,257

2.4.3 Calculating Point Cloud Moments

Statistical moments of $z_{detrended}$, namely the standard deviation (σ_z), skewness (S_{kz}), and kurtosis (K_{uz}), were calculated using R (R Core Team, 2013). S_{kz} and K_{uz} were calculated using the *e1071* package (Meyer *et al.* 2017). Moments were calculated for a) the entire cloud, and b) for each cell of grid 1 and grid 2 to show the spatial variation in surface texture and structure. For the spatially varied calculations the *lidR* package (Roussel & Auty, 2017) was used in R to grid the data and apply the calculations of σ_z, S_{kz}, and K_{uz} on a cell by cell basis for grid 1 and grid 2. The grid of spatially varied TLS moments was subtracted from the SfMp grid for each survey date and grid resolution to show variations in moments calculated with each method.

It is important to note that many statistical software packages calculate excess kurtosis, which differs from traditional kurtosis values (Joanes & Gill, 1998). Traditional kurtosis gives a coefficient of 3 for normal distributions. Modern calculations of kurtosis tend to report the excess kurtosis, which uses the same calculation of kurtosis but subtracts 3 from the result so a normal distribution has a coefficient of 0. Negative excess kurtosis values therefore always represent a platykurtic distribution, and positive values a leptokurtic distribution. To enable comparison of our kurtosis coefficients with those of Aberle & Nikora (2006) who report the traditional kurtosis values we subtracted 3 from the coefficients reported by Aberle & Nikora (2006) to give the excess kurtosis. All comparisons discussed in this paper therefore refer to the excess kurtosis unless otherwise stated.

2.4.4 Pebble Counts

A pebble count was conducted with a pebble template (gravelometer) following the Wolman (1954) protocol to provide a comparison between characterising gravel surfaces using point clouds and conventional pebble counts. The Wolman method was chosen over other methods such as sieving as it is commonly used to describe surface gravels given its ease and rapidity of use in the field, so provides a meaningful representation of the conventional approach. Pebble templates eliminate observer errors associated with identifying the b-axis (Bunte *et al.* 2009; Daniels & McCusker, 2010). The pebble template had 0.5 ϕ increments (cf. Bunte *et al.* 2009). 100 clasts were randomly sampled from the surface over the survey area extent using the big toe (boot) method to maintain sampling randomness (Bunte *et al.* 2009; Neverman *et al.* 2016). Representative clast sizes (D_{50} and D_{84}) were derived using cumulative frequency plots of D. Inclusive graphic standard deviation (σ_i), inclusive graphic skewness (S_{ki}), and inclusive graphic kurtosis (K_{ui}) were also derived from the grain-size distributions following Folk (1980). It is critical to note that the graphical kurtosis used by Folk (1980) gives a coefficient of 1 for a normal distribution. We therefore subtracted 1 from these coefficients to give the excess kurtosis, enabling easier comparison with the point cloud K_{uz} coefficients.

2.5 Results

2.5.1 Pebble Counts

Metrics derived from the Pebble counts are presented in Table 2.2. The pebble counts show an increase in D_{50} and D_{84} from October 2015 to December 2015, followed by a decrease to August 2016. σ_i ranged from -0.32 to 0.07. Skewness was near symmetrical for October 2015 and August 2016, but skewed towards fines (<12 mm diameter) for the December 2015 survey. The K_{ui} coefficients show the December 2015 survey was slightly leptokurtic whilst the October 2015 and August 2016 surveys were very platykurtic (*sensu* Folk, 1980). The sorting coefficients indicate October 2015 was well sorted, and the December 2015 and August 2016 surveys were moderately well sorted (*sensu* Folk, 1980).

2.5.2 Point Clouds

2.5.2.1 Standard deviation

Point cloud moments are presented in Table 2.3. σ_z coefficients for the complete clouds range from 15 to 28 mm. No systematic difference between survey method was observed, but grid 2 consistently produced lower σ_z coefficients than grid 1. Grid 1 TLS σ_z followed

Table 2.2: Statistics for the pebble count surveys following Folk (1980), and the D_{50} and D_{84} characteristic grain sizes.

Survey Date	σ_i	S_{ki}	K_{ui}	**Excess Kurtosis**	D_{50} **mm**	D_{84} **mm**
October 2015	-0.44	0.07	0.49	-0.51	37	55
December 2015	-0.63	-0.32	1.06	0.06	39	61
August 2016	-0.51	-0.03	0.68	-0.32	36	56

the trend of the D_{50} and D_{84} closer than SfMp. Grid 2 SfMp had an inverse trend to the D_{50} and D_{84}.

The D_{50} and D_{84} were divided by σ_z (D_{50}/σ_z and D_{84}/σ_z, respectively) to calculate the multiplier coefficients needed to convert σ_z to the D_{50} and D_{84} (c.f. Heritage & Milan, 2009; Vázquez-Tarrío *et al.* 2017). These values are presented in Table 2.4. On average the D_{50} was twice the σ_z, but ranged from 1.4 - 2.6 x σ_z. The D_{84} was on average 3 x the σ_z, but ranged from 2.2 - 4 x σ_z.

Spatially varied σ_z ranged from 0.02 mm to 103 mm. Grid 2 produced more extreme minimum and maximum σ_z coefficients, but had systematically lower first quartile (Q1), median, and third quartile (Q3) values, and smaller Inter Quartile Ranges (IQRs), excepting the December 2015 SfMp (Figure 2.6). Figure 2.7 shows an example of the difference in the spatial distribution of σ_z coefficients between TLS and SfMp. Differences in σ_z between SfMp and TLS ($\Delta\sigma_z$) ranged from 0 - 94.7 mm for grid 2, and 0.001 - 65.8 for grid 1. IQRs for$\Delta\sigma_z$ ranged from 3.5 - 8.3 mm. $\Delta\sigma_z$ is plotted in Figure 2.6. Grid 1 had no cells with equal σ_z, whereas grid 2 had at least one cell with equal σ_z, with three matching cells for the October 2015 survey (Table 2.5).

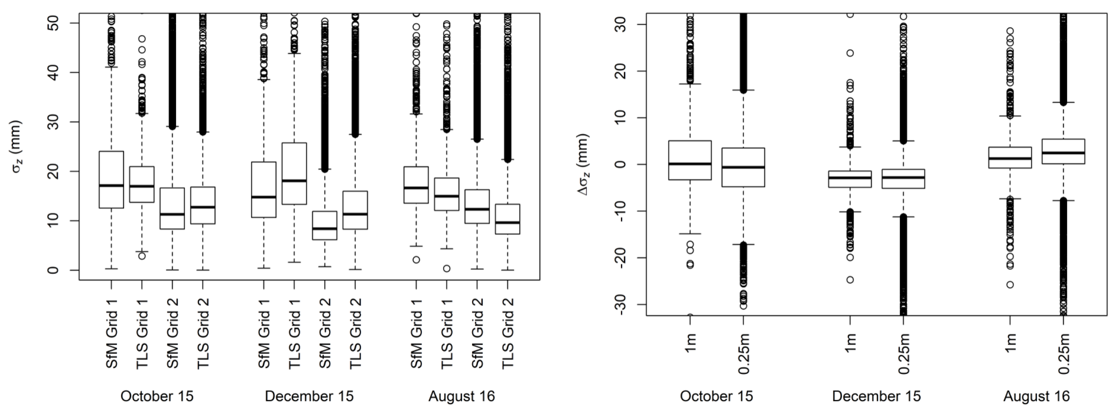

Figure 2.6: Box and whisker plots of the spatially varied σ_z (left) and $\Delta\sigma_z$ (right). Note the y-axis has been scaled to make the IQR legible, so some data points beyond the whiskers are not included in the plots.

2.5.3 Skewness and Kurtosis

2.5.3.1 Complete clouds

For the complete clouds skewness ranged from -1.06 to 0.68 (Table 2.3). A systematic bias was apparent between detrending cell resolutions with grid 1 producing negative skewness, whilst grid 2 produced positive skewness, excepting the October 2015 SfMp

Table 2.3: Moments of $z_{detrended}$ for each survey and detrending grid resolution (not spatially varied). Note the kurtosis coefficients (K_{uz}) are excess kurtosis.

Detrending Grid	**Survey Date**	**Survey Method**	σ_z	S_{kz}	K_{uz}
Grid 1	October 2015	TLS	20	-0.02	2.77
		SfMp	26	-0.27	6.79
	December 2015	TLS	28	-0.50	10.28
		SfMp	24	-0.58	15.10
	August 2016	TLS	23	-1.06	13.01
		SfMp	23	-0.17	6.75
Grid 2	October 2015	TLS	15	0.68	1.97
		SfMp	19	-0.23	7.20
	December 2015	TLS	20	0.51	5.05
		SfMp	15	0.50	6.04
	August 2016	TLS	16	0.62	9.28
		SfMp	18	0.32	6.44

Table 2.4: Statistics for the pebble count surveys following Folk (1980), and the D_{50} and D_{84} characteristic grain sizes.

Detrending Grid	**Survey Date**	**Survey Method**	D_{50}/σ_z	D_{84}/σ_z
Grid 1	October 2015	TLS	1.8	2.7
		SfMp	1.4	2.2
	December 2015	TLS	1.4	2.2
		SfMp	1.7	2.6
	August 2016	TLS	1.6	2.5
		SfMp	1.6	2.5
Grid 2	October 2015	TLS	2.4	3.6
		SfMp	1.9	2.9
	December 2015	TLS	2.0	3.1
		SfMp	2.6	4.0
	August 2016	TLS	2.2	3.5
		SfMp	2.0	3.1

survey. Trends in skewness varied between survey method and grid size. Grid 1 TLS surveys showed increasing negative skew from October 2015 to August 2016. Grid 2 TLS showed similar positive skew from October 2015 and August 2016 with a decreased skew for December 2015. Grid 1 SfMp showed negative skewness for all surveys with highest skew for December 2015. Grid 2 SfMp showed negative skew for October 2015, and the

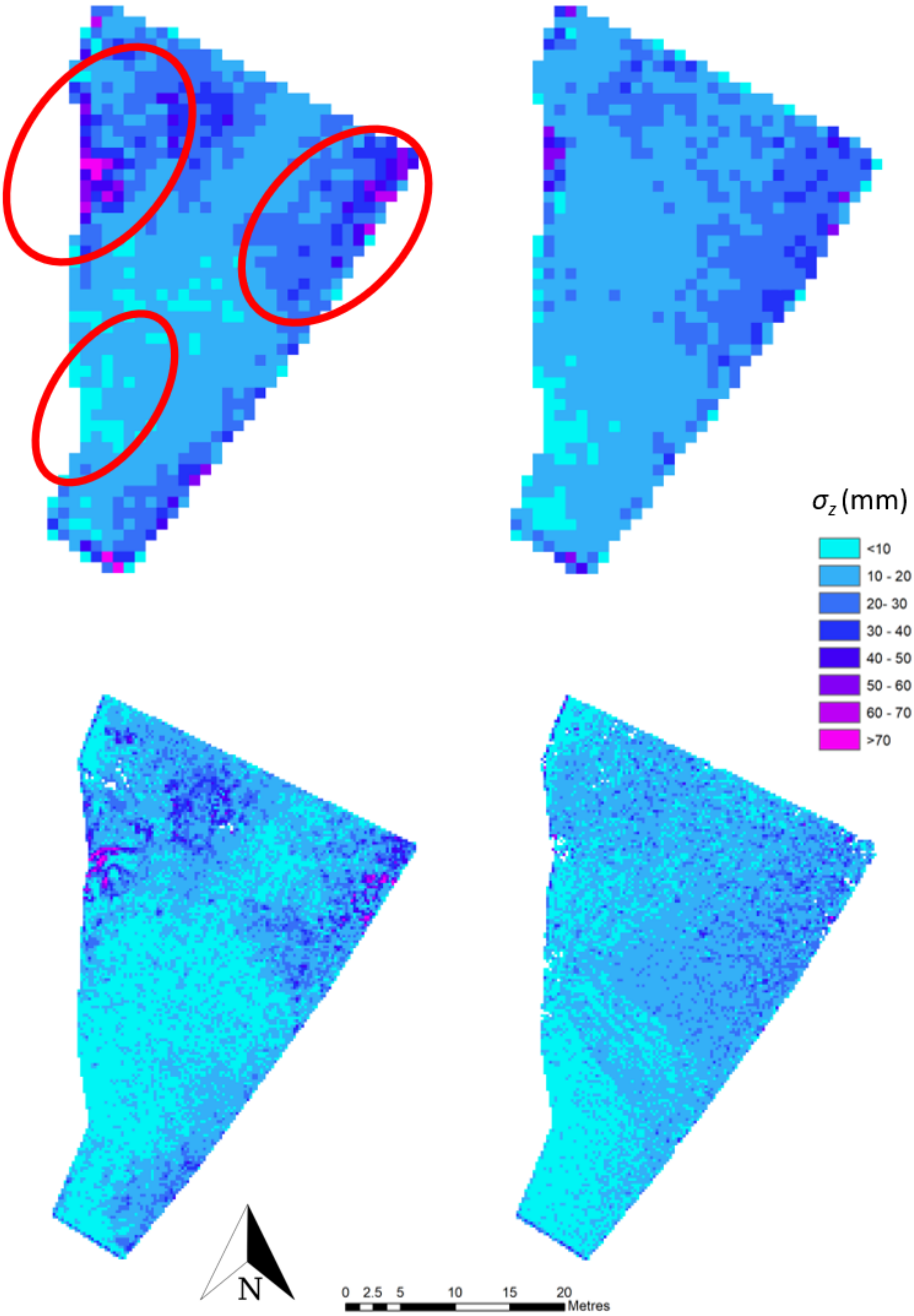

Figure 2.7: Rasters showing the spatial variation of σ_z for the October 2015 survey 1 m (top) and 0.25 m (bottom) cell resolutions. SfMp surveys are on the left and TLS on the right. Red circles highlight some of the roughness patches which are evident in the clouds.

Table 2.5: Number of cells in each spatially differenced moment raster which had equal values for the TLS and SfMp surveys.

Grid	Date	σ_z	S_{kz}	K_{uz}
1	October 2015	0	1	0
	December 2015	0	1	0
	August 2016	0	0	0
2	October 2015	1	3	1
	December 2015	1	2	1
	August 2016	3	7	5

highest skew for December 2015, which was positive. K_{uz} coefficients ranged from 1.97 to 15.10 (Table 2.3). SfMp produced higher K_{uz} coefficients for the 2015 surveys, but lower for the 2016 survey for both grids. Grid 1 produced higher K_{uz} coefficients than grid 2, excepting the October 2015 SfMp survey. The TLS surveys showed increasing positive kurtosis from October 2015 to August 2016 for both grids. The SfMp surveys showed the same trend as the pebble count data for grid 1 with lower K_{uz} for October 2015 and August 2016, and higher for December 2015, and the opposite trend for grid 2. However, all SfMp K_{uz} values were positive.

2.5.3.2 Spatially varied moments

S_{kz} coefficients ranged from -3.4 to 5.8 for grid 1, and -8.15 to 6.39 for grid 2. Grid 2 resulted in a larger range of S_{kz} than grid 1 for the October 2015 and August 2016 surveys, but lower for the December 2015 survey. TLS systematically had higher positive S_{kz} IQR for grid 1, but lower S_{kz} for two out of three surveys using grid 2 (Figure 2.8). K_{uz} coefficients for the spatially varied moments ranged from -2.75 to 66 for grid 1 and -2.75 to 113 for grid 2. Grid 2 produced greater ranges of K_{uz} coefficients, but systematically lower Q1, median, and Q3 values than grid 1 (Figure 2.9). The K_{uz} IQRs ranged from 0.7 to 2.1.

The spatially varied moments were also differenced for each matching pair. The difference in S_{kz} (ΔS_{kz}) ranged from 0 to 9.7. Table 2.5 shows all surveys except August 2016 had at least one cell with matching S_{kz} between methods. Grid 2 produced more cells with matching S_{kz} than grid 1. ΔS_{kz} IQRs varied from 0.5 to 1 (Figure 2.8). All surveys except grid 2 December 2015 and August 2016 had negative median ΔS_{kz}, suggesting TLS cells tended to have higher skewness for grid 1, but lower for grid 2.

Differenced grids had kurtosis differences (ΔK_{uz}) ranging from 0 to 110. Grid 1 did not produce any cells with equal K_{uz} coefficients (Table 2.5). Grid 2 produced at least 1 cell with matching K_{uz} for all surveys. The IQRs for ΔK_{uz} ranged from 1 to 1.7. All surveys except the grid 1 December 2015 survey had positive median differences (Figure 2.9), indicating SfMp surveys tended to have higher K_{uz} coefficients. Figure 2.9 shows grid 2 consistently produced higher Q1, median, and Q3 values.

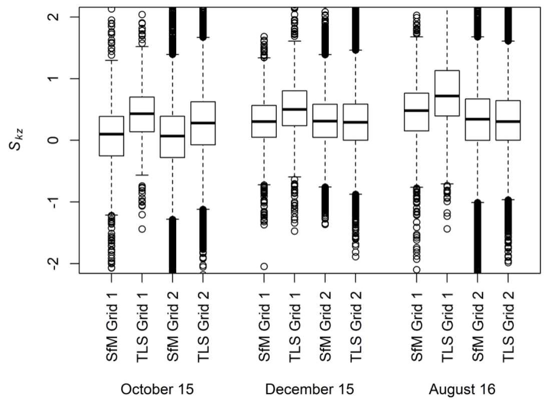

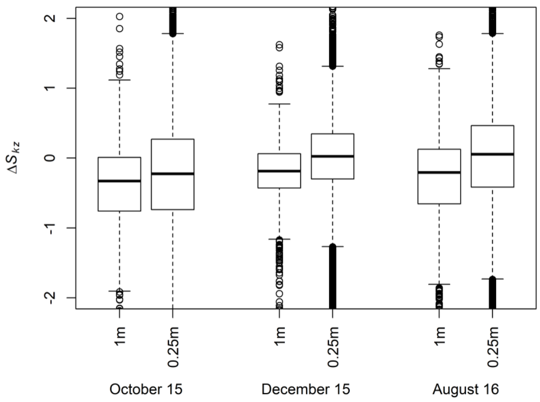

Figure 2.8: Box and whisker plots of the spatially varied S_{kz} (left) and ΔS_{kz} (right). Note the y-axis has been scaled to make the IQR legible, so some data points beyond the whiskers are not included in the plots.

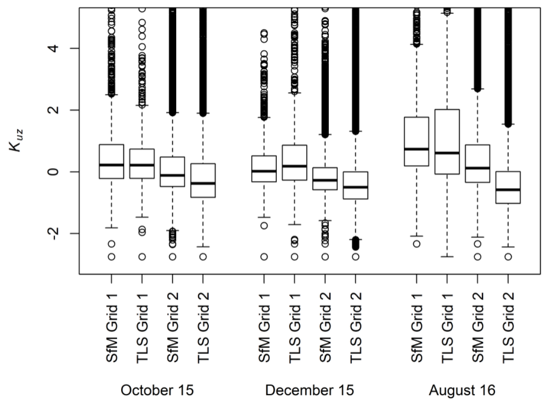

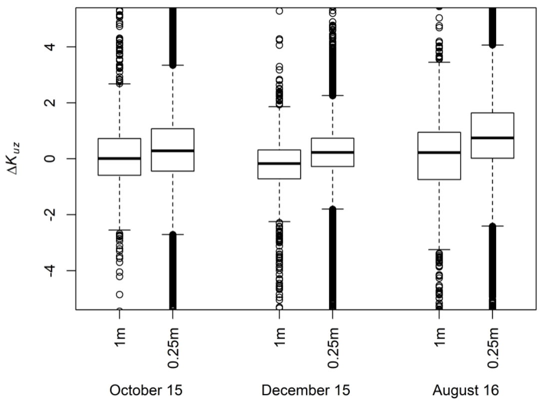

Figure 2.9: Box and whisker plots of the spatially varied K_{uz} (left) and ΔK_{uz} (right). Note the y-axis has been scaled to make the IQR legible, so some data points beyond the whiskers are not included in the plots.

2.6 Discussion

2.6.1 Characterising Surface Roughness

Surface roughness has a significant effect on near-bed hydrodynamics and is a key parameter to include in entrainment models. Conventional approaches to quantifying surface roughness have relied on relationships with a characteristic grain size (e.g. Clifford *et al.* 1992; Gomez, 1993; Fuller *et al.* 2003a; Neverman *et al.* 2016). This relationship is altered by local variations in substrate structure. Due to the labour-intensive and intrusive nature of manually sampling grain size, spatial representation of surface roughness is rarely quantified, yet is an important aspect of moving towards calculation of spatially varied entrainment thresholds and transport rates. Hyper-resolution topographic surveys of *in situ* gravels allow the characterisation of surface roughness by calculating the standard deviation of surface elevations about the mean bed elevation (Heritage & Milan, 2009; Hodge *et al.* 2009b; Brasington *et al.* 2012; Vázquez-Tarrío & Menéndez-Duarte, 2015; Woodget *et al.* 2015; Pearson *et al.* 2017; Woodget & Austrums, 2017). These calculations may be spatially varied, offering the opportunity to represent spatial differences in surface roughness and model spatial variability in hydrodynamics and entrainment forces. The measurements are also non-intrusive, so the bed structure is not altered during sampling.

The rasters presented in Figure 2.7 show the TLS and SfMp spatially varied σ_z maps identified similar patches of surface roughness differences, despite absolute values varying between survey methods. Figure 2.6 shows the $\Delta\sigma_z$ between the surfaces had small IQRs of 3.5 to 8.5 mm. This means that 50% of grid cells had differences in σ_z smaller than the laser beam footprint, so are below the minimum level of detection.

The conventional approach to characterising roughness with the D_{84} suggests increases in the D_{84} should be reflected by increases in surface roughness, not accounting for variations in substrate structure. σ_z for the TLS surveys showed a similar trend to the D_{50} and D_{84} between surveys for both grid resolutions. The SfMp σ_z showed the opposite trend to D_{84} and D_{50}, with successive decreases in σ_z for grid 1, and lowest σ_z for the December 2015 survey for grid 2. This suggests TLS is most consistent with field-derived pebble count metrics. However, this does not imply it is the most accurate means of assessing surface roughness.

Pearson *et al.* (2017) and Woodget *et al.* (2018) note the limitations of estimating grain size from surface roughness measurements, as the relationship between axis length and protrusion is altered by the arrangement of clasts in the bed, with factors such as sorting, imbrication, clustering, and packing altering the protrusion or hiding of individual grains (see Clifford *et al.* 1992, for further discussion). These same factors inhibit the estimation of surface roughness from grain size measurements. Pearson *et al.* (2017) found no relationship between surface roughness and grain size in poorly sorted gravels, but found significant linear relationships in moderately- and well-sorted gravels. The gravel bar at Mais Reach was moderately- to well- sorted for all surveys presented in this study (Table 2.2). We could therefore expect to see significant relationships between grain size and surface roughness.

However, the Wolman (1954) protocol used for measuring grain size is significantly biased towards sampling of coarse grains (Bunte *et al.* 2009). The higher correlation between TLS estimates and measured grain size may reflect the bias of both methods towards larger grains. The lower correlation seen between SfMp and measured grain size may therefore result from better representation of fines and hidden grains in the SfMp point cloud (Figure 2.1). This is due to the use of nadir and oblique imagery reducing the sampling bias introduced by occlusion and higher oblique scanning angles in the TLS point clouds. Given a lack of representation of fines and structure in the grain size samples we would expect to see this weaker correlation with SfMp. This may also explain why the SfMp data did not show the same grain size trends as the pebble counts and TLS, as changing structure between surveys may have more significantly altered the SfMp results. The relationship between SfMp and manually sampled grain size data may have been stronger if grain size sampling methods which include fine material (i.e. $<$12 mm) were used, such as sieving.

It is important to highlight here that this grain size bias is not necessarily related to photogrammetric vs LiDAR biases, but rather the different platforms used for each method (i.e. airborne nadir and low oblique surveying vs proximal oblique surveying). sUAS-borne LiDAR may not have the same biases as TLS towards larger/protruding grains.

It is also critical to note that whilst estimation of particle b-axis lengths from point cloud elevations has been popular in the literature, stronger relationships between the c-axis length and σ_z have been demonstrated by numerous authors (Pearson *et al.* 2017; Vázquez-Tarrío *et al.* 2017). This is a result of the typical alignment of grains to flow, resulting in the a- b-axis plane aligning parallel with the bed surface, and the c-axis aligning normal to the bed surface. Reported relationships between σ_z and the b-axis may therefore be a product of site specific relationships between the b- and c-axis lengths of particles.

Further work is still required to improve the estimation of grain size from point clouds, but these results support the use of both TLS and SfMp as a tool for quantifying surface roughness. Understanding how sensitive entrainment models are to the surface roughness measurements is also a critical avenue for future research.

2.6.2 Describing Surface Texture

S_{kz} and K_{uz} coefficients may be used to describe the distribution of particle sizes on the bed surface, which may provide a means to quantify resistance to entrainment (see Aberle & Nikora, 2006). Following the rationale of Aberle & Nikora (2006) we would expect to see high S_{kz} coefficients for our surveys due to the fine sediment deposited between protruding clasts (Figure 2.10), assuming the fines formed a flat surface, and skewness would be increasingly positive with increasing armouring (higher frequency of coarse particles). We would also expect leptokurtic K_{uz} coefficients as more data points should be distributed around the centre (in this case the mean $z_{detrended}$). All grid 1 detrended surfaces produced negative skewness, whilst all grid 2 produced positive skewness, excepting the October 2016 SfMp survey which was negatively skewed. For the spatially varied S_{kz} data the median values were all positive, and 75% of Q1 values were 0; the three which werent were all from the October 2015 survey. The spatially varied S_{kz} therefore suggest an armoured surface. TLS data tended to show higher S_{kz} than SfMp.

K_{uz} coefficients for both point cloud survey methods varied more than those of Aberle & Nikora (2006) whose K_{uz} coefficients ranged from 3.1 - 5.4 over 13 surveys. With the large amount of fines in the surface layer we would expect to see a greater sorting towards the centre of the distribution, or the mean $z_{detrended}$. We would also expect to see higher K_{uz} coefficients for the Grid 2 $z_{detrended}$ data from less influence of bedforms on the mean surface height, which we observe for all surveys. The complete cloud analyses supported these hypotheses with both survey methods and grid sizes returning high positive K_{uz} coefficients. The spatially varied K_{uz} values did not show the leptokurtic distributions expected, particularly for grid 2 which had consistently more platykurtic coefficients than their grid 1 counterparts. This is evident in Figure 2.11. Our analysis suggests the moments of the elevation data are increasingly affected by gridding resolution, with less systematic influence of survey method.

2.6.3 Implications for Modelling and Management

Our results have shown both TLS and SfMp identified similar patches of σ_z subclasses. The greatest impact on σ_z was grid size used for detrending or spatial variation. There was also no clear bias towards one survey method producing larger or smaller calculations of σ_z.

σ_z is also commonly used to estimate a characteristic grain size. Quantification of grain size is a key component of accurately estimating particle entrainment thresholds and transport rates, but the representative percentile used varies within the literature (Green, 2003; Neverman *et al.* 2016). Green (2003) suggests the selection of a representative grain size percentile for flow competency modelling should consider the sampling precision for each percentile. TLS derived σ_z was shown to be better related to the D_{50} and D_{84} than the SfMp for the study area as a whole (i.e. not spatially differenced), and grid 2 SfMp was inversely related to the pebble counts. But as discussed previously the direct relationship between the b-axis and σ_z may not be valid as many factors influence the relationship between the b-axis length and surface roughness, in particular, grain alignment and burial. Several authors have highlighted that the c-axis is better related to surface roughness as the c-axis tends to align normal to the bed surface (i.e. in the direction of the z axis

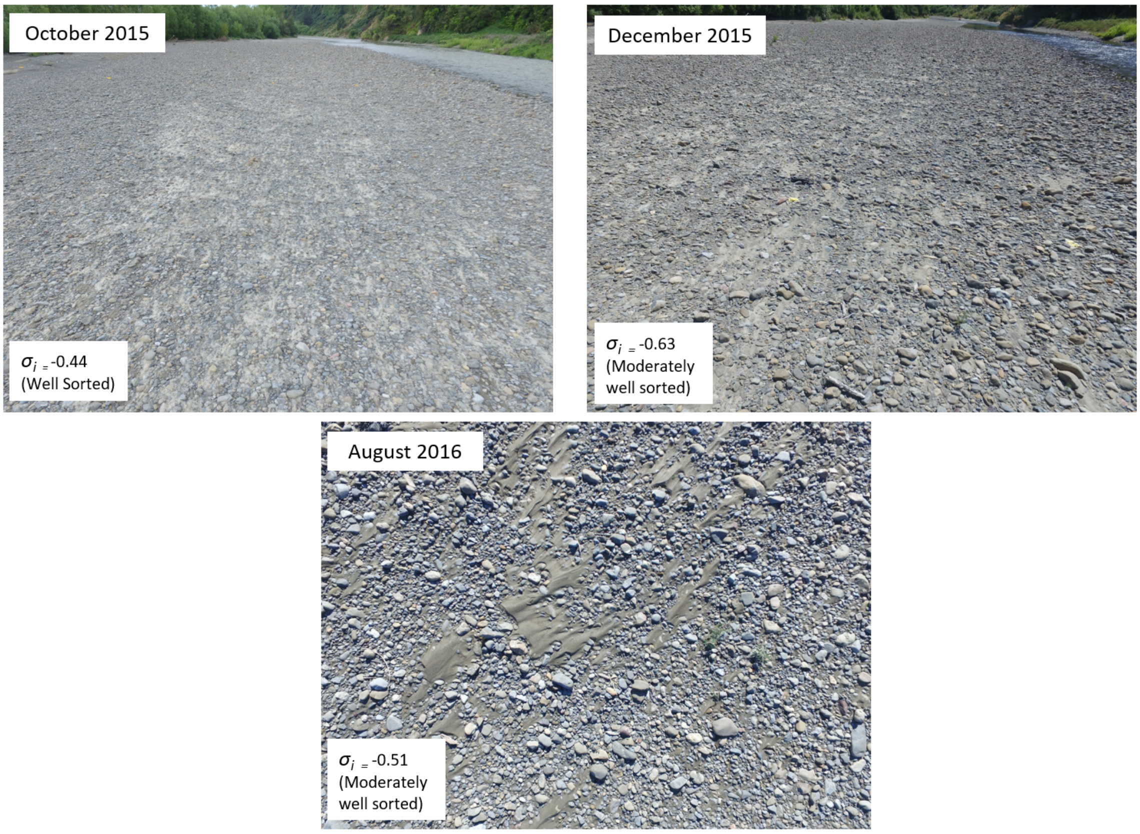

Figure 2.10: Images of the substrate surface for each survey, along with sorting coefficients derived from the pebble count data.

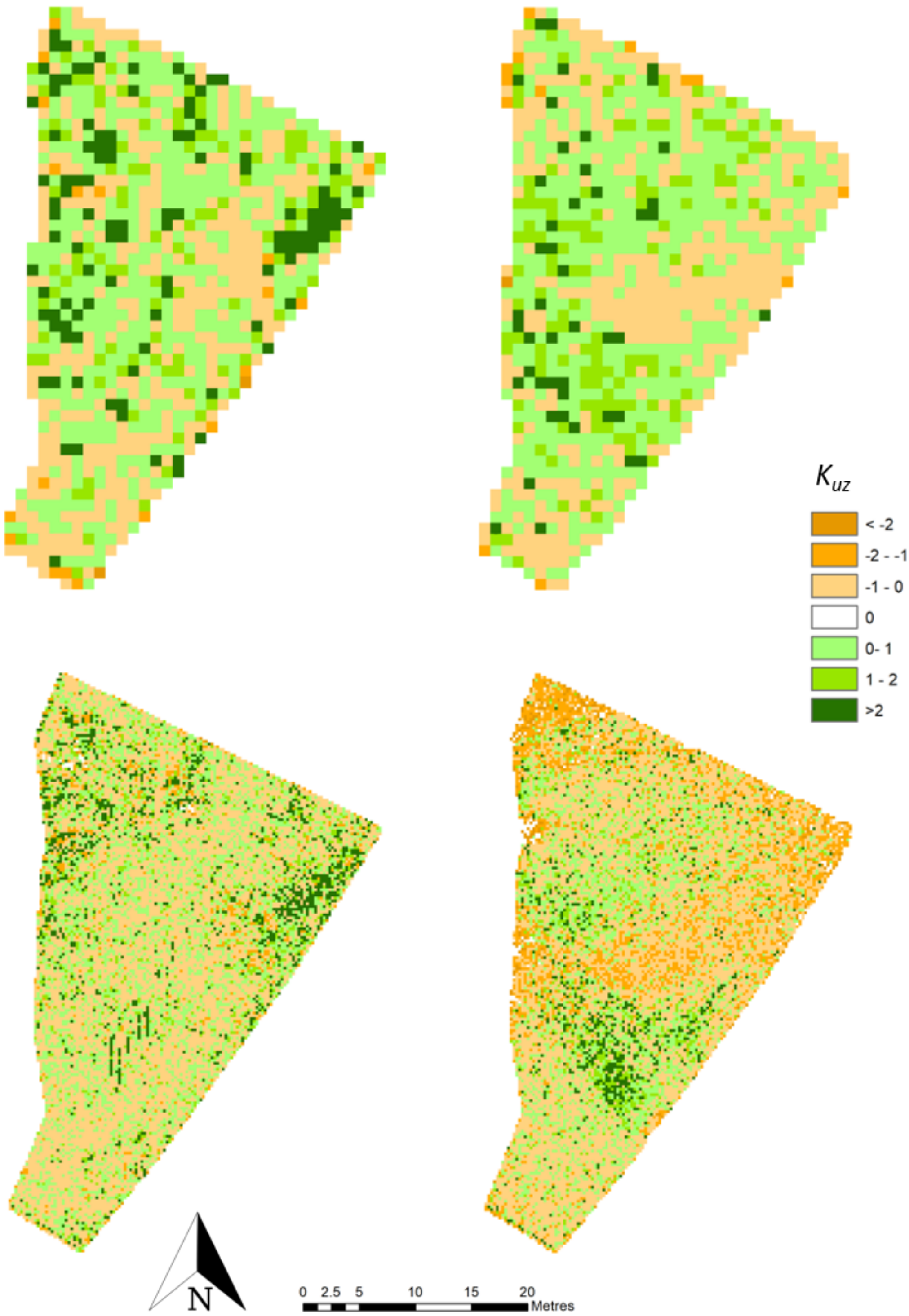

Figure 2.11: Rasters showing the spatial variation of K_{uz} for the October 2015 survey 1 m (top) and 0.25 m (bottom) cell resolutions. SfMp surveys are on the left and TLS on the right. Note the higher frequency of more extreme platykurtic cells in the 0.25 m rasters, particularly the TLS.

used to calculate roughness). However, entrainment formulae often rely on the b-axis measurement for calculating or proxying particle volume. Unless relationships between the c- and b-axes can be derived and used to better estimate b-axis length from surface roughness, which would involve site specific relationships, it may be more appropriate to measure b-axes for entrainment formulae using methods such as photo-sieving which are capable of planimetric measurement of particles. Carbonnneau *et al.* (2018) have provided a proof-of-concept for including the SfMp process in a pipeline for photo-sieving. It may therefore be possible to extend the use of SfMp datasets to the measurement of planimetric grain axis, which TLS is not as suited for. Although grain edge detection from point clouds has been demonstrated (e.g. Measures & Tait, 2008) the occlusion present in many field TLS datasets makes this challenging. sUAS-bourne LiDAR surveys may help to reduce the occlusion in grain-scale point clouds, but the impact on grain size estimates is yet to be demonstrated.

It is also important to understand the limitations of the pebble count derived metrics used for comparison in this paper. This method is biased towards sampling of coarse particles, and poorly accounts for fines. Rice & Church (1996) suggest the D_{50} may be the most poorly estimated percentile due to the often bimodal distribution of fluvial sediments (Sambrook Smith, 1996). Percentiles above the D_{50} have been found to have lower sampling errors, and sampling errors were lower than expected based on a theoretical log-normal distribution (Rice & Church, 1996; Green, 2003). Given these limitations, photo-sieving techniques may be better suited to derivation of characteristic grains sizes than conventional Wolman samples, and may make spatially varied sampling more logistically feasible.

Using moments of point cloud elevation data has proven challenging, and appears to be significantly affected by gridding parameters for higher moments. Further work is required to better understand the relationship between these moments and surface texture and structure of gravel beds. It is important to understand what values of these coefficients are significant for representing different degrees of resistance to entrainment, and how these can be included as parameters for entrainment modelling. However, quantifying resistance to entrainment using other objective techniques in a way which can be compared with these coefficients is challenging.

It is also critical to understand how fine registration errors may impact the spatially varied moment calculations. The analyses presented in this paper have shown that spatially varied metrics vary between TLS and SfM surfaces, and assumed these variations are a result of different representations of surface elevations between these methods. However, different sources of registration errors are also present in each model and these may result in differences in the data points being represented by each cell of the detrending and spatial variation grids. There is a need for future research to address the impacts of point cloud registration on the calculation of spatially varied metrics, and provide suggestions on appropriate gridding resolutions. This will be particularly critical if researchers seek to quantify spatial changes in surface texture and structure between surveys.

2.7 Conclusions

Terrestrial Laser Scanning and Structure-from-Motion photogrammetry both provide opportunities to quantify surface layer texture, structure, and development in natural heterogeneous gravel-bed rivers. Accurate quantification of surface layer characteristics is critical for progressing our ability to predict substrate scour events by providing much needed parameters for entrainment threshold and transport rate models. Through better measurement and prediction of the magnitude, frequency, and extent of scour events, managers will be able to improve the assessment of the impact of restoration schemes on habitat structure and physical processes and improve predictions of system trajectories. However, the impact of sampling biases and errors between TLS and SfMp on the metrics derived from their point clouds needs to be better understood so the optimal method can be chosen for data acquisition, and for understanding the limitations of analyses performed using either technique.

Our results have shown SfMp and TLS provide similar quantification of surface roughness based on σ_z of $z_{detrended}$. This is the most commonly derived metric from point clouds at present for the description of gravel surfaces. Higher order moments were also calculated to describe the texture of the gravel surface, but these results were found to be significantly influenced by the cell size used for detrending and spatial analysis, which made it challenging to discern a methodological influence on coefficient differences.

However, the SfMp workflow offers several other advantages for surface characterisation that TLS struggles to offer presently. In particular, the robotic photo-sieving method described by Carbonnneau *et al.* (2018), which may utilise the SfMp dataset, offers the potential to combine photo-sieving measurements of the planimetric measurements of particles with the metrics derived from point cloud elevations, potentially allowing a wider range of metrics to be derived from the same dataset.

This paper has demonstrated the significant progress in our ability to quantify the texture and structure of the surface layer of gravel beds using remote sensing approaches over conventional, manual sampling procedures. The metrics derived from these remote sensing approaches provide a step-change in our ability to parameterise entrainment and transport rate models for gravel beds by quantifying texture and structure characteristics. Surface texture and structure has been challenging to quantify continuously over spatial extents and resolutions suitable for entrainment parameterisation. This progress is critical for improving the management of physical processes in riverine systems, and thus enhancing the health of degraded rivers. As highlighted by Moore & Rutherfurd (2017) river management schemes are often not maintained, leading to poor performance. Identifying changing trajectories and adjusting management practices accordingly is a key step towards improving the maintenance of river systems. The relatively rapid data collection over large spatial extents afforded by SfMp given the ability to capitalise on sUAS may improve the temporal resolution and spatial extent of surface layer characterisation, and afford higher frequency repeat monitoring, allowing changes in entrainment thresholds and system trajectories to be identified, and management practices to be adjusted in a timely manner.

2.8 Notation

D	Grain b-axis length (grain diameter)
D_{50}	50^{th} percentile grain b-axis length
D_{84}	84^{th} percentile grain b-axis length
K_{ui}	Inclusive Graphic Kurtosis (pebble count)
K_{uz}	Point Cloud Kurtosis
σ_i	Sorting (Inclusive Graphic Standard Deviation)
σ_z	The Standard Deviation of $z_{detrended}$
S_{ki}	Inclusive Graphic Skewness (pebble count)
S_{kz}	Point Cloud Skewness
$z_{detrended}$	Bed elevations with the local trend removed
ΔK_{uz}	Difference in K_{uz} between SfMp and TLS
$\Delta\sigma_{\mathrm{z}}$	Difference in σ_z between SfMp and TLS
ΔS_{kz}	Difference in S_{kz} between SfMp and TLS
Δz	Difference in elevation between SfMp and TLS

2.9 Acknowledgements

The authors wish to thank Charlotte Holdsworth, Matthew Hemler, Nathan Forrester, and Szabolcs Kosik for their assistance with field work. We also thank Gabor Kereszturi for his instruction on using the MS50, and Jon Tunnicliffe for his assistance with establishing our SfMp capabilities.

2.10 Funding

Andrew Neverman is in receipt of a Massey University Doctoral Scholarship, and fieldwork was in part funded by grants provided by the Institute of Professional Engineers New Zealand (IPENZ) Rivers Group [2015 Student Research Grant] and the New Zealand Hydrological Society. Manaaki Whenua is thanked for supporting this research from Strategic Science Investment Funding.

Summary of Chapter 2 for Thesis

This chapter has compared the description of surface layer structure development using TLS and SfMp point clouds. The results revealed both methods provided a similar quantification of surface roughness, but the metrics used to quantify surface layer structure were affected by both the survey method and some data processing parameters. The chapter highlighted the potential for these metrics to be used to improve the description of surface structure, which is important for understanding how substrate structure affects bed resistance measurements (Chapter 3), and for balancing hydrodynamic forces to understand variations in flow thresholds for particle entrainment (Chapter 5). Further work is required to understand how the metrics derived from these point clouds relate to armouring, and how the metrics can be used to model surface layer resistance. The chapter also identified emerging techniques which may be more suitable for quantifying grain size, which is a critical component of entrainment modelling. The metrics identified in this chapter may also be used to indirectly assess bed mobility potential, and may be used for future development of high-technology bed stability indicies as an alternative to the low-cost index presented in Chapter 4.

Chapter 3

Rapidly Quantifying Compactness of the Active Layer in Gravel-Bed Streams

Introduction of Chapter 3 to Thesis

Chapter 3 addresses the present gap in methodologies for quantifying the compactness of the active layer in gravel beds. Chapter 3 accomplishes objective ii-b by developing a protocol for using a penetrometer to quantify the resistive force of the bed, providing a value which is directly comparable to entrainment forces. This protocol improves on the methods of Sear (1992), Sear (1995), and Pedersen & Friberg (2007) who used a penetrometer to derive an index which indicates the relative compactness of the bed when compared to other sites, but do not provide a quantification of resistive forces. The protocol developed in this chapter also accounts for active layer thickness, ensuring only the compaction of the active layer is assessed. This chapter also provides the development of a modified Mackintosh probe penetrometer which was designed to be sensitive to variations in active layer compactness, and has modifications which reduce observer bias and blunders. The protocol therefore provides a valuable tool for improving the assessment of bed resistance, developing entrainment models, and tracking changes in armour layer development and habit change. As such, it develops our understanding of bed structure derived from Chapter 2, and provides a rapid, low-cost, low-technology approach to link bed structure with potential bed mobility.

This chapter is in preparation as a manuscript for Earth Surface Processes and Landforms as:

Neverman, A.J., Fuller, I.C., & Death, R.G. (In Prep). Rapidly quantifying compactness of the active layer in gravel-bed streams.

3.1 Abstract

The ability to predict the entrainment of gravel particles is essential to improve management of river systems. The frequency and magnitude of gravel movement affects ecological health and hazard risk. Improved prediction of bed moving events relies on accurate calculation of bed resistance and hydraulic entrainment forces. Bed compactness is an important parameter of bed resistance but is rarely quantified and is often missing from resistance assessment. This likely results from a lack of appropriate methodologies for measuring compactness. A limited number of published studies have used penetrometers to assess substrate stability in gravel-bed channels, but there is no consistent methodology, and they rarely produce values which can be used in flow competency equations. This paper presents a technique to quantify the compactness of gravel stream beds using a modified Mackintosh probe penetrometer. The modified penetrometer limits the introduction of observer error, and ensures measurements are comparable between penetrometer designs, observers, and sites. Most importantly, the protocol presented here converts the Penetration Rate into Substrate Resistance, measured as force in Newtons, which is the unit used in hydraulic force measurements and therefore provides a means to directly compare bed resistance with entrainment force. The method was trialled at six sites to test co-dependency of the outputs with other characteristics of the active layer as a technique to provide comparative assessment of compactness is not available. A case study from a separate site, the Waikanae River, New Zealand, is presented to demonstrate application of the technique to quantify habitat modification following river engineering. This case study demonstrated the ability of the methodology to distinguish between modified and unmodified beds, and provide an assessment of the degree of modification to assess the impact on habitat quality. In particular, the method identified the downstream impact of engineering, and provided a valuation around the degree of weakening or strengthening of the active layer.

3.2 Introduction

The entrainment and transport of gravel particles has received considerable attention in the literature for over a century (Herschel, 1878; Shields, 1936; Einstein, 1937; Javernick *et al.* 2018; Liedermann *et al.* 2018; Rickenmann, 2018), yet the prediction of substrate movement events in natural channels remains elusive. Estimation of substrate entrainment thresholds and quantification of substrate stability are key objectives for river managers and scientists because the frequency and magnitude of entrainment events is important for structuring benthic communities and habitat (Resh *et al.* 1988; Death, 2008, 2010), and driving morphological adjustment of the channel with associated implications for flooding and erosion (Raven *et al.* 2009, 2010; Guan *et al.* 2016; Slater, 2016). Predicting the magnitude and frequency of bed movement is vital for understanding riverine system trajectories under forecast flow conditions. This is essential for the development of effective management plans for infrastructure, flooding and erosion hazards, ecological health, and improving the maintenance of implemented management schemes; where many schemes often fail (Moore & Rutherfurd, 2017).

The estimation of entrainment thresholds is frequently simplified to a function of individual particle submerged weight and streamwise hydraulic forces, with little consideration of the complex variability in resistance forces created by particle interactions (Laronne & Carson, 1976). Lorang & Hauer (2003) attribute this reliance on overly-simplified flow competency equations to the difficulty of finding alternative equations in the literature. Another factor leading to the limited inclusion of substrate resistance parameters in flow competency models is a lack of methodologies to quantify the sources of resistance, thus preventing their inclusion in equations.

Substrate resistance is largely a product of the changed propensity for individual grains to become mobile due to the grain-on-grain interactions caused by arrangement of particles in the bed. This arrangement of particles in referred to as bed structure (Buffington & Montgomery, 1999; Bertin & Friedrich, 2018), and is a product of the grain size distribution (bed texture), particle form, flow regime, and channel morphology (Wittenberg, 2002). In natural gravel riverbed environments, a wide range of substrate textures and structures can be encountered, and lead to distinct bed morphologies with characteristic stability. Distinct morphologies include stepped-bed channels, cascades, plane bed, and riffle-pool morphologies . Gravel beds can be defined as matrix- or framework-supported depending on whether the bed structure is held together by fines (sands and smaller) or gravel, respectively (Lisle, 1989; Wilcock & Southard, 1989; Wilcock, 2001). Open-work or closed structure (Laronne & Carson, 1976) beds may also be encountered, which describes the presence or lack of fine material in the void spaces of the framework. Closed-structure beds may be referred to as embedded or mortared (mortared beds usually consist of sticky sediments which cement the framework particles into a cohesive bed) (Osmundson & Scheer, 1998; Bunte & Abt, 2001; Hodge *et al.* 2013). Fines enter the bed through a process known as colmation, also referred to as clogging, ingress, infilling, or siltation (Wharton *et al.* 2017). Removal of finer sediment fractions from the bed via size-selective entrainment at lower flows leads to restructuring of the bed, and these beds are termed winnowed or water-worked beds. Each of these beds has a characteristic level of stability due to the resistance created by the characteristic structure of the beds.

Beds may also be described as unstructured or structured depending on the degree of structural elements present. Recognisable structural elements include features such as grain protrusion/surface roughness (Fenton & Abbott, 1977; Buffington *et al.* 1992; Ferguson, 2005); bed packing (Downes *et al.* 1998; Papanicolaou *et al.* 2002); pebble clusters (Dal Cin, 1968; Church *et al.* 1998; Wittenberg & Newson, 2005), and imbrication (Millane *et al.* 2006; Qin *et al.* 2012). Advancements in remote and proximal sensing data collection and analysis have generated methods capable of quantifying grain protrusion/surface roughness (e.g. Heritage & Milan, 2009; Brasington *et al.* 2012; Rychkov *et al.* 2012), pebble clusters (e.g. Papanicolaou *et al.* 2012), and imbrication (e.g. Millane *et al.* 2006). However, quantification of bed packing remains elusive.

Bed packing refers to the arrangement of grains with respect to one another in the bed (Church, 2006). In heterogenous substrates packing results in the interlocking of particles due to variations in particle shape and size. The more interlocked the particles are, the more resistant they are to movement, and the more tightly packed the bed is said to be. Tightly packed beds reduce the mobility of individual particles (Church, 2006). Hereafter we refer to the tightness of bed packing as the *compactness* of the bed. Compactness relates to the particle density per unit volume. As beds become more compact, they either decrease in volume (reduction of void spaces as interlocking increases) or become denser (intrusion of particles into void spaces). Compactness is therefore related to porosity.

Civil engineers and geotechnical surveyors frequently measure the compactness of soils to test their load bearing capacity. The standard methodology for measuring soil compactness is via a *penetration test* using a device known as a *penetrometer* (Fakher *et al.* 2006; Rahman *et al.* 2016). Penetrometers comprise a rod with a pointed tip which is driven into the soil with a drop weight of consistent mass and travel distance (Rahman *et al.* 2016).

Narahari *et al.* (1967) demonstrated the application of penetrometers for measuring the compactness of gravel foundations. A limited number of studies have adapted the approach of Narahari *et al.* (1967) to quantify bed stability in gravelly stream beds using a penetrometer (e.g. Sear, 1992; Sear, 1995; Pedersen & Friberg, 2007). Sear (1992) and Sear (1995) used a penetrometer to test compactness of the bed surface and found a statistically significant difference between regulated and unregulated riffles, and between riffles and pools, as is to be expected (Grant, 1982). Pedersen & Friberg (2007) used a penetrometer to classify the compactness of two riffles and compared the results with tracer particle data. The authors recorded greater penetration (less compactness) at the riffle with the highest rate of tracer movement. Penetrometers have therefore shown promise for assessing compactness in gravel-bed rivers, producing results which were consistent with expectations, but these studies lacked any consistent methodology and produced index values, inhibiting comparisons using the datasets. Pedersen & Friberg (2007) measured penetration at 36 spots over a survey area, using a consistent number of blows (hammer drops), and using the depth of penetration to quantify compactness. Sear (1995) measured penetration four times at 10 locations across a transect using a consistent depth of 0.05 m, and therefore using the blow count (number of times the hammer was dropped on the anvil) to compare compactness. The four recordings were averaged at each location to give a score, then the scores for each location were averaged to give a score for the site. Sear (1992) tested compactness of the first 50 mm and 100 mm of the bed surface.

This paper presents a new technique for using penetrometers to test active layer compactness in gravel bed streams, referred to as the *Bed Compactness Index*, with the aim to establish a consistent method to enable dataset comparisons. The technique has been trialled at six sites with varying substrate characteristics. As there are no tools currently available to measure bed compactness, the results from the study are compared with other substrate properties to assess dependence of the penetration tests on substrate properties other than compactness. A case study is then presented to demonstrate the application of the Bed Compactness Index for quantifying the impact of engineering works on bed substrate as a means of assessing habit modification.

3.3 Study Sites

The Bed Compactness Index (*BCI*) was trialled at six sites in the Manawatu and Hawke‘s Bay regions, North Island, New Zealand (Figure 3.1). These sites offered a range of low to middle order gravel-bed channels (Figure 3.2), with a range of substrate compositions (Table 3.1). Surveying was conducted between January and June 2017.

A seventh site, the Waikanae River, Wellington, New Zealand (Figure 3.1), was used as a case study to demonstrate the application of the *BCI* for river management. The Waikanae River is a 5$^{\text{th}}$ order gravel-bed river which flows from the western side of the Tararua Ranges, through the settlement of Waikanae to the coast at Waikanae Beach. Channel engineering works on a section of the Waikanae River afforded the opportunity to use the *BCI* to measure bed compactness before and after river engineering works at control and engineered sites, and provide a quantification of the change in substrate resistance. Four reaches were surveyed. Reaches 1 and 2 were used as control sites where no channel engineering was planned, and reaches 3 and 4 were located within the planned engineering works. The bench mark survey was conducted during December 2016. The repeat survey was conducted during June 2017.

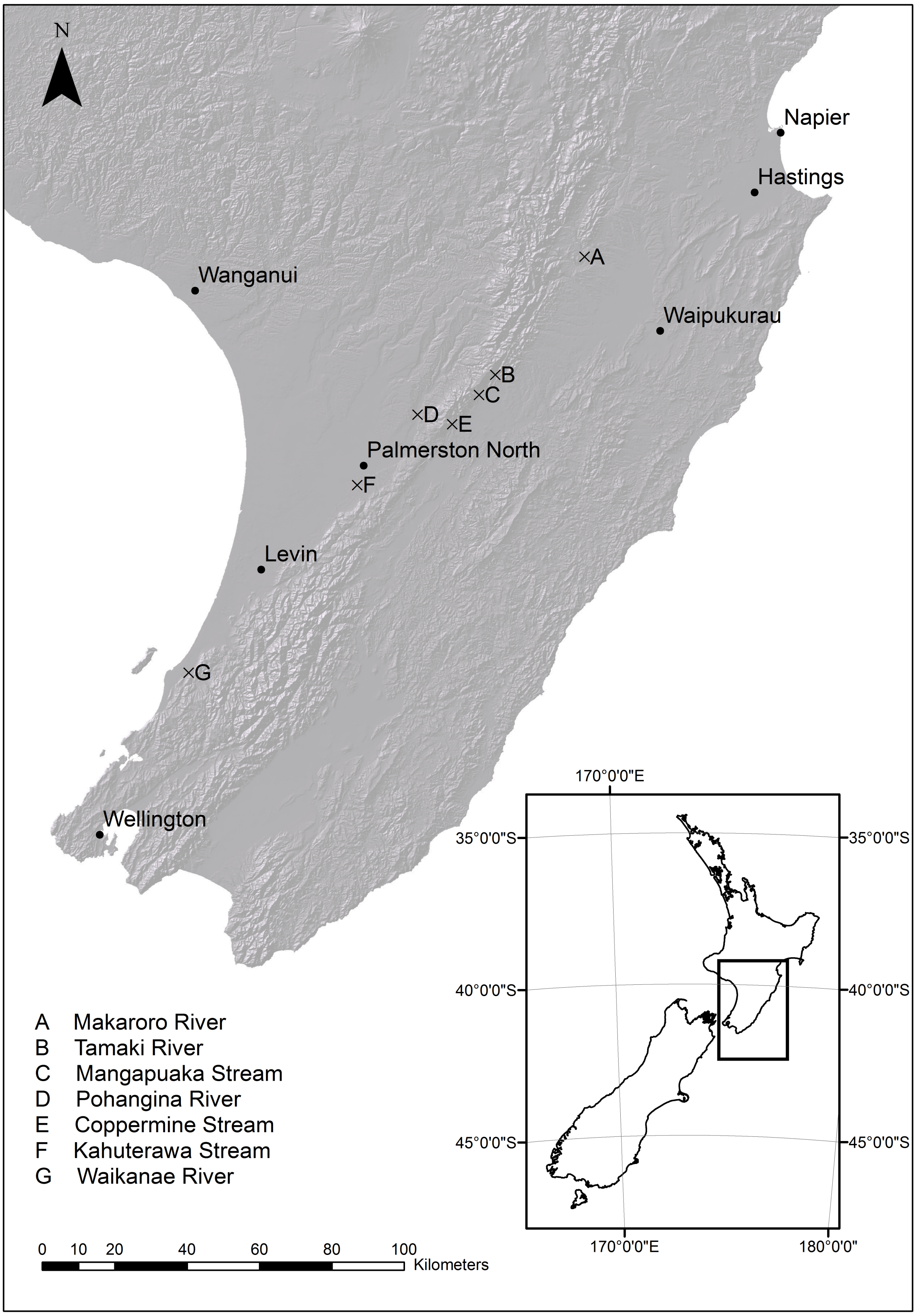

Figure 3.1: Site locations. Sites A-F are the trial sites.

Table 3.1: Site characteristics. Grain size for the Waikanae shows range between the study reaches.

Label	**Site**	D_{50} **mm**	D_{84} **mm**	D_{90} **mm**	**Stream Order**	**Sinuosity**	**Sorting**
A	Makaroro River	35	58	62	4	1.67	Moderately Well Sorted
B	Tamaki River	52	79	89	3	1.12	Moderately Well Sorted
C	Mangapuaka Stream	34	64	82	3	1.09	Moderately Sorted
D	Pohangina River	89	122	127	5	1.1	Moderately Well Sorted
E	Coppermine Stream	62	196	287	3	1.07	Poorly Sorted
F	Kahuterawa Stream	54	91	104	4	1.26	Moderately Well Sorted
G	Waikanae River	20-42	32-77	46-93	5	1.25	Moderately Sorted

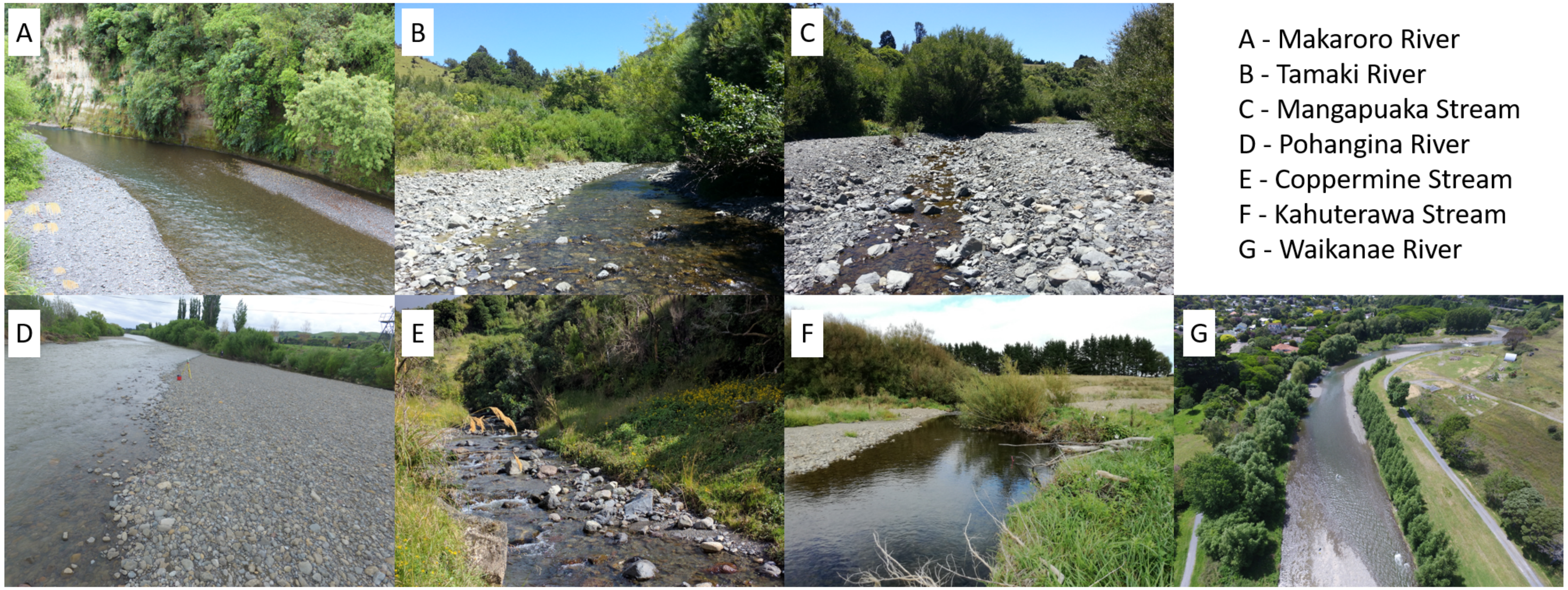

Figure 3.2: Photographs showing the characteristics of the six trial sites, ranging from third order boulder-bed headwater streams to 6$^{\text{th}}$ order wandering lowland rivers.

3.4 Methodology

The *BCI* presented here improves on previous compactness tests in gravel-bed streams by a) developing a penetrometer which is suitable for use in gravel beds and limits observer bias, b) standardising the approach used to conduct the penetration tests, and c) converts the compactness index to a measure of material strength measured in Newtons, allowing direct comparison with stress measurements.

3.4.1 Conducting Penetration Tests

The *BCI* uses a modified version of the Mackintosh probe (c.f. Clayton *et al.* 1995), here after referred to as the penetrometer (Figure 3.3). The penetrometer has a total length of 1.152 m, and consists of a 12 mm long rounded tip, a 2.2 kg brass slide hammer, an anvil, and a hammer stop. The hammer has a drop height of 300 mm. Early designs used a nylon ring to mark penetration depth, but this was found to wear quickly and become loose. The ring was also affected by protruding grains and debris resulting in false depth readings. To overcome this limitation, a depth reader attachment was made for the penetrometer which consists of a flat foot, a vertical rod, supports (Figures 3.3 & 3.4), and a tape measure added to the hammer (Figure 3.4). The top of the rod aligns with the base of the tape measure when the foot and penetrometer tip are aligned (i.e. both sitting flush on the bed surface). As the penetrometer is driven into the bed, the top of the rod reads higher up the tape measure, allowing penetration depth to be measured accurately (Figure 3.4).

Penetration tests are performed by placing the penetrometer tip between surface grains, with care taken not to drive the rod into the bed. The depth marking foot sits on the surface of the bed. The starting depth is read using the depth reader and recorded. The hammer is lifted to the hammer stop and released. The hammer free falls on to the anvil, driving the tip in to the bed, and 1 *blow* is counted. The new depth is read, and the starting depth is subtracted to give the penetration depth (d).

As the intended use of the *BCI* is to estimate substrate resistance to entrainment, the *BCI* aims to quantify compactness of the active layer only, and not subsurface material. The *BCI* therefore limits d so the Penetration Rate (*PR*) is only calculated in the active layer. However, d could be adjusted if compactness measurements of the subsurface are desired. There is no clear value in the literature defining armour layer thickness, nor a definitive way to measure armour layer thickness easily in the field. DeVries (2002) defines a *disturbance depth*, which is the depth of the substrate which the surface flow may act upon, and is associated with 2 times the D_{90}. For the purposes of this study, we have defined the armour layer as the surface layer of grains which the surface flow may act on, as this will be the layer which is first entrained and whose resistance to entrainment therefore relates to entrainment thresholds. This is also often referred to as the active layer, and this will be the terminology used in this paper. We can therefore define the active layer following DeVries (2002) as the surface material to a depth equivalent to $2D_{90}$. As the penetrometer tip begins in the interstitial spaces of the surface material, we suggest the first layer is not completely sampled by the penetrometer. We are therefore left with approximately the D_{90} depth to sample. d should therefore equal the D_{90}.

If the penetration depth is less than the D_{90} after the first blow the hammer is dropped again until the D_{90} depth is reached (i.e. $d = D_{90}$). The number of blows (n_{blows}) required to reach d are counted and recorded. In cases where the penetration of the penetrometer is inhibited by a particle, the penetrometer may be moved to a neighbouring interstitial space. If the penetrometer still cannot reach a depth equal to the D_{90} the number of blows and penetration depth up until the inhibiting clast are recorded as n_{blows} and d, respectively. These values are used to calculate the Penetration Rate (PR), using Equation 3.1:

$$PR = \frac{d}{n_{blows}} \tag{3.1}$$

where n_{blows} is the blow count (number of blows) and d is the penetration depth. To maintain consistency for the survey area and number of measurements taken, PR was measured at 30 spots over a reach with length equal to the pool-pool spacing, or five times the wetted channel width (c.f. Montgomery *et al.* 1995). This allows for variability in compactness between subaqueous geomorphic units to be accounted for in the compactness score. We focused on the wetted channel as that is relevant for high frequency bed movement and aquatic habitat. The 30 PR measurements were distributed over six evenly spaced transects (spaced at distances equal to the wetted channel width), with five PR measurements conducted at even spacing across each transect. To give a final quantification of compactness at the site, the Bed Compactness Index (BCI) is calculated as the mean of the 30 PR measurements from the reach. The BCI is therefore calculated using Equation 3.2, and provides a spatially-integrated quantification of compactness.

$$BCI = \frac{1}{n}\sum_{i=1}^{n} PR_i \tag{3.2}$$

3.4.2 Calculating the D_{90}

The D_{90} was derived from a cumulative frequency plot of a 100 clast sample of the surface grains collected using the Wolman (1954) protocol. A gravelometer (pebble template) was used to measure the b-axis of the clasts to reduce observer error (Green, 2003; Daniels & McCusker, 2010). The gravelometer sampled at 0.5 ϕ intervals from 3.5 - 8 ϕ (12 - 256 mm) (c.f. Wentworth, 1922; Krumbein, 1936). To ensure sampling randomness the boot (Bunte *et al.* 2009) or big toe (Neverman *et al.* 2016) method was used.

3.4.3 Calculating Substrate Resistance

Following the Energy-Work theorem of Halliday & Resnick (1962) the work done by the substrate to stop the penetrometer can be calculated and used to describe the substrate penetration resistance. Herrick & Jones (2002) apply the Energy Work theorem to penetration tests, defining penetration resistance as the force applied to the penetrometer causing deceleration from initial velocity to zero velocity, where initial velocity results from the hammer striking the anvil. Substrate penetration resistance is therefore calculated following Herrick & Jones (2002) using Equation 3.3:

$$R_s = \frac{W_s}{P_d} \tag{3.3}$$

where R_s is the substrate resistance (N), W_s is the work done by the substrate, and P_d is the penetration depth (m) (equivalent to d in the BCI). Equation 3.1 can be reworked using the PR (m) in place of P_d to calculate the depth-integrated R_s for each measurement spot. P_d can also be replaced by the BCI score (m) to calculate the depth- and spatially-integrated (double-averaged) substrate resistance for the reach, giving Equation 3.4:

$$R_s = \frac{W_s}{BCI} \tag{3.4}$$

The work done by the substrate (W_s) can be substituted with the kinetic energy (KE) of the hammer as it strikes the anvil, which is calculated using Equation 3.5:

$$W_s = KE = \frac{1}{2}mv^2 \tag{3.5}$$

where m is the mass of the hammer (kg), and v is the travelling velocity of the hammer as it strikes the anvil (m s^{-1}). v is calculated using Equation 3.6:

$$v = \sqrt{v_2^0 + 2a(x)} \tag{3.6}$$

where v_o is the velocity at time 0, a is the acceleration due to gravity, and x is the negative change in height (i.e. the hammer drop height).

Working through these equations for the penetrometer used in this paper, Equation 3.6 gives a travelling velocity for the hammer as 2.4 m s^{-1}, with $v_o = 0$, $a = 9.8\ ms^{-2}$, and $x = 0.3$ m. The kinetic energy of the hammer as it strikes the anvil is 6.468 J, with $m =$ 2.2 kg, and $v = 2.4$ m s^{-1}. Equation 3.4 is then used to calculate the substrate penetration resistance (R_s) for each site. Alternatively, a conversion curve (Figure 3.5) may be used for conversion in the field.

3.4.4 Comparison Substrate Characteristics

To identify the potential dependence of PR on substrate characteristics other than compactness, the shape, characteristic grain sizes, form, grain size distribution moments, and alignment of particles on the bed surface were measured.

Sorting, graphical skewness, and graphical kurtosis were calculated using the equations of Folk (1980) to characterise the size distribution of particles. Clast roundness was calculated using Callieux roundness for a sample of 30 clasts. "Flatness" of the substrate was calculated using the C_{40} index of Benn & Ballantyne (1994). The C_{40} index is a measure of the percentage of clasts whose c:a axis ratio is ≤0.4 (i.e. elongated clasts). The C_{40} index was calculated from the 30 clasts used to measure roundness.

Grain alignment was quantified by measuring the alignment of the b-axis relative to flow using a compass for 30 *in situ* clasts. The standard deviation (σ) of the sample was used to quantify alignment to account for the range of alignment angles. A low standard deviation relates to sites where most clasts have similar alignment, and are therefore more structured.

Imbrication of the substrate is also likely to have a significant effect on compactness. Visual assessment at each site suggested imbrication was low at all sites, and penetration tests were not conducted in imbricate structures. The substrates were also all framework-supported, and only the subaqueous bed was included, therefore the impact of bed saturation was not examined.

Pearsons correlation coefficients and the coefficient of determination were calculated in R using the stats package (R Core Team, 2013) for all relationships between the BCI and the comparison substrate characteristics.

3.5 Results

At the six trial sites the BCI scores ranged from 2.6 to 7.2, with σ ranging from 1 to 5.7 (Table 3.2). These scores are equivalent to penetration rates of 2.6 mm and 7.2 mm per

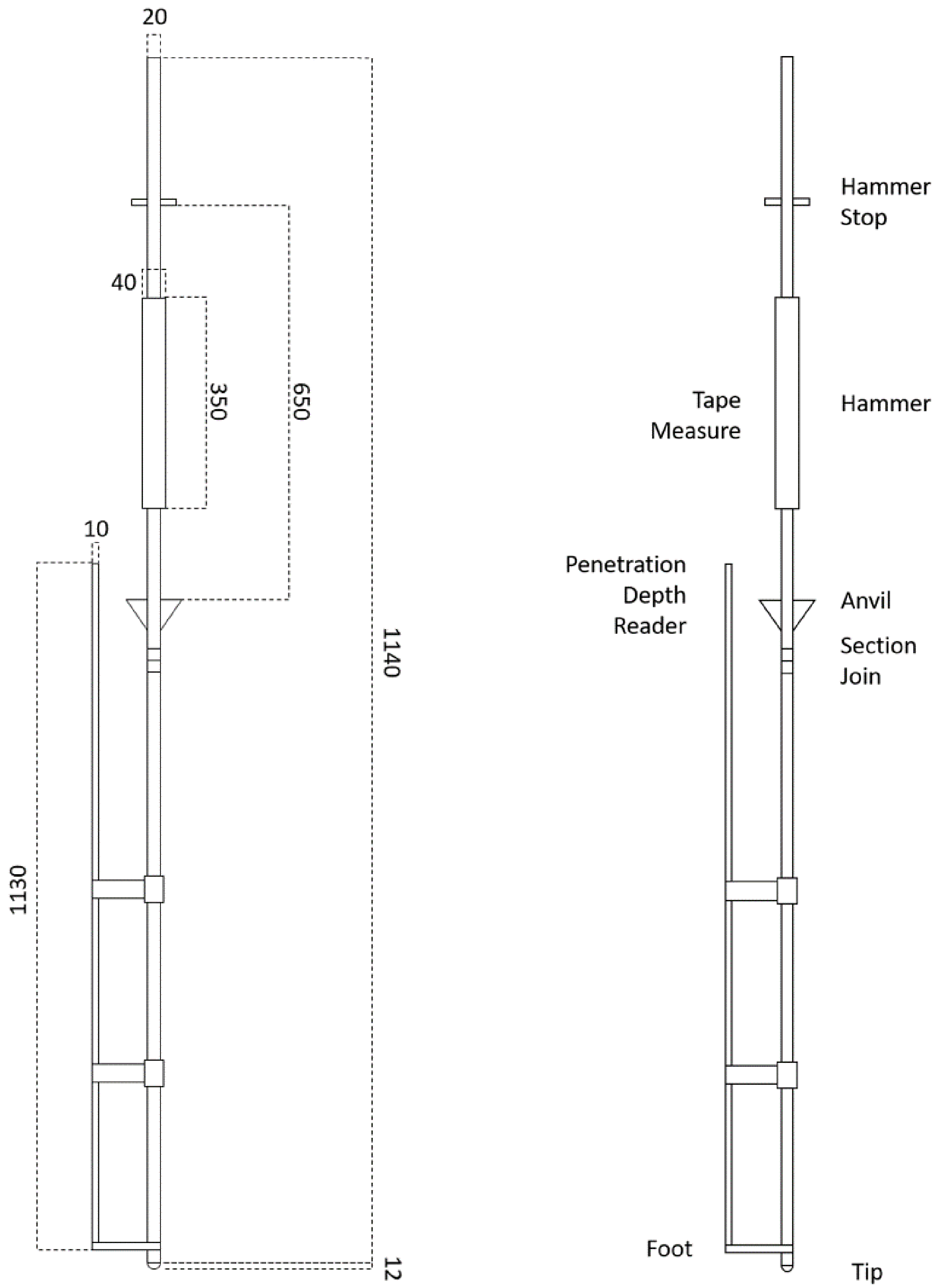

Figure 3.3: Schematic of the penetrometer design, showing dimensions and part names.

blow. Following Herrick & Jones (2002) the substrate penetration resistance was calculated using Equations 3.4 - 3.6. The results are presented in Table 3.6. Substrate resistance ranged from 894 N to 2,490 N. Table 3.3 presents the substrate characteristics for each site alongside the *BCI*. Substrate sorting values ranged from -0.62 to -1.48 indicating

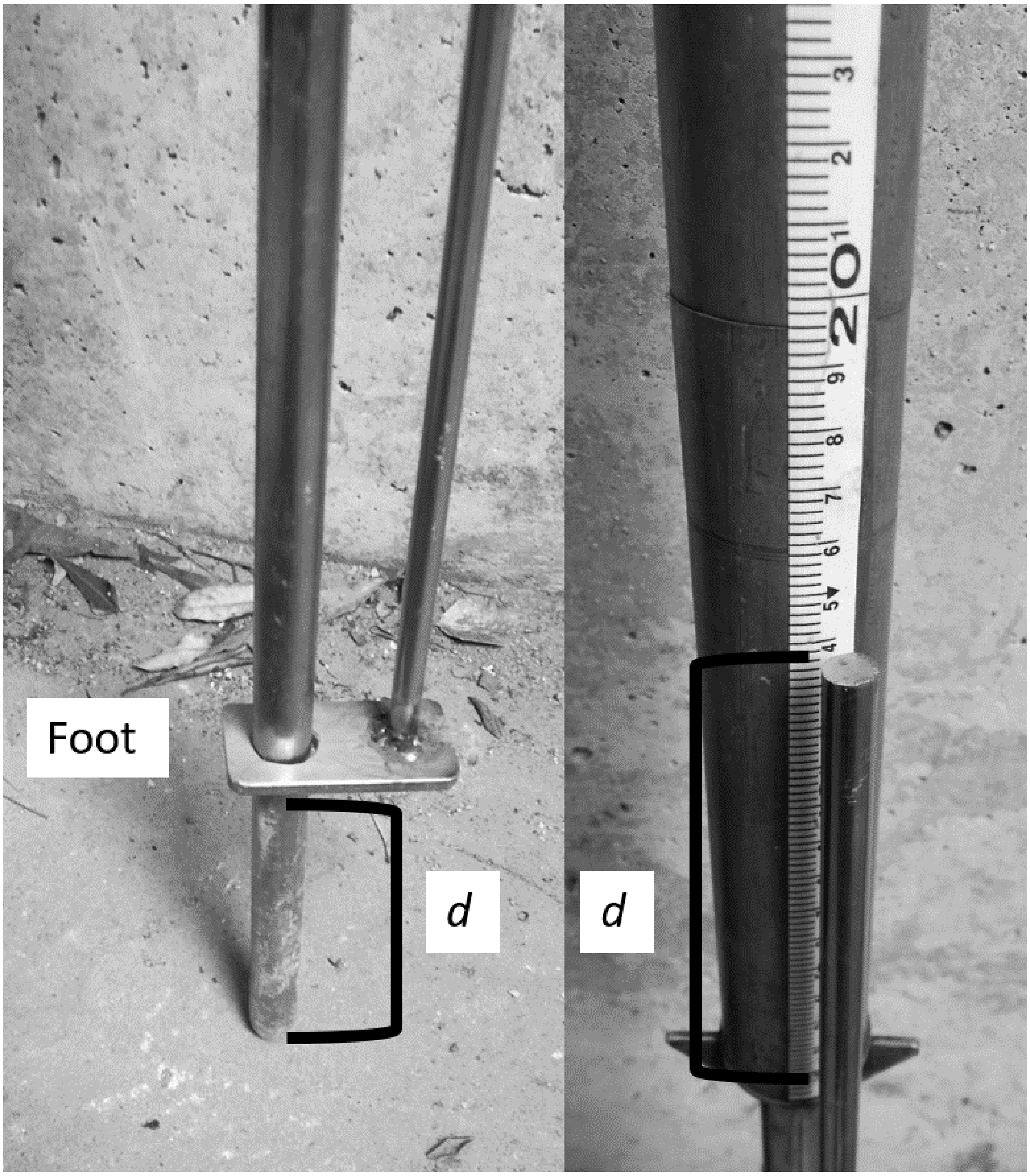

Figure 3.4: Illustration of how the depth reader attachment is used to measure penetration depth (d), assuming the foot started level with the penetrometer tip.

moderately well to poorly sorted gravels (Folk, 1980). Skewness values indicate grain size distributions ranged from strongly negatively skewed (i.e. dominated by finer particles) to positively skewed (distributed toward coarser material). Distributions ranged from very platykurtic to extremely leptokurtic. The sites therefore represent a suitable range of grain size distributions to test the protocol.

Regression analysis of the *BCI* score vs substrate characteristics (Table 3.4) shows poor relationships between the *BCI* and all substrate characteristics, with all p-values $\geq$0.14. Given the logarithmic relationship between the *BCI* score and substrate resistance demonstrated in Figure 3.5, the *BCI* score was log transformed (BCI') and regressed against the substrate characteristics. During this analysis, the grain size data was also transformed to the Krumbein phi scale (Krumbein, 1936). The results are reported in Table 3.5 and plotted in Figures 3.6 & 3.7, and show improved relationships between the

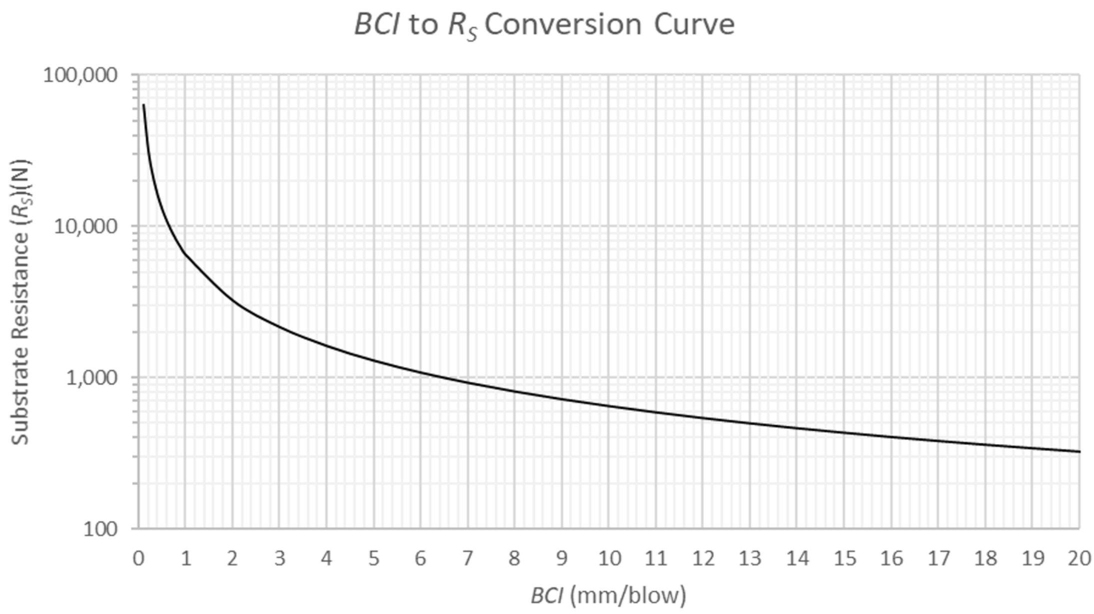

Figure 3.5: Conversion curve for the relationship between the *BCI* and substrate resistance (R_s) for the penetrometer described in this paper.

BCI and all parameters except for C_{40}.

Table 3.7 presents the *BCI* scores and R_s values for the Waikanae River at the control and engineered reaches for December 2016 and June 2017. The change in *BCI* (Δ *BCI*) shows minimal alteration at the control sites between December and June, with 0.1 and 0.2 mm per blow difference. This is within the operator error range (1 mm tape measure increments) and therefore suggests no detectable change in compactness at these two sites. The two engineered sites saw a significant change in bed compactness, with a 71% increase in the *BCI* score at reach 3 (less compact) and 60% reduction at reach 4 (more compact). This change in the *BCI* at the engineered sites equates to a 42% decrease, and 147% increase in bed resistance at reaches 3 and 4, respectively.

Table 3.2: Statistics for the 30 penetration rates (*PR*) measured at each site. We propose the use of the mean *PR* to represent compactness at the site, termed the *BCI*.

Label	**Site**	**Mean**	**Median**	**Mode**	σ	**Range**
A	Makaroro River	7.2	5.6	5.6	5.7	28.4
B	Tamaki River	2.9	2.8	3.1	1.0	4.7
C	Mangapuaka Stream	4.5	3.6	2.7	2.5	11.3
D	Pohangina River	2.6	2.3	4.7	1.0	3.7
E	Coppermine Stream	2.6	2.5	2.5	1.4	5.7
F	Kahuterawa Stream	3.9	3.5	4.5	1.4	5.3

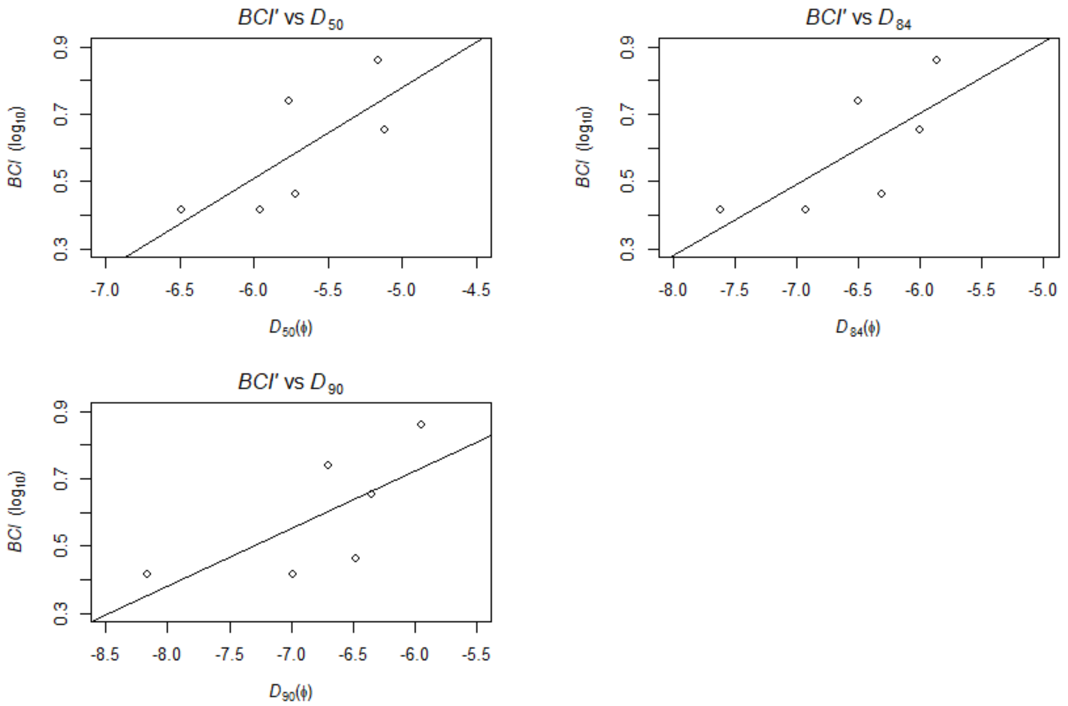

Figure 3.6: Scatterplots showing relationship between BCI' and grain size metrics.

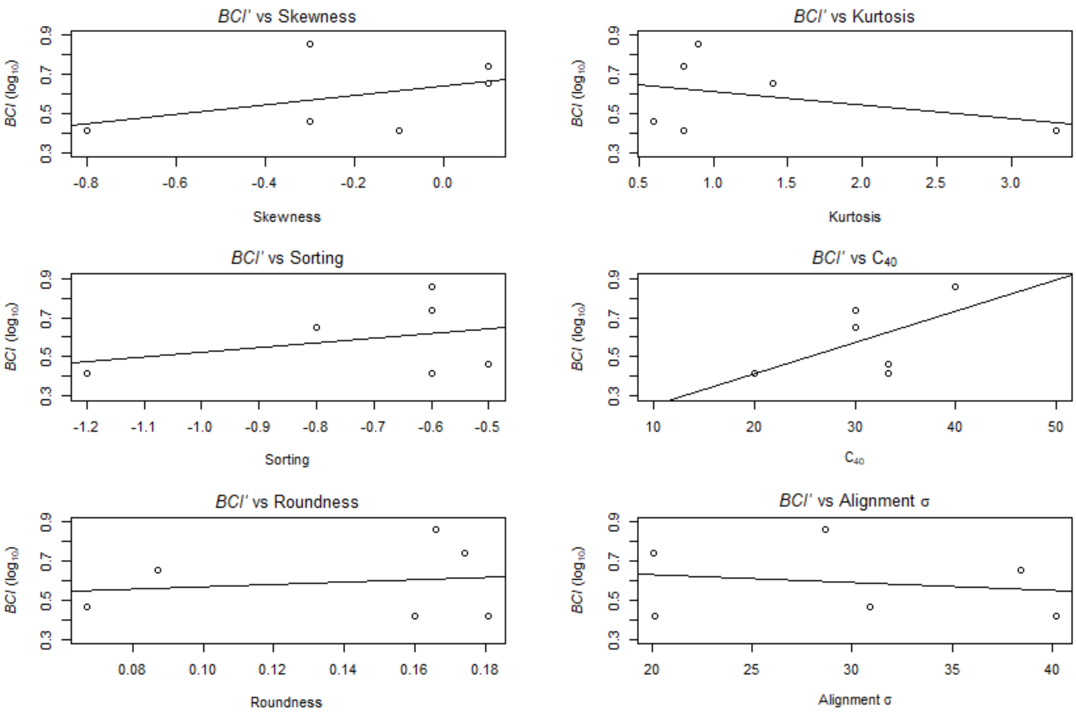

Figure 3.7: Scatterplots showing relationship between BCI' and substrate characteristics.

Table 3.3: *BCI* score and substrate characteristics for each site.

Label	**Site**	***BCI***	**Sorting**	**Skewness**	**Kurtosis**	**C_{40}**	**Cailleux' Roundness**	**Alignment σ (degrees)**
A	Makaroro River	7.2	-0.66	-0.3	0.9	40.0	0.17	28.7
B	Tamaki River	2.9	-0.64	-0.3	0.6	33.3	0.07	30.9
C	Mangapuaka Stream	4.5	-0.86	0.1	1.4	30.0	0.09	38.4
D	Pohangina River	2.6	-0.62	-0.8	0.8	20.0	0.18	20.1
E	Coppermine Stream	2.6	-1.48	-0.1	3.3	33.3	0.16	40.2
F	Kahuterawa Stream	3.9	-0.69	0.1	0.8	30.0	0.17	20.1

Table 3.4: Regression coefficients for the linear models of the *BCI* score vs various substrate characteristic metrics, ranked by statistical significance.

Regressed Against *BCI*	r	r^2	p	*df*
D_{50} (mm)	-0.68	0.46	0.14	4
D_{84} (mm)	-0.64	0.41	0.17	4
C40 Index	0.59	0.35	0.22	4
D_{90} (mm)	-0.58	0.33	0.23	4
Skewness	0.35	0.12	0.49	4
Kurtosis	-0.35	0.12	0.50	4
Sorting	0.33	0.11	0.53	4
Cailleux' Roundness	0.23	0.05	0.67	4
Alignment σ (degrees)	-0.20	0.04	0.71	4

Table 3.5: Regression coefficients for the linear models of the $\log_{10}$ transformed *BCI* score (BCI') vs various substrate characteristic metrics, ranked by statistical significance

Regressed Against BCI'	r	r^2	p	**df**
D_{50} (ϕ)	0.74	0.55	0.09	4
D_{84} (ϕ)	0.73	0.54	0.10	4
D_{90} (ϕ)	0.70	0.49	0.12	4
Sorting	0.56	0.31	0.25	4
Skewness	0.44	0.19	0.39	4
Kurtosis	-0.37	0.13	0.47	4
C_{40} Index	0.33	0.11	0.52	4
Alignment σ (degrees)	-0.18	0.03	0.73	4
Cailleux' Roundness	0.16	0.03	0.76	4

3.5.1 Discussion/Conclusions

Bed compactness has long been recognised as an important parameter of gravel substrate resistance, but due to a lack of suitable measurement techniques, it has not been used in most entrainment formulae. Being able to quantify compactness and include it as a parameter in entrainment formulae is a critical step for improving the accuracy of entrainment estimations and providing more robust management decisions. Penetrometers are used extensively in civil engineering and geotechnical surveys to quantify the compactness of soils. A few studies have used them in gravel-bed rivers, but their use has lacked a consistent methodology that has inhibited comparison between datasets. We have presented a protocol for measuring bed compactness in gravel bed streams using penetration tests which aimed to improve on previous approaches by a) developing a penetrometer which is suitable for use in gravel beds and limits observer bias, b) standardising the approach

Table 3.6: *BCI* scores converted to substrate resistance (R_s) following Herrick & Jones (2002). R_s values are in Newtons.

Label	**Site**	***BCI***	R_s **(N)**
A	Makaroro River	7.2	894
B	Tamaki River	2.9	2251
C	Mangapuaka Stream	4.5	1430
D	Pohangina River	2.6	2448
E	Coppermine Stream	2.6	2490
F	Kahuterawa Stream	3.9	1644

Table 3.7: *BCI* score and substrate resistance (R_s) for the control reaches (1 and 2) and engineered reaches (3 and 4) of the Waikanae River. Change in the *BCI* (Δ *BCI*) and R_s (Δ R_s) are also shown.

Reach	***BCI***	R_s **(N)**	***BCI***	R_s **(N)**	Δ ***BCI***	Δ R_s **(N)**
1	2.5	2587	2.7	2396	0.2	-192
2	3.6	1797	3.7	1748	0.1	-49
3	5.2	1244	8.9	727	3.7	-517
4	13.1	494	5.3	1220	-7.8	727

used to conduct penetration tests, and c) converting the compactness index to a measure of force which allows direct comparison with stress measurements.

During earlier development of this method a Scala penetrometer was trialled in gravel-bed streams. The Scala penetrometer was not sensitive to variations in bed compactness, and tended to travel straight through the active layer and deep into the subsurface within the first blow. The modified Mackintosh Probe presented in this paper proved itself to be sensitive to the variations in active layer compactness. The use of a set a) slide hammer weight and b) drop height ensure consistent travelling velocity and kinetic energy between users, reducing observer bias.

A review of previous uses of penetration tests in gravel-bed streams revealed two different approaches to quantifying the penetration rate: 1) through measuring penetration depth after a consistent number of blows (Pedersen & Friberg, 2007); or 2) counting the blows required to achieve a consistent penetration depth (Sear, 1992; Sear, 1995). Early trials of the adapted penetrometer used in this paper showed that using a consistent number of blows can result in the penetrometer moving well into the subsurface material, which plays no role in armouring (Laronne & Carson, 1976). Thus we have limited penetration depth to ensure only the active layer compactness is measured. This also requires the penetration depth to vary between sites to account for differing active layer thickness. As the armour layer thickness may be difficult to identify in the field, we have used the disturbance depth identified by DeVries (2002) (and referred to commonly as the active layer) for calculating armour layer thickness, ensuring compactness is measured within the bed layers which are most relevant for entrainment thresholds.

A further limitation of penetration tests is the different metrics used to quantify resistance in the literature. For such a protocol to be adopted by river managers a meaningful, standardised metric needs to be produced. The *BCI* uses the penetration rate (*PR*) which is a standard metric used for penetration tests. A significant advantage of this approach is that PR can be converted into substrate resistance force (R_s), measured in Newtons. This has two key advantages. Firstly, this overcomes the issue of different penetrometer designs being used by different operators if datasets are compared. The most significant difference in designs will be the hammer weight and drop height, which will produce different kinetic energy and will therefore produce different penetration rates for a given substrate. These parameters are used in the calculation of R_s, which essentially normalises the PR by the penetrometer properties. Secondly, quantifying the substrate resistance force in Newtons may also be more meaningful for use in entrainment formulae as a resistance parameter, as entrainment forces are calculated in Newtons (e.g. shear stress calculated using Du Boys and Shields equations). As the Waikanae case study shows this also allows for the change in substrate resistance to be quantified and a percentage change calculated which may be more meaningful for managers and regulation.

An important point to note when presenting the change in substrate resistance as change in Newtons is the effect of the logarithmic decay relationship between the BCI score and substrate resistance. Low BCI scores (i.e. 0.1 - 2) represent exponentially higher substrate resistance values than high BCI scores (i.e. 13 - 15), so a 5% change at the low BCI end of the scale is significantly higher in terms of Newtons of resistance than a 5% change at the high BCI end (Figure 3.5). Consideration therefore needs to be given when presenting values of change. For example, a 5% change in highly compacted beds (low BCI score) may have a greater effect on entrainment resistance as the total change in resistance force is greater, and vice versa.

Percentage change is likely to be more meaningful for river managers than actual resistance values as percentage change provides a means of quantifying the degree of impact floods and engineering works have on in-stream habitat. R_s also provides a better quantification of the longer-term effects of engineering and floods on aquatic communities, sediment processes, and hazards. Change in compactness should therefore be reported as R_s not BCI.

Whilst compactness is a product of a range of substrate properties, such as grain size heterogeneity and clast form (Sear, 1995), it is important to assess the dependency of the BCI score on any one of these properties. No statistically significant relationship (p-values <0.05) was found between the BCI score and any of the individual substrate parameters measured at each site.

The notable linear relationship between the BCI and grain size (Figure 3.6) is to be expected as particle mass has a significant effect on resistance, with larger particles requiring more force to move, hence particle mass is the key variable in entrainment formulae. Beds with higher grain size metrics would therefore be expected to require a linear increase in force from the penetrometer to move the bed particles (c.f. Figure 3.6). It is important to note here that the BCI was tested at sites with a limited diversity of bed morphologies, and in particular, the study did not include matrix-supported beds, stepped-bed channels, or subaerial units. Future research should seek to test this methodology and penetrometer design in a wider range of bed morphologies to provide a more complete assessment of the limitations of this method. It would also be valuable to test the methodology controlling for median particle size to test the sensitivity of the method to changes in bed structure.

The BCI proved to be a useful tool for assessing geomorphic impact of engineering works on the Waikanae River. Minimal change in the BCI score occurred in reaches 1 and 2 between December 2016 and June 2017. The change which did occur at these reaches was 0.1 and 0.2 mm per blow, which is considered to be within the error range of the operator given the tape measure used had 1 mm increments. Interestingly, unplanned engineering work was carried out at reach 2 between the surveys, with the channel straightened and rip rap bank protection established adjacent to the survey area. Despite this work being implemented, the *BCI* score change was lower than that of reach 1 where no engineering works occurred. Given the engineering work was adjacent to the survey area it is possible it did not affect the substrate at reach 2. Significant change occurred at reaches 3 and 4, which were downstream of engineering works. Reach 3 was located immediately downstream of a ford crossing used by heavy vehicles. Riparian strip and bar vegetation had also been removed immediately upstream of the ford. Reach 4 occurred downstream of channel widening and riparian vegetation removal, and at the tail end of a large lateral point bar which was lowered in height, and the wetted channel infilled with gravel. These results show the importance of monitoring downstream of engineering works, as the results at reach 2 show the works may not affect the immediate area.

In summary, the *BCI* presented in this paper offers a means for quantifying substrate resistance, and has overcome several of the limitations in previous work. Of particular importance is the reduction in opportunity for observer bias, and the output of a metric which is capable of accounting for key differences in penetrometer designs and is directly related to calculations of hydraulic forces. We contend the *BCI* provides a valuable means for geomorphologists, ecologists, and river managers to quantify bed compaction. The results have implications for improving particle entrainment and bedload transport models, aquatic habitat assessment, flood and engineering impact assessment, and riverine system trajectory modelling.

3.6 Notation

n_{blows}	Blow count
d	Penetration depth
BCI	Bed Compactness Index
PR	Penetration Rate
D_{90}	Characteristic grain size, at which 90% of grains are smaller
$\Delta\ BCI$	Change in BCI between two samples
R_s	Substrate Resistance
W_s	Work done by the substrate to stop the penetrometer
KE	Kinetic Energy of the hammer as it strikes the anvil
m	Mass of the hammer
v	Travelling velocity of the hammer as it strikes the anvil
ϕ	Wentworth exponent, as described by Krumbein (1936)

3.7 Acknowledgements

We would like to thank David Feek from Massey University for his assistance with designing and constructing the penetrometer. We also thank Charlotte Holdsworth, Renae Pratt, Will Conley, James Veitch, Ioan Fuller and Steffan Fuller for their assistance with fieldwork.

Summary of Chapter 3 for Thesis

This chapter has developed a protocol for measuring compaction of the armour (active) layer in gravel-bed rivers which limits observer bias, allows for comparison of measurements between sites and studies, and produces a quantification of bed resistive force which is directly comparable with entrainment force measurements. This provides a step towards accurate assessment of bed resistance, filling a substantial gap in particle entrainment research to date, and moves on from a quantification of structure (Chapter 2) to relate structure to potential bed mobility. The method has also been shown to be useful for assessing the impact of river management on instream habitat. This chapter has directly addressed objective ii-b of this thesis which was to improve the quantification of the resistance of gravel beds for entrainment and transport model parameterisation by developing a method to quantify active layer compaction.

Chapter 4

A New Rapid Assessment Technique for Measuring Stability in Gravel Substrates

Introduction of Chapter 4 to Thesis

This chapter addresses objective iii by developing a method to rapidly assess reach-scale bed stability using an index, referred to as the Bed Stability Index (BSI). Similar indices have been popular in ecology as a cheap, rapid means for assessing bed stability without the need to perform repeat site visits to collect bed movement data. These methods allow relationships between bed stability and benthic communities to be studied, for benthic community composition to be predicted, and to track habitat changes. Such a method therefore lends itself to periphyton management by enabling sites with high bed stability to be identified to alert managers to potential sites of excess periphyton accrual, and for the effect of flushing flows on bed stability to be quantified. Assessment of bed stability is also required to improve the study of periphyton-bed stability relationships so effective hydrological limits can be designed. The BSI presented in this study improves on previous methods by reducing the subjectivity of measurements, and including an assessment of bed compactness using an early version of the Bed Compactness Index presented in Chapter 3.

This chapter is in preparation as a manuscript for Freshwater Biology as:

Neverman, A.J., Death, R.G., Fuller, I.C., McAllister, T.G. (In Prep). A new rapid assessment technique for measuring stability in gravel substrates.

4.1 Summary

1. Substrate disturbance has a strong influence on benthic communities in streams. Both too much and too little disturbance can alter the stream bed, affecting ecosystem condition. Embedded substrate can reduce the magnitude of substrate movement during high flow events, remove habitat, increase periphyton and macrophyte accrual, and consequently alter the functioning of riverine food webs. Increasing embeddedness is a growing global phenomenon, largely as a result of impoundment and/or water abstraction and increasing fine sediment deposition.

2. The importance of assessing disturbance regimes and their effect on bed movement is reflected in the wide range of techniques that have been adopted by river ecologists to measure substrate movement. These techniques range from the direct measurement of bed movement, to estimating bed mobility using indices that assess the potential for substrate movement. The latter provide a valuable tool for stream ecologists as they allow rapid and cost-effective quantification of bed stability. However, they can suffer from limited accuracy and precision because they use subjective assessment approaches.

3. We present a new index for rapid bed stability assessment that requires minimal training to use, but eliminates the subjectivity of similar approaches. The index incorporates a range of geomorphic and hydraulic parameters which are known to impact intrinsic thresholds on substrate stability. As part of the index we adopt a novel quantification of bed compactness using a penetrometer.

4. We provide an example of how the index may be used to explore the relationship between substrate stability and cyanobacteria accrual at sites which lack hydrological and sediment regime time-series data, and discuss the implications this may have for river management.

5. As a rapid, simple, and quantitative approach, we contend this methodology has considerable potential for improving the accuracy and understanding of benthic community-substrate stability relationships.

4.2 Introduction

Substrate disturbance is a critical process in riverine systems and often plays a major role in structuring the composition and diversity of benthic communities (Resh *et al.* 1988; Lake, 2000; Death, 2008, 2010). The effect of substrate disturbance on biological communities was initially made by linking high flow events with changes in periphyton biomass (Biggs, 1985; Clausen & Biggs, 1997), and invertebrate abundance and diversity (Carling, 1987; Resh *et al.* 1988; Reice *et al.* 1990; Lake, 2000; Death, 2008). More direct measurement of substrate stability, assessed by tracking marked substrates, was subsequently linked with invertebrate community composition in numerous studies (Stevenson, 1990; Death & Winterbourn, 1995; Death, 2002; Death & Zimmermann, 2005). Cobb *et al.* (1992) actually compared measures of flow and sediment movement and found variation in insect density was better explained by sediment entrainment models than discharge models. Hoyle *et al.* (2017) similarly found sediment entrainment models more closely related to periphyton removal than the commonly used hydrological metric three times the median flow, also known as FRE_3 (Clausen & Biggs, 1997). Thus direct or indirect measurement of substrate movement is critical to understanding the structure and function of benthic communities (Death, 2008).

Measuring substrate movement directly is notoriously difficult, and typically requires long-term monitoring to capture multiple events. Another approach is to use substrate entrainment and transport models to estimate the frequency of transport events (e.g. Hoyle *et al.* 2017), but this requires long-term hydrological time series data. One-off assessment of channel and sediment characteristics may yield estimates of substrate stability without monitoring stations, and have been used to develop indices linked with biological communities (e.g. Pfankuch, 1975; Rounick & Winterbourn, 1982; Greenwood & McIntosh, 2008; Schwendel *et al.* 2012a). However, the indices developed are subjective, suffer from inter-observer bias, and/or often provide poor estimates of actual bed movement.

In this paper we describe the development of a new index for quantifying substrate stability with one site visit that improves on previous indicies by providing a more objective assessment of individual channel and substrate parameters. We also demonstrate how the index may be used to study the relationship between bed stability and benthic communities.

4.3 Methodology

4.3.1 Study sites

The bed stability index was developed using data collected at 10 sites in the axial Ruahine Ranges, North Island, New Zealand, with available bed movement data (Fuller & Death, 2018). These sites offered a range of channel types and substrate characteristics (Table 4.1), with planforms ranging from cobbly pool-riffle reaches to bouldery step-pool channels. The catchment area upstream of the sites is conservation estate under native vegetation (mixed podocarp forest), with little to no anthropogenic impact (Schwendel *et al.* 2012a).

The developed index was then used to quantify bed stability at eight sites in the Canterbury region, South Island, New Zealand (Table 4.2), where the biomass of the cyanobacterium Phormidium was measured (McAllister *et al.* 2018). These sites were in high order, predominantly braided rivers, downstream of agricultural anthropogenic influences.

Table 4.1: Location, planform, channel parameters, and sediment characteristics of the 10 study sites in the Ruahine Ranges, North Island, New Zealand.

Site	**Latitude/Longitude**	**Section Planform**	**Width (m)**	**Stream Order**	D_{50} **(mm)**	D_{84} **(mm)**	**Slope (m/m)**
Coal Creek	40°14'34.59"S, 175°53'51.64"E	Single-thread	3	1	43	63	0.11
Coppermine Stream	40°14'45.98"S, 175°53'42.32"E	Single-thread	5	3	20	45	0.007
Limestone Creek	39°58'34.08"S, 176°00'13.20"E	Single-thread	7	2	35	57	0.044
Managatautou Stream	40°09'11.55"S, 175°53'08.58"E	Single-thread	5	2	29	64	0.087
Manawatu River	40°01'51.90"S, 176°08'36.73"E	Single-thread	3	3	32	64	0.042
Mangapuaka Stream	40°10'16.50"S, 175°58'42.72"E	Single-thread	25	3	27	55	0.044
Matanganui Stream	40°11'09.36"S, 175°52'06.06"E	Single-thread	5	2	21	55	0.115
Matanganui Tributary	40°11'54.96"S, 175°51'15.13"E	Single-thread	3	1	41	76	0.093
Ngamoko Stream	40°03'15.30"S, 176°09'43.93"E	Single-thread	1	1	15	27	0.031
Tamaki Stream	40°07'11.28"S, 176°01'44.76"E	Single-thread	15	3	28	53	0.014

Table 4.2: Location, planform, channel parameters, and sediment characteristics of the eight study sites in the South Island, New Zealand.

Site	**Latitude/Longitude**	**Section Planform**	**Width (m)**	**Stream Order**	D_{50} **(mm)**	D_{84} **(mm)**	**Slope (m/m)**
Ashley River	43°16’40.17”S, 172°41’17.72”E	Multi-thread	173	7	30	53	0.008
Opihi River	44°15’50.08”S, 171°16’24.32”E	Multi-thread	177	6	26	36	0.017
Orari River	43°59’22.45”S, 171°14’15.89”E	Multi-thread	164	6	72	113	0.009
Pareora River	44°24’41.19”S, 171°03’26.66”E	Multi-thread	80	6	15	24	0.009
Selwyn River	43°29’11.12”S, 171°56’08.62”E	Single-thread	17	5	77	124	0.009
Te Muka River	44°14’43.18”S, 171°16’08.10”E	Single-thread	54	5	29	48	0.017
Te Ngawai River	44°17’52.59”S, 170°59’32.03”E	Multi-thread	68	5	32	86	0.017
Waipara River	43°03’45.63”S, 172°40’00.24”E	Single-thread	30	6	29	57	0.007

4.3.2 Index Development

There are differences in how geomorphologists and ecologists define bed stability. Geomorphologists tend to use stability in reference to reach scale morphological adjustments (e.g. Kuo *et al.* 2017; MacKenzie & Eaton, 2017), whereas ecologists refer to stability in terms of patch-scale mobility. Physically, the geomorphic definition requires topographic change, whereas the ecological definition only requires the substrate to move, regardless of whether or not it creates topographic change. This study takes an ecological view and defines bed stability as the magnitude of movement of the coarse surface layer of the bed. This definition is also relevant to geomorphologists as movement of the surface layer often leads to topographic change, depending on sediment supply conditions (notwithstanding compensating scour and fill, cf. Lindsay & Ashmore, 2002). Using this definition as a framework for developing the assessment tool ensures it is useful for geomorphic, ecological, and inter-disciplinary studies.

Suitable methodologies for measuring bed stability were examined in the literature and deconstructed to identify the key variables measured and the methods used to quantify the variables. Advantages and disadvantages of the methodologies for quantifying bed stability were also identified. This literature review revealed two common approaches to estimating substrate stability: approach 1) using time series data, usually discharge, to identify the frequency of exceedance of flow thresholds for substrate entrainment (e.g. Newbury, 1984; Cobb *et al.* 1992; Duncan *et al.* 1999); or approach 2) measuring parameters which control intrinsic thresholds, using discrete datasets, to estimate the potential for substrate entrainment (e.g. Pfankuch, 1975; Schwendel *et al.* 2011). We judged approach 2 to be the best for our aims as it does not require long term monitoring.

A bottom-up approach was then used to develop a new methodology by first identifying what intrinsic variables should be measured based on substrate entrainment (initiation of motion) formulae, what methods are available for their measurement, which methods best suit the objectives, and then combining these into an index.

4.3.3 Index Variable Selection

Substrate movement occurs when thresholds for initiation of motion are exceeded. Predicting substrate movement therefore requires an index which measures drivers of that initiation of motion. Initiation of motion is the product of an interaction between hydrologic and geomorphic processes. These components can be categorised as *particle resistance* and *fluid entrainment forces* (Komar & Li, 1988). Particle resistance is controlled by characteristics of the substrate, such as grain protrusion (Fenton & Abbott, 1977); bed packing (Papanicolaou *et al.* 2002); grain size and placement (Downes *et al.* 1998); and pebble clusters (Wittenberg & Newson, 2005). Entrainment forces are produced by fluid flow dynamics such as velocity, turbulence, and pressure fluctuations (Smart & Habersack, 2007; Smart *et al.* 2010; Paiement-Paradis *et al.* 2011), which are conditioned by channel parameters, such as slope, and complex feedback between hydraulics and substrate characteristics. See Neverman *et al.* (2018) for a review of entrainment and resistance thresholds, and the mechanisms of entrainment.

In order for a bed stability index to be effective it therefore needs parameters which measure a range of substrate characteristics and channel properties which condition flow hydraulics. Visual evidence of substrate movement, such as the presence of active erosion surfaces, may also be valuable as they provide visual confirmation that substrate movement is occurring.

Parameters which measure substrate and channel properties in the Pfankuch (1975) and Schwendel *et al.* (2012a) indices were identified and combined into the new index. Parameters were also added for other hydraulic and geomorphic properties not considered in these indices which condition either entrainment or resistance thresholds, or may be visual indicators of potential for substrate movement. The pilot index variables are presented in Table 4.3. Objective approaches to measuring these variables were then sought, and selected on the basis of ease of use, cost, and speed. Where variables could not be easily or cheaply measured objectively a numeric rating system was used based on visual assessment. The development process sought to reduce the subjectivity in the visual assessment approach by providing guidelines for rating, similar to the style of Pfankuch (1975) and Schwendel *et al.* (2012a), such as estimating the percentage of the bed covered by signs of active erosion. This is referred to as Guided Visual Assessment in Table 4.3. This is particularly important if non-expert users are to collect data with this index without having experienced a range of river types.

Table 4.3: Parameters initially trialled for the index during the pilot surveys, prior to optimisation. The parameter type indicates whether the parameter is measuring a driver of resistance or entrainment, or a product of bed movement. The scoring approach differentiates between the use of objective scoring, using physical measurements of parameters e.g. with a tape measure; visual assessment where the observer assigns a numeric rating for the parameter; or categorised visual assessment where the observer uses a guide which provides categories to follow for visual estimation, such as percentage of subaerial active channel.

Parameter	**Parameter Type**	**Description**	**Rationale**	**Scoring Approach**	**Measurement Method**
Bed Compactness	Substrate - Resistance	Measurement of armour layer compactness/cohesion/clast interlocking	Packing of the armour layer affects the resistance of clasts to entrainment. Higher compactness means the clasts are more interlocked and individual clasts are less readily available for entrainment.	Objective	Use of a penetrometer following Sear (1995), Narahari *et al.* (1967), and Pedersen & Friberg (2007). The method of Pedersen & Friberg (2007) was followed for this study, where a consistent number of blows was used, in this case 10 blows.
Development of geomorphic units	Geomorphic - Product	The extent to which distinct geomorphic units are pronounced. i.e. how clearly developed pools and riffles are.	Riffles and pools are considered to be relatively stable features (Robert, 1997) and are recognised as maintaining quasi-equilibrium (Milan *et al.* 2001).	Visual Assessment	Observer visually assesses how developed geomorphic units are at the site, and records an appropriate rating. A score of 1 is given for well developed pools and riffles, and the highest score for no pool or riffle development.
Active erosion	Geomorphic - Product	Visual erosion evident on bed/banks	Visible erosion features suggest channel is near erosion thresholds	Categorised Visual Assessment	Observer visually assesses the extent of active erosion visible on the banks and bed. The observer estimates and records the percentage of the active channel which shows active erosion. A rating is then assigned based on the percentage.
Armour layer clast range (D_{16}-D_{84})	Substrate Resistance	Quantification of the range of clast sizes as a proxy for protrusion/hiding.	A larger range of clast sizes in the armour layer would be indicative of higher grain protrusion/hydraulic roughness, and hiding of smaller clasts. In this case the D_{16} to D_{84} has been used as the D_{84} is commonly used to characterise roughness, and the D_{16} represents bedload fraction.	Objective	D_{16} andD_{84} derived from Wolman (1954) sample of surface grains.
Substrate homogeneity	Substrate - Product	The uniformity of clast sizes in the surface layer	Homogenous, well-sorted substrates are indicative of stable beds as the smaller material which can be mobilised at daily flows has already been preferentially sorted. Sorting also effects pivoting angles, with lower pivoting angles found in poorly sorted beds for grains larger than the mean, making them more easily entrained (Buffington *et al.* 1992).	Visual Assessment	Observer visually assesses whether the surface gravels are well sorted or poorly sorted, and records an appropriate rating.

Bar development	Geomorphic - Product	Assessment of the degree to which bars are developed in the active channels.	Bars are indicative of high sediment supply which is stored between high magnitude events. Channels which have well developed bars therefore have the potential for frequent substrate movement due to high sediment supply, which decreases the ability of channels to become well armoured providing high magnitude events occur frequently enough.	Categorised Visual Assessment	Observer estimates the percentage of the active bed which is subaerial. A rating is then assigned based on the percentage.
Water surface slope	Hydraulic - Entrainment	Slope of the water surface	Steep slopes produce higher stream power and therefore higher shear stresses and potential for substrate entrainment.	Objective	Measure the gradient of the water surface by recording the length of longitudinal profile of the reach, and recording the vertical drop in height from the top to the bottom of the reach. The water surface slope is measured rather than the bed slope to reduce effect of bed undulations and roughness on measurements (pole placement errors, see Neverman *et al.* 2016)
Bankfull hydraulic radius	Hydraulic - Entrainment	Measurement of channel area in contact with flow	The hydraulic radius is a key component of shear stress based competence equations, such as Du Boys (Baker & Ritter, 1975), as it plays a role in the development of friction and therefore shear stress.	Objective	The bankfull hydraulic radius is derived by measuring the active channel cross-sectional area and dividing by the wetted perimeter, using bankfull to determine depth.
Bankfull width to depth ratio	Hydraulic - Entrainment	Ratio between the depth and width of the active channel.	High width to depth ratios are often attributed to streams which transport coarse bedload (Schumm, 1968). Channels with large widths may also indicate highly erodible banks which contribute material for mobilisation, such as in braided rivers.	Objective	The width of the active channel is measured, and the depth is measured based on the determined bankfull channel top.
Pebble cluster development	Substrate Resistance	Assessment of the degree of pebble cluster development in the reach.	Pebble clusters develop as obstacle clasts trap larger clasts on their stoss side, and smaller clasts on their lee side by altering local hydraulics.	Categorised Visual Assessment	Observer estimates the percentage of the bed surface covered by pebble clusters. A rating is then assigned based on the percentage.
Shannon index (substrate diversity index)	Substrate - Resistance	The Shannon Index describes the degree of diversity of the clast sizes. It is therefore an objective scoring approach for bed homogeneity	See Substrate Homogeneity	Objective	Shannon Index applied to grain size data derived from Wolman (1954) sample of surface grains.

Degree of mortaring	Substrate - Resistance	Mortaring (*sensu* Hodge *et al.* 2013) describes filling of interstitial spaces by fines. Also referred to as clogging, fine sediment infiltration, fine sediment deposition, ingress, infilling, intrusion of fines, and siltation (Wharton *et al.* 2017).	Mortaring can act as cement, increasing the resistance of the bed to entrainment (Hodge *et al.* 2013)	Visual Assessment	Observer visually assesses the degree of fines infilling interstitial spaces, and records an appropriate rating.
Active channel width vs. wetted channel width	Hydraulic - Product	Ratio of the active channel to wetted channel widths.	The ratio between active and wetted widths is used here as an indicator of the potential magnitude of high flow events, following the rationale of Pickup & Warner (1976) and Wolman & Miller (1960) that bankfull events condition channel form. A high ratio indicates that active channel width is much higher than wetted channel width, and therefore high flow events are likely to be significantly larger than daily flows, and the site therefore likely experiences high disturbance.	Objective	Active and wetted channel widths are measured. This may be with a tape measure in smaller channels, or using GPS or GIS-based methods for larger channels. The ratio between the measurements is then calculated.

4.3.4 Optimising the Index

In order to optimise the index, data were collected using the pilot index parameters at 10 sites in the Ruahine Ranges, where bed movement data were available. Bed movement was quantified as the percentage of the bed which is regularly mobilised (Fuller & Death, 2018), and was calculated using tracer particle data following the method of Death & Winterbourn (1994). A correlation matrix was produced between the raw data for each parameter and the bed movement data. The results are summarised in Table 4.4. The correlation matrix was used to assess how strongly parameters were linked with bed movement, and remove parameters which showed weak correlation. Parameters which were strongly intercorrelated were also removed, leaving the most objective parameter. In this instance a threshold of $r < 0.25$ was used to separate poorly correlated parameters from acceptably correlated parameters, as this appeared to be a natural break between parameter correlations. It was also necessary to have a positive relationship between parameters and bed movement. Scores with a negative relationship were rescaled (described below) to produce a positive relationship.

Following the methodology of Pfankuch (1975) and Schwendel *et al.* (2012a) the aim was to produce a final index score which was the sum of the parameter scores, each with a different weighting. To achieve the parameter weighting each parameter was first rescaled from 1 to 5. The parameters were then weighted by adjusting the scores to scales between 1 and 10, 15, or 20, effectively allowing some scores to contribute up to 4 times more to the final score than other parameters.

Table 4.4: Correlations between pilot index parameters and bed movement at 10 sites in the Ruahine Ranges.

Parameter	r
Bankfull Width to Depth Ratio	0.47
Bed Compactness	0.44
Bar Development	0.42
Development of Geomorphic Units	0.42
Pebble Clusters	0.42
Active vs Wetted Width	0.40
Bankfull Hydraulic Radius	0.33
Water Surface Slope	0.29
Degree of Mortaring	0.27
Substrate Homogeneity	0.26
Active Erosion	0.16
Armour Layer Clast Range (D_{16} - D_{84})	0.12
Shannon Index	0.07

4.3.5 Calibrating the Index

The index was calibrated to find the best weighting for each parameter by considering all possible permutations and weightings for the index, and correlating the scores with measured bed movement data. Parameters (notated as P1, P2, ..., P9) were weighted by rescaling the data between 1 and a maximum value of either 5, 10, 15, or 20 using a standard feature scaling normalisation procedure following Equation 4.1:

$$x' = (b - a)\frac{x - min(x)}{max(x) - min(x)} + a \tag{4.1}$$

where x' is the rescaled score, a is the minimum score (always 1 in this case), b is the maximum score (5, 10, 15, or 20), x is the raw value for the parameter, *min(x)* and *max(x)* are the minimum and maximum for the range of values for x recorded in the dataset. This therefore meant the extreme values in the dataset were given the minimum or maximum score possible. The rescaled data were stored in a matrix for each respective weighting class. The weighted parameters are notated as $\mathrm{P1_x}$, $\mathrm{P2_x}$, ..., $\mathrm{P9_x}$, where x denotes the weighting class. A matrix of all permutations of the index (PerMatrix) was created, each stored as a row in PerMatrix, and denoted as $\mathrm{PerMatrix_i}$. R (R Core Team, 2013) was then used to produce a m x 1 matrix (CorMatrix), with each row representing the correlation coefficient between $\mathrm{PerMatrix_i}$ and the bed movement data. This process was performed 10 times using a Hold Out approach, where a different site was left out (test site) of the dataset each time (training dataset), creating matrices $\mathrm{HOMatrix}_{1...10}$. The maximum correlation coefficient value was found in each HOMatrix ($\mathrm{HOMatrix_{nmax}}$). The row number (i) for the maximum correlation coefficient ($\mathrm{HOMatrix_{ni}}$) was used to find the correlating index permutation, $\mathrm{PerMatrix_i}$, which therefore had the optimal parameter weightings for each Hold Out dataset. The most frequently occurring optimal weighting for each parameter was then found, and the calibrated bed stability index was created using these weightings, here after referred to as the Bed Stability Index (BSI).

4.3.6 Validating the Index

To estimate the performance of the calibrated index for data outside of the calibration set, a Leave One Out Cross Validation (LOOCV) approach was used. Using each of the Hold Out datasets, the calibrated index was used with the training dataset to predict bed movement (%) at the test site. A linear regression model was used to find the coefficient of determination for the relationship between the predicted and observed bed movement for all 10 sites combined.

4.3.7 Case Study

To demonstrate the application of the index for ecological studies, the index was used to predict bed movement at eight sites in the Canterbury region to examine the relationship between bed stability and *Phormidium* accrual. Three *in situ* cobbles covered with *Phormidium* mats in a riffle or run were randomly collected from each site weekly over a 30-week period for biomass analysis based on chlorophyll-*a* analysis (see McAllister *et al.* 2018). Chlorophyll-*a* was extracted in boiling ethanol (96%; 10 mL) for 2 minutes. Samples were shaken manually until the mat turned grey, centrifuged (3000g, 15 min) and absorbances measured spectrophotometrically (HACH DR390, USA). An acidification step was carried out to account for phaeopigments as suggested by Biggs & Kilroy (2000). To assess the relationship between bed stability and *Phormidium* accrual the minimum and maximum values for chlorophyll-a over the 30 week period were compared to predicted bed movement using linear regression in R (R Core Team, 2013).

The Bed Stability Index was used at each of the *Phormidium* sampling sites to quantify bed stability at each site.

Rescaling of the index constituent parameters was performed using Equation 4.1, with *min(x)* and *max(x)* set using the values from the Ruahine dataset to maintain consistent normalisation and allow estimation of bed movement using the model developed at the Ruahine sites. For example, the maximum bed compactness measured in the Ruahine dataset was 0.18 (*max(x)* for bed compactness). If bed compactness at a site in the Canterbury dataset exceeded 0.18, the site would be given the maximum score possible for bed compactness.

4.4 Results

4.4.1 Index Optimisation and Performance

Optimisation of the index involved removing parameters which either poorly correlated with measured substrate movement and/or were highly intercorrelated with other parameters (Table 4.4). Active erosion, armour layer clast range, and the substrate diversity index all had weak correlations with substrate movement and were removed. Bar development was removed as it was visually assessed, but highly correlated (r = 0.90) with active channel width vs wetted channel width. These two parameters were essentially measuring the same thing; accommodation space and in-channel storage, which leads to exposed gravel surfaces (bars) during average daily flow conditions.

In 70% of Hold Out iterations permutation 17104 (PerMatrix_{17104}) produced the best correlation with bed movement data. In the three Hold Out datasets where PerMatrix_{17104} did not have the highest correlation, its correlation coefficient exceeded 0.96. Correlation coefficients for PerMatrix_{17104} vs bed movement data for each Hold Out dataset are present in Table 4.5, and the relationships plotted in Figure 4.1. PerMatrix_{17104} was therefore the best combination of parameter weightings (Table 4.6). These parameters and weightings therefore make up the Bed Stability Index (BSI).

The predictive power of the BSI was tested using a Leave One Out Cross-Validation approach (Figure 4.2). Variation between predicted and observed bed movement ranged from - 0.1% to 10.8%, with RMSE = 5.3% and r = 0.94.

Table 4.5: Correlation Coefficients for predicted bed movement using PerMatrix$_{17104}$ at the test sites for each Hold Out dataset correlated with bed movement. Based on these results PerMatrix$_{17104}$ became the BSI.

Test Site	$\boldsymbol{r}$
Coal Creek	0.966
Coppermine Stream	0.981
Limestone Creek	0.983
Manawatu River	0.964
Mangapuaka Stream	0.967
Mangatautou Stream	0.966
Matanganui Stream	0.967
Matanganui Tributary	0.968
Ngamoko Stream	0.968
Tamaki Stream	0.963

Table 4.6: Optimised weightings for the BSI parameters. These are the parameter weightings for PerMatrix$_{17104}$ which had the highest frequency of maximum correlation with observed bed movement in the 10 Hold Out datasets.

Parameter	**BSI Parameter Weightings**
Bed Compactness	1-20
Development of Geomorphic Units	1-20
Substrate Homogeneity	1-5
Water Surface Slope	1-20
Bankfull Hydraulic radius	1-15
Bankfull Width:Depth	1-5
Pebble Clusters	1-5
Degree of Mortaring	1-10
Active Channel Width vs. Wetted Channel Width	1-5

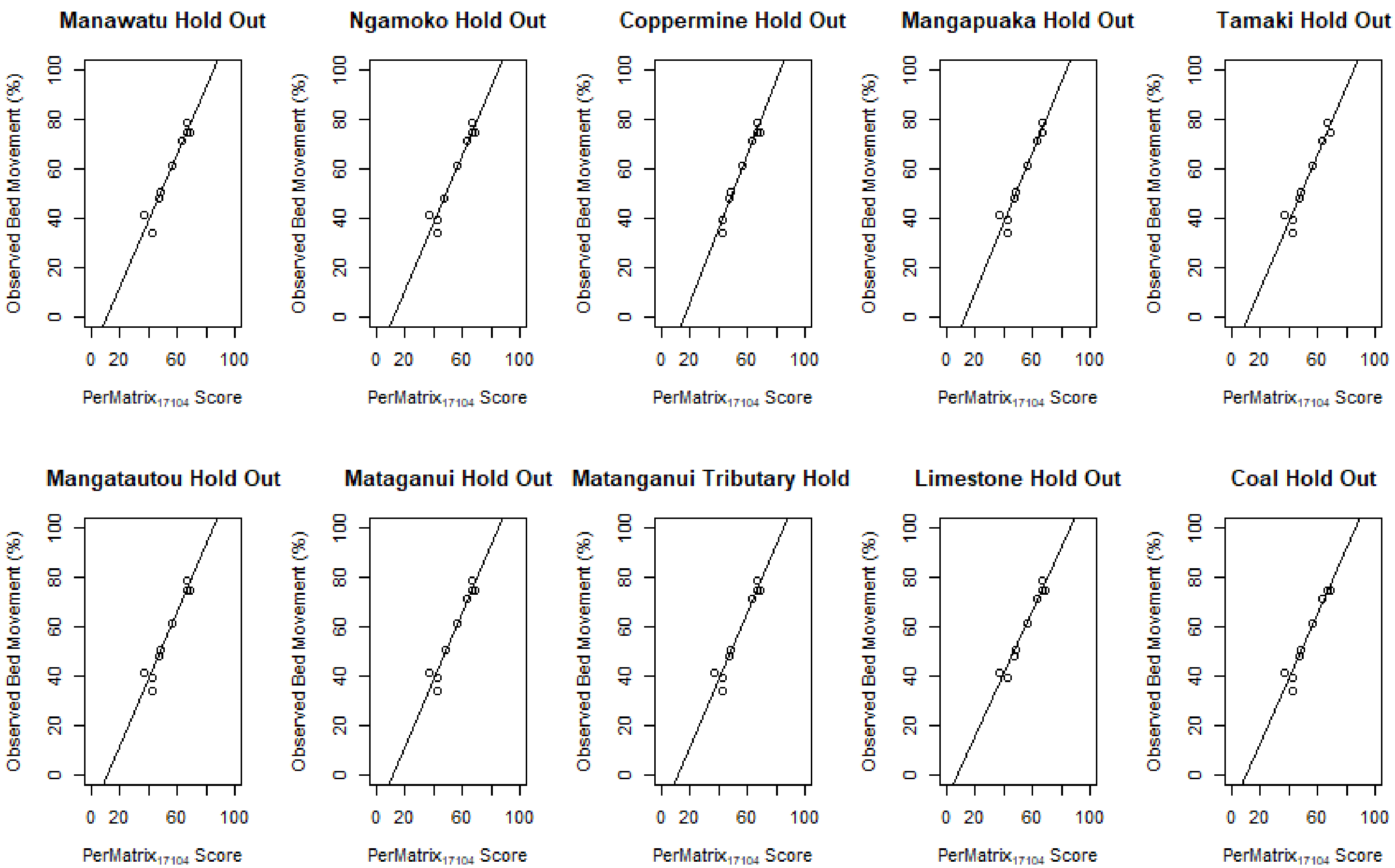

Figure 4.1: Relationships between the bed stability score calculated using PerMatrix_{17104} and observed bed movement for each Hold Out test. The title above each plot indicates which site was withheld.

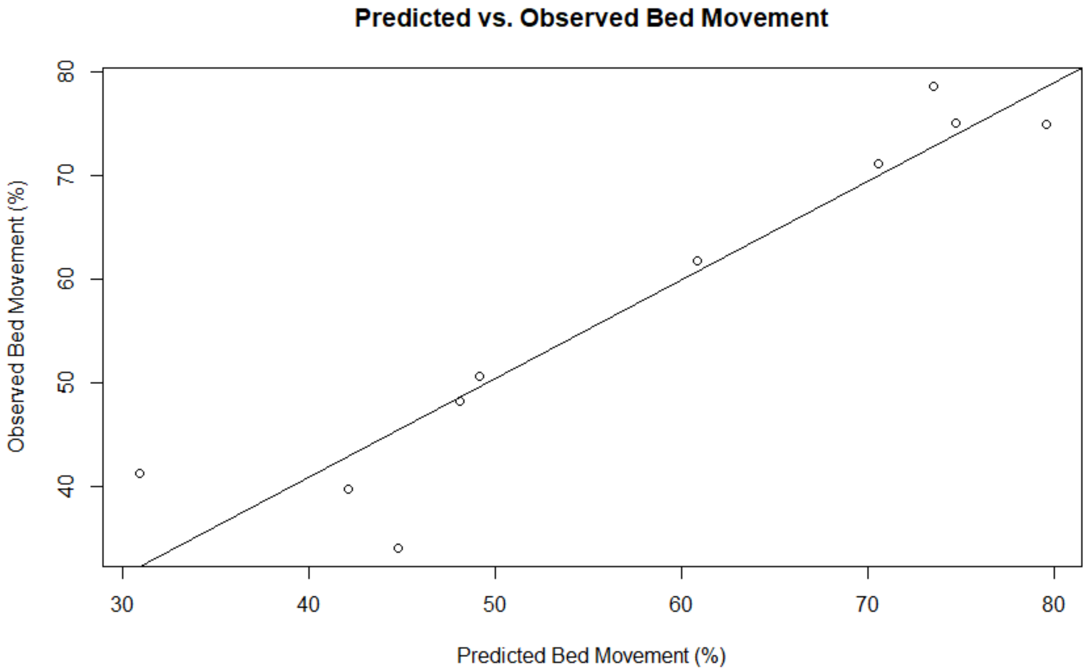

Figure 4.2: Observed vs. predicted bed movement for the cross-validation procedure.

4.4.2 Predicting Phormidium Accrual

To demonstrate the application of the BSI for ecological studies, the index was used to quantify bed stability at eight sites and the index scores were regressed against chlorophyll-a measures (Figure 4.3) to assess the relationship between *Phormidium* biomass and degree of bed stability (Table 4.7). There was no significant relationship between the index score and minimum and median chlorophyll-a, however the index was correlated with maximum and range of chlorophyll-a ($p < 0.1$). The correlation coefficients for the relationship between the index scores and the maximum and range of chlorophyll-a show strong negative relationships with r = -0.67 and -0.69, respectively.

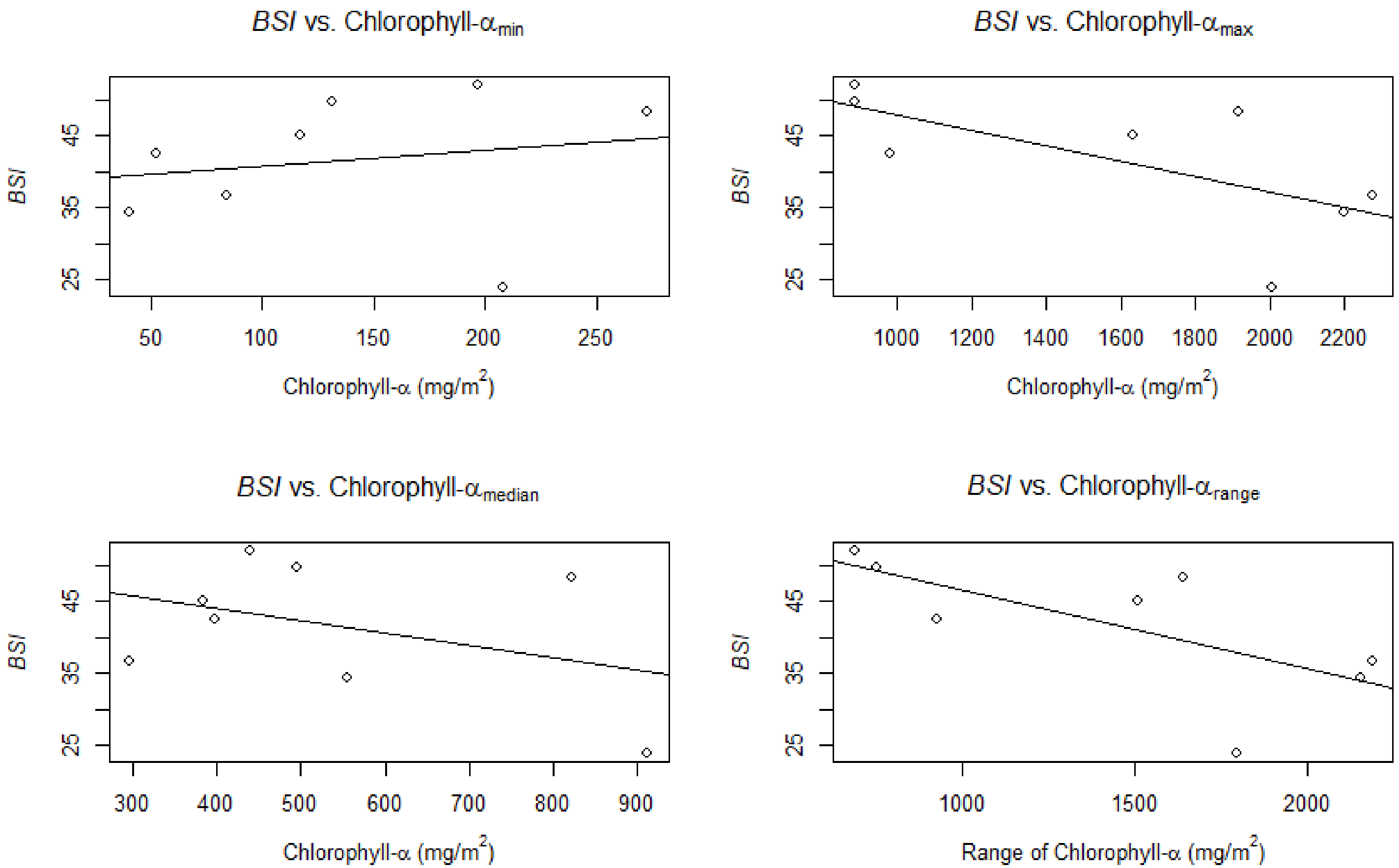

Figure 4.3: BSI score vs biomass metrics for the Canterbury case study.

Table 4.7: Regression statistics for BSI score vs selected metrics for chlorophyll-a as measures for *Phormidium* biomass.

Metric regressed against BSI score	r	r^2	p	df	F
Min Chlorophyll-a	0.19	0.04	0.650	6	0.23
Max Chlorophyll-a	-0.67	0.45	0.067	6	4.99
Range Chlorophyll-a	-0.69	0.48	0.058	6	5.50
Median Chlorophyll-a	-0.39	0.16	0.334	6	1.10

4.5 Discussion

Substrate movement is an important structuring force for benthic communities (Death, 2008), however, the stochastic nature of bed movement events has made their accurate measurement and prediction difficult in natural channels (Gomez, 1991; Fuller & Basher, 2013). Whilst a range of high-resolution techniques are being developed to measure bed-load movement (see Neverman *et al.* 2018), these are often expensive, labor intensive, and require long term data collection. Several rapid, inexpensive techniques for estimating bed movement have been adopted by ecologists to assess bed movement, but have produced poor results to date. In this paper we have developed a new index for the rapid, accurate, and inexpensive assessment of bed movement in gravelly bedded streams; the Bed Stability Index (BSI). Calibration of the BSI with measured particle movement produced good correlations. Leave One Out Cross-Validation was used to assess the predictive power of the BSI, and produced a strong correlation between predicted and observed bed movement. These results suggest the BSI provides an accurate assessment of bed movement, and may prove a useful tool for accurate and rapid quantification of substrate stability.

Schwendel *et al.* (2012a) compared the Stream Bed Stability for Invertebrates (SBSI) protocol and the bottom component of the Pfankuch (1975) index (BCP) with bed movement using tracer particles at 46 streams in New Zealand, including many of the streams from this paper. Schwendel *et al.* (2012a) reported correlation coefficients of 0.48 and 0.46 between bed movement and the SBSI and BCP, respectively. One of the major differences in the performance between the indices presented by Schwendel *et al.* (2012a) and the BSI may be the inclusion of an objective approach to quantifying bed compactness, which plays a major role in substrate resistance to entrainment. The BSI also included more channel hydraulic parameters, which were objectively measured, providing more consideration of entrainment forces as opposed to the focus on substrate resistance in the SBSI. The BSI also removed the use of biological indicators of stability, such as aquatic vegetation growth used in the Pfankuch (1975) index. This was done for two reasons: firstly, vegetation growth is affected by other factors, such as light availability (Minchin & Death, 2002), and secondly, so the BSI can be used to examine the relationship between stability and instream vegetation biomass accrual. Including biomass in the index scoring would obviously bias any relationship. The objective measurement of parameters may also explain the improved performance over the Pfankuch (1975) index.

Future research should seek to improve the BSI by conducting a comparison between the index score and observed movement at a wider range of sites. One of the limitations of the study presented in this paper is the relatively small number of sites used in the calibration dataset, which largely consisted of low order streams with stable planforms. More accurate rating of the parameters may be achieved by including a broader range of channel types, which include extremes of the parameter measurements which can be found in natural channels.

Future research may also seek to improve the objectivity of parameter rating in the BSI by replacing some of the visual assessment approaches. For example, remote sensing techniques may be used to objectively measure some parameters. Papanicolaou *et al.* (2012) have demonstrated the ability to quantify clusters using image analysis techniques. Aberle & Nikora (2006) demonstrated that gravel surfaces could be characterised using 3D point clouds, with skewness of the elevation data relating to the filling of interstitial spaces by fines, potentially offering a means to quantify mortaring and armouring (Neverman *et al.* In Press). Sieving may also be implemented to quantify composition of the surface sediment, with dominance of fines relating to mortaring. Including such methodologies may further improve the index, however, such approaches are time consuming, may require expensive apparatus, and require expertise to collect, process, and analyse the data.

To demonstrate the application of the index to ecological research, bed stability was quantified at eight sites using the BSI and compared to *Phormidium* accrual. Hoyle *et al.* (2017) concluded that sediment mobility parameters may improve the identification of sites which are at risk of nuisance periphyton accrual, and provide a better understanding of the links between flow, nutrients, and periphyton accrual. As bed movement acts as a removal mechanism for periphyton, we hypothesised that sites with higher stability (i.e. less bed movement, lower index score) would have higher *Phormidium* accrual and therefore higher chlorophyll-a. But as re-establishment following removal can be rapid (i.e. within days), and it is unlikely that all biomass is removed during an event, we expect to see weaker relationships between the index and minimum chlorophyll-a. The regression model p-values (Table 4.7) show a relationship exists between maximum chlorophyll-a and the BSI score at the 10% significance level, but no relationship between minimum chlorophyll-a and the BSI score for the 30 week period. The direction of the relationship between BSI score and maximum chlorophyll-a was negative, suggesting higher bed stability was related to sites with higher *Phormidium* accrual and vice versa. These results support our hypothesis, suggesting bed movement may be a controlling factor in peak *Phormidium* accrual (Biggs, 1985, 1990; Minchin & Death, 2002; McAllister *et al.* 2016; Hoyle *et al.* 2017). The weak correlation between movement and minimum *Phormidium* accrual may reflect that presence/absence of *Phormidium* is a product of other factors such as stream shading and nutrient availability. However, it is more important to explain maximum chlorophyll-a for sites at risk of nuisance periphyton accrual. We therefore contend the BSI may be a valuable tool in identifying sites at risk of nuisance periphyton accrual.

The BSI may also be used to build temporal datasets to identify changes in bed stability. Such datasets may be useful for assessing the impact of land use changes, engineering works, management strategies, or river restoration projects. Predictions could then be made on ecosystem trajectories. The BSI may also be reverse engineered and used as a model to see how changes to certain parameters affect bed stability. Such predictions and identification of system changes are critical for the maintenance of river management schemes; an aspect of river management which has been poorly carried out to date (Moore & Rutherfurd, 2017).

The BSI may be used in a similar manor to explore other relationships between benthic communities and disturbance events, such as identifying the main physical driver of catastrophic drift, and providing better understanding of sensitivity and resilience. Such insights will enable better predictions of ecosystem trajectories under changing land use and climatic conditions, and underpin more effective mitigation and management decisions.

We conclude that the BSI offers an inexpensive, rapid approach for accurately quantifying bed stability and estimating bed movement. A case study of the application of the BSI as a tool for river management has shown that the BSI provides a means of identifying sites which are at risk of nuisance periphyton accrual, and is a valuable tool for river scientists, managers, and stewards.

4.6 Acknowledgements

We thank Charlotte Holdsworth, Matt Hemler, Laura Kelsey, and Erica Smith for their assistance in the field.

Summary of Chapter 4 for Thesis

This chapter addresses objective iii by developing a method to rapidly assess reach-scale bed stability indirectly using an index, referred to as the Bed Stability Index (BSI). The BSI lends itself to periphyton management by enabling sites with high bed stability (low frequency of bed mobilisation) to be identified to alert managers to potential sites of excess periphyton accrual, and for the effect of flushing flows on bed stability to be quantified. Assessment of bed stability is also required to improve the study of periphyton-bed stability relationships so effective hydrological limits can be designed. The BSI presented in this study improves on previous methods by reducing the subjectivity of measurements, and including an assessment of bed compactness using an early version of the Bed Compactness Index presented in Chapter 3. The BSI moves on from Chapters 2 & 3 by providing an indirect assessment of bed mobility, which considers hydraulic forcing as opposed to just dealing with substrate resistance. Whilst this indirect approach has some benefits in terms of rapidity and cost for broader studies, there remains a need to directly measure the onset of motion to more reliably link with hydrodynamics to develop predictive models and establish site-specific hydrological limits (c.f. Chapter 1). Chapter 5 addresses this need for a direct approach.

Chapter 5

Implementation of a Multi-Sensor System to Identify Streamwise Hydrodynamic and Vertical Bed Seepage Thresholds for Particle Entrainment in Gravel-Bed Rivers

Introduction of Chapter 5 to Thesis

Whilst Chapter 1 identified a significant need to improve the quantification of substrate structure (2) and the resistance to entrainment created by that structure (3), there remains a need to identify thresholds for entrainment forces if correctly balanced entrainment models are to be developed. This requires direct measurement of bed mobilisation and coincident hydrodynamics, as opposed to indirect bed mobility assessment (4), which forms the basis of objective iv of this thesis. Chapter 5 addresses objective iv by developing a multi-sensor system which records continuous high temporal resolution bedload transport data suitable for identifying the onset of bedload transport, and recording near-bed velocity at the same location and resolution as the bedload data. This dataset makes it possible to identify the moment of initial bed movement and identify corresponding entrainment thresholds from the velocity data. The multi-sensor system also recorded vertical bed seepage head, providing the first assessment of seepage as an initiation threshold in a natural channel. Seepage has been identified as a key parameter of entrainment and resistance forces in flumes, but has not been recorded alongside bedload transport data in a natural channel. Chapter 5 presents a pilot study which captured five bedload transport events using the multi-sensor system. Analysis of the data reveals bed seepage has the strongest relationship with the bedload entrainment. This result, along with support from the literature, suggests seepage needs to be included in entrainment models to improve their accuracy, and challenges the use of discharge and mean velocity for setting hydrological limits which aim to use bed mobility to manage periphyton accrual.

This chapter is in review as a manuscript to Journal of Geophysical Research: Earth Surface as:

Neverman, A.J., Fuller, I.C., Procter, J.N., Singh, R., & Death, R.G. (In Review). Implementation of a multi-sensor system to identify streamwise hydrodynamic and vertical bed seepage thresholds for particle entrainment in gravel-bed rivers.

5.1 Abstract

This paper presents a multi-sensor system which was deployed in a dynamic, coarse gravel-bed river to collect data on particle entrainment with relatively little expense, without permanent infrastructure. The system utilises an impact plate geophone, ultrasonic velocity sensor, and standpipe piezometers to collect high temporal resolution data on the timing of particle movement and hydrodynamics. The system was used to collect data for five bedload transport events. The results found no consistent threshold in any measured variable for particle entrainment over the five events. Mean velocity was found to be the worst predictor of particle entrainment despite being one of the most commonly measured parameters in initiation of motion research. Seepage was found to have a strong relationship with both the initiation and cessation of transport. This phenomenon has been demonstrated in flume experiments, but this paper is the first to demonstrate this relationship in a natural channel.

5.2 Introduction

Bedload transport processes are the main driver of morphodynamics in gravel-bed rivers. Being able to model bedload transport and predict morphological change is a principal interest for fluvial geomorphologists, civil and environmental engineers, ecologists, and river managers (Gilvear, 1999; Mao, 2012; Gilvear *et al.* 2013). Morphological changes have implications for flooding, erosion, hillslope processes, and aquatic and riparian habitat (e.g. Gilvear, 1999; Raven *et al.* 2010; Fuller & Basher, 2013; Fuller & Death, 2018). Accurate modelling of bedload transport processes is therefore critical for effective river management. However, present models frequently produce several magnitudes of variation between observed and predicted values for bedload transport (Recking *et al.* 2012). The inaccuracy of the models is largely attributed to them being derived from flume experiments (e.g. Meyer-Peter & Müller, 1948; Ackers & White, 1973; Parker *et al.* 1982), which are known to provide poor approximations of the flow dynamics and substrate structure found in natural channels. The core function of entrainment models is to equate particle resistance forces to hydraulic entrainment forces (Andrews, 1983), which relies on accurate quantification of flow dynamics and substrate structure.

5.2.1 Quantifying Thresholds

Field-based quantification of substrate resistance has traditionally been very challenging, and largely limited to using a representative particle size to characterise bed roughness, if it is considered at all. A significant focus in fluvial geomorphology in recent years has been on the description of gravel substrates using high resolution topographic surveying and image processing techniques (e.g. Dugdale *et al.* 2010; Woodget *et al.* 2015; Pearson *et al.* 2017; Vázquez-Tarrío *et al.* 2017; Woodget & Austrums, 2017; Neverman *et al.* In Press). Methodologies for quantifying other parameters of bed resistance are also emerging (Aberle & Nikora, 2006; Millane *et al.* 2006; Qin *et al.* 2012; Neverman *et al.* In Prep). These methods show promise for improving our ability to quantify bed resistance in entrainment models.

The inclusion of fluid forces in entrainment models has largely been limited by our ability to record and represent hydrodynamics at suitable spatio-temporal scales in the field. Much of the early entrainment literature sought to identify a critical discharge, time-averaged velocity, or shear stress for the entrainment of a given particle size fraction (e.g. Carling, 1983; Komar, 1987), under the assumption that flow effectiveness was linear (c.f. discussion of geomorphic effectiveness in Lisenby *et al.* 2018). As the non-linearity of fluvial systems became more widely acknowledged entrainment research began to emphasise the limitations of the effective flow paradigm and stressed the stochastic nature and spatial variability of entrainment and resistance forces (Wilcock *et al.* 1996; Milan *et al.* 2001). Numerous authors have observed counter-clockwise hysteresis patterns in bedload transport, where peak transport occurs on the falling limb of the hydrograph (Mao, 2012), which further complicates the identification of effective flows and highlights the non-linearity between discharge and entrainment.

Reliance on discharge as the metric for quantifying bedload transport thresholds is largely a result of the challenge in measuring and representing the temporal and spatial fluctuations in velocity, and lack of high temporal resolution velocity data recorded in natural channels. Yet, many entrainment mechanisms are driven by fluctuations in velocity, known as turbulence and manifested as eddies and vortices (Papanicolaou *et al.* 2002; Wu & Chou, 2003; Zanke, 2003; Smart & Habersack, 2007; Smart *et al.* 2010; Jaeger & Smart, 2012). Exchange of flow between the bed and open channel (seepage) has also been shown to have an effect on entrainment by altering near-bed velocity, turbulence, and the submerged weight of particles (Chen & Chiew, 2004; Lu *et al.* 2008; Dey & Nath, 2009; Patel *et al.* 2017). In fact, Rao & Sitaram (1999) found seepage can generate a $\pm$ 40% deviation between observed and estimated critical shear stress. Rao & Sitaram (1999) attribute this deviation to the effect seepage has on both hydrodynamic and resistance forces and their balance. Francalanci *et al.* (2008) suggest it is the reliance on entrainment models which assume hydrostatic conditions, such as the bottom component of Shields equation, despite the characteristic non-hydrostatic nature of natural flows, which causes the deviation between estimated and observed thresholds.

5.2.2 Identifying Incipient Motion

A further difficulty to the challenges of quantifying resistance and entrainment forces is the identification of incipient motion. This begins with variations in the definition of incipient motion, such as individual initial motion, several grains moving, and weak movement (Kramer, 1935; Miller *et al.* 1977; Buffington & Montgomery, 1997; Alfadhli & Yang, 2014). Variation in the definition of incipient motion has been attributed to deviations from Shields curve between observed and estimated onset of motion, with up to a two-fold variation in critical shear stress estimates (Buffington & Montgomery, 1997; Alfadhli & Yang, 2014).

Measurement of entrainment thresholds in the field has often relied on tracer particles and bedload traps (e.g. Reid *et al.* 1980; Ashworth & Ferguson, 1989; Death & Winterbourn, 1995; Leopold & Emmett, 1997). The major limitation with earlier implementation of these methods is their inability to record the exact timing of clast movement, low recovery rates of tagged clasts, and ability to only sample portions of the mobilised substrate (Sterling & Church, 2002; Bunte & Abt, 2003; Gottesfeld *et al.* 2004; Snyder *et al.* 2009; Cadol & Wohl, 2011). With limited understanding of when particles move it is difficult at best to identify coincident hydrodynamic forces to derive entrainment thresholds. Some of these limitations have been overcome through the use of pressure cells in traps, or smart tracers and magnetometers used for particle tracking (e.g. Rickenmann *et al.* 2012; Cassel *et al.* 2017). However, these methods still suffer from limited ability to sample the entire bed movement event, are limited to sites with appropriate infrastructure, require maintenance post-event, and are relatively expensive to implement and maintain and are therefore not widely adopted. Surrogate devices such as impact plate geophones and acoustic pipes are becoming popular methods for direct, continuous measurement of bedload transport. However, their installation is often limited to sites with solid permanent structures (sills, weirs) which can be used to secure the sensors (Rickenmann *et al.* 2017; Rickenmann & Fritschi, 2017; Tsutsumi *et al.* 2018). Some studies have overcome this issue by placing acoustic pipes in logs (Dell'Agnese *et al.* 2014; Mao *et al.* 2014) or impact plates in garden paving stones (Downs *et al.* 2016). These approaches either limit installation to sites with stable beds, or risk losing the sensors during an event.

To improve bedload entrainment models a new approach is required for collecting empirical datasets in the field which capture all mechanisms of entrainment using reliable techniques (Recking *et al.* 2012). It is apparent that advancing the study of particle entrainment requires simultaneous continuous monitoring of bedload transport and fluid dynamics at suitably high resolutions to capture their temporal and spatial variations. This will provide a better understanding of the mechanisms of entrainment in natural channels, and lead to the development of more robust entrainment models. This paper presents the development and implementation of a multi-sensor system designed to achieve:

1. Continuous recording of bedload transport without requiring significant infrastructure;

2. Coincident recording of continuous high-resolution near-bed velocity alongside the bedload transport data;

3. Identification of bed seepage direction prior to and during bedload transport events.

This paper focuses on the development of the multi-sensor system, as advancing the methodologies for field-based entrainment studies is a critical first step towards improving entrainment models. The methods were trialled in the Pohangina River, New Zealand to demonstrate their ability to record bedload transport initiation and local hydrodynamics. The datasets produced by the system are analysed to demonstrate how they may assist in advancing particle entrainment studies in gravel-bed rivers.

5.3 Study Site

The Pohangina River is a 5$^{\text{th}}$ order wandering gravel-bed river (*sensu* Ferguson & Werritty, 1983) located northeast of Palmerston North, New Zealand (Figure 5.1). The Pohangina runs parallel to the western front of the Ruahine Ranges, draining a 547 km^2 valley in the eastern Wanganui Basin (Fuller, 2007; Clement *et al.* 2010). The catchment has a steep 0.004 gradient, and the channel has a sinuosity of 1.3 (Fuller, 2007). A temperate maritime climate exists in the Manawatu region with rainfall ranging from 800 mm at the coast to >5000 mm in the ranges (Clement *et al.* 2010).

The study site is located at a regional council monitoring site known as Mais Reach on the lower Pohangina (Figure 5.1). The study site has been monitored since 1969 and is known to have frequent bed movement events. Henderson & Diettrich (2007) analysed the flow record from 1969 to 2005 and report a mean annual flow of 17 m^3 s^{-1}, MALF of 2 m^3 s^{-1}, and MAF of 490 m^3 s^{-1}. FRE$_3$ at Mais Reach is 30 m^3 s^{-1} and occurs 12.5 times per year on average. The MAF/Median is 48.94, indicating a relatively disturbed regime. The Pohangina has a measured sediment load of 499,830 t yr^{-1}, and a sediment yield of 978 t km^{-2} yr^{-1} (Dymond *et al.* 2016). During a 150-year storm event in 2004 the Pohangina expended ~14,400 x 103 J, eroding 0.36 km^2 of floodplain (Fuller, 2007). The Pohangina River therefore represents a site with a dynamic flow and sediment regime.

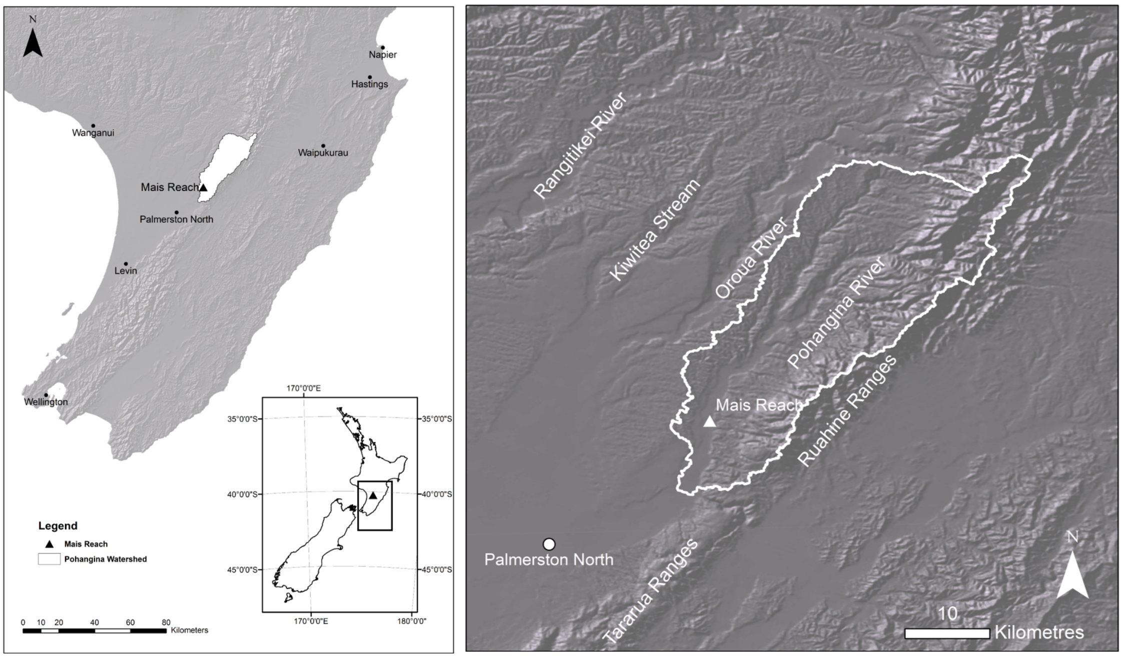

Figure 5.1: Location of the Mais Reach study site and Pohangina River catchment within the context of the North Island (left), and the Ruahine Ranges and neighbouring catchments (right). The head of the catchment is in the north with the river flowing southward, running parallel with the axial Ruahine Range.

5.4 Methodology

There are four main methodological components to this research:

1. record continuous, high temporal resolution bedload transport data which are suitable for identifying the onset of motion for bed particles;
2. record high temporal resolution velocity data to characterise a range of hydrodynamic characteristics shown to relate to bedload entrainment mechanisms;
3. measure the seepage regime at the site during bedload transport events, particularly at the onset of motion; and
4. use the datasets to identify entrainment thresholds and dominant entrainment mechanisms at the site.

5.4.1 Identifying the Onset of Motion

Identifying the onset of motion requires a time series dataset capable of recording precise instants of particle movement. Given the stochastic nature of entrainment events it is critical to record bed movement automatically and continuously, with minimal maintenance of apparatus required (i.e. minimal downtime). Conventional approaches to measuring bedload transport, such as tracer particles (Ashworth & Ferguson, 1989; Hassan *et al.* 1991; Death & Winterbourn, 1995; Death, 2002; Chapuis *et al.* 2015; Houbrechts *et al.* 2015) and bedload traps (Milhous, 1973; Leopold & Emmett, 1976; Reid *et al.* 1980; Garcia *et al.* 2000; Sear *et al.* 2000) do not give good indications of the timing of movement, require regular maintenance, have sampling biases (Sterling & Church, 2002; Bunte & Abt, 2003), or have inconsistent success rates (e.g. Gottesfeld *et al.* 2004; Snyder *et al.* 2009; Cadol & Wohl, 2011) and are therefore unsuitable for incipient motion study.

Impact plate geophones were identified as the most suitable method to achieve the research objectives. The use of impact plate geophones has been covered in previous literature (e.g. Rickenmann *et al.* 2014; Tsakiris *et al.* 2014) and will not be repeated here. This section focuses on the novel installation system used to install the impact plate, which will enable wider adoption of impact plates.

A literature review of impact plate installations suggested present methods were not suitable for use in dynamic, coarse gravel beds, such as the Pohangina River, as they required extensive permanent support structures such as sills (e.g. Rickenmann & Fritschi, 2017) or were likely to be washed away (e.g. Downs *et al.* 2016). To overcome these issues a novel installation method was developed. A 750 mm x 500 mm plate was constructed from 4 mm mild steel (Figure 5.2). A housing was constructed at one end of the impact plate for the geophone and velocity sensor. The impact plate was secured to the bed of the channel in the thalweg at baseflow (Figure 5.3) using three securing rods constructed from 25 mm diameter mild steel. The securing rods were installed in sections of variable lengths to enable on-the-fly adjustment for local bed conditions (i.e. some spots in the bed were difficult to penetrate and required shorter rods). This ensured the top of the rods were always flush with the bed surface. The securing rods were installed to a maximum depth of 3 m, where they were believed to have hit bedrock. 22 mm male threads were inserted in the top of the securing rods. The impact plate was attached to the threads using large washers and nuts. This system allowed the impact plate to be installed anywhere within the channel and ensured the plate could be installed flush with the bed surface. Adjustments could also be made following bed level adjustments post-flood. A 6 mm galvanised chain was used to connect the impact plate to a railway iron post, which was located 15 m away at the channel margin, to retain the plate if it was removed from the bed during a flood event. Fortunately, the impact plate was never removed by a flood, but the chain was occasionally broken.

A 10 Hz geophone was attached to the impact plate. A datalogger was built which pre-processed the raw geophone signal by converting the waveform amplitude (the impact magnitude) from volts to a 10-bit value (0 to 1023). These 10-bit values are referred to as *impact units*. The average and maximum impact magnitude ($MaxA$) measured per second were recorded. Impact magnitude has been found to relate to grain size (Turowski & Rickenmann, 2009; Rickenmann *et al.* 2014; Wyss *et al.* 2016), and is used in this study as a proxy for grain size when identifying threshold relationships with entrainment. The datalogger was located on the elevated floodplain and powered by a battery and solar panel. Power and data transmission cables were run from the datalogger to the impact plate along the galvanised chain. This system acted as a safeguard in the event of the impact plate being washed away, allowing the cables to break and retaining the datalogger (and the data) on the floodplain.

Analysis of the geophone data revealed that a new cable which was installed to repair the system had introduced noise in later datasets. Signal processing revealed a consistent background noise of $\leq$60 impact units. Given this meant the average impacts per second were skewed by background noise, the maximum impact per second ($MaxA$) was solely used for subsequent analysis. Background noise in geophone signals is a common issue and is resolved by signal filtering (Wyss *et al.* 2016). The $MaxA$ data was filtered using a threshold of 70 impact units. Using $MaxA$ also helps to eliminate noise caused by a single grain creating multiple impacts or resonating vibrations (Rickenmann *et al.* 2014), and allows thresholds to be found for the maximum grain in motion.
Bedload events were identified in the datasets by finding the instant when impacts $\geq$70 began to occur in succession, following the several grains moving definition of incipient motion (Alfadhli & Yang, 2014). The change in state to the onset of motion was quite distinct in all five recorded events. The time stamp accompanying the first impact of the

event was used to identify the values for the hydrodynamic parameters occurring simultaneously with the onset of motion.

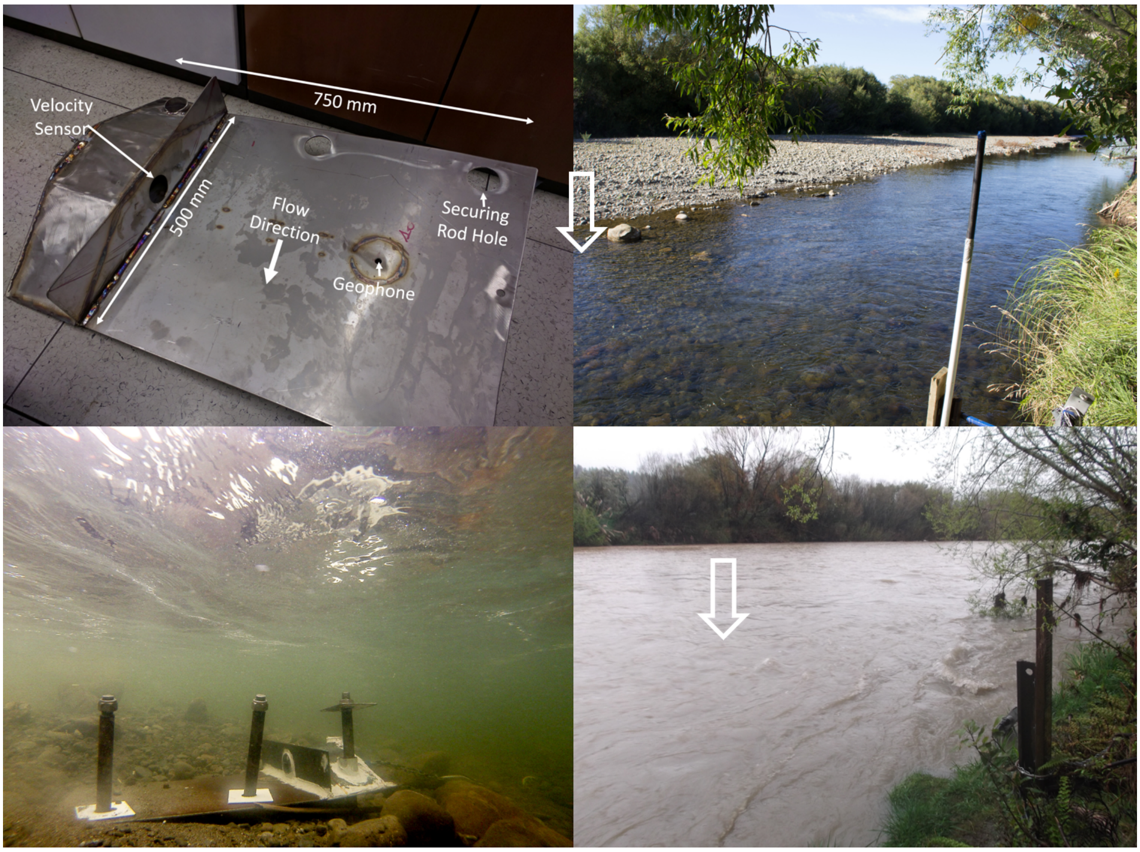

Figure 5.2: Top left: Dimensions and layout of the impact plate. Bottom left: Impact plate sitting on the bed showing securing rods as they were being driven in to the bed. Right: White arrows show location of the impact plate at low flow (top) and during a high flow event (bottom).

5.4.2 Near-Bed Velocity

5.4.3 Near-Bed Velocity

Given the strong spatial variation inherent in velocity it was important to record velocity as close to the impacts as possible to ensure congruency between thresholds and movement. An AIRMAR® CS4500 ultra-sonic velocity sensor was installed in the impact plate instrument housing, with the sensor face mounted in a side scanning position (Figure 5.2). The centre of the sensor was mounted 50 mm above the impact plate. The CS4500 has a screening distance of 77 mm to 127 mm to avoid measuring in the boundary layer created by the sensor face/mounting surface. This design ensured velocity was measured approximately 50 mm above the centre of the impact plate. Velocity was recorded at 1 Hz alongside impacts using the same datalogger.

The velocity data were used to calculate the instantaneous velocity ($\tilde{u}$), time-averaged velocity (U_i), turbulence (u_i), and turbulence intensity (I) following Reynolds decomposition (Tennekes & Lumley, 1972). U_i was calculated for each time series datum with a 30-second moving window using Equation 5.1:

$$U_i = \frac{\tilde{u}_t + \tilde{u}_{t\text{-}1} + \tilde{u}_{t\text{-}(n\text{-}1)}}{n} \tag{5.1}$$

Figure 5.3: Location of the impact plate and piezometers within the context of the channel planform. The stage gauge is mounted alongside the piezometers. The black box on the left image indicates the extent of the right image. Note there are no major source areas of sediment near the study site, although some erosion of the true left bank did occur, this mainly supplied sand to the channel.

where U_{it} is the time-averaged velocity at time t, $\tilde{u}_t$ is the instantaneous velocity at time t, and n is the number of samples in the moving average, in this case n =30. u_i was calculated using Equation 5.2:

$$u_{\text{it}} = U_{\text{it}} - \tilde{u}_t \tag{5.2}$$

where u_{it} is the turbulence at time t. I was then calculated from u_i using Equation 5.3:

$$I_t = \frac{\sqrt{u_{it}^2 + u_{it-1}^2 + ... + u_{it-(n-1)}^2}}{U_{it}} \tag{5.3}$$

where I_t is the turbulence intensity at time t.

5.4.4 Seepage

Given the inherent difficulty in using seepage meters in high flow events, differential standpipe piezometers (also known as miniature piezometers or hydraulic-potential probes) were used to provide an estimate of vertical seepage direction (upward or downward) based on Darcy's principle where flow is driven from areas of higher total head (h) to areas of lower h. This is a well-established method for measuring seepage (Lee & Cherry, 1979; Winter *et al.* 1988). In the case of vertical seepage in the river bed, upward seepage (injection) occurs when flow moves from the bed into the open flow, and downward seepage (suction) when flow moves from the open channel flow into the bed (Rao & Sitaram, 1999). Injection therefore occurs when pore pressure in the bed is greater than the pressure of the open flow (stage), and suction occurs when the bed pore pressure is lower than that of the open flow.

Figure 5.4 demonstrates the differential standpipe piezometer system installed at Mais Reach, and the parameters used to derive the total head difference and therefore the direction of seepage. Two standpipe piezometers (SP1 and SP2) were installed at the margin of the wetted channel, at a vertical bank, in line with the impact plate to measure pressure head (h_w) of the open channel (h_{w_1} in SP1) and intra-gravel flows (h_{w_2} in SP2). Pore pressure (p) at point x_n is calculated using Equation 5.4:

$$p = h_w \cdot y_{\mathrm{w}} \tag{5.4}$$

where y_w is the unit weight of water (9.81 kN/m^3), and h_w is the pressure head (m). Given the unit weight of water is constant, h_{w_2} - h_{w_1} can be used to indicate the difference between pore pressures at x_1 and x_2, assuming they are measured from the same height datum.

The standpipes were constructed from 40 mm diameter steel tube, with a 10 cm long screen and end cap at the base of SP2, and an open end for SP1. SP1 was installed in the open channel flow. SP2 was installed in the bed with the top of the screen 0.6 m below the surface (further penetration could not be achieved). Solinst® Levelogger Edge Junior Model 3001 pressure transducers were installed inside the standpipes to measure the pressure head. The Leveloggers are battery powered with onboard dataloggers, making them a self-contained unit. The Leveloggers recorded water level in the standpipes at 15-minute intervals beginning on the hour to ensure measurements were consistent with the regional council discharge data. A Solinst® Barologger Edge Model 3001 barometer was installed at the site and used to compensate the Leveloggers for atmospheric pressure.

The bed surface was used as a height datum (A) and was monitored regularly to ensure a constant datum, but no change in bed surface height was observed throughout the study period. A was used to calculate the elevation head (h_z) for SP1 (h_{z_1}) and SP2 (h_{z_2}) using Equation 5.5:

$$h_z = A + x \tag{5.5}$$

where h_z is the elevation head, A is the datum elevation, x is the elevation of the point where pore pressure is being measured. Total head or piezometric head (h) for SP1 (h_1) and SP2 (h_2) was calculated using Equation 5.6:

$$h = h_z + h_w \tag{5.6}$$

where h is the piezometric head. The difference in the piezometric head (Δh, subsequently referred to as the seepage head) between SP1 and SP2 was calculated to identify the direction of the hydraulic gradient and indicate direction of flow between the bed and open channel using Equation 5.7:

$$\Delta h = h_2 - h_1 \tag{5.7}$$

where Δh is the seepage head, and h_1 and h_2 are the piezometric head for SP1 and SP2, respectively. Positive Δh indicates injection, negative Δh indicates suction.

Figure 5.4 models three scenarios and their implication for seepage direction. In scenario 1 $h_1 = h_2$, indicating that the difference between x_1 and x_2 is due to the difference in depth between the points (h_{z_2} - h_{z_1}), and no seepage is occurring. Scenario 2 occurs when $h_2 > h_1$, and the difference between x_1 and x_2 is not explained by h_{z_2} - h_{z_1}. In this instance injection would occur. In Scenario 3 $h_2 < h_1$, and the difference between x_1 and x_2 is not explained by h_{z_2} - h_{z_1}. Suction is expected to occur during scenario 3. The piezometric head for SP1 was used as the stage (St) data. Discharge (Q) data was not derived from St but was instead independently measured and provided by Horizons Regional Council. Q data were provided at 15-minute intervals for the entire study period.

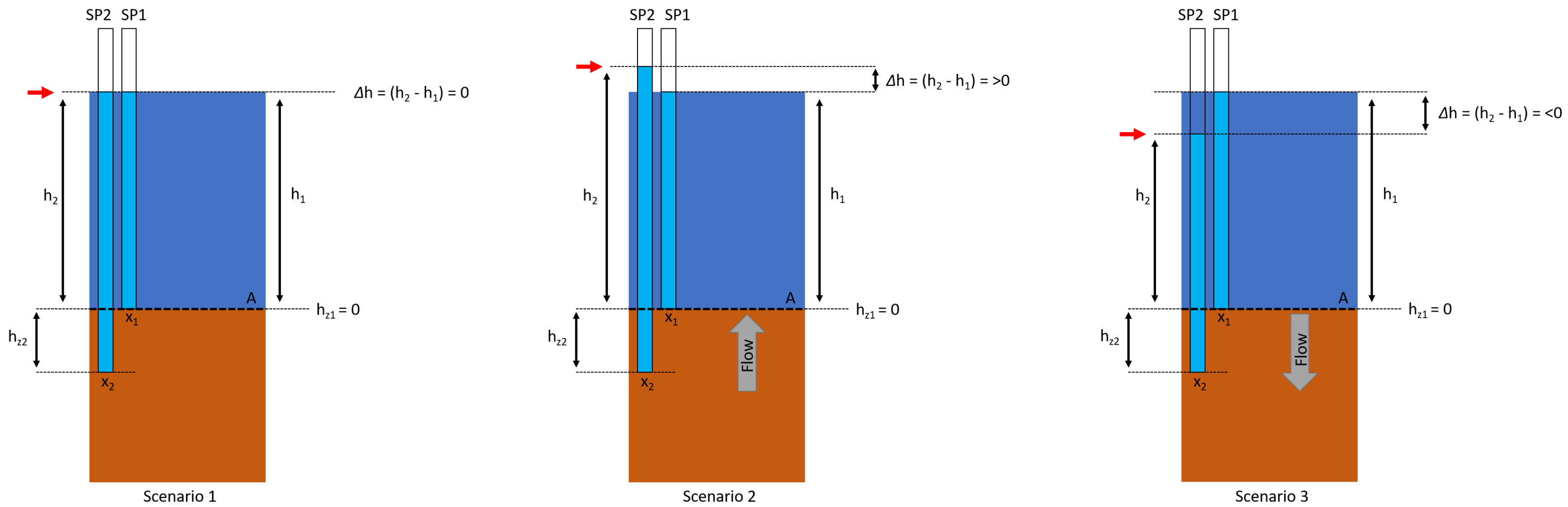

Figure 5.4: Diagram demonstrating the application of the differential standpipe piezometers (SP1 and SP2) for measuring seepage direction. Scenario 1 demonstrates a state of no seepage, scenario 2 demonstrates injection due to high pore pressure at x_2, and scenario 3 demonstrates suction due to low pore pressure at x_2.

5.5 Results

Five bedload transport events (Table 5.1) were recorded over the study period with corresponding hydrodynamic data. Figure 5.5 shows the timing of these events on the hydrograph for the site. The data record for Event 5 ended ~2 hours after the initiation of bedload transport as the datalogger malfunctioned, so the entire event was not captured. Table 5.2 presents the values recorded for St_{cr}, Q_{cr}, Δh_{cr}, $\tilde{u}_{cr}$, U_{icr}, u_{icr}, and I_{cr} (cr denotes critical value for the respective metric) which correspond with the initial impact for each event.

Table 5.1: Bedload transport events recorded by the impact plate which also had corresponding hydrodynamic data.

Event Number	**Bedload Initiation Date**
1	05/09/2016
2	06/10/2016
3	08/11/2016
4	18/11/2016
5	23/01/2017

5.5.1 Event 1

Event 1 occurred on September 5, 2016, 9 days after the previous high flow event (which peaked at 100 $m^3 s^{-1}$). The initial impact for the event was the largest initial impact for the five recorded events. Event 1 had the lowest triggering Q_{cr} and Δh_{cr} for the five events. Initiation occurred on the rising limb at 3.7 times the median flow (Figure 5.6). Initiation occurred as seepage switched from injection to suction (Figure 5.7). Velocity metrics were relatively high, along with the lowest u_i and second lowest I. Event 1 had an average duration with bedload transport lasting approximately 19 hours. Cessation of movement occurred as suction switched to injection.

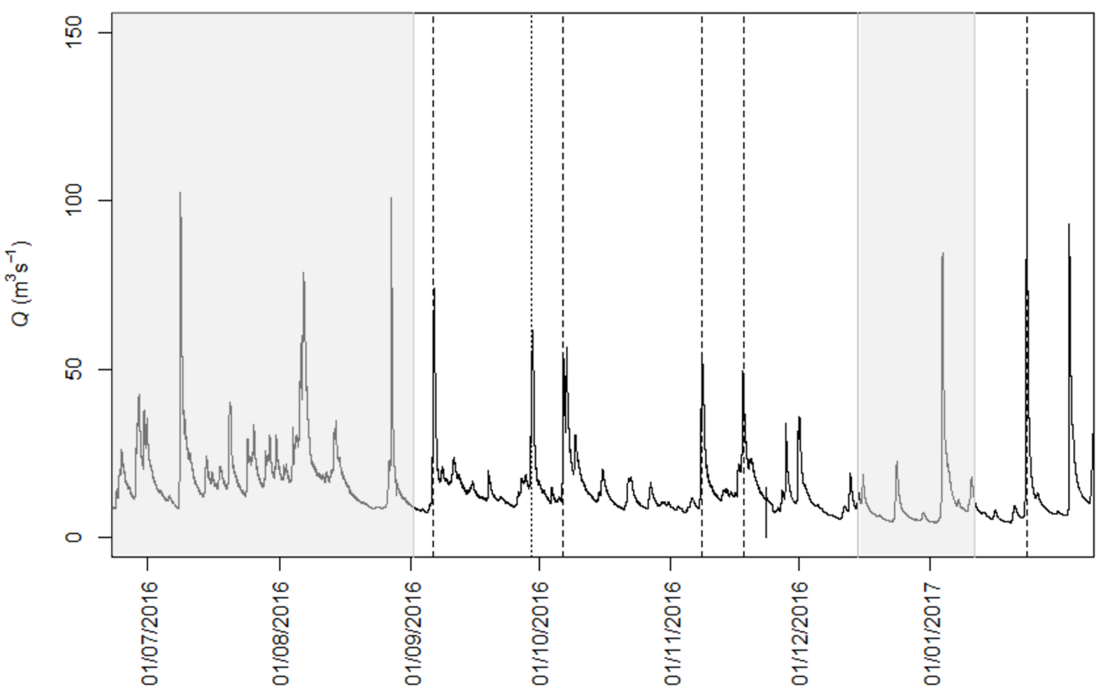

Figure 5.5: Hydrograph for Mais Reach from July 2016 to January 2017. Initiation of bedload events 1-5 are indicated by vertical dashed lines. The dotted vertical line indicates a bedload event recorded by the geophone, but no velocity data was recorded during the onset of bedload transport, so this event was not analysed in this paper. The grey boxes are sections of the hydrograph where no bedload or velocity data was recorded.

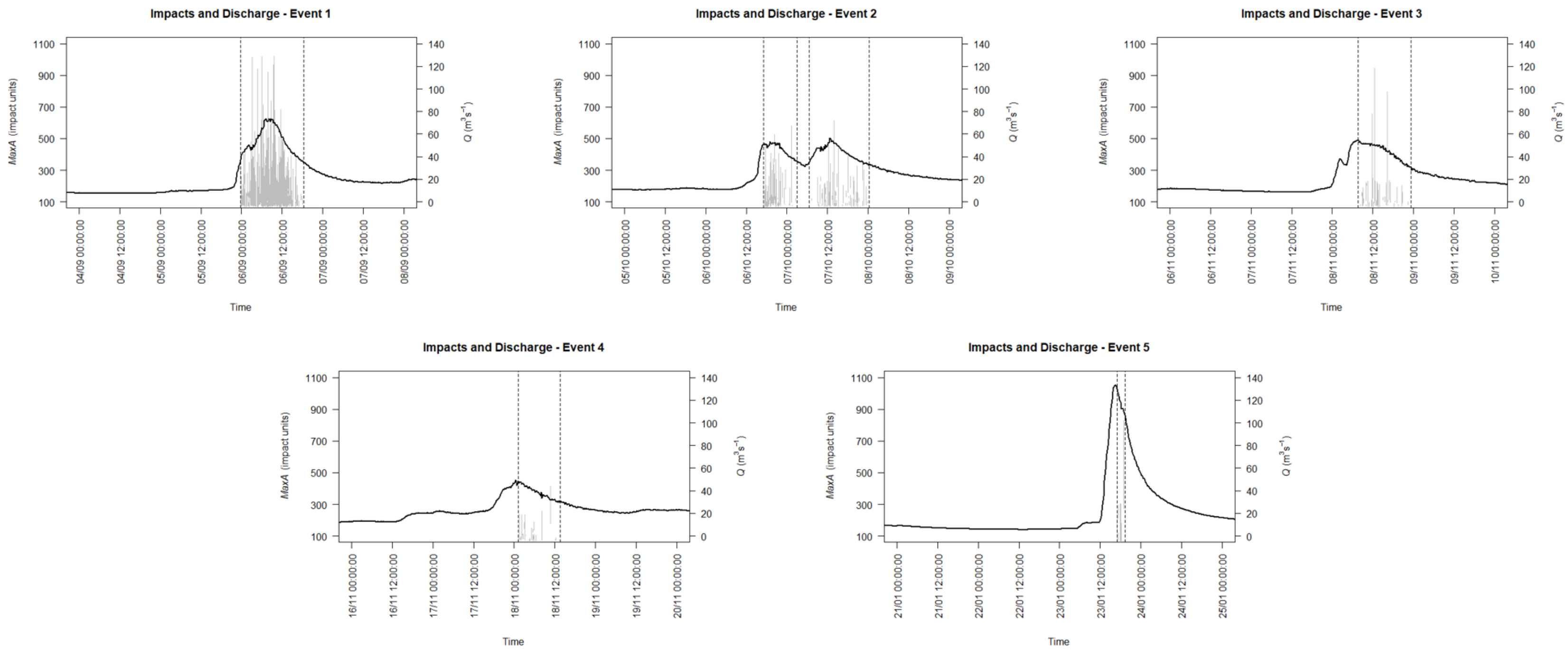

Figure 5.6: Plots showing geophone impacts ($MaxA$) and discharge (Q) for each event. Axis extents are the same for all plots. The initiation and cessation of each event are indicated by the dashed vertical lines. Event 1 represents a textbook case where bedload transport initiates at a critical discharge on the rising limb. Events 2-4 show initiation occurred at peak discharge. It is interesting to note Event 2 had two phases of bedload transport as a second flood peak occurred shortly after the first cessation of bedload transport. Event 5 shows a case where initiation occurred on the failing limb of the hydrograph. Note: during Event 5 the data cables were damaged, so the cessation of transport was not truly captured. The second vertical dashed line for Event 5 therefore represents the end of the data set rather than end of transport.

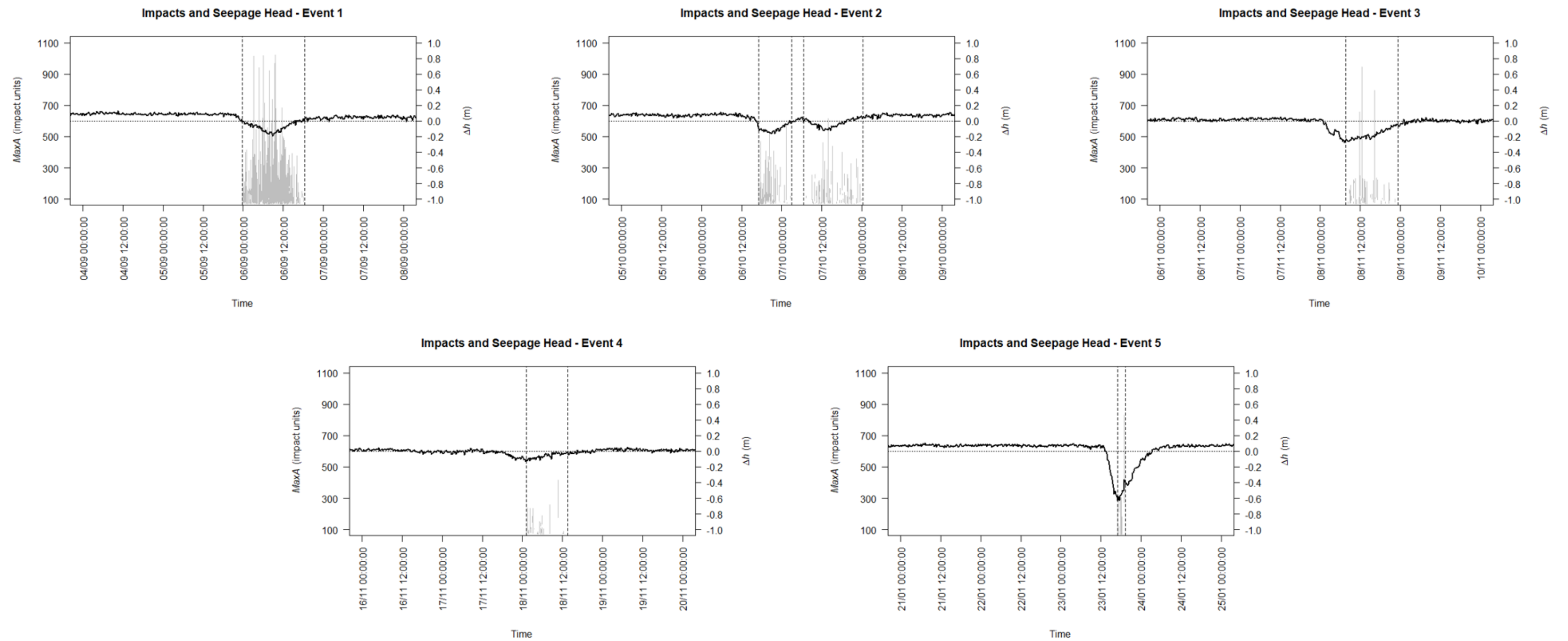

Figure 5.7: Plots showing geophone impacts ($MaxA$) and seepage head (Δh) for each event. Axis extents are the same for all plots. The initiation and cessation of each event are indicated by the dashed vertical lines. The horizontal dotted line represents 0 m seepage head, indicating the point where seepage switches between suction and injection. During Events 1 and 2 it is apparent that initiation and cessation of bedload transport occurs around the point of injection switching to suction and vice versa. During Events 3-5 initiation coincides with peak suction, and cessation occurs as suction switches to injection. Note: during Event 5 the data cables were damaged, so the cessation of transport was not truly captured. The second vertical dashed line for Event 5 therefore represents the end of the data set rather than end of transport.

5.5.2 Event 2

Event 2 occurred on October 6, 31 days after event 1. However, there was an event on September 29 between event 1 and 2 (Figure 5.5). Velocity data did not record during the initiation period of the September 29 event, but did record again an hour after initiation. It is thought an object blocked the sensor for this period. The data for this event was therefore unusable for this study.

Event 2 therefore occurred 7 days after the previous event on September 29. Event 2 had two hydrograph peaks of similar magnitudes, and two phases of bedload movement (Figure 5.7). Initiation of the first phase occurred with an impact of 96 impact units at 50 $m^3\,s^{-1}$, five times the median flow, at the first hydrograph peak as injection switched to suction with $\mathit{\Delta} h_{cr}$ of -0.073 m. Event 2 was triggered at the lowest recorded $\tilde{u}_{cr}$ and U_{icr}, the second lowest u_{icr}, and the second highest I_{cr}. The second phase occurred at a lower Q_{cr}, but as with the first phase initiation occurred as injection switched to suction. Cessation occurred as suction switched to injection for both phases.

5.5.3 Event 3

Event 3 occurred on November 8, 33 days after event 2. Event 3 had the lowest initial impact magnitude of 79 impact units, and the fourth highest Q and $\mathit{\Delta} h$ thresholds of 54 $m^3\,s^{-1}$ and -0.258 m, respectively. Initiation again occurred at the hydrograph peak, but this time at peak suction. Event 3 had an equal $\tilde{u}_{cr}$ as event 2, with a slightly higher U_{icr}. Event 3 u_{icr} was the second highest, and I_{cr} was the highest recorded. Cessation occurred as suction switched to injection.

5.5.4 Event 4

Event 4 occurred on November 18, 10 days after event 3. Event 4 had the second lowest Q_{cr}, with motion occurring at the hydrograph peak which coincided with peak suction. All other thresholds were the median recorded of the five events. The initial impact was also the median recorded at 134 impact units. Cessation occurred as suction became injection.

5.5.5 Event 5

Event 5 occurred on January 23, 2017, 66 days after event 4. A high flow event did occur between events 4 and 5 on January 3, but due to sensor malfunction no data was recorded for this event. Given this event reached a peak discharge of 84 $m^3\,s^{-1}$ it is likely that bedload transport did occur, however, the peak of this event was smaller than Q_{cr} for event 5 so may not have produced bedload transport.

The initial impact magnitude for event 5 was the second highest recorded at 146 impact units. Event 5 had the highest thresholds for all parameters, except for I which was the lowest recorded. Initiation occurred on the falling limb, meaning the triggering discharge had already been exceeded on the rising limb without initiating movement. However, this triggering discharge coincided with higher suction on the falling limb. Cessation of event 5 was not recorded due to sensor malfunction ˜2 hours after initiation.

Table 5.2: Critical threshold values (denoted by cr) for the range of hydraulic parameters which were recorded at the onset of bedload transport for the five events. The table shows the large variation in thresholds, with no consistent threshold for incipient motion being identified.

Event	$\boldsymbol{Q_{cr}}$ $(\mathbf{m^3\,s^{-1}})$	$\boldsymbol{St_{cr}}$ **(m)**	$\boldsymbol{\Delta h_{cr}}$ **(m)**	$\tilde{u}_{cr}$ $(\mathbf{m\,s^{-1}})$	$\boldsymbol{U_{icr}}$ $(\mathbf{m\,s^{-1}})$	$\boldsymbol{u_{icr}}$ $(\mathbf{m\,s^{-1}})$	$\boldsymbol{I_{cr}}$	**First Impact** $\boldsymbol{MaxA}$
1	37	1.63	-0.013	0.37	0.37	0.006	0.177	310
2	50	1.7	-0.073	0.09	0.15	-0.056	0.77	96
3	54	1.84	-0.258	0.09	0.21	-0.12	0.89	79
4	46	1.73	-0.13	0.19	0.3	-0.11	0.28	134
5	130	2.73	-0.633	1.50	1.3	0.20	0.09	146

5.5.6 Parameter Relationships

Table 5.3 presents the correlation coefficients for each parameter vs $MaxA$ at the instant of initiation for each event. Over the five events no consistent critical threshold for entrainment was found. $MaxA$ was better predicted by Δh than Q or St, but statistical significance was low. Δh also had a stronger relationship than $\tilde{u}$, U_i, and u_i. I had the highest predictive power with a significantly higher correlation coefficient and a significantly lower p-value, followed by Δh, and u_i. Figure 5.6 shows time series plots of Q and $MaxA$, and Figure 5.7 shows plots of Δh and $MaxA$ for each event. These figures show initiation occurs on the rising limb for Event 1, at the peak of the hydrograph for Events 2-4, and on the falling limb for Event 5. Initiation occurs at the change from injection to suction for Events 1 & 2, and at peak suction for Events 3-5. Cessation of motion occurs as suction turns to injection for events 1-4, but was not recorded for event 5 due to sensor malfunction.

Intra-event thresholds showed weak relationships with $MaxA$ for events 1-4. Event 5 showed stronger relationships (Table 5.4). The parameters were ranked from 1-4 in order of relationship strength. Overall, I was the best predictor based on aggregated scores, followed by $\tilde{u}$, u_i, and U_i, respectively.

Table 5.3: Correlation coefficients for each hydrodynamic parameter threshold regressed against $MaxA$ for the initiation of each event, listed in descending order of relationship strength.

Parameter	r	p	df
I	-0.66	0.23	3
Δh	0.31	0.61	3
u_i	0.27	0.65	3
Q	-0.20	0.74	3
St	-0.17	0.78	3
$\tilde{u}$	0.15	0.81	3
U_i	0.11	0.86	3

5.6 Discussion

This study has developed a multi-sensor system capable of recording hydrodynamic and bedload transport data in the field. This has been achieved by developing and successfully deploying a geophone impact plate coupled with a near-bed velocity sensor and measurement of the seepage regime. The multi-sensor system presented in this paper has demonstrated significant utility for advancing incipient motion research in natural channels.

5.6.1 Identifying entrainment thresholds

Critical discharge is often identified for bedload events. As our results have shown, critical discharge would be an inappropriate metric for a bedload initiation target in the Pohangina River during this study period as critical discharge ranged from 4 to 13 times the median flow. Time-averaged velocity is also commonly measured as a threshold for

Table 5.4: Correlation coefficients for each velocity and turbulence parameter regressed against *MaxA* for each impact record over the duration of each event (*intra-event thresholds*). Thresholds are ordered by significance for each event.

Number	**Parameter regressed against *MaxA***	r	p	**Rank**
1	I	-0.04	0.01	1
	U_i	0.02	0.13	2
	$\tilde{u}$	0.01	0.35	3
	u_i	-0.01	0.55	4
2	I	-0.02	0.24	1
	$\tilde{u}$	0.02	0.30	2
	u_i	0.02	0.32	3
	U_i	0.00	0.84	4
3	u_i	-0.04	0.22	1
	U_i	0.03	0.33	2
	I	-0.01	0.71	3
	$\tilde{u}$	0.01	0.85	4
4	u_i	-0.08	0.05	1
	$\tilde{u}$	-0.06	0.13	2
	U_i	0.02	0.64	3
	I	0.00	0.98	4
5	$\tilde{u}$	-0.52	0.00	1
	I	0.50	0.00	2
	U_i	-0.48	0.00	3
	u_i	-0.29	0.00	4

entrainment, but this study found U_i had the weakest relationship with *MaxA* at the onset of motion, and ranked as the worst intra-event predictor of *MaxA* over the five events. In fact, no consistent critical threshold for initiation of motion was found for the five events for any parameter (Table 5.2).

I had the strongest relationship with *MaxA* for the onset of motion, and the strongest intra-event relationship with *MaxA* throughout events 1 & 2. I also ranked as the best predictor for intra-event thresholds over the five events. These results indicate turbulence intensity may be a critical parameter to include in entrainment equations, yet I is rarely mentioned in incipient motion studies. I has been shown to affect the drag coefficient (c_d) of objects (Ko & Graf, 1972; Surry, 1972; Yeboah *et al.* 1997; Younis, 2010), with an inverse relationship between I and c_d. If the alteration of c_d were significant enough it could lead to the crossing of the entrainment threshold at a consistent velocity/boundary shear stress. The relationship between I and *MaxA* at the onset of motion was found to be negative for the Mais Reach dataset. This relationship suggests higher *MaxA* occurred during moments of lower I and therefore higher c_d at Mais Reach. Particle resistance may therefore be better assessed if I and c_d are included in entrainment models.

Δh was also found to have a stronger linear relationship with $MaxA$ than Q, St, $\tilde{u}$, U_i, and u_i. This is likely a result of the affect seepage has on the balance between resistance and entrainment forces for a given particle size by affecting both the relative submerged weight of particles and the local hydrodynamics (Maclean, 1991; Chen & Chiew, 2004; Lu *et al.* 2008; Deshpande & Kumar, 2016). Flume studies have also shown I decreases under suction. The relationship between Δh and $MaxA$ may relate to Δh decreasing I, leading to increased c_d. This relationship between Δh and I may explain why these two parameters had the strongest relationship with $MaxA$ at incipient motion.

5.6.2 Mechanisms

Whilst no critical thresholds were identified, some trends in the balance of thresholds were apparent. Flume studies have demonstrated the role seepage may play in initiating entrainment by altering the balance of resistance and hydrodynamic forces (Chen & Chiew, 2004; Lu *et al.* 2008; Dey & Nath, 2009; Patel *et al.* 2017), but to the authors knowledge this is the first measurement of seepage alongside bedload transport in natural channels. The relationship between $MaxA$ and Δh at Mais Reach appear to be consistent with flume studies as substrate motion occurred under suction during all five bedload transport events. Suction was also present throughout the duration of all bedload transport events, with cessation of motion occurring as suction switched to injection. This is evident in Figure 5.6 which shows entrainment occurs at changes in seepage direction or peak intensity, which coincided with peak discharge during events 2-4 and on the falling limb during event 5. However, no consistent Δh_{cr} was found. The concept of pseudo-motion proposed by Rao & Sitaram (1999) may explain why incipient motion occurred on the falling limb during event 5, with increased suction magnitude on the falling limb reducing critical shear stress and allowing particles to be mobilised at flows which were unable to move particles on the rising limb when higher critical shear stress would be required. Event 5 also has the lowest I suggesting c_d was high at the onset of motion on the falling limb.

Seepage also appears to affect the cessation of movement which occurred at the onset of injection during events 1-4 (cessation was not recorded during event 5 due to sensor malfunction). Event 2 provides an interesting example of this phenomenon as event 2 had two phases of bedload transport, with the initiation and cessation of each phase occurring at the onset of suction and injection, respectively.

5.6.3 Intra-Event Thresholds

As shown in Table 5.4, the correlation between $MaxA$ and the hydrodynamic parameters was low for events 1-4, but reasonable for event 5. This may be explained by equal mobility transport (Parker *et al.* 1982; Andrews, 1983) occurring in the later stages of events 1-4 as the bed becomes more mobile throughout the event due to break up of the armour layer and increased exposure of particles. Given event 5 had a short duration, equal mobility transport may not have been reached. Equal mobility would result in a range of particle sizes moving at once, but the thresholds only relate to the larger particles, leading to poor correlation between $MaxA$ and the hydrodynamic parameters when all $MaxA$ values are considered. It may be more appropriate to use the hydrodynamic parameters to estimate transport rates, similar to the application of reference shear stress (Parker *et al.* 1982; Mueller *et al.* 2005), rather than predicting the entrainment of individual particle size fractions during an event.

5.6.4 Key Outcomes

We have demonstrated that single parameter thresholds are not suitable for consistently identifying entrainment thresholds. Instead, a multi-parameter approach is required for entrainment models to balance resistance and entrainment forces. It is also critical to note that hydrodynamic forces act as both entrainment and resistance forces. In particular, turbulence intensity and seepage are key to determining resistance thresholds and therefore need to be considered in entrainment models. This relationship between $MaxA$, Δh, and I has been apparent in all five events recorded at Mais Reach, highlighting the need to consider these parameters in entrainment models. Doing so may provide a better balance of entrainment and resistance thresholds in the models. This should also be extended by improving the measurement of substrate characteristics which contribute to particle resistance and include these as parameters in entrainment models (Neverman *et al.* 2018). This study has assumed equivalent resistance thresholds for all events. It is unlikely that this was the case, and variations in substrate resistance are expected to at least partially contribute to the variations in critical entrainment thresholds.

Improving entrainment models will require bedload transport to be measured in natural channels along with quantification of substrate composition and structure prior to entrainment, 4-dimensional hydrodynamics before, during, and after transport events, and information on the quality and quantity of material being transported. As entrainment mechanisms and thresholds are likely to vary between sites, datasets are required from a wide range of sites to ensure robust models are developed which are widely applicable. This requires instrumentation to be developed which can be installed in diverse natural settings without infrastructure such as sills and weirs, is capable of recording data continuously at high temporal resolutions, and all at relatively low expense.

The multi-sensor system presented in this paper has attempted to address this need for multi-parameter data by capturing high resolution bedload transport and hydrodynamic data, and for the first time in a natural channel including data on the seepage regime. However, the seepage data was limited to a lower temporal resolution dataset than the bedload and velocity data due to limitations with the battery life of the piezometers used in the standpipes. Whilst the 15-minute recording interval used for seepage was adequate for showing the trend in seepage direction, higher temporal resolution seepage data may be valuable for better understanding the effect of seepage on entrainment thresholds, particularly how this balance fluctuates with other flow characteristics such as turbulence intensity. It may also be valuable to quantify seepage velocity, but this will rely on a range of assumptions such as substrate conductivity remaining constant if seepage meters cannot be used.

5.7 Conclusions

Accurate understanding of bedload transport and associated morphodynamic responses is central to effective management of gravel-bed rivers, with implications for hazard management, resource use, and ecological health (Gilvear, 1999; Gilvear *et al.* 2013). New sediment data collected with reliable techniques is required to further our understanding of bedload transport dynamics (Recking *et al.* 2012). Coupled fluid dynamics data is also required to better model the mechanisms of entrainment in natural channels and develop accurate entrainment models. The multi-sensor system installed at Mais Reach has demonstrated an ability to provide improved empirical datasets on the timing of particle movement and coincident hydrodynamics in challenging-to-measure natural channels. The novel inclusion of seepage data in the analysis revealed the initiation and cessation of bedload transport coincided with key changes in seepage. Numerous flume experiments have demonstrated the ability of seepage to initiate or cease bedload transport (Cheng & Chiew, 1999; Francalanci *et al.* 2008; Dey & Nath, 2009), even under constant discharge, but to the authors knowledge this paper provides a first demonstration of this phenomenon in a natural channel.

The interplay of flow parameters which balance resistance and entrainment forces is complex. It is apparent from this study that entrainment cannot be predicted from one parameter alone. Particle stability is dependent on the relative increase in entrainment and resistance forces (Rao & Sitaram, 1999), which are affected by the balance between a range of flow characteristics. Some parameters, such as seepage, affect both entrainment and resistance parameters meaning their effect on entrainment thresholds may not be linear, depending on the balance of forces resulting from other parameters. Considerable work is required to better understand and model this balance.

Based on the results from Mais Reach and numerous results from flume experiments there is a need to include seepage direction in entrainment formulae as seepage affects key entrainment parameters. In particular, the relationship between seepage and turbulence intensity appears to be important for entrainment thresholds. The multi-sensor approach demonstrated in this paper offers significant potential for further developing our understanding and models of bedload entrainment in natural channels.

5.8 Notation

c_d	Drag coefficient
Δh	Difference in piezometric head, calculated as h_2 - h. Referred to as seepage head
Δh_{cr}	Critical seepage head threshold
h	Total head - height of water column in the pipe above height datum (i.e. the piezometric head)
h_w	Pressure head (height of water column in pipe above the screen)
h_z	Elevation head height of a point (i.e. screen top) above a height datum (i.e. bed surface)
I	Turbulence intensity
I_{cr}	Critical turbulence intensity threshold
$MaxA$	Impact magnitude, or maximum amplitude following Rickenmann *et al.* (2014). Used as a proxy for the size of the impacting grain
p	Pore pressure
Q	Discharge
Q_{cr}	Critical discharge threshold
SP1 and SP2	Standpipe piezometers: SP1 = open flow, SP2 = bed pore pressure at 0.6 m
St	Stage
St_{cr}	Critical stage threshold
$\tilde{u}$	Instantaneous velocity
$\tilde{u}_{cr}$	Critical instantaneous velocity threshold
U_i	Time-averaged velocity
U_{icr}	Critical time-averaged velocity threshold
u_i	Turbulence
u_{icr}	Critical turbulence threshold

5.9 Acknowledgements

We would like to thank David Feek from Massey University for his patience with this project. David was instrumental in developing and installing the sensor system. Brent Watson and the Horizons Regional Council team are thanked for their support of this project through financial assistance with development of the impact plate, provision of data, assistance with installation of equipment, and discussion during the early development of the project. Dave Reid from Essential Electronics and Security Limited is thanked for his assistance developing and maintaining the datalogger, and his in-kind support of the project is greatly appreciated. Volcanic Risk Solutions are thanked for their financial support of the geophone development. IPENZ Rivers Group, New Zealand Hydrological Society, TrustPower, and Tilt Renewables are thanked for financial assistance. Mai Farm are thanked for allowing continual access to the site through their farm. Charlotte Holdsworth is thanked for her assistance with fieldwork on many occasions.

Andrew Neverman was in receipt of a Massey University Doctoral Scholarship. Manaaki Whenua are thanked for supporting the publication of this research through Strategic Science Investment Funding.

Summary of Chapter 5 for Thesis

Chapter 1 identified the challenge of obtaining bedload initiation data in natural channels as a significant factor inhibiting the development of accurate entrainment models, along with measuring coinciding data to capture initiation thresholds. Objective iv aimed to address this issue by developing a methodology to record the onset of initiation along with entrainment thresholds. Chapter 1 highlighted near-bed velocity data to be a key parameter for identifying entrainment mechanisms, but also identified bed seepage as a parameter which is not measured alongside bedload transport data in natural channels but has been identified as a mechanism of entrainment in flume studies, and has been directly attributed to the deviations between predicted and observed entrainment thresholds. Chapter 1 identified impact plate geophones as a potential sensor for recording the initiation of bedload transport, but identified a significant challenge with installing impact plates without significant support infrastructure. The multi-sensor system presented in Chapter 5 has addressed these issues by: 1) developing a method to install impact plates in dynamic gravel beds without requiring significant infrastructure, 2) capturing continuous bedload transport and near-bed velocity data at a suitable temporal resolution to identify the instant of bed movement and coincident hydrodynamics, and 3) capturing continuous bed seepage data alongside bedload transport data. This system advances the ability to directly measure bed mobility and identify hydrodynamic thresholds for bedload entrainment and transport rates in natural channels.

The following, final chapter provides a synthesis of this body of work, highlighting how these methods work together to address the challenge of quantifying bed mobility, and outlining a direction for future research to advance this work to set mechanistic hydrological limits for periphyton management.

Chapter 6

Synthesis

This thesis aimed to identify and develop a suite of tools to advance the measurement of bed stability and identification of coarse particle entrainment and transport thresholds in gravel-bed rivers as a step towards using sediment transport thresholds to set hydrological limits for periphyton management. A comprehensive literature synthesis of the mechanisms of bedload entrainment and methods to measure bedload transport, entrainment forces, and resistance forces (Chapter 1) identified four key limitations for improving the measurement and estimation of bedload entrainment and transport (bed mobility): 1) a lack of ability to quantify substrate structure to calculate bed resistance in the field, 2) challenges recording the instant of bedload movement so accurate hydrodynamic thresholds can be identified, 3) challenges measuring hydrodynamic thresholds and entrainment mechanisms in the near-bed region of flow where they are most applicable to particle entrainment, and 4) a lack of consideration for non-streamwise flow and its effect on entrainment, in particular bed seepage, in natural channels. These knowledge/methodological gaps need to be addressed in order to advance research on the effects of sediment transport on benthic communities, and to improve the design of hydrological limits. Objectives ii-iv aimed to address these gaps. These objectives were achieved in Chapters 2-5.

In order to use hydrological limits to control bed mobility as a mechanism for periphyton management it is critical that bed resistance and near-bed hydrodynamics can be measured and modelled (Hoyle *et al.* 2017). A suite of methods were tested or developed in Chapters 2 & 3 to advance the measurement of substrate structure and resistance (objectives ii-a and ii-b). Measuring characteristics of the bed structure beyond grain size has remained challenging, ultimately due to a lack of methods which can quantify the variability in bed structure at suitable spatial scales over extents relevant to river management. Two remote sensing methods, Structure-from-Motion photogrammetry (SfMp) and Terrestrial Laser Scanning (TLS), were compared for their ability to quantify surface layer structural development (Chapter 2). Grain-scale TLS point clouds have previously been shown to be capable of describing bed armouring (Aberle & Nikora, 2006), but SfMp is rapidly becoming the most popular method for collecting grain-scale topographic point clouds in the geosciences due to the low cost of small Unmanned Aerial Systems (sUAS) compared to Terrestrial Laser Scanners, making the SfMp data more accessible to practitioners. Differences in errors and bias between ranging and optical remote sensing lead to variations in the point clouds produced by both methods, yet only Woodget (2015) has compared the correspondence of these methods for describing substrates beyond an estimate of grain size. It is therefore critical to compare the methods to see if the same process used by Aberle & Nikora (2006) to describe armouring with TLS can be used to describe armouring with SfMp. Chapter 2 found both methods provide a relatively consistent quantification of spatial variation in surface roughness, with a majority of the variability falling below the minimum level of detection based on survey error. Quantification of surface roughness is critical to developing effective near-bed hydrodynamics models, and being able to spatially vary the analysis is important for assessing substrate stability at the patch scale to make it relevant to periphyton management (Hoyle *et al.* 2017). Quantification of grain size is also important for calculating bed resistance. Chapter 2 found careful consideration is required when estimating grain size from point clouds based on the point elevations as these relate best to the c-axis length of grains (Pearson *et al.* 2017; Vázquez-Tarrío *et al.* 2017), but the b-axis length is often used in entrainment formulae. Grain hiding and protrusion also affects the relationship between point elevations and grain axis lengths. Chapter 2 suggested photo-sieving approaches (Carbonneau *et al.* 2004; Dugdale *et al.* 2010; Carbonnneau *et al.* 2018) may be more appropriate than point cloud methods for estimating grain size relevant for entrainment modelling. Chapter 2 also found metrics derived from point cloud elevations could be used to identify surface layer development, but further work is required to understand the impacts of data processing parameters on the computation of these metrics. This task remains challenging as methods to provide a comparison assessment of surface structure are not available. Chapter 2 concluded that methods which utilise aerial surveying platforms rather than terrestrial platforms have the greatest advantage for characterising gravel bed surface structure as aerial platforms reduce occlusion issues and allow more rapid and extensive surveying. At present, the use of aerial systems generally limits practitioners to using optical methods as these are widely available on sUAS, whereas sUAS laser ranging systems are only just emerging on the market and are relatively expensive, limiting their accessibility. Optical remote sensing using sUAS therefore appears to be the best method for characterising substrate structure for river management at present as the surveying platforms are readily available, enable suitable spatial resolution datasets to be obtained at extents relevant to river management, and a wider range of processing methods are available for imagery data, allowing more substrate characteristics to be measured than using ranging techniques. However, the methods for characterising gravel structure using either ranging or optical techniques are still in their infancy and require further development and validation. Current technology also limits the use of these techniques to subaerial gravels, missing the subaqueous bed structure which is arguably more relevant to periphyton management. Some studies have demonstrated utility of SfMp for subaqueous surface reconstruction (Woodget *et al.* 2015; Dietrich & Woodget, 2018), and bathymetric laser ranging sensors are appearing on the market, but these techniques have so far been limited to shallow flows (>1.5 m) with undisturbed (flat, calm) water surfaces and low turbidity. Bathymetric sonar faces similar challenges, with flow depth and spatial resolution limitations. There also remains the challenge of associating the metrics derived from these methods to bed resistive force, and incorporating the metrics in entrainment and bed mobility models before they can be used to study periphyton dynamics, or in hydrological limits setting. Addressing these challenges may be facilitated by the methods developed in Chapters 3-5.

To move beyond characterisation of substrate structure to incorporating structural parameters in entrainment formulae requires a means to measure the resistance force of different structural arrangements of the armour (active) layer. Chapter 1 identified bed compactness as a significant feature of armouring which results from substrate structure and has a substantial impact on bed resistance, but is rarely quantified due to a lack of methodologies to do so. Bed compactness describes the interlocking of particles, which leads to the resistance of individual particles being influenced by neighbouring particles. It is necessary to be able to measure bed compactness to understand the influence of structure on particle resistance. A limited number of published studies have attempted to measure bed compactness and relate differences in compactness to particle mobility (Sear, 1992; Sear, 1995; Pedersen & Friberg, 2007), but these methods lacked a standardised methodology and their results were not comparable. Furthermore, the methods did not go beyond a relative comparison of compactness to actually quantify the resistive force created by compactness. Chapter 3 developed a methodology to objectively quantify compactness of the active layer, using the novel Bed Compactness Index (BCI), and provide a measure of the active layer resistive force. The method developed in Chapter 3 provides a measure of the resistive force of the active layer measured in Newtons, allowing direct comparison with entrainment forces. The measure of resistance can therefore be used directly as a parameter in entrainment models to balance entrainment and resistance forces . This is a significant step towards improving the estimation of particle entrainment and relating bed structure to bed mobility as practitioners have previously been unable to measure the resistive force of the bed, and have instead been limited to semi-qualitatively relating bed structure to changes in entrainment thresholds and tracer particle movement (Laronne & Carson, 1976; Aberle & Smart, 2003; Yu *et al.* 2012; Chen *et al.* 2017). Chapter 3 also developed a modified Mackintosh probe penetrometer which enabled the penetration test depth to be controlled. This modification allowed the penetration test to be limited to the active layer, and for the penetration depth to be varied to account for different active layer thickness between sites. This provides a significant improvement on previous uses of penetration tests in gravel beds which were indiscriminate in regards to active layer and subsurface material (e.g. Pedersen & Friberg, 2007). It is crucial that resistance of the active layer is measured independent of the subsurface using methodologies such as penetration tests which integrate over depth as the subsurface is significantly less compact than the surface layers, leading to skewed estimates of active layer resistance. For setting hydrological limits which aim to entrain the bed it is vital that accurate active layer resistance is measured as it is the active layer which will be entrained first, and hydraulic forces therefore need to exceed the resistive force of the active layer to mobilise the bed and induce molar action. This is why the disturbance depth as defined by DeVries (2002) was used to define the penetration depth in the BCI. Chapter 3 therefore provides a means to quantify the resistance force created by the substrate structure quantified in Chapter 2. This is a critical step to understand the relationship between the metrics used to quantify bed structure in Chapter 2 and bed mobility, and to balance entrainment forces to understand particle entrainment thresholds (Chapter 5) under different bed conditions. The protocol developed in Chapter 3 also proved to be a useful tool for quantifying habitat change, which may be critical for assessing the impact of hydrological limits beyond periphyton removal.

In order for managers to identify sites where hydrological limits are necessary an assessment of potential bed mobility is required which requires site hydraulic parameters to be related to substrate resistance to estimate the potential for bed mobilisation. This assessment allows sites with low potential for bed mobility to be identified as sites at risk of excess periphyton accrual. Such a tool is also needed to track changes in bed mobility at a site so hydrological limits can be adjusted accordingly. Direct measurement of bed mobility can be expensive, requiring installation of sensors or repeat site visits to survey tracer particles or changes in topography (e.g. Death & Winterbourn, 1995; Death, 2002; Schwendel *et al.* 2012b). Practitioners require a relatively cheap, rapid approach for quantifying bed stability if regular monitoring is to be logistically feasible. Index-type assessments of bed stability are popular means of indirect bed mobility assessment in ecology (e.g. Pfankuch, 1975; Schwendel *et al.* 2012a) as they require only a single site visit, but present methods perform poorly. Objective iii therefore sort to fill this gap by developing a new method for rapidly quantifying reach scale bed stability. Chapter 4 achieved this objective by developing a new index for the rapid assessment of bed stability, referred to as the Bed Stability Index (BSI), which improved on previous methods by reducing the subjectivity in parameter scoring. The BSI also incorporated a measure of bed compactness using an earlier version of the BCI presented in Chapter 3, which was a key parameter in the index as indicated by the high parameter weighting for bed compactness. The BSI calibrated strongly with bed movement rates calculated from tracer particle data, suggesting the BSI is a suitable proxy for bed mobility. The BSI took 1-2 hours to complete data collection in the field, enabling multiple sites in close proximity to be assessed in a single day of fieldwork. The BSI therefore provides a rapid estimation of bed mobility without the need for long-term monitoring, providing a logistically feasible method for ecologists to assess bed stability to study the relationship with benthic communities. This was demonstrated by comparing the BSI with *Phormidium* accrual, which found a significant relationship between the BSI score and maximum chlorophyll-a, suggesting 1) periphyton biomass is partially controlled by bed mobility, supporting the application of inducing bed instability to manage periphyton accrual, and 2) the index may be used to identify sites at risk of excess periphyton accrual. The BSI may also provide assessment of bed stability change, allowing the impact of hydrological limits to be assessed, and management practices altered accordingly. A lack of consideration for system trajectories and suitable adjustment of management is a major issue for stream restoration (Moore & Rutherfurd, 2017). The BSI is therefore a valuable tool for hydrological limits setting as it addresses some key challenges, including: identifying sites at risk of excess periphyton accrual, allowing managers to target their efforts; tracking changes in bed stability to assess the impact of river management; and providing a tool for ecologists to quantify bed stability so relationships between bed stability and periphyton removal can be identified and converted to thresholds for removal so hydrological limits can be more objectively set.

Whilst Chapters 2 & 3 have advanced the ability to measure substrate characteristics and resistance to entrainment, which has been a significant challenge to date (Chapter 1) and is critical to improving estimates and models of gravel entrainment, there remains a need to improve the identification of hydrodynamic entrainment thresholds in natural channels due to the limitations of flumes (Chapter 1). The measurement and estimation of entrainment force thresholds has remained challenging despite receiving significant focus for the past century (Herschel, 1878; Shields, 1936; Einstein, 1937; Javernick *et al.* 2018; Liedermann *et al.* 2018; Rickenmann, 2018). Chapter 1 identified the difficulty of measuring the instant of particle motion and obtaining high frequency velocity data as being a significant challenge which has inhibited identification of entrainment thresholds in the field. Chapter 1 also identified bed seepage as a hydrodynamic component which has been demonstrated in flume studies as having a significant impact on entrainment thresholds, but bed seepage is not measured in field studies. Objective iv therefore sought to develop a methodology to improve the identification of site-specific bedload transport thresholds by recording bedload transport events and obtaining corresponding data suitable for identifying entrainment thresholds. Chapter 1 identified impact plates as being a suitable sensor for obtaining continuous high temporal resolution bedload data (Turowski & Rickenmann, 2009; Rickenmann *et al.* 2014; Tsakiris *et al.* 2014), but highlighted the limited ability to install them without permanent support structures such as sills and weirs. This limits the application of impact plates in many locations where the bed is dynamic, or permanent structures cannot be built, which is likely to be many of the locations where hydrological limits will be implemented, or bedload transport studied. Chapter 5 addressed all of these issues by developing an approach to install impact plate geophones combined with a high frequency velocity sensor in dynamic, coarse gravel beds to obtain continuous measurement of bedload transport and streamwise hydrodynamics data without the need for extensive support structures such as sills or weirs. The installation was also cheap and easy to deploy, making the system easily accessible to practitioners, and proved to be stable in a coarse dynamic gravel bed. The temporal resolution of the data obtained from the impact plate was suitable to identify the instant of entrainment and corresponding hydrodynamic thresholds. This system therefore fills a large gap between cheap and easily deployed bedload measuring apparatus such as bedload traps which lack data on the timing or duration of bedload transport (Leopold & Emmett, 1976; Reid *et al.* 1980; Leopold & Emmett, 1997; Garcia *et al.* 2000; Bunte & Abt, 2003), and the permanent monitoring stations (Turowski & Rickenmann, 2009; Rickenmann *et al.* 2012; Aigner *et al.* 2017; Rainato *et al.* 2017) which offer timing and duration data but require significant investment to establish, and are often not logistically feasible.

Chapter 5 also demonstrated the application of differential standpipe piezometers to measure bed seepage, which provided the ability to identify relationships between seepage direction and bedload transport, which is the first time this has been done in natural channels. The research revealed seepage direction and turbulence intensity had the strongest relationship with bedload transport, likely due to their impact on altering the resistance thresholds of particles (Ko & Graf, 1972; Surry, 1972; Maclean, 1991; Yeboah *et al.* 1997; Chen & Chiew, 2004; Lu *et al.* 2008; Younis, 2010; Deshpande & Kumar, 2016). Frequently used metrics for entrainment thresholds such as discharge and mean velocity had the weakest relationships. This is a critical finding for hydrological limits which are frequently based on discharge targets, such as FRE_3 or the Montana Method (Tennant, 1976; Clausen & Biggs, 1997). Hoyle *et al.* (2017) demonstrated that periphyton abundance was better predicted by frequency of sediment mobility thresholds than by FRE_3, which is widely used in New Zealand, and suggested management of periphyton requires better data to predict sediment mobility if management is to move beyond the present method of setting limits based on discharge-based rules-of-thumb. The multi-sensor system developed in Chapter 5 is a critical tool for making this transition as it enables collection of continuous bedload, velocity, turbulence, and bed seepage data. With the support of the methods for characterising substrate structure and resistance from Chapters 2 & 3, Chapter 5 makes a substantial contribution towards the shift away from simplistic rules-of-thumb toward the site-specific characterisation called for by Hoyle *et al.* (2017).

Beyond the study of entrainment thresholds the sensor system developed in Chapter 5 has wider implications for hydrological limits and periphyton management. Where the BSI developed in Chapter 4 provides a low-cost, rapid, indirect assessment of bed mobility, some research and management objectives may require a more accurate, direct assessment of mobility. The system in Chapter 5 affords the opportunity for bed mobility to be directly assessed, enabling questions around the magnitude, frequency, and duration of bed movement to be answered more accurately, but at a higher financial and labour cost than using the BSI. This will be particularly critical for addressing questions regarding the frequency, duration, and magnitude of bed movement required to remove periphyton, which is a present knowledge gap, whereas the BSI provides analysis of the impact of general bed stability on periphyton abundance. The geophone impact plate will also be critical for ensuring hydrological limits are inducing suitable levels of bed movement to manage periphyton, enabling real-time monitoring of flow effectiveness. This is crucial for compliance monitoring and maintenance of management practices.

Chapter 5 also highlights the need to consider the seepage regime, which is not commonly measured as part of routine monitoring. If bed seepage is critical to bed mobility this has wider implications for management of hydrological connectivity within a catchment, particularly connection between the channel and groundwater, which implies management of aquifers needs to be considered for instream ecological health, and variations in groundwater levels may impact instream ecology.

6.1 Conclusions

This thesis highlights the limitations of the conventional approach to hydrological limits setting and illustrates the benefit of using sediment process thresholds as a foundation for establishing hydrological limits instead of flow-ecology relationships. Before this can be achieved practitioners need accurate methods to measure and model sediment process thresholds both to establish effective limits and, more importantly, to study the relationships between sediment processes and benthic community response. Without more work on the latter achieving the former will be problematic. This thesis has focused on improving the ability of practitioners to measure and model the entrainment of bedload, as this marks the upper phase of sediment movement and periphyton removal processes, and is arguably the most challenging phase to predict.

This thesis highlights a significant need to improve the quantification of substrate resistance as entrainment is a product of the balance between entrainment and resistance forces, yet resistance is poorly represented in entrainment models. This poor representation is predominantly due to a lack of methods to quantify the characteristics of gravel substrates which condition particle resistance, and to measure bed resistive force. This thesis has contributed to the advancement of substrate resistance quantification by identifying and comparing remote sensing methods to characterise substrate structure, and by developing a protocol to quantify active layer resistance based on measurements of compactness using a modified penetrometer developed in this thesis specifically for use in gravel stream beds. A method to rapidly quantify bed stability was also developed, providing a means for ecologists to quantify bed mobility without the need for long-term monitoring of tracer particles. The Bed Stability Index was demonstrated to relate significantly to maximum chlorophyll-a for *Phormidium*, demonstrating its utility to identify sites prone to excess accrual of periphyton.

Recording the instant of particle entrainment and coincident hydrodynamic thresholds in natural channels has also proven challenging. The often large discrepancy between predicted and observed entrainment has been attributed to reliance on flume-derived entrainment formulae which poorly represent the complexity of natural channels. Acquiring data from natural channels is a critical step towards improving the accuracy of entrainment models. This thesis identified the challenges of recording continuous high frequency bedload transport and hydrodynamic data in natural channels as being a significant limiting factor for model development. This thesis also highlights a shortcoming of conventional entrainment studies as they only consider streamwise hydrodynamics, but vertical bed seepage has been demonstrated to have a significant influence on entrainment thresholds, yet it is never measured in field-based entrainment studies. This thesis has contributed to the advancement of field-based entrainment studies by developing a method to install an impact plate geophone, near-bed velocity sensor, and standpipe piezometers in dynamic gravel beds without the need for extensive infrastructure. This system was demonstrated to be capable of indentifying the instant of bedload entrainment and coincident velocity and turbulence thresholds, and provided the first assessment of bed seepage thresholds for bedload entrainment in a natural channel. Five bedload events were recorded with the system, and the data revealed bed seepage and turbulence were more strongly correlated with particle entrainment than mean velocity and discharge, despite mean velocity and discharge being the most common flow parameters used as entrainment thresholds, and more importantly the only metrics used as hydrological limits. These findings have significant implications for improving bedload entrainment and transport models, and ultimately improving the effectiveness of hydrological limits.

The aims of this thesis have been met successfully, with a range of tools developed to measure substrate resistance, bed mobility, and entrainment forces. Whilst this thesis has not been able to provide a model to establish hydrological limits, it has provided tools required to address some of the knowledge gaps in our ability to set mechanistic hydrological limits for periphyton removal. Many of these knowledge gaps exist due to a lack of suitable data to understand the complex relationships between flow, geomorphic processes, and ecological responses. The key take home message from this thesis for river managers is the need to collect site-specific time series data on substrate texture and structure, bed mobility, and entrainment thresholds, so a large dataset can be created to help develop bedload entrainment models. Data on these parameters is not often captured during the regular monitoring activities of local authorities and is often limited to capture by researchers during limited field campaigns. This thesis has developed several tools which would assist with regular monitoring of these parameters. These data also need to be coupled with regular monitoring of benthic communities to help understand the interactions between hydraulic, geomorphic, and ecological processes if effective mechanistic hydrological limits are ever to be achieved. The steps needed to improve our understanding of these interactions, and to develop suitable models, are expanded upon below.

This thesis has also highlighted a need for river managers to consider the impact of bed seepage when setting mechanistic hydrological limits, and not just setting limits based on streamwise flow. As bed seepage may be strongly connected to groundwater dynamics, this suggests river managers need to look beyond the river channel when setting hydrological limits, and actively manage groundwater to ensure environmental flows remain effective.

6.2 Future Research

This thesis has provided a first step towards improving the measurement and modelling of bedload entrainment and transport by developing a toolkit to quantify substrate resistance and record empirical datasets for the initiation of motion and associated thresholds. Further work is required to use these tools to build datasets to develop new entrainment and transport models which have improved quantification of substrate resistance and 4-Dimensional hydrodynamics. Approaches for quantifying surface structure were outlined and tested, but further work is required to fully understand how these metrics relate to armouring magnitude, and to understand how the calculation of the metrics and the relationship with armouring is affected by various data acquisition and processing parameters. This remains challenging as comparative assessments of surface structure and armouring are challenging. This thesis also developed a method to quantify substrate resistance based on bed compactness, but further work is required to relate this measure of resistance to entrainment forces. This is somewhat complicated by the influence of other characteristics of the substrate and flow on resistance. This thesis also highlighted the significant impact of bed seepage on entrainment and demonstrated the need to include seepage in entrainment models. However, the effect of bed seepage on entrainment thresholds is complicated and not very well understood. This presents a valuable avenue for future research. This thesis has only presented a small dataset on seepage thresholds for entrainment in the field and obtaining a much larger dataset will be required to model this phenomena accurately.

Developing better measurements and models for bedload entrainment will have little impact on hydrological limits if the relationship between periphyton removal and sediment processes is not well understood. This has been a challenging area of research as bed stability has been challenging to quantify. The tools developed in this thesis provide a means to extend this area of research. Developing effective hydrological limits for periphyton removal using bedload transport will require an understanding of the magnitude, frequency, and duration of bedload transport events required to maintain a healthy level of periphyton biomass. This will be site and species dependent, and will depend on the level of periphyton biomass the desired local biotic community can support. Further research is required to understand these dynamics so the required bedload transport regime can be identified to maintain ecosystem health at a site, and hydrological limits to achieve that regime can be developed. A key next step toward developing effective hydrological limits is therefore to use the suite of tools developed in this body of work to link sediment mobility with observations and analysis of periphyton.

Bibliography

Aberle, J., Nikora, V. (2006). Statistical properties of armored gravel bed surfaces. *Water Resources Research* 42 (11), 1–11. DOI: 10.1029/2005WR004674.

Aberle, J., Smart, G.M. (2003). The influence of roughness structure on flow resistance on steep slopes. *Journal of Hydraulic Research* 41 (3), 259–269. DOI: 10.1080/00221680309499971.

Aberle, J., Nikora, V., Walters, R. (2006). Data interpretation for in situ measurements of cohesive sediment erosion. *Journal of Hydraulic Engineering* 132 (6), 581–588.

Aberle, J. (2007). Measurements of armour layer roughness geometry function and porosity. *Acta Geophysica* 55 (1), 23–32.

Ackers, P., White, W.R. (1973). Sediment transport: new approach and analysis. *Journal of the Hydraulics Division* 99 (hy11).

Acreman, M.C., Dunbar, M.J. (2004). Defining environmental river flow requirements? A review. *Hydrology and Earth System Sciences Discussions* 8 (5), 861–876.

Adams, J. (1979). Gravel size analysis from photographs. *Journal of the Hydraulics Division* 105 (10), 1247–1255.

Adin, A., Alon, G. (1986). Mechanisms and process parameters of filter screens. *Journal of Irrigation and Drainage Engineering* 112 (4), 293–304.

Aigner, J., Kreisler, A., Rindler, R., Hauer, C., Habersack, H. (2017). Bedload pulses in a hydropower affected alpine gravel bed river. *Geomorphology* 291, 116–127. DOI: http://dx.doi.org/10.1016/j.geomorph.2016.05.015.

Alfadhli, I., Yang, S.-Q. (2014). Influence of vertical motion on initiation of sediment movement. *Journal of Water Resource and Protection* 6 (18), 1666–1681.

Andrews, E.D. (1983). Entrainment of gravel from naturally sorted riverbed material. *Geological Society of America Bulletin* 94 (10), 1225–1231. DOI: Doi10.1130/0016-7606(1983)94<1225:Eogfns>2.0.Co;2.

Ashmore, P., Parker, G. (1983). Confluence scour in coarse braided streams. *Water Resources Research* 19 (2), 392–402. DOI: 10.1029/WR019i002p00392.

Ashworth, P.J., Ferguson, R.I. (1986). Interrelationships of Channel Processes, Changes and Sediments in a Proglacial Braided River. *Geografiska Annaler. Series A, Physical Geography* 68 (4), 361–371. DOI: 10.2307/521527.

Ashworth, P.J., Ferguson, R.I., Powell, M. (1992). Bedload transport and sorting in braided channel. In: Billi, P., Hey, R.D., Thorne, C.R., Tacconi, P. (Eds). Dynamics of Gravel-Bed Rivers. John Wiley, New York, pp. 497–515.

Ashworth, P.J., Ferguson, R.I. (1989). Size-selective entrainment of bed load in gravel bed streams. *Water Resources Research* 25 (4), 627–634. DOI: 10.1029/WR025i004p00627.

Baewert, H., Bimböse, M., Bryk, A., Rascher, E., Schmidt, K.-H., Morche, D. (2014). Roughness determination of coarse grained alpine river bed surfaces using Terrestrial Laser Scanning data. *Zeitschrift für Geomorphologie, Supplementary Issues* 58 (1), 81–95.

Baker, P.D., Steffensen, D.A., Humpage, A.R., Nicholson, B.C., Falconer, I.R., Lanthois, B., Fergusson, K.M., Saint, C.P. (2001). Preliminary evidence of toxicity associated with the benthic cyanobacterium Phormidium in South Australia. *Environmental Toxicology* 16 (6), 506–511.

Baker, V.R., Ritter, D.F. (1975). Competence of rivers to transport coarse bedload material. *Geological Society of America Bulletin* 86 (7), 975–978.

Barrière, J., Krein, A., Oth, A., Schenkluhn, R. (2015). An advanced signal processing technique for deriving grain size information of bedload transport from impact plate vibration measurements. *Earth Surface Processes and Landforms* 40 (7), 913–924. DOI: `10.1002/esp.3693`.

Benn, D.I., Ballantyne, C.K. (1994). Reconstructing the transport history of glacigenic sediments: a new approach based on the co-variance of clast form indices. *Sedimentary Geology* 91 (1), 215–227. DOI: `10.1016/0037-0738(94)90130-9`.

Bertin, S., Friedrich, H. (2013). Measurement of gravel-bed topography: Evaluation study applying statistical roughness analysis. *Journal of Hydraulic Engineering* 140 (3), 269–279.

Bertin, S., Friedrich, H. (2016). Field application of close-range digital photogrammetry (CRDP) for grain-scale fluvial morphology studies. *Earth Surface Processes and Landforms* 41 (10), 1358–1369. DOI: `10.1002/esp.3906`.

Bertin, S., Friedrich, H. (2018). Effect of surface texture and structure on the development of stable fluvial armors. *Geomorphology* 306, 64–79.

Bertin, S., Groom, J., Friedrich, H. (2017). Isolating roughness scales of gravel-bed patches. *Water Resources Research* 53, 6841–6856. DOI: `10.1002/2016WR020205`.

Biggs, B.J.F. (1985). Algae, a blooming nuisance in rivers. *Soil and Water* 21 (2), 27–31.

Biggs, B.J.F. (1990). Periphyton communities and their environments in New Zealand rivers. *New Zealand Journal of Marine and Freshwater Research* 24 (3), 367–386. DOI: `10.1080/00288330.1990.9516431`.

Biggs, B.J., Gerbeaux, P. (1993). Periphyton development in relation to macro-scale (geology) and micro-scale (velocity) limiters in two gravel-bed rivers, New Zealand. *New Zealand Journal of Marine and Freshwater Research* 27 (1), 39–53.

Biggs, B.J., Goring, D.G., Nikora, V.I. (1998). Subsidy and stress responses of stream periphyton to gradients in water velocity as a function of community growth form. *Journal of Phycology* 34 (4), 598–607. DOI: `10.1046/j.1529-8817.1998.340598.x`.

Biggs, B.J., Smith, R.A., Duncan, M.J. (1999). Velocity and sediment disturbance of periphyton in headwater streams: biomass and metabolism. *Journal of the North American Benthological Society* 18 (2), 222–241. DOI: `10.2307/1468462`.

Biggs, B., Kilroy, C. (2000). *Stream periphyton monitoring manual. National Institute of Water and Atmospheric Research, Christchurch, New Zealand*. Report. Niwa.

Billi, P. (1988). A note on cluster bedform behaviour in a gravel-bed river. *Catena* 15 (5), 473–481. DOI: `10.1016/0341-8162(88)90065-3`.

Booker, D.J. (2013). Spatial and temporal patterns in the frequency of events exceeding three times the median flow (FRE3) across New Zealand. *Journal of Hydrology* 52 (1), 15–39.

Bourassa, N., Cattaneo, A. (1998). Control of periphyton biomass in Laurentian streams (Quebec). *Journal of the North American Benthological Society* 17 (4), 420–429. DOI: `10.2307/1468363`.

Brasington, J., Vericat, D., Rychkov, I. (2012). Modeling river bed morphology, roughness, and surface sedimentology using high resolution terrestrial laser scanning. *Water Resources Research* 48 (11), 1–11. DOI: `10.1029/2012wr012223`.

Brayshaw, A.C. (1985). Bed microtopography and entrainment thresholds in gravel-bed rivers. *Geological Society of America Bulletin* 96 (2), 218–223. DOI: 10.1130/0016-7606(1985)96<218:Bmaeti>2.0.Co;2.

Brodu, N., Lague, D. (2012). 3D terrestrial lidar data classification of complex natural scenes using a multi-scale dimensionality criterion: Applications in geomorphology. *ISPRS Journal of Photogrammetry and Remote Sensing* 68, 121–134. DOI: `http://dx.doi.org/10.1016/j.isprsjprs.2012.01.006`.

Buffington, J.M., Dietrich, W.E., Kirchner, J.W. (1992). Friction angle measurements on a naturally formed gravel streambed: Implications for critical boundary shear stress. *Water Resources Research* 28 (2), 411–425. DOI: `10.1029/91WR02529`.

Buffington, J.M., Montgomery, D.R. (1997). A systematic analysis of eight decades of incipient motion studies, with special reference to gravel-bedded rivers. *Water Resources Research* 33 (8), 1993–2029.

Buffington, J.M., Montgomery, D.R. (1999). A procedure for classifying textural facies in gravel-bed rivers. *Water Resources Research* 35 (6), 1903–1914.

Bunte, K., Abt, S.R. (2001). Sampling surface and subsurface particle-size distributions in wadable gravel-and cobble-bed streams for analyses in sediment transport, hydraulics, and streambed monitoring. *Gen. Tech. Rep. RMRS-GTR-74. Fort Collins, CO: US Department of Agriculture, Forest Service, Rocky Mountain Research Station. 428 p.* 74.

Bunte, K., Abt, S.R. (2003). Sampler size and sampling time affect bed load transport rates and particle sizes measured with bed load traps in gravel-bed streams. *IAHS Publication* (283), 126–133.

Bunte, K., Abt, S.R., Potyondy, J.P., Swingle, K.W. (2009). Comparison of three pebble count protocols (EMAP, PIBO, and SFT) in two mountain gravel-bed streams. *JAWRA Journal of the American Water Resources Association* 45 (5), 1209–1227.

Cadol, D., Wohl, E. (2011). Coarse sediment movement in the vicinity of a logjam in a neotropical gravel-bed stream. *Geomorphology* 128 (3–4), 191–198. DOI: `http://dx.doi.org/10.1016/j.geomorph.2011.01.007`.

Carbonneau, P.E., Bergeron, N., Lane, S.N. (2005). Automated grain size measurements from airborne remote sensing for long profile measurements of fluvial grain sizes. *Water Resources Research* 41 (11). DOI: `10.1029/2005wr003994`.

Carbonneau, P.E., Dietrich, J.T. (2017). Cost-effective non-metric photogrammetry from consumer-grade sUAS: implications for direct georeferencing of structure from motion photogrammetry. *Earth Surface Processes and Landforms* 42 (3), 473–486. DOI: `10.1002/esp.4012`.

Carbonneau, P.E., Lane, S.N., Bergeron, N.E. (2004). Catchment-scale mapping of surface grain size in gravel bed rivers using airborne digital imagery. *Water Resources Research* 40 (7). DOI: 10.1029/2003wr002759.

Carbonnneau, P., Bizzi, S., Marchetti, G. (2018). Robotic photosieving from low-cost multirotor sUAS: A proof-of-concept. *Earth Surface Processes and Landforms* 43, 1160–1166. DOI: 0.1002/esp.4298.

Carling, P.A. (1983). Threshold of coarse sediment transport in broad and narrow natural streams. *Earth Surface Processes and Landforms* 8 (1), 1–18. DOI: 10.1002/esp.3290080102.

Carling, P. (1987). Bed stability in gravel streams, with reference to stream regulation and ecology. In: River channels: environment and process. Basil Blackwell Inc., New York, NY, pp. 321–347.

Cassel, M., Dépret, T., Piégay, H. (2017). Assessment of a new solution for tracking pebbles in rivers based on active RFID. *Earth Surface Processes and Landforms*. DOI: 10.1002/esp.4152.

Chapuis, M., Dufour, S., Provansal, M., Couvert, B., Linares, M. de (2015). Coupling channel evolution monitoring and RFID tracking in a large, wandering, gravel-bed river: Insights into sediment routing on geomorphic continuity through a riffle–pool sequence. *Geomorphology* 231, 258–269. DOI: http://dx.doi.org/10.1016/j.geomorph.2014.12.013.

Chen, S.-C., Yang, C.-N., Tsou, C.-Y. (2017). Bedform development and its effect on bed stabilization and sediment transport based on a flume experiment with non-uniform sediment. *International Journal of Sediment Research* 32 (3), 305–312. DOI: 10.1016/j.ijsrc.2017.05.003.

Chen, X., Chiew, Y.-M. (2004). Velocity distribution of turbulent open-channel flow with bed suction. *Journal of Hydraulic Engineering* 130 (2), 140–148. DOI: 10.1061/(Asce)0733-9429(2004)130:2(140).

Chen, Y.-C., Kao, S.-P., Wu, J.-H. (2014). Measurement of stream cross section using ground penetration radar with Hilbert–Huang transform. *Hydrological Processes* 28 (4), 2468–2477. DOI: 10.1002/hyp.9755.

Cheng, N.-S., Chiew, Y.-M. (1999). Incipient sediment motion with upward seepage. *Journal of Hydraulic Research* 37 (5), 665–681.

Church, M.A., McLean, D., Wolcott, J. (1987). River bed gravels: sampling and analysis. In: Thorne, C., and, J.B., Hey, R. (Eds). Sediment Transport in Gravel-Bed Rivers. John Wiley & Sons, Chichester, pp. 43–88.

Church, M. (2006). Bed Material Transport and the Morphology of Alluvial River Channels. *Annual Review of Earth and Planetary Sciences* 34 (1), 325–354. DOI: 10.1146/annurev.earth.33.092203.122721.

Church, M., Hassan, M.A., Wolcott, J.F. (1998). Stabilizing self-organized structures in gravel-bed stream channels: Field and experimental observations. *Water Resources Research* 34 (11), 3169–3179. DOI: 10.1029/98wr00484.

Clapuyt, F., Vanacker, V., Van Oost, K. (2016). Reproducibility of UAV-based earth topography reconstructions based on Structure-from-Motion algorithms. *Geomorphology* 260, 4–15. DOI: 10.1016/j.geomorph.2015.05.011.

Clausen, B., Biggs, B. (1997). Relationships between benthic biota and hydrological indices in New Zealand streams. *Freshwater Biology* 38 (2), 327–342. DOI: `10.1046/j.1365-2427.1997.00230.x`.

Clayton, C.R.I., Matthews, M.C., Simons, N.E. (1995). Site investigation: a handbook for engineers. Blackwell Science, Oxford.

Clement, A.J., Sloss, C.R., Fuller, I.C. (2010). Late quaternary geomorphology of the Manawatu coastal plain, North Island, New Zealand. *Quaternary International* 221 (1), 36–45.

Clifford, N., Robert, A., Richards, K. (1992). Estimation of flow resistance in gravel-bedded rivers: A physical explanation of the multiplier of roughness length. *Earth Surface Processes and Landforms* 17 (2), 111–126.

Cobb, D., Galloway, T., Flannagan, J. (1992). Effects of Discharge and Substrate Stability on Density and Species Composition of Stream Insects. *Canadian Journal of Fisheries and Aquatic Sciences* 49, 1788–1795.

Dal Cin, R. (1968). "Pebble clusters": Their origin and utilization in the study of palaeocurrents. *Sedimentary Geology* 2 (4), 233–241.

Daniels, M.D., McCusker, M.H. (2010). Operator bias characterizing stream substrates using Wolman pebble counts with a standard measurement template. *Geomorphology* 115 (1-2), 194–198. DOI: `10.1016/j.geomorph.2009.09.038`.

Davie, A.W., Mitrovic, S.M. (2014). Benthic algal biomass and assemblage changes following environmental flow releases and unregulated tributary flows downstream of a major storage. *Marine and Freshwater Research* 65 (12), 1059–1071. DOI: `http://dx.doi.org/10.1071/MF13225`.

de Haas, T., Ventra, D., Carbonneau, P.E., Kleinhans, M.G. (2014). Debris-flow dominance of alluvial fans masked by runoff reworking and weathering. *Geomorphology* 217, 165–181.

de Jalón, D.G., Bussettini, M., Rinaldi, M., Grant, G., Friberg, N., Cowx, I.G., Magdaleno, F., Buijse, T. (2017). Linking environmental flows to sediment dynamics. *Water Policy* 19 (2), 358–375.

Death, R.G. (2002). Predicting invertebrate diversity from disturbance regimes in forest streams. *Oikos* 97 (1), 18–30.

Death, R.G. (2008). The Effect of Floods on Aquatic Invertebrate Communities. In: Lancaster, J., Briers, R. (Eds). Aquatic Insects: Challenges to Populations. Proceedings of the Royal Entomological Society's 24th Symposium. CAB International, Wallingford, Oxfordshire. Chap. 6, pp. 103–121.

Death, R.G. (2010). Disturbance and riverine benthic communities: What has it contributed to general ecological theory? *River Research and Applications* 26 (1), 15–25.

Death, R.G., Winterbourn, M.J. (1994). Environmental stability and community persistence: a multivariate perspective. *Journal of the North American Benthological Society* 13, 125–139.

Death, R.G., Winterbourn, M.J. (1995). Diversity patterns in stream benthic invertebrate communities: the influence of habitat stability. *Ecology* 76 (5), 1446–1460. DOI: `10.2307/1938147`.

Death, R.G., Zimmermann, E.M. (2005). Interaction between disturbance and primary productivity in determining stream invertebrate diversity. *Oikos* 111 (2), 392–402.

Dell'Agnese, A., Mao, L., Comiti, F. (2014). Calibration of an acoustic pipe sensor through bedload traps in a glacierized basin. *CATENA* 121, 222–231. DOI: `https://doi.org/10.1016/j.catena.2014.05.021`.

Deshpande, V., Kumar, B. (2016). Turbulent flow structures in alluvial channels with curved cross-sections under conditions of downward seepage. *Earth Surface Processes and Landforms* 41 (8), 1073–1087. DOI: `10.1002/esp.3889`.

DeVries, P. (2002). Bedload Layer Thickness and Disturbance Depth in Gravel Bed Streams. *Journal of Hydraulic Engineering* 128 (11), 983.

Dey, S., Nath, T.K. (2009). Turbulence characteristics in flows subjected to boundary injection and suction. *Journal of Engineering Mechanics* 136 (7), 877–888.

Dietrich, J., Woodget, A. (2018). Bathymetric Structure from Motion: Change Detection and Technical Improvements.

Dietrich, J.T. (2016). Bathymetric Structure-from-Motion: extracting shallow stream bathymetry from multi-view stereo photogrammetry. *Earth Surface Processes and Landforms* 42 (2), 355–364. DOI: `10.1002/esp.4060`.

Dietrich, W.E., Kirchner, J.W., Ikeda, H., Iseya, F. (1989). Sediment supply and the development of the coarse surface layer in gravel-bedded rivers. *Nature* 340 (6230), 215–217.

Downes, B.J., Lake, P.S., Glaister, A., Webb, J.A. (1998). Scales and frequencies of disturbances: rock size, bed packing and variation among upland streams. *Freshwater Biology* 40 (4), 625–639. DOI: `10.1046/j.1365-2427.1998.00360.x`.

Downs, P.W., Soar, P.J., Taylor, A. (2016). The anatomy of effective discharge: the dynamics of coarse sediment transport revealed using continuous bedload monitoring in a gravel-bed river during a very wet year. *Earth Surface Processes and Landforms* 41 (2), 147–161.

Dugdale, S.J., Carbonneau, P.E., Campbell, D. (2010). Aerial photosieving of exposed gravel bars for the rapid calibration of airborne grain size maps. *Earth Surface Processes and Landforms* 35 (6), 627–639. DOI: `10.1002/esp.1936`.

Duncan, M.J., Suren, A.M., Brown, S.L. (1999). Assessment of streambed stability in steep, bouldery streams: development of a new analytical technique. *Journal of the North American Benthological Society*, 445–456.

Dymond, J.R., Herzig, A., Basher, L., Betts, H.D., Marden, M., Phillips, C.J., Ausseil, A.-G.E., Palmer, D.J., Clark, M., Roygard, J. (2016). Development of a New Zealand SedNet model for assessment of catchment-wide soil-conservation works. *Geomorphology* 257, 85–93.

Einstein, H. (1937). Bedload transport as a probability problem. *Sedimentation (reprinted in 1972). Water Resources Publications, Colorado*, 105–108.

Einstein, H.A., El-Samni, E.-S.A. (1949). Hydrodynamic forces on a rough wall. *Reviews of Modern Physics* 21 (3), 520–524. DOI: `10.1103/RevModPhys.21.520`.

Entwistle, N.S., Fuller, I.C. (2009). Terrestrial laser scanning to derive the surface grain size facies character of gravel bars. In: Heritage, G.L., Large, A. (Eds). Laser Scanning for the Environmental Sciences. John Wiley & Sons, Chichester, pp. 102–114.

Ergenzinger, P., De Jong, C. (2003). Perspectives on bed load measurement. *Erosion and Sediment Transport Measurement in Rivers: Technological and Methodological Advances* (283), 113–125.

Fakher, A., Khodaparast, M., Jones, C. (2006). The use of the Mackintosh Probe for site investigation in soft soils. *Quarterly Journal of Engineering Geology and Hydrogeology* 39 (2), 189–196.

Fenton, J., Abbott, J. (1977). Initial movement of grains on a stream bed: The effect of relative protrusion. *Proceedings of the Royal Society of London. Series A, Mathematical and Physical Sciences* 352 (1671), 523–537.

Ferguson, R.I. (1994). Critical discharge for entrainment of poorly sorted gravel. *Earth Surface Processes and Landforms* 19 (2), 179–186.

Ferguson, R.I. (2005). Estimating critical stream power for bedload transport calculations in gravel-bed rivers. *Geomorphology* 70 (1-2), 33–41. DOI: `10.1016/j.geomorph.2005.03.009`.

Ferguson, R.I., Werritty, A. (1983). Bar development and channel changes in the gravelly River Feshie. In: Collison, J.D., Lewin, J. (Eds). Modern and Ancient Fluvial Systems, pp. 133–143. DOI: `doi:10.1002/9781444303773.ch14`.

Flinders, C.A., Hart, D.D. (2009). Effects of pulsed flows on nuisance periphyton growths in rivers: a mesocosm study. *River Research and Applications* 25 (10), 1320–1330. DOI: `10.1002/rra.1244`.

Folk, R.L. (1980). Petrology of sedimentary rocks. Hemphill Publishing Company.

Fovet, O., Belaud, G., Litrico, X., Charpentier, S., Bertrand, C., Dollet, P., Hugodot, C. (2012). A model for fixed algae management in open channels using flushing flows. *River Research and Applications* 28 (7), 960–972. DOI: `10.1002/rra.1495`.

Fraccarollo, L., Marion, A. (1995). Statistical approach to bed-material surface sampling. *Journal of Hydraulic Engineering* 121 (7), 540–545.

Francalanci, S., Parker, G., Solari, L. (2008). Effect of seepage-induced nonhydrostatic pressure distribution on bed-load transport and bed morphodynamics. *Journal of Hydraulic Engineering* 134 (4), 378–389. DOI: `10.1061/(Asce)0733-9429(2008)134:4(378)`.

Francoeur, S., Biggs, B.F. (2006). Short-term effects of elevated velocity and sediment abrasion on benthic algal communities. In: Stevenson, R.J., Pan, Y., Kociolek, J.P., Kingston, J. (Eds). Advances in Algal Biology: A Commemoration of the Work of Rex Lowe. Vol. 185. Developments in Hydrobiology. Springer Netherlands, Dordrecht, The Netherlands. Chap. 4, pp. 59–69. DOI: `10.1007/1-4020-5070-4_4`.

Fuller, I.C., Basher, L.R. (2013). Riverbed digital elevation models as a tool for holistic river management : Motueka River , Nelson , New Zealand. *River Research and Applications* 633 (29), 619–633. DOI: `10.1002/rra`.

Fuller, I.C., Death, R.G. (2018). The science of connected ecosystems: what is the role of catchment-scale connectivity for healthy river ecology? *Land Degradation & Development* 29 (5), 1413–1426.

Fuller, I.C. (2007). Geomorphic work during a “150-year” storm: contrasting behaviors of river channels in a New Zealand catchment. *Annals of the Association of American Geographers* 97 (4), 665–676.

Fuller, I.C., Large, A.R.G., Charlton, M.E., Heritage, G.L., Milan, D.J. (2003a). Reach-scale sediment transfers: an evaluation of two morphological budgeting approaches. *Earth Surface Processes and Landforms* 28 (8), 889–903. DOI: 10.1002/esp.1011.

Fuller, I.C., Large, A.R.G., Milan, D.J. (2003b). Quantifying channel development and sediment transfer following chute cutoff in a wandering gravel-bed river. *Geomorphology* 54 (3-4), 307–323. DOI: 10.1016/S0169-555X(02)00374-4.

Garcia, C., Laronne, J.B., Sala, M. (2000). Continuous monitoring of bedload flux in a mountain gravel-bed river. *Geomorphology* 34 (1), 23–31.

Gilvear, D.J. (1999). Fluvial geomorphology and river engineering: future roles utilizing a fluvial hydrosystems framework. *Geomorphology* 31 (1), 229–245. DOI: https://doi.org/10.1016/S0169-555X(99)00086-0.

Gilvear, D.J., Spray, C.J., Casas-Mulet, R. (2013). River rehabilitation for the delivery of multiple ecosystem services at the river network scale. *Journal of Environmental Management* 126 (Supplement C), 30–43. DOI: https://doi.org/10.1016/j.jenvman.2013.03.026.

Girardeau-Montaut, D., Roux, M., Marc, R., Thibault, G. (2005). Change detection on points cloud data acquired with a ground laser scanner. *International Archives of Photogrammetry, Remote Sensing and Spatial Information Sciences* 36 (Part 3), 30–35.

Gomez, B. (1991). Bedload transport. *Earth-Science Reviews* 31 (2), 89–132. DOI: 10.1016/0012-8252(91)90017-A.

Gomez, B. (1993). Roughness of stable, armored gravel beds. *Water Resources Research* 29 (11), 3631–3642.

Gottesfeld, A.S., Hassan, M.A., Tunnicliffe, J.F., Poirier, R.W. (2004). Sediment dispersion in salmon spawning streams: the influence of floods and salmon redd construction. *Journal of the American Water Resources Association* 40 (4), 1071–1086.

Graf, W.L. (2006). Downstream hydrologic and geomorphic effects of large dams on American rivers. *Geomorphology* 79 (3), 336–360. DOI: http://dx.doi.org/10.1016/j.geomorph.2006.06.022.

Graham, D.J., Reid, I., Rice, S.P. (2005a). Automated Sizing of Coarse-Grained Sediments: Image-Processing Procedures. *Mathematical Geology* 37 (1), 1–28. DOI: 10.1007/s11004-005-8745-x.

Graham, D.J., Rice, S.P., Reid, I. (2005b). A transferable method for the automated grain sizing of river gravels. *Water Resources Research* 41 (7).

Grant, P.J. (1982). Course Sediment Yields from the Upper Waipawa River Basin, Ruahine Range. *Journal of Hydrology (NZ)* 21 (2), 81–97.

Gray, J.R., Laronne, J.B., Marr, J.D. (2010). *Bedload-surrogate monitoring technologies.* Report 1411328485. US Department of the Interior, US Geological Survey.

Green, J.C. (2003). The precision of sampling grain-size percentiles using the Wolman method. *Earth Surface Processes and Landforms* 28 (9), 979–991. DOI: http://dx.doi.org/10.1002/esp.513.

Greenwood, M.J., McIntosh, A.R. (2008). Flooding impacts on responses of a riparian consumer to cross-ecosystem subsidies. *Ecology* 89 (6), 1489–1496.

Guan, M., Carrivick, J.L., Wright, N.G., Sleigh, P.A., Staines, K.E.H. (2016). Quantifying the combined effects of multiple extreme floods on river channel geometry and on flood hazards. *Journal of Hydrology* 538 (Supplement C), 256–268. DOI: 10.1016/j.jhydrol.2016.04.004.

Halliday, D., Resnick, R. (1962). Physics: for students of science and engineering; combined ed. Wiley.

Hamill, D., Buscombe, D., Wheaton, J.M. (2018). Alluvial substrate mapping by automated texture segmentation of recreational-grade side scan sonar imagery. *PloS one* 13 (3), e0194373.

Hamill, K.D. (2001). Toxicity in benthic freshwater cyanobacteria (blue-green algae): First observations in New Zealand. *New Zealand Journal of Marine and Freshwater Research* 35 (5), 1057–1059. DOI: 10.1080/00288330.2001.9517062.

Hassan, M.A., Church, M., Schick, A.P. (1991). Distance of movement of coarse particles in gravel bed streams. *Water Resources Research* 27 (4), 503–511.

Heerdegen, R.G., Shepherd, M. (1992). Manawatu landforms–product of tectonism, climate change and process. *Landforms of New Zealand*, 308–333.

Henderson, R., Diettrich, J. (2007). *Statistical analysis of river flow data in the Horizons Region.* Report NIWA Client Report: CHC2006-154. NIWA.

Heritage, G.L., Milan, D.J. (2009). Terrestrial Laser Scanning of grain roughness in a gravel-bed river. *Geomorphology* 113 (1-2), 4–11. DOI: 10.1016/j.geomorph.2009.03.021.

Herrick, J.E., Jones, T.L. (2002). A dynamic cone penetrometer for measuring soil penetration resistance. *Soil Science Society of America Journal* 66 (4), 1320–1324.

Herschel, C. (1878). On the erosive and abrading power of water upon the sides and the bottom of rivers and canals. *Journal of the Franklin Institute* 105 (6), 393–403. DOI: https://doi.org/10.1016/0016-0032(78)90380-0.

Hodge, R., Brasington, J., Richards, K. (2009a). Analysing laser-scanned digital terrain models of gravel bed surfaces: linking morphology to sediment transport processes and hydraulics. *Sedimentology* 56 (7), 2024–2043. DOI: 10.1111/j.1365-3091.2009.01068.x.

Hodge, R., Brasington, J., Richards, K. (2009b). In situ characterization of grain-scale fluvial morphology using Terrestrial Laser Scanning. *Earth Surface Processes and Landforms* 34 (7), 954–968. DOI: 10.1002/esp.1780.

Hodge, R., Sear, D., Leyland, J. (2013). Spatial variations in surface sediment structure in riffle-pool sequences: a preliminary test of the Differential Sediment Entrainment Hypothesis (DSEH). *Earth Surface Processes and Landforms* 38 (5), 449–465. DOI: 10.1002/esp.3290.

Horner, R.R., Welch, E. (1981). Stream periphyton development in relation to current velocity and nutrients. *Canadian Journal of Fisheries and Aquatic Sciences* 38 (4), 449–457.

Horner, R.R., Welch, E.B., Seeley, M.R., Jacoby, J.M. (1990). Responses of periphyton to changes in current velocity, suspended sediment and phosphorus concentration. *Freshwater biology* 24 (2), 215–232.

Houbrechts, G., Levecq, Y., Peeters, A., Hallot, E., Van Campenhout, J., Denis, A.-C., Petit, F. (2015). Evaluation of long-term bedload virtual velocity in gravel-bed rivers (Ardenne, Belgium). *Geomorphology* 251, 6–19. DOI: 10.1016/j.geomorph.2015.05.012.

Hoyle, J.T., Kilroy, C., Hicks, D.M., Brown, L. (2017). The influence of sediment mobility and channel geomorphology on periphyton abundance. *Freshwater Biology* 62 (2), 258–273. DOI: 10.1111/fwb.12865.

Ibbeken, H., Schleyer, R. (1986). Photo-sieving: A method for grain-size analysis of coarse-grained, unconsolidated bedding surfaces. *Earth Surface Processes and Landforms* 11 (1), 59–77. DOI: doi:10.1002/esp.3290110108.

Jackson, W., Beschta, R. (1982). A model of two-phase bedload transport in an Oregon Coast Range stream. *Earth Surface Processes and Landforms* 7 (6), 517–527.

Jaeger, M., Smart, G. (2012). Flow induced pressure fluctuations with a gravel bed. In: Murillo Muñoz, R. (Ed). River Flow 2012, pp. 435–441.

James, M.R., Robson, S., d'Oleire-Oltmanns, S., Niethammer, U. (2017). Optimising UAV topographic surveys processed with structure-from-motion: Ground control quality, quantity and bundle adjustment. *Geomorphology* 280, 51–66. DOI: http://dx.doi.org/10.1016/j.geomorph.2016.11.021.

James, M.R., Robson, S. (2014). Mitigating systematic error in topographic models derived from UAV and ground-based image networks. *Earth Surface Processes and Landforms* 39 (10), 1413–1420. DOI: 10.1002/esp.3609.

Javernick, L., Redolfi, M., Bertoldi, W. (2018). Evaluation of a numerical model's ability to predict bed load transport observed in braided river experiments. *Advances in Water Resources* 115, 207–218. DOI: https://doi.org/10.1016/j.advwatres.2018.03.012.

Joanes, D., Gill, C. (1998). Comparing measures of sample skewness and kurtosis. *Journal of the Royal Statistical Society: Series D (The Statistician)* 47 (1), 183–189.

Jowett, I.G., Biggs, B.J. (1997). Flood and velocity effects on periphyton and silt accumulation in two New Zealand rivers. *New Zealand Journal of Marine and Freshwater Research* 31 (3), 287–300.

Kammerlander, J., Gems, B., Kößler, D., Aufleger, M. (2017). Effect of bed load supply on sediment transport in mountain streams. *International journal of sediment research* 32 (2), 240–252. DOI: http://dx.doi.org/10.1016/j.ijsrc.2017.03.004.

Kenyon, N.H., Belderson, R.H. (1973). Bed forms of the Mediterranean undercurrent observed with side-scan sonar. *Sedimentary Geology* 9 (2), 77–99. DOI: http://dx.doi.org/10.1016/0037-0738(73)90027-4.

Ko, S.C., Graf, W.H. (1972). Drag coefficient of cylinders in turbulent flow. *Journal of the Hydraulics Division* 98 (5), 897–912.

Komar, P.D. (1987). Selective gravel entrainment and the empirical evaluation of flow competence. *Sedimentology* 34 (6), 1165–1176. DOI: 10.1111/j.1365-3091.1987.tb00599.x.

Komar, P.D., Li, Z. (1988). Applications of grain-pivoting and sliding analyses to selective entrapment of gravel and to flow-competence evaluations. *Sedimentology* 35 (4), 681–695. DOI: 10.1111/j.1365-3091.1988.tb01244.x.

Kondolf, G.M., Wilcock, P.R. (1996). The flushing flow problem: defining and evaluating objectives. *Water Resources Research* 32 (8), 2589–2599. DOI: 10.1029/96wr00898.

Kramer, H. (1935). Sand mixtures and sand movement in fluvial model. *Transactions of the American Society of Civil Engineers* 100 (1), 798–838.

Krumbein, W.C. (1936). Application of logarithmic moments to size frequency distributions of sediments. *Journal of Sedimentary Petrology* 6 (1), 35–47.

Kuo, C.-W., Chen, C.-F., Chen, S.-C., Yang, T.-C., Chen, C.-W. (2017). Channel Planform Dynamics Monitoring and Channel Stability Assessment in Two Sediment-Rich Rivers in Taiwan. *Water* 9 (2), 84.

Lacey, R., Roy, A.G. (2007). A comparative study of the turbulent flow field with and without a pebble cluster in a gravel bed river. *Water Resources Research* 43 (5). DOI: 10.1029/2006wr005027.

Lague, D., Brodu, N., Leroux, J. (2013). Accurate 3D comparison of complex topography with terrestrial laser scanner: Application to the Rangitikei canyon (NZ). *ISPRS Journal of Photogrammetry and Remote Sensing* 82, 10–26.

Lake, P.S. (2000). Disturbance, patchiness, and diversity in streams. *Journal of the North American Benthological Society* 19 (4), 573–592. DOI: 10.2307/1468118.

Laronne, J.B., Carson, M.A. (1976). Interrelationships between bed morphology and bed-material transport for a small, gravel-bed channel. *Sedimentology* 23 (1), 67–85. DOI: 10.1111/j.1365-3091.1976.tb00039.x.

Larsen, D.P., Kaufmann, P.R., Kincaid, T.M., Urquhart, N.S. (2004). Detecting persistent change in the habitat of salmon-bearing streams in the Pacific Northwest. *Canadian Journal of Fisheries and Aquatic Sciences* 61 (2), 283–291.

Lee, D.R., Cherry, J.A. (1979). A field exercise on groundwater flow using seepage meters and mini-piezometers. *Journal of Geological Education* 27 (1), 6–10.

Leica Geosystems AG (2014). *WFD – Wave Form Digitizer Technology White Paper.* Report.

Leopold, L.B., Emmett, W.W. (1976). Bedload measurements, East Fork River, Wyoming. *Proceedings of the National Academy of Sciences* 73 (4), 1000–1004.

Leopold, L.B., Emmett, W.W. (1997). Bedload and river hydraulics: inferences from the East Fork River, Wyoming. US Geological Survey.

Lessard, J., Hicks, D.M., Snelder, T.H., Arscott, D.B., Larned, S.T., Booker, D., Suren, A.M. (2013). Dam design can impede adaptive management of environmental flows: a case study from the Opuha Dam, New Zealand. *Environmental Management* 51 (2), 459–73. DOI: 10.1007/s00267-012-9971-x.

Liedermann, M., Gmeiner, P., Kreisler, A., Tritthart, M., Habersack, H. (2018). Insights into bedload transport processes of a large regulated gravel-bed river. *Earth Surface Processes and Landforms* 43 (2), 514–523. DOI: doi:10.1002/esp.4253.

Lindsay, J.B., Ashmore, P.E. (2002). The effects of survey frequency on estimates of scour and fill in a braided river model. *Earth Surface Processes and Landforms* 27 (1), 27–43.

Lisenby, P.E., Croke, J., Fryirs, K.A. (2018). Geomorphic effectiveness: a linear concept in a non-linear world. *Earth Surface Processes and Landforms* 43 (1), 4–20. DOI: 10.1002/esp.4096.

Lisle, T.E. (1989). Sediment Transport and Resulting Deposition in Spawning Gravels, North Coastal California. *Water Resources Research* 25 (6), 1303–1319.

Lisle, T.E., Nelson, J.M., Pitlick, J., Madej, M.A., Barkett, B.L. (2000). Variability of bed mobility in natural, gravel-bed channels and adjustments to sediment load at local and reach scales. *Water Resources Research* 36 (12), 3743–3755. DOI: 10.1029/2000WR900238.

Lisle, T.E., Iseya, F., Ikeda, H. (1993). Response of a channel with alternate bars to a decrease in supply of mixed-size bed load: A flume experiment. *Water Resources Research* 29 (11), 3623–3629.

Lisle, T.E., Madej, M. (1992). Spatial variation in armouring in a channel with high sediment supply. In: Billi, P., Hey, R., Thorne, C., Tacconi, P. (Eds). Dynamics of Gravel-Bed Rivers. Chap. 13, pp. 277–293.

Litrico, X., Belaud, G., Fovet, O. (2011). "Adaptive control of algae detachment in regulated canal networks". In: *2011 International Conference on Networking, Sensing and Control (ICNSC)*, pp. 197–202. DOI: 10.1109/ICNSC.2011.5874878.

Lorang, M.S., Tonolla, D. (2014). Combining active and passive hydroacoustic techniques during flood events for rapid spatial mapping of bedload transport patterns in gravel-bed rivers. *Fundamental and Applied Limnology* 184 (3), 231–246. DOI: 10.1127/1863-9135/2014/0552.

Lorang, M.S., Hauer, F.R. (2003). Flow competence and streambed stability: an evaluation of technique and application. *Journal of the North American Benthological Society* 22 (4), 475–491. DOI: 10.2307/1468347.

Lozano, D., Arranja, C., Rijo, M., Mateos, L. (2010). Simulation of automatic control of an irrigation canal. *Agricultural Water Management* 97 (1), 91–100. DOI: 10.1016/j.agwat.2009.08.016.

Lu, Y., Chiew, Y.-M., Cheng, N.-S. (2008). Review of seepage effects on turbulent open-channel flow and sediment entrainment. *Journal of Hydraulic Research* 46 (4), 476–488. DOI: 10.3826/jhr.2008.2942.

MacKenzie, L.G., Eaton, B.C. (2017). Large grains matter: contrasting bed stability and morphodynamics during two nearly identical experiments. *Earth Surface Processes and Landforms*. DOI: 10.1002/esp.4122.

Maclean, A. (1991). Open channel velocity profiles over a zone of rapid infiltration. *Journal of Hydraulic Research* 29 (1), 15–27.

Mao, L., Carrillo, R., Escauriaza, C., Iroume, A. (2016). Flume and field-based calibration of surrogate sensors for monitoring bedload transport. *Geomorphology* 253, 10–21. DOI: http://dx.doi.org/10.1016/j.geomorph.2015.10.002.

Mao, L. (2012). The effect of hydrographs on bed load transport and bed sediment spatial arrangement. *Journal of Geophysical Research: Earth Surface* 117 (F3). DOI: 10.1029/2012JF002428.

Mao, L., Dell'Agnese, A., Huincache, C., Penna, D., Engel, M., Niedrist, G., Comiti, F. (2014). Bedload hysteresis in a glacier-fed mountain river. *Earth Surface Processes and Landforms* 39 (7), 964–976. DOI: 10.1002/esp.3563.

McAllister, T.G., Wood, S.A., Atalah, J., Hawes, I. (2018). Spatiotemporal dynamics of Phormidium cover and anatoxin concentrations in eight New Zealand rivers with contrasting nutrient and flow regimes. *Science of the Total Environment* 612, 71–80. DOI: 10.1016/j.scitotenv.2017.08.085.

McAllister, T.G., Wood, S.A., Hawes, I. (2016). The rise of toxic benthic Phormidium proliferations: A review of their taxonomy, distribution, toxin content and factors regulating prevalence and increased severity. *Harmful Algae* 55, 282–294. DOI: http://dx.doi.org/10.1016/j.hal.2016.04.002.

Measures, R., Tait, S. (2008). Quantifying the role of bed surface topography in controlling sediment stability in water-worked gravel deposits. *Water Resources Research* 44 (4), 1–17. DOI: 10.1029/2006wr005794.

Meyer-Peter, E., Müller, R. (1948). "Formulas for bed-load transport". In: *IAHSR 2nd meeting, Stockholm, appendix 2*. IAHR.

Meyer, D., Dimitriadou, E., Hornik, K., Weingessel, A., Leisch, F. (2017). "e1071: Misc Functions of the Department of Statistics, Probability Theory Group (Formerly: E1071), TU Wien".

Milan, D.J. (2009). Terrestrial laser scan-derived topographic and roughness data for hydraulic modelling of gravel-bed rivers. Wiley-Blackwell: Oxford, UK.

Milan, D.J., Heritage, G.L. (2012). LiDAR and ADCP Use in Gravel-Bed Rivers: Advances Since GBR6. In: Michael, C., Biron, P.M., Roy, A.G. (Eds). Gravel-bed Rivers: Processes, Tools, Environments. John Wiley & Sons, Ltd, pp. 286–302. DOI: 10.1002/9781119952497.ch22.

Milan, D., Heritage, G., Large, A., Charlton, M. (2001). Stage dependent variability in tractive force distribution through a riffle–pool sequence. *Catena* 44 (2), 85–109. DOI: 10.1016/S0341-8162(00)00155-7.

Milhous, R.T. (1973). Sediment transport in a gravel-bottomed stream. PhD Thesis. Oregon State University.

Millane, R.P., Weir, M.I., Smart, G.M. (2006). Automated Analysis of Imbrication and Flow Direction in Alluvial Sediments Using Laser-Scan Data. *Journal of Sedimentary Research* 76 (8), 1049–1055. DOI: 10.2110/jsr.2006.098.

Miller, M., McCave, I., Komar, P. (1977). Threshold of sediment motion under unidirectional currents. *Sedimentology* 24 (4), 507–527.

Minchin, S., Death, R. (2002). Invertebrate species richness in New Zealand forest streams. *Internationale Vereinigung fur Theoretische und Angewandte Limnologie Verhandlungen* 28 (1), 311–314.

Mizuyama, T., Oda, A., Laronne, J.B., Nonaka, M., Matsuoka, M. (2010). Laboratory tests of a Japanese pipe geophone for continuous acoustic monitoring of coarse bedload. *US Geological Survey Scientific Investigations Report* 5091, 319–335.

Montgomery, D.R., Buffington, J.M., Smith, R.D., Schmidt, K.M., Pess, G. (1995). Pool spacing in forest channels. *Water Resources Research* 31 (4), 1097–1105.

Moore, H.E., Rutherfurd, I.D. (2017). Lack of maintenance is a major challenge for stream restoration projects. *River Research and Applications* 33 (9), 1387–1399. DOI: 10.1002/rra.3188.

Mueller, E.R., Pitlick, J., Nelson, J.M. (2005). Variation in the reference Shields stress for bed load transport in gravel-bed streams and rivers. *Water Resources Research* 41 (4), W04006. DOI: 10.1029/2004WR003692.

Narahari, D., Rao, B., Jain, R. (1967). "Dynamic cone penetration tests in gravels and gravely soils". In: *Symposium on Site Investigation Foundation, Roarkee, India.* Vol. 1, pp. 317–325.

Neverman, A.J., Fuller, I.C., Death, R.G., Singh, R., Procter, J. (2018). Towards Mechanistic Hydrological Limits: A Literature Synthesis to Improve the Study of Direct Linkages between Sediment Transport and Periphyton Accrual in Gravel-Bed Rivers. *Environmental Management* 62 (4), 740–755. DOI: 10.1007/s00267-018-1070-1.

Neverman, A.J., Fuller, I.C., Death, R. (In Prep). Rapidly quantifying compactness of the active layer in gravel-bed streams.

Neverman, A.J., Fuller, I.C., Procter, J.N., Death, R.G. (In Press). Terrestrial Laser Scanning and Structure-from-Motion Photogrammetry concordance analysis for describing the surface layer of gravel beds.

Neverman, A., Fuller, I.C., Procter, J. (2016). Application of Geomorphic Change Detection (GCD) to quantify morphological budgeting error in a New Zealand gravel-bed river: a case study from the Makaroro River, Hawke's Bay. *Journal of Hydrology (NZ)* 55 (1), 45–63.

Newbury, R.W. (1984). Hydrologic determinants of aquatic insect habitats. In: Ecology of Aquatic Insects. Chap. 11, pp. 323–357.

Nikora, V., Ballio, F., Coleman, S., Pokrajac, D. (2013). Spatially averaged flows over mobile rough beds: Definitions, averaging theorems, and conservation equations. *Journal of Hydraulic Engineering* 139 (8), 803–811.

Nikora, V., Goring, D., McEwan, I., Griffiths, G. (2001). Spatially averaged open-channel flow over rough bed. *Journal of Hydraulic Engineering* 127 (2), 123–133.

Nouwakpo, S.K., Weltz, M.A., McGwire, K. (2016). Assessing the performance of structure-from-motion photogrammetry and terrestrial LiDAR for reconstructing soil surface microtopography of naturally vegetated plots. *Earth Surface Processes and Landforms* 41 (3), 308–322. DOI: 10.1002/esp.3787.

Ockelford, A., Haynes, H. (2013). The impact of stress history on bed structure. *Earth Surface Processes and Landforms* 38 (7), 717–727.

Osmundson, D., Scheer, B. (1998). Monitoring cobble-gravel embeddedness in the streambed of the upper Colorado River, 1996–1997. *US Fish and Wildlife Service, Grand Junction, CO.*

Paiement-Paradis, G., Marquis, G., Roy, A. (2011). Effects of turbulence on the transport of individual particles as bedload in a gravel-bed river. *Earth Surface Processes and Landforms* 36 (1), 107–116. DOI: 10.1002/esp.2027.

Papanicolaou, A., Diplas, P., Evaggelopoulos, N., Fotopoulos, S. (2002). Stochastic incipient motion criterion for spheres under various bed packing conditions. *Journal of Hydraulic Engineering* 128 (4), 369–380. DOI: 10.1061/(Asce)0733-9429(2002)128:4(369).

Papanicolaou, A., Tsakiris, A.G., Strom, K.B. (2012). The use of fractals to quantify the morphology of cluster microforms. *Geomorphology* 139, 91–108. DOI: 10.1016/j.geomorph.2011.10.007.

Parker, G., Dhamotharan, S., Stefan, H. (1982). Model experiments on mobile, paved gravel bed streams. *Water Resources Research* 18 (5), 1395–1408.

Patel, M., Majumder, S., Kumar, B. (2017). Effect of seepage on flow and bedforms dynamics. *Earth Surface Processes and Landforms.* DOI: `10.1002/esp.4134`.

Pearson, E., Smith, M.W., Klaar, M.J., Brown, L.E. (2017). Can high resolution 3D topographic surveys provide reliable grain size estimates in gravel bed rivers? *Geomorphology* 293, 143–155. DOI: `10.1016/j.geomorph.2017.05.015`.

Pedersen, M.L., Friberg, N. (2007). Two lowland stream riffles – linkages between physical habitats and macroinvertebrates across multiple spatial scales. *Aquatic Ecology* 41 (3), 475–490. DOI: `10.1007/s10452-004-1584-x`.

Pfankuch, D.J. (1975). Stream reach inventory and channel stability evaluation. *US Department of Agriculture Forest Service, Region,* 1.

Pickup, G., Warner, R.F. (1976). Effects of hydrological regime on magnitude and frequency of dominant discharge. *Journal of Hydrology* 29, 51–75.

Piedra, M.M., Haynes, H., Hoey, T.B. (2012). The spatial distribution of coarse surface grains and the stability of gravel river beds. *Sedimentology* 59 (3), 1014–1029. DOI: `doi:10.1111/j.1365-3091.2011.01290.x`.

Poff, N.L., Allan, J.D., Bain, M.B., Karr, J.R., Prestegaard, K.L., Richter, B.D., Sparks, R.E., Stromberg, J.C. (1997). The natural flow regime. *BioScience* 47 (11), 769–784. DOI: `10.2307/1313099`.

Poff, N.L., Brown, C.M., Grantham, T.E., Matthews, J.H., Palmer, M.A., Spence, C.M., Wilby, R.L., Haasnoot, M., Mendoza, G.F., Dominique, K.C., Baeza, A. (2015). Sustainable water management under future uncertainty with eco-engineering decision scaling. *Nature Climate Change* 6 (1), 25–34. DOI: `10.1038/NCLIMATE2765`.

Poff, N.L., Olden, J.D., Merritt, D.M., Pepin, D.M. (2007). Homogenization of regional river dynamics by dams and global biodiversity implications. *Proceedings of the National Academy of Sciences* 104 (14), 5732–5737. DOI: `10.1073/pnas.0609812104`.

Poff, N.L. (2017). Beyond the natural flow regime? Broadening the hydro-ecological foundation to meet environmental flows challenges in a non-stationary world. *Freshwater Biology*, 1–11. DOI: `10.1111/fwb.13038`.

Poff, N.L., Zimmerman, J.K.H. (2010). Ecological responses to altered flow regimes: a literature review to inform the science and management of environmental flows. *Freshwater Biology* 55 (1), 194–205. DOI: `10.1111/j.1365-2427.2009.02272.x`.

Pokrajac, D., McEwan, I., Nikora, V. (2008). Spatially averaged turbulent stress and its partitioning. *Experiments in Fluids* 45 (1), 73–83. DOI: `10.1007/s00348-008-0463-y`.

Poole, G.C. (2010). Stream hydrogeomorphology as a physical science basis for advances in stream ecology. *Journal of the North American Benthological Society* 29 (1), 12–25.

Powell, D.M. (1998). Patterns and processes of sediment sorting in gravel-bed rivers. *Progress in Physical Geography* 22 (1), 1–32.

Qin, J., Zhong, D., Wang, G., Ng, S.L. (2012). On characterization of the imbrication of armored gravel surfaces. *Geomorphology* 159, 116–124.

R Core Team (2013). “R: A language and environment for statistical computing. R Foundation for Statistical Computing, Vienna, Austria.”

Radice, A., Nikora, V., Campagnol, J., Ballio, F. (2013). Active interactions between turbulence and bed load: Conceptual picture and experimental evidence. *Water Resources Research* 49 (1), 90–99. DOI: 10.1029/2012WR012255.

Rahman, N.K.A., Kaamin, M., Suwandi, A.K., Sahat, S., Kesot, M.J. (2016). “Development of Mackintosh Probe Extractor”. In: *IOP Conference Series: Materials Science and Engineering.* Vol. 160. IOP Publishing. DOI: doi:10.1088/1757-899X/160/1/012015.

Rainato, R., Mao, L., García-Rama, A., Picco, L., Cesca, M., Vianello, A., Preciso, E., Scussel, G.R., Lenzi, M.A. (2017). Three decades of monitoring in the Rio Cordon instrumented basin: Sediment budget and temporal trend of sediment yield. *Geomorphology* 291, 45–56. DOI: http://dx.doi.org/10.1016/j.geomorph.2016.03.012.

Rao, A.R., Sitaram, N. (1999). Stability and mobility of sand-bed channels affected by seepage. *Journal of Irrigation and Drainage Engineering* 125 (6), 370–379.

Raven, E.K., Lane, S.N., Bracken, L.J. (2010). Understanding sediment transfer and morphological change for managing upland gravel-bed rivers. *Progress in Physical Geography* 34 (1), 23–45. DOI: 10.1177/0309133309355631.

Raven, E.K., Lane, S.N., Ferguson, R.I., Bracken, L.J. (2009). The spatial and temporal patterns of aggradation in a temperate , upland , gravel-bed river. *Earth Surface Processes and Landforms* (34), 1181–1197. DOI: 10.1002/esp.

Recking, A., Liébault, F., Peteuil, C., Jolimet, T. (2012). Testing bedload transport equations with consideration of time scales. *Earth Surface Processes and Landforms* 37 (7), 774–789. DOI: 10.1002/esp.3213.

Reice, S.R., Wissmar, R.C., Naiman, R.J. (1990). Disturbance regimes, resilience, and recovery of animal communities and habitats in lotic ecosystems. *Environmental Management* 14 (5), 647–659.

Reid, I., Layman, J., Frostick, L. (1980). The continuous measurement of bedload discharge. *Journal of Hydraulic Research* 18 (3), 243–249.

Reid, I., Brayshaw, A.C., Frostick, L.E. (1984). An electromagnetic device for automatic detection of bedload motion and its field applications. *Sedimentology* 31 (2), 269–276. DOI: 10.1111/j.1365-3091.1984.tb01963.x.

Reid, I., Frostick, L.E. (1986). Dynamics of bedload transport in Turkey Brook, a coarse-grained alluvial channel. *Earth Surface Processes and Landforms* 11 (2), 143–155.

Rennie, C.D., Villard, P.V. (2004). Site specificity of bed load measurement using an acoustic Doppler current profiler. *Journal of Geophysical Research: Earth Surface* 109 (F3). DOI: 10.1029/2003JF000106.

Resh, V.H., Brown, A.V., Covich, A.P., Gurtz, M.E., Li, H.W., Minshall, G.W., Reice, S.R., Sheldon, A.L., Wallace, J.B., Wissmar, R.C. (1988). The Role of Disturbance in Stream Ecology. *Journal of the North American Benthological Society* 7 (4), 433–455. DOI: 10.2307/1467300.

Rice, S., Church, M. (1996). Sampling surficial fluvial gravels: the precision of size distribution percentile estimates. *Journal of Sedimentary Research* 66 (3).

Richter, B.D., Mathews, R., Harrison, D.L., Wigington, R. (2003). Ecologically sustainable water management: Managing river flows for ecological integrity. *Ecological Applications* 13 (1), 206–224. DOI: 10.1890/1051-0761(2003)013[0206:ESWMMR]2.0.CO;2.

Rickenmann, D., Antoniazza, G., Wyss, C.R., Fritschi, B., Boss, S. (2017). Bedload transport monitoring with acoustic sensors in the Swiss Albula mountain river. *Proc. IAHS* 375, 5–10. DOI: `10.5194/piahs-375-5-2017`.

Rickenmann, D., Turowski, J.M., Fritschi, B., Klaiber, A., Ludwig, A. (2012). Bedload transport measurements at the Erlenbach stream with geophones and automated basket samplers. *Earth Surface Processes and Landforms* 37 (9), 1000–1011. DOI: `10.1002/esp.3225`.

Rickenmann, D., Turowski, J.M., Fritschi, B., Wyss, C., Laronne, J., Barzilai, R., Reid, I., Kreisler, A., Aigner, J., Seitz, H., Habersack, H. (2014). Bedload transport measurements with impact plate geophones: comparison of sensor calibration in different gravel-bed streams. *Earth Surface Processes and Landforms* 39 (7), 928–942. DOI: `10.1002/esp.3499`.

Rickenmann, D. (2018). Variability of Bed Load Transport During Six Summers of Continuous Measurements in Two Austrian Mountain Streams (Fischbach and Ruetz). *Water Resources Research* 54 (1), 107–131. DOI: `doi:10.1002/2017WR021376`.

Rickenmann, D., Fritschi, B. (2017). Bedload transport measurements with impact plate geophones in two Austrian mountain streams (Fischbach and Ruetz): system calibration, grain size estimation, and environmental signal pick-up. *Earth Surface Dynamics* 5 (4), 669.

Robert, A. (1997). Characteristics of velocity profiles along riffle-pool sequences and estimates of bed shear stress. *Geomorphology* 19 (1–2), 89–98. DOI: `https://doi.org/10.1016/S0169-555X(96)00049-9`.

Rounick, J., Winterbourn, M. (1982). Benthic faunas of forested streams and suggestions for their management. *New Zealand Journal of Ecology*, 140–150.

Roussel, J.-R., Auty, D. (2017). "lidR: Airborne LiDAR Data Manipulation and Visualization for Forestry Applications. R package version 1.2.0."

Rychkov, I., Brasington, J., Vericat, D. (2012). Computational and methodological aspects of terrestrial surface analysis based on point clouds. *Computers & Geosciences* 42, 64–70. DOI: `10.1016/j.cageo.2012.02.011`.

Ryder, D.S., Watts, R.J., Nye, E., Burns, A. (2006). Can flow velocity regulate epixylic biofilm structure in a regulated floodplain river? *Marine and Freshwater Research* 57 (1), 29–36.

Sambrook Smith, G.H. (1996). Bimodal fluvial bed sediments: origin, spatial extent and processes. *Progress in Physical Geography* 20 (4), 402–417.

Schumm, S.A. (1968). River adjustment to altered hydrologic regimen, Murrumbidgee River and paleochannels, Australia. Vol. 598. US Government Printing Office.

Schwendel, A.C., Death, R.G., Fuller, I.C., Joy, M.K. (2011). Linking disturbance and stream invertebrate communities: how best to measure bed stability. *Journal of the North American Benthological Society* 30 (1), 11–24. DOI: `10.1899/09-172.1`.

Schwendel, A.C., Death, R.G., Fuller, I.C., Tonkin, J.D. (2012a). A New Approach to Assess Bed Stability Relevant for Invertebrate Communities in Upland Streams. *River Research and Applications* 28 (10), 1726–1739. DOI: `10.1002/rra.1570`.

Schwendel, A.C., Fuller, I.C., Death, R.G. (2012b). Assessing dem interpolation methods for effective representation of upland stream morphology for rapid appraisal of bed stability. *River Research and Applications* (2010), 567–584. DOI: `10.1002/rra`.

Sear, D.A. (1995). Morphological and sedimentological changes in a gravel-bed river following 12 years of flow regulation for hydropower. *Regulated Rivers: Research & Management* 10 (2-4), 247–264. DOI: `10.1002/rrr.3450100219`.

Sear, D. (1992). Impact of hydroelectric power releases on sediment transport processes in pool-riffle sequences. In: Billi, P., Hey, R.D., Thorne, C.R., Tacconi, P. (Eds). Dynamics of Gravel-Bed Rivers. John Wiley, New York. Chap. 32, pp. 629–650.

Sear, D. (1996). Sediment transport processes in pool–riffle sequences. *Earth Surface Processes and Landforms* 21 (3), 241–262.

Sear, D., Damon, W., Booker, D., Anderson, D. (2000). A load cell based continuous recording bedload trap. *Earth Surface Processes and Landforms* 25 (6), 659–672.

Shields, A. (1936). Application of Similarity Mechanics and Turbulence Research to Bedload Movement. PhD Thesis. Technical University Berlin.

Shrestha, S., Shibata, K., Hirano, K., Takahara, T., Matsumura, K. (2005). “River Bedload Monitoring Using a Radar System”. In: *International Bedload Surrogates Monitoring Workshop*.

Slater, L.J. (2016). To what extent have changes in channel capacity contributed to flood hazard trends in England and Wales? *Earth Surface Processes and Landforms* 41 (8), 1115–1128. DOI: `10.1002/esp.3927`.

Smart, G.M., Habersack, H.M. (2007). Pressure fluctuations and gravel entrainment in rivers. *Journal of Hydraulic Research* 45 (5), 661–673.

Smart, G., Plew, D., Gateuille, D. (2010). “Eddy educed entrainment”. In: Dittrich Koll, A.G. (Ed). *River Flow 2010*. Bundesanstalt für Wasserbau, pp. 747–754.

Smart, G., Aberle, J., Duncan, M., Walsh, J. (2004). Measurement and analysis of alluvial bed roughness. *Journal of Hydraulic Research* 42 (3), 227–237.

Smith, H., Yager, E. (2012). “An investigation into the turbulence parameter responsible for the onset of grain motion”. In: *AGU Fall Meeting Abstracts*.

Snelder, T.H., Booker, D.J., Quinn, J.M., Kilroy, C. (2014). Predicting Periphyton Cover Frequency Distributions across New Zealand’s Rivers. *JAWRA Journal of the American Water Resources Association* 50 (1), 111–127. DOI: `10.1111/jawr.12120`.

Snyder, N.P., Castele, M.R., Wright, J.R. (2009). Bedload entrainment in low-gradient paraglacial coastal rivers of Maine, U.S.A.: Implications for habitat restoration. *Geomorphology* 103 (3), 430–446. DOI: `http://dx.doi.org/10.1016/j.geomorph.2008.07.013`.

Soar, P.J., Downs, P.W. (2017). Estimating bedload transport rates in a gravel-bed river using seismic impact plates: Model development and application. *Environmental Modelling & Software* 90, 182–200. DOI: `http://dx.doi.org/10.1016/j.envsoft.2017.01.012`.

Sotoodeh, S. (2006). Outlier detection in laser scanner point clouds. *International Archives of Photogrammetry, Remote Sensing and Spatial Information Sciences* 36 (5), 297–302.

Spicer, K.R., Costa, J.E., Placzek, G. (1997). Measuring flood discharge in unstable stream channels using ground-penetrating radar. *Geology* 25 (5), 423–426. DOI: `10.1130/0091-7613(1997)025<0423:Mfdius>2.3.Co;2`.

Stark, N., Hay, A.E., Cheel, R., Zedel, L., Barclay, D. (2014). Laboratory Measurements of Coarse Sediment Bedload Transport Velocity Using a Prototype Wideband Coherent Doppler Profiler (MFDop). *Journal of Atmospheric and Oceanic Technology* 31 (4), 999–1011. DOI: `10.1175/Jtech-D-13-00095.1`.

Sterling, S.M., Church, M. (2002). Sediment trapping characteristics of a pit trap and the Helley-Smith sampler in a cobble gravel bed river. *Water Resources Research* 38 (8), 19-1-19-11. DOI: `10.1029/2000WR000052`.

Stevenson, R.J. (1990). Benthic algal community dynamics in a stream during and after a spate. *Journal of the North American Benthological Society*, 277–288.

Surry, D. (1972). Some effects of intense turbulence on the aerodynamics of a circular cylinder at subcritical Reynolds number. *Journal of Fluid Mechanics* 52 (3), 543–563.

Tamminga, A., Hugenholtz, C., Eaton, B., Lapointe, M. (2015). Hyperspatial Remote Sensing of Channel Reach Morphology and Hydraulic Fish Habitat Using an Unmanned Aerial Vehicle (UAV): A First Assessment in the Context of River Research and Management. *River Research and Applications* 31 (3), 379–391. DOI: `10.1002/rra.2743`.

Tennant, D.L. (1976). Instream flow regimens for fish, wildlife, recreation and related environmental resources. *Fisheries* 1 (4), 6–10.

Tennekes, H., Lumley, J.L. (1972). A first course in turbulence. MIT press.

Townsend, S.A., Padovan, A.V. (2005). The seasonal accrual and loss of benthic algae (Spirogyra) in the Daly River, an oligotrophic river in tropical Australia. *Marine and Freshwater Research* 56 (3), 317–327.

Traykovski, P., Irish, J.D., Lynch, J.F. (1998). Motivations for using a pulsed full spectrum Doppler to measure bedload and near-bottom suspended sediment transport. *The Journal of the Acoustical Society of America* 103 (5), 2866–2866.

Trevisani, S., Cavalli, M. (2016). Topography-based flow-directional roughness: potential and challenges. *Earth Surface Dynamics* 4, 343–358.

Tsakiris, A.G., Papanicolaou, A.N., Lauth, T.J. (2014). Signature of bedload particle transport mode in the acoustic signal of a geophone. *Journal of Hydraulic Research* 52 (2), 185–204. DOI: `10.1080/00221686.2013.876454`.

Tsujimoto, T., Tashiro, T. (2004). Application of Population Dynamics Modeling to Habitat Evaluation–Growth of Some Species of Attached Algae and Its Detachment by Transported Sediment. *Hydroécologie Appliquée* 14 (1), 161–174.

Tsutsumi, D., Fujita, M., Nonaka, M. (2018). Transport measurement with a horizontal and a vertical pipe microphone in a mountain stream: taking account of particle saltation. *Earth Surface Processes and Landforms* 43 (5), 1118–1132. DOI: `10.1002/esp.4297`.

Tunnicliffe, J., Gottesfeld, A.S., Mohamed, M. (2000). High resolution measurement of bedload transport. *Hydrological Processes* 14 (15), 2631–2643. DOI: `10.1002/1099-1085(20001030)14:15<2631::Aid-Hyp83>3.0.Co;2-C`.

Turowski, J.M., Rickenmann, D. (2009). Tools and cover effects in bedload transport observations in the Pitzbach, Austria. *Earth Surface Processes and Landforms* 34 (1), 26–37. DOI: 10.1002/esp.1686.

Van der Lingen, G.J. (1968). Preliminary sedimentological evaluation of some flysch-like deposits from the Makara Basin, Central Hawke's Bay, New Zealand. *New Zealand Journal of Geology and Geophysics* 11 (2), 455–477. DOI: 10.1080/00288306.1968.10423662.

Vázquez-Tarrío, D., Borgniet, L., Liébault, F., Recking, A. (2017). Using UAS optical imagery and SfM photogrammetry to characterize the surface grain size of gravel bars in a braided river (Vénéon River, French Alps). *Geomorphology* 285, 94–105. DOI: 10.1016/j.geomorph.2017.01.039.

Vázquez-Tarrío, D., Menéndez-Duarte, R. (2015). Assessment of bedload equations using data obtained with tracers in two coarse-bed mountain streams (Narcea River basin, NW Spain). *Geomorphology* 238, 78–93. DOI: http://dx.doi.org/10.1016/j.geomorph.2015.02.032.

Venditti, J.G., Dietrich, W.E., Nelson, P.A., Wydzga, M.A., Fadde, J., Sklar, L. (2010). Mobilization of coarse surface layers in gravel-bedded rivers by finer gravel bed load. *Water Resources Research* 46 (7). DOI: 10.1029/2009WR008329.

Verdú, J.M., Batalla, R.J., Martínez-Casasnovas, J.A. (2005). High-resolution grain-size characterisation of gravel bars using imagery analysis and geo-statistics. *Geomorphology* 72 (1–4), 73–93. DOI: http://dx.doi.org/10.1016/j.geomorph.2005.04.015.

Viles, H. (2016). Technology and geomorphology: Are improvements in data collection techniques transforming geomorphic science? *Geomorphology* 270, 121–133. DOI: http://dx.doi.org/10.1016/j.geomorph.2016.07.011.

Vollmer, S., Kleinhans, M.G. (2007). Predicting incipient motion, including the effect of turbulent pressure fluctuations in the bed. *Water Resources Research* 43 (5). DOI: 10.1029/2006WR004919.

Wang, H.-W., Hong, J.-H., Huang, C.-J. (2016). Analysis of ground-penetrating radar signal reflected from the water volume influenced by sediment concentration. In: Huang, C.-J. (Ed). River Flow 2016: Iowa City, USA, July 11-14, 2016, p. 345.

Watts, R.J., Ryder, D.S., Burns, A., Wilson, A.L., Nye, E., Zander, A., Dehaan, R. (2006). *Responses of biofilms to cyclic releases during a low flow period in the Mitta Mitta River, Victoria, Australia.* Report. Institute for Land Water & Society - Charles Sturt University.

Wentworth, C.K. (1922). A Scale of Grade and Class Terms for Clastic Sediments. *The Journal of Geology* 30 (5), 377–392.

Westoby, M.J., Dunning, S.A., Woodward, J., Hein, A.S., Marrero, S.M., Winter, K., Sugden, D.E. (2015). Sedimentological characterization of Antarctic moraines using UAVs and Structure-from-Motion photogrammetry. *Journal of Glaciology* 61 (230), 1088–1102. DOI: 10.3189/2015JoG15J086.

Westoby, M., Brasington, J., Glasser, N., Hambrey, M., Reynolds, J. (2012). 'Structure-from-Motion'photogrammetry: A low-cost, effective tool for geoscience applications. *Geomorphology* 179, 300–314.

Wharton, G., Mohajeri, S.H., Righetti, M. (2017). The pernicious problem of streambed colmation: a multi-disciplinary reflection on the mechanisms, causes, impacts, and management challenges. *Wiley Interdisciplinary Reviews: Water*.

White, C. (1940). The equilibrium of grains on the bed of a stream. *Proceedings of the Royal Society of London. Series A, Mathematical and Physical Sciences*, 322–338.

Wilcock, P.R. (2001). Toward a practical method for estimating sediment-transport rates in gravel-bed rivers. *Earth Surface Processes and Landforms* 26 (13), 1395–1408. DOI: `10.1002/esp.301`.

Wilcock, P.R., Barta, A.F., Shea, C.C., Kondolf, G.M., Matthews, W.V.G., Pitlick, J. (1996). Observations of Flow and Sediment Entrainment on a Large Gravel-Bed River. *Water Resources Research* 32 (9), 2897–2909. DOI: `10.1029/96WR01628`.

Wilcock, P.R., Southard, J.B. (1989). Bed load transport of mixed size sediment: Fractional transport rates, bed forms, and the development of a coarse bed surface layer. *Water Resources Research* 25 (7), 1629–1641. DOI: `10.1029/WR025i007p01629`.

Williams, R.D., Brasington, J., Hicks, M., Measures, R., Rennie, C.D., Vericat, D. (2013). Hydraulic validation of two-dimensional simulations of braided river flow with spatially continuous aDcp data. *Water Resources Research* 49 (9), 5183–5205. DOI: `10.1002/wrcr.20391`.

Williams, R.D., Brasington, J., Vericat, D., Hicks, D.M. (2014). Hyperscale terrain modelling of braided rivers: fusing mobile terrestrial laser scanning and optical bathymetric mapping. *Earth Surface Processes and Landforms* 39 (2), 167–183. DOI: `10.1002/esp.3437`.

Winter, T.C., LaBaugh, J.W., Rosenberry, D.O. (1988). The design and use of a hydraulic potentiomanometer for direct measurement of differences in hydraulic head between groundwater and surface water. *Limnology and Oceanography* 33 (5), 1209–1214. DOI: `10.4319/lo.1988.33.5.1209`.

Wittenberg, L. (2002). Structural patterns in coarse gravelriver beds: typology, survey and assessment of the roles of grain size and river regime. *Geografiska Annaler: Series A, Physical Geography* 84 (1), 25–37.

Wittenberg, L., Newson, M.D. (2005). Particle clusters in gravel-bed rivers: an experimental morphological approach to bed material transport and stability concepts. *Earth Surface Processes and Landforms* 30 (11), 1351–1368. DOI: `10.1002/esp.1184`.

Wohl, E.E., Anthony, D.J., Madsen, S.W., Thompson, D.M. (1996). A comparison of surface sampling methods for coarse fluvial sediments. *Water Resources Research* 32 (10), 3219–3226.

Wolman, M.G. (1954). A Method of Sampling Coarse River-Bed Material. *Transactions, American Geophysical Union* 35, 951–956. DOI: `10.1029/TR035i006p00951`.

Wolman, M.G., Miller, J.P. (1960). Magnitude and frequency of forces in geomorphic processes. *Journal of Geology* 68, 54–74.

Wood, S.A., Selwood, A.I., Rueckert, A., Holland, P.T., Milne, J.R., Smith, K.F., Smits, B., Watts, L.F., Cary, C.S. (2007). First report of homoanatoxin-a and associated dog neurotoxicosis in New Zealand. *Toxicon* 50 (2), 292–301. DOI: `http://dx.doi.org/10.1016/j.toxicon.2007.03.025`.

Woodget, A.S., Carbonneau, P.E., Visser, F., Maddock, I.P. (2015). Quantifying submerged fluvial topography using hyperspatial resolution UAS imagery and structure from motion photogrammetry. *Earth Surface Processes and Landforms* 40 (1), 47–64. DOI: 10.1002/esp.3613.

Woodget, A.S., Fyffe, C., Carbonneau, P.E. (2018). From manned to unmanned aircraft: Adapting airborne particle size mapping methodologies to the characteristics of sUAS and SfM. *Earth Surface Processes and Landforms* 43 (4), 857–870. DOI: 10.1002/esp.4285.

Woodget, A. (2015). Quantifying physical river habitat parameters using hyperspatial resolution UAS imagery and SfM-photogrammetry. PhD Thesis. University of Worcester.

Woodget, A.S., Austrums, R. (2017). Subaerial gravel size measurement using topographic data derived from a UAV-SfM approach. *Earth Surface Processes and Landforms* 42 (9), 1434–1443. DOI: 10.1002/esp.4139.

World Commission on Dams (2000). Dams and Development: A New Framework for Decision-making: the Report of the World Commission on Dams. Earthscan Publications Ltd.

Wu, F.-C., Chou, Y.-J. (2003). Rolling and lifting probabilities for sediment entrainment. *Journal of Hydraulic Engineering* 129 (2), 110–119. DOI: 10.1061/(Asce)0733-9429(2003)129:2(110).

Wyss, C.R., Rickenmann, D., Fritschi, B., Turowski, J.M., Weitbrecht, V., Boes, R.M. (2016). Laboratory flume experiments with the Swiss plate geophone bed load monitoring system: 1. Impulse counts and particle size identification. *Water Resources Research* 52 (10), 7744–7759. DOI: 10.1002/2015WR018555.

Yager, E.M., Kenworthy, M., Monsalve, A. (2015). Taking the river inside: Fundamental advances from laboratory experiments in measuring and understanding bedload transport processes. *Geomorphology* 244, 21–32. DOI: http://dx.doi.org/10.1016/j.geomorph.2015.04.002.

Yeboah, E., Rahai, H., LaRue, J. (1997). "The effects of external turbulence on mean pressure distribution, drag coefficient, and wake characteristics of smooth cylinders". In: *ASME Fluids Engineering Division Summer Meeting, FEDSM*. Vol. 97, pp. 22–26.

Younis, N. (2010). The role of turbulent integral length scale on the drag of a circular cylinder in cross flow. PhD thesis. Universoty of Windsor.

Yu, G.A., Wang, Z.Y., Huang, H.Q., Liu, H.X., Blue, B., Zhang, K. (2012). Bed load transport under different streambed conditions - a field experimental study in a mountain stream. *International Journal of Sediment Research* 27 (4), 426–438. DOI: 10.1016/S1001-6279(13)60002-5.

Zanke, U. (2003). On the influence of turbulence on the initiation of sediment motion. *International Journal of Sediment Research* 18 (1), 17–31.

Zarfl, C., Lumsdon, A.E., Berlekamp, J., Tydecks, L., Tockner, K. (2015). A global boom in hydropower dam construction. *Aquatic Sciences* 77 (1), 161–170. DOI: 10.1007/s00027-014-0377-0.

Zhu, T., Fu, D., Jenkinson, B., Jafvert, C.T. (2015). Calibration and application of an automated seepage meter for monitoring water flow across the sediment-water interface. *Environmental Monitoring and Assessment* 187 (4), 1–11. DOI: 10.1007/s10661-015-4388-7.

Appendix A

Statements of Contribution

MASSEY UNIVERSITY
GRADUATE RESEARCH SCHOOL

STATEMENT OF CONTRIBUTION TO DOCTORAL THESIS CONTAINING PUBLICATIONS

(To appear at the end of each thesis chapter/section/appendix submitted as an article/paper or collected as an appendix at the end of the thesis)

We, the candidate and the candidate's Principal Supervisor, certify that all co-authors have consented to their work being included in the thesis and they have accepted the candidate's contribution as indicated below in the *Statement of Originality*.

Name of Candidate: Andrew Neverman

Name/Title of Principal Supervisor: Professor Ian Fuller

Name of Published Research Output and full reference:

Neverman, A. J., Fuller, I. C., Death, R. G., Singh, R., & Procter, J. N. (2018). Towards mechanistic hydrological limits: a literature synthesis to improve the study of direct linkages between sediment transport and periphyton accrual in gravel-bed rivers. Environmental Management. 62(4), 740-755. DOI : 10.1007/s00267-018-1070-1

In which Chapter is the Published Work: Chapter 1

Please indicate either:

- The percentage of the Published Work that was contributed by the candidate:

  and / or

- Describe the contribution that the candidate has made to the Published Work:

  Andrew Neverman was the principal author in the review of literature, manuscript preparation, submission, and revision. Review and editing of the manuscript was provided by co-authors.

Andrew Neverman
Digitally signed by Andrew Neverman
DN: cn=Andrew Neverman, email=a.neverman@massey.ac.nz, c=NZ
Date: 2018.12.09 20:00:37 +13'00'

Candidate's Signature

9/12/2018

Date

Principal Supervisor's signature

10/12/2018

Date

MASSEY UNIVERSITY
GRADUATE RESEARCH SCHOOL

STATEMENT OF CONTRIBUTION TO DOCTORAL THESIS CONTAINING PUBLICATIONS

(To appear at the end of each thesis chapter/section/appendix submitted as an article/paper or collected as an appendix at the end of the thesis)

We, the candidate and the candidate's Principal Supervisor, certify that all co-authors have consented to their work being included in the thesis and they have accepted the candidate's contribution as indicated below in the *Statement of Originality*.

Name of Candidate: Andrew Neverman

Name/Title of Principal Supervisor: Professor Ian Fuller

Name of Published Research Output and full reference:

Neverman, A. J., Fuller, I. C., Procter, J. N., & Death, R. G. (In Press). Terrestrial Laser Scanning and Structure-from-Motion Photogrammetry concordance analysis for describing the surface layer of gravel beds. Progress in Physical Geography.

In which Chapter is the Published Work: Chapter 2

Please indicate either:

- The percentage of the Published Work that was contributed by the candidate:

  and / or

- Describe the contribution that the candidate has made to the Published Work:

  Andrew Neverman carried out all fieldwork with minor assistance. Andrew Neverman carried out all processing and analysis with guidance from co-authors. Andrew Neverman was the principal author in the manuscript preparation, submission, and revision. Review and editing of the manuscript was provided by co-authors.

Andrew Neverman
Digitally signed by Andrew Neverman
DN: cn=Andrew Neverman, email=a.neverman@massey.ac.nz, c=NZ
Date: 2018.12.09 20:03:23 +13'00'

Candidate's Signature

9/12/2018

Date

Principal Supervisor's signature

10/12/2018

Date

MASSEY UNIVERSITY
GRADUATE RESEARCH SCHOOL

STATEMENT OF CONTRIBUTION TO DOCTORAL THESIS CONTAINING PUBLICATIONS

(To appear at the end of each thesis chapter/section/appendix submitted as an article/paper or collected as an appendix at the end of the thesis)

We, the candidate and the candidate's Principal Supervisor, certify that all co-authors have consented to their work being included in the thesis and they have accepted the candidate's contribution as indicated below in the *Statement of Originality*.

Name of Candidate: Andrew Neverman

Name/Title of Principal Supervisor: Professor Ian Fuller

Name of Published Research Output and full reference:

Neverman, A.J., Fuller, I.C., & Death, R.G. (In Prep). A technique to rapidly quantify active layer compactness in gravel-bed streams. Earth Surface Processes and Landforms.

In which Chapter is the Published Work: Chapter 3

Please indicate either:

- The percentage of the Published Work that was contributed by the candidate:

  and / or

- Describe the contribution that the candidate has made to the Published Work:

  Andrew Neverman carried out all fieldwork with minor assistance. Andrew Neverman carried out all processing and analysis with guidance from co-authors. Andrew Neverman was the principal author in the manuscript preparation and submission. Review and editing of the manuscript was provided by co-authors.

Andrew Neverman
Digitally signed by Andrew Neverman
DN: cn=Andrew Neverman, email=a.neverman@massey.ac.nz, c=NZ
Date: 2018.12.09 20:05:06 +13'00'

Candidate's Signature

9/12/2018

Date

Principal Supervisor's signature

10/12/2018

Date

MASSEY UNIVERSITY
GRADUATE RESEARCH SCHOOL

STATEMENT OF CONTRIBUTION TO DOCTORAL THESIS CONTAINING PUBLICATIONS

(To appear at the end of each thesis chapter/section/appendix submitted as an article/paper or collected as an appendix at the end of the thesis)

We, the candidate and the candidate's Principal Supervisor, certify that all co-authors have consented to their work being included in the thesis and they have accepted the candidate's contribution as indicated below in the *Statement of Originality*.

Name of Candidate: Andrew Neverman

Name/Title of Principal Supervisor: Professor Ian Fuller

Name of Published Research Output and full reference:

Neverman, A.J., Death, R.G., Fuller, I.C., McAllister, T.G. (In Prep). A new rapid assessment technique for measuring bed stability in gravel substrates. Freshwater Biology.

In which Chapter is the Published Work: Chapter 4

Please indicate either:

- The percentage of the Published Work that was contributed by the candidate:

  and / or

- Describe the contribution that the candidate has made to the Published Work:

  Andrew Neverman carried out all fieldwork for the development of the index with minor assistance. Tara McAllister supplied the periphyton biomass data. Andrew Neverman carried out all processing and analysis with guidance from co-authors. Andrew Neverman was the principal author in the manuscript preparation, submission, and revision. Review and editing of the manuscript was provided by co-authors.

Andrew Neverman
Digitally signed by Andrew Neverman
DN: cn=Andrew Neverman, email=a.neverman@massey.ac.nz, c=NZ
Date: 2018.12.09 20:07:13 +13'00'

Candidate's Signature

9/12/2018

Date

Principal Supervisor's signature

10/12/2018

Date

MASSEY UNIVERSITY
GRADUATE RESEARCH SCHOOL

STATEMENT OF CONTRIBUTION TO DOCTORAL THESIS CONTAINING PUBLICATIONS

(To appear at the end of each thesis chapter/section/appendix submitted as an article/paper or collected as an appendix at the end of the thesis)

We, the candidate and the candidate's Principal Supervisor, certify that all co-authors have consented to their work being included in the thesis and they have accepted the candidate's contribution as indicated below in the *Statement of Originality*.

Name of Candidate: Andrew Neverman

Name/Title of Principal Supervisor: Professor Ian Fuller

Name of Published Research Output and full reference:

Neverman, A.J., Fuller, I.C., Procter, J.N., Singh, R., & Death, R.G. (In Review). Implementation of a multi-sensor system to identify streamwise hydrodynamic and vertical bed seepage thresholds for particle entrainment in gravel-bed rivers. Journal of Geophysical Research: Earth Surface.

In which Chapter is the Published Work: Chapter 5

Please indicate either:

- The percentage of the Published Work that was contributed by the candidate:

  and / or

- Describe the contribution that the candidate has made to the Published Work:

  Andrew Neverman carried out all fieldwork with minor assistance. Andrew Neverman carried out all processing and analysis with guidance from co-authors. Andrew Neverman was the principal author in the manuscript preparation and submission.

Andrew Neverman
Digitally signed by Andrew Neverman
DN: cn=Andrew Neverman, email=a.neverman@massey.ac.nz, c=NZ
Date: 2018.12.09 20:08:40 +13'00'

Candidate's Signature

9/12/2018

Date

Principal Supervisor's signature

10/12/2018

Date